



RV SONNE
CRUISE REPORT SO109
HYDROTRACE

SO109-1: Astoria - Victoria
May 23 - June 5, 1996

SO109-2: Victoria - Astoria
June 6 - June 25, 1996

SO109-3: Astoria - Victoria
June 26 - July 8, 1996

Edited by
Peter Herzig (Project Coordinator, TU Freiberg),
Erwin Suess & Peter Linke (GEOMAR Kiel)
with contributions by the cruise participants

GEOMAR
Forschungszentrum
für marine Geowissenschaften
der Christian-Albrechts-Universität
zu Kiel

Kiel 1997
GEOMAR REPORT 58

GEOMAR
Research Center
for Marine Geosciences
Christian Albrechts University
in Kiel

Redaktion der Serie
Umschlag

Gerhard Haass
Kerstin Kreis, Harald Gross,
GEOMAR Technologie GmbH

Managing Editor:
Cover:

Gerhard Haass
Kerstin Kreis, Harald Gross,
GEOMAR Technologie GmbH

GEOMAR REPORT
ISSN 0936 - 5788

GEOMAR REPORT
ISSN 0936 - 5788

GEOMAR
Forschungszentrum
für marine Geowissenschaften
D-24148 Kiel
Wischhofstr. 1-3
Telefon (0431) 600-2555, 600-2505

GEOMAR
Research Center
for Marine Geosciences
D-24148 Kiel / Germany
Wischhofstr. 1-3
Telephone (49) 431 / 600-2555, 600-2505

Contents

Preface	1
Vorwort	5
1. Cruise Participants and Schedule	8
1.1 Scientists	8
1.1.1 Leg SO 109-1	8
1.1.2 Leg SO 109-2	8
1.1.3 Leg SO 109-3	9
1.2 Participating Institutions	9
1.3 Ship's Crew	10
1.4 Summary of Activities of Participating Institutions	11
2. Geologic Settings of the Vent Fields	17
2.1 Juan de Fuca Ridge	17
2.1.1 Background	17
2.1.2 ASHES Vent Field	19
2.1.3 CASM Site	20
2.1.4 North Rift Zone	22
2.1.5 South Rift Zone	23
2.1.6 CoAxial Site	23
2.2 Cascadia Accretionary Margin	26
2.2.1 Background	26
2.2.2 Second Accretionary Ridge	27
2.2.3 Bottom Simulating Reflector	27
2.2.4 Bioherm Carbonate	29
3. Leg SO 109-1	31
3.1 Cruise Objectives and Operations Background	31
3.2 Fahrtverlauf und Zusammenfassung der Ergebnisse	32
3.3 Cruise Narrative and Summary of Results	36
3.4 Results:	39
3.4.1 Water Column Program.....	39
3.4.2 Methane Analyses on Hydrocast Samples.....	51
3.4.3 Hydrosweep and Parasound Seafloor Mapping	55
3.4.4 Sediment Sampling and Sedimentology.....	68
3.4.5 Pore Water Studies	71
3.4.6 Biomarker Sampling	79
3.5 Appendix: Station list	82

4.	Leg SO 109-2	98
4.1	Cruise Objectives	98
4.2	Cruise Narrative and Summary of Results	102
4.3	Operations Background	106
4.4	Results:	108
4.4.1	EXPLOS Camera tows	108
4.4.2	Hydrothermal Venting and Sulfide Deposits	115
4.4.3	Water Column Program	146
4.4.4	Methane Analyses on Hydrocast Samples	151
4.4.5	Nutrient and Pore Water Studies	157
4.4.6	SUAVE Operations	161
4.4.7	Biology Report	170
4.4.8	Microbiology	175
4.4.9	Petrology and Volcanology	177
4.4.10	Acoustic Extensometer Deployment	195
4.4.11	Appendix: Station list	198
	Cruise statistics	204
	Maps	211
5.	Leg SO 109-3	214
5.1	Cruise Objectives	214
5.2	Cruise Narrative and Summary of Results	215
5.3	Operations Background	217
5.4	ROPOS Operation	217
5.4.1	Specifications	217
5.4.2	Technical Problems	221
5.5	Results:	223
5.5.1	ROV Operation	223
5.5.2	Mapping and Sulfide Sampling	224
5.5.3	Water Sampling	230
5.5.4	Microbiology	231
5.5.5	EXPLOS Operation	232
5.5.5.1	Survey	232
5.5.5.2	Eh Measurements	234
5.5.6	Appendix: Station list	238
	ROPOS Logs	239
	Sample list	249

Preface

by Erwin Suess and Peter Herzig

The general objective of the project HYDROTRACE on hot vents at the Juan de Fuca Ridge as well as the cold seeps of the Cascadia margin is the evaluation of their vent fluid transport for the material balance of the ocean. Furthermore it was of interest what kind of tracer distribution patterns develop, e.g. how far from their immediate source the influence of discharged fluids, of tracer, and particle distribution can be tracked in the water as well as in the sediments. Hereby the sediment record provides an integrated long-term signal of fluid discharge spanning the divergent plate boundary of the Axial Seamount to the convergent plate boundary, the accretionary ridge off Oregon (Fig. 1). These two areas were the focus of an multidisciplinary project by RV SONNE with Canadian and US participation.

As the hydrothermal and cold seep signals decrease in a non-linear function with increasing distance from the vents, the strategy called for a detailed and high-resolution study of the immediate vicinity of active vents using the unmanned submersible ROPOS, and then proceeding along a regional section with conventional survey methods and sampling farther away from the active discharge zones. For this purpose the RV SONNE cruise SO109 was divided into three legs. The first leg, SO109-1, was to provide an extensive survey and sampling program at the Axial Seamount and the accretionary ridge off Oregon, without the ROPOS system. For this reconnaissance, RV SONNE departed Astoria/Oregon on 23 May, worked at the eastern flank of the Juan de Fuca Ridge from 25-29 May and then on the accretionary continental margin off Oregon from 30 May to 3 June. This leg was completed in Victoria/ Canada on 4 June. For the second leg, SO109-2, RV SONNE departed Victoria on 8 June, though without an operational ROPOS system on board as technical problems had delayed completion of the drum for the new cable winch. Instead of deploying ROPOS as planned, an intense sampling program was carried out from 9-20 June in the northern and southern rift zones of the Axial Seamount and in the hydrothermal fields CASM and ASHES on the Juan de Fuca Ridge. This activity was followed from 22-25 June by a detailed sampling program of the second accretionary ridge off Oregon, where during leg SO109-1 new vents and an extraordinarily strong methane anomaly in the water column had been observed. Eventually during the third leg, SO109-3, the ROPOS system became available and was successfully deployed on the Juan de Fuca Ridge. This leg started from Astoria on 27 June and ended on 8 July in Victoria, a few days shorter than originally planned because the new winch had been completed in the meantime and was to be put aboard ship for the following cruise SO-RO (SO110). The ROPOS deployment at the second accretionary ridge off Oregon, which had been cut short during SO109-3, was successfully completed at the beginning of cruise SO110.

This cruise report, however, details only the activity of SO109 and is structured according to the three legs SO109-1, SO109-2 and SO109-3 which were divided for logistic, technical and scientific reasons as explained above. Each of the three legs is represented by a separate self-contained report not only because the objectives and methods used were different for each leg but also because the participating groups provided a different expertise and addressed correspondingly different partial objectives. Nevertheless, the report should be regarded as a single unit since later groups built their work on the results of former ones and also because the partial objectives all contributed a single overall objective to trace the vent fluids away from their respective sources. The common objectives and the general tectonic framework of each of the targeted areas Axial Seamount and second accretionary ridge are detailed in the introductory chapter.

This cruise report should also be seen in conjunction with that of SO110. Both projects represent a landmark in German marine geoscience research. For the first time the unmanned deep-sea diving system ROPOS was deployed in a joint effort with Canadian and US groups and as part of a research program which was exclusively driven by scientific objectives. During both cruises technical problems with the new fiber optic deep-sea cable developed which had to be overcome at the expense of a considerable loss of deployment time of the ROV-system. Nevertheless, significant scientific and technical success was achieved. The highlights of this success are the quality of documentation of vent processes not previously achieved, the documentation of phase separation observed by boiling fluids at the Axial Seamount, the mapping of cold vents off Alaska, as well as new insights into the specialized ecosystems of cold seep communities. This could not have been achieved by conventionally towed systems. Accurate sampling, especially of vent fluids and sulfide chimneys in the area of the phase separation, provided unique sample material which when fully analyzed and evaluated will provide new and basic knowledge about vent processes. The technology success of the ROPOS system is two-fold: reaching a record diving-depth of 4.960 m with all systems operating and accomplishing the longest continuous deployment of the system of almost 30 hours. This demonstrates the greater economic viability and superiority of an unmanned diving system compared to manned submersibles. For the German marine research community it could thus be shown convincingly that the RV SONNE with her superior equipment and experienced crew can proficiently handle such ROV deployments. The unanimous opinion of all participating national and international groups was that a leading role in marine research has been achieved through the ROPOS deployments during projects SO109 and SO110. This success was only possible through the cooperation of numerous scientific and administrative departments of reviewing, funding, and scheduling agencies, and their intention and good will to see this project through in spite of setbacks.

The project HYDROTRACE was planned, coordinated, and carried out by the Technische Universität Bergakademie Freiberg and the GEOMAR Research Center for Marine Geosciences and the project SO-RO by the GEOMAR Research Center and Rutgers University. Both projects were financed by the Bundesministerium für Bildung, Wissenschaft, Forschung und Technologie, Bonn (Project Nos. 03G0109 and 03G0110) as part of their deep-sea research initiative. Project review and administration was handled proficiently by BEO Warnemünde. On behalf of all participants we wish to thank these departments and their staff for their support and flexibility in overcoming problems and to eventually succeed in “getting the ROPOS system on the bottom“. Additional financial support was also provided by the Canadian side through the National Science and Engineering Council (NSERC) and the US side through the National Science Foundation (NSF). The Reedereigemeinschaft Forschungsschiffahrt (RF) also provided extra funds for technical requirements to accommodate the ROPOS system on board RV SONNE. We would like to especially acknowledge the vessel's master Henning Papenhagen and his crew for their highly professional conduct, their continued flexibility, patience and their contribution to provide an extraordinary pleasant working atmosphere during both cruises. The ROPOS system was originally developed through funds from the Canadian government and is currently available for research through charter by the Canadian Scientific Submersible Facility (CSSF) in Montreal/Toronto. Finally, the success would not have been achieved without the enormous commitment and expertise of the ROPOS team, their enthusiasm and cooperation to work with the crew of the RV SONNE and the science groups.

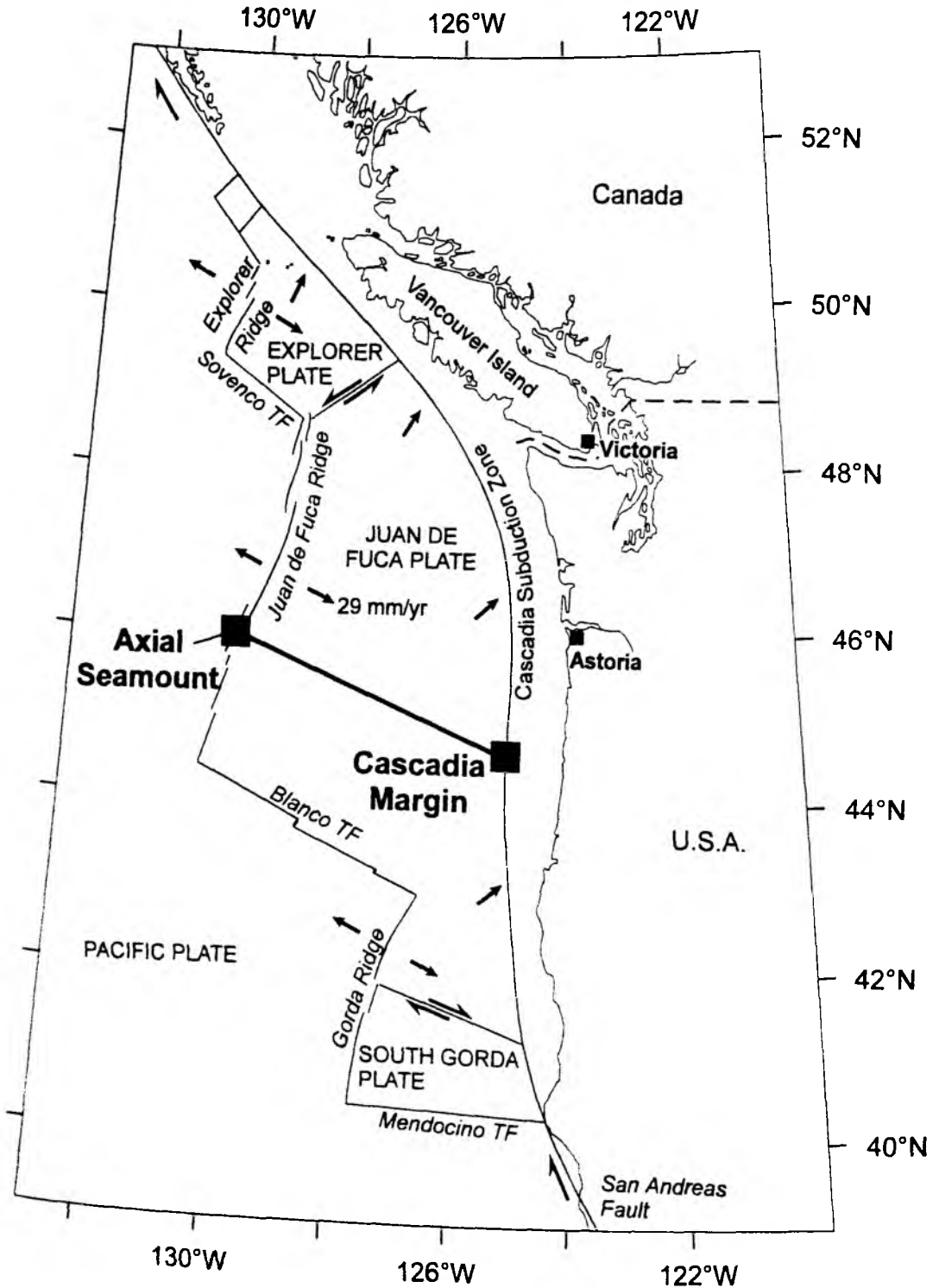


Fig. 1 Übersichtskarte mit dem generellen tektonischen Regime des Nordost-Pazifiks. Dargestellt sind die durch ein Transekt verbundenen zentralen Arbeitsgebiete am Axial Seamount und an der Cascadia Subduktionszone.
Overview of the tectonic regime of NE Pacific. The transect depicts the main working areas at Axial Seamount and the Cascadia Subduction Zone.

Vorwort

Erwin Suess und Peter Herzig

Das übergeordnete Ziel der Bearbeitung von submarinen Quellen, sowohl an Riftzonen als auch an Subduktionszonen, ist die Untersuchung ihrer Bedeutung für den marinen Stoffhaushalt. Hierzu ist u. a. zu klären, welcher Art die Verteilungsmuster sind. Insbesondere ist von Interesse, wie weit der Einfluß der austretenden Fluide mit gelösten Tracern und den enthaltenen Partikel von der unmittelbaren Quelle aus in die Wassersäule einerseits und die Sedimente andererseits verfolgt und ihre Verteilung bestimmt werden kann. Diese Fragen wurden in einem multidisziplinären Ansatz mit kanadischer und amerikanischer Beteiligung entlang der divergierenden Plattengrenze im Gebiet des Axial Seamount (Juan de Fuca Ridge) und der konvergierenden Plattengrenze im Gebiet der Cascadia Subduktionszone (Oregon Margin) bearbeitet (Abb. 1).

Da die Tracer-Signale mit zunehmender Entfernung von den Quellen in einer nicht linearen Weise abnehmen, lief die Untersuchungsstrategie darauf hinaus, eine detaillierte und hochauflösende Bearbeitung jeweils im proximalen Bereich der Fluid-Quellen, unter Einsatz des unbemannten Unterwasserfahrzeuges ROPOS zu beginnen, um dann mit herkömmlichen Methoden der Vermessung und der Probenahme das überregionale Profil zu vervollständigen. Dazu wurde die Expedition HYDROTRACE SO109 in drei Fahrtabschnitte aufgeteilt. Hierbei wurde auf dem Abschnitt SO109-1 zunächst eine großräumige Vermessung und Beprobung des Axial Seamount und der Akkretionsrücken vor Oregon ohne das ROPOS-System vorgenommen. Dazu verließ FS SONNE am 23.05.1996 den Hafen von Astoria, arbeitete vom 25.05. - 29.05. an der östlichen Flanke des Juan de Fuca Rückens und vom 30.05. - 03.06. am Kontinentalrand vor Oregon. Am 04.06. ging dieser erste Fahrtabschnitt in Victoria zu Ende.

Der zweite Fahrtabschnitt SO109-2 begann am 08.06. in Victoria, allerdings ohne ein einsatzfähiges ROPOS System an Bord, da technische Gründe die Fertigstellung der Windentrommel zur Aufnahme des neuen 5000 m Glasfaserkabels verzögerten. Statt dessen wurde vom 09.06. bis zum 20.06. ein intensives Beprobungsprogramm, das ursprünglich alternierend mit den ROPOS-Einsätzen vorgesehen war, in der nördlichen und südlichen Riftzone und den Hydrothermalfeldern CASM und ASHES des Axial Seamount durchgeführt. Danach erfolgte vom 22.06.- 25.06. eine detaillierte Bearbeitung des zweiten Akkretionsrückens vor Oregon: Hier waren während des ersten Fahrtabschnittes neue Vents und eine außerordentlich starke Methananomalie in der Wassersäule festgestellt worden. In beiden Gebieten wurden durch die erneute Detailbearbeitung die genauen Einsatzziele für ROPOS festgelegt. Das ROV-System, inzwischen mit dem alten, aber kürzeren Kabel

funktionstüchtig gemacht, wurde dann erfolgreich auf dem dritten Fahrtabschnitt (SO109-3), der am 27.06. in Astoria begann, eingesetzt. Dieser Fahrtabschnitt war kürzer als geplant und endete am 08.07., weil inzwischen die Fertigstellung der neuen Kabeltrommel zur Aufnahme des 5000 m Glasfaserkabels soweit gediehen war, daß eine Übernahme für die folgende Reise SO110 bevorstand. Die Untersuchung des zweiten Akkretionsrückens vor Oregon durch ROPOS, für die während der Reise SO109 nunmehr keine Arbeitstage mehr zur Verfügung standen, wurde zu Beginn der folgenden Reise SO110 nachgeholt.

Entsprechend dieser, aus logistischen, technischen und wissenschaftlichen Gründen erfolgten Aufteilung der Reise SO109, ist auch dieser Fahrtbericht angelegt. Jeder der drei Abschnitte wird als eigenständiger Bericht dargestellt, da nicht nur die Ziele und Geräteeinsätze unterschiedlich waren, sondern die beteiligten Arbeitsgruppen auch größtenteils unterschiedliche Expertisen besaßen und entsprechend unterschiedliche Teilziele verfolgten. Dennoch ist dieser Bericht als Einheit zu betrachten, da die jeweils folgenden Gruppen auf den Ergebnissen der vorhergehenden aufbauen konnten und das übergeordnete Ziel stets die unterschiedlichen Teilziele miteinander verband. Diese Gemeinsamkeiten wie die Grundzüge der Tektonik der beiden Zielgebiete Axial Seamount und Second Accretionary Ridge sind in dem einleitenden Kapitel dargestellt.

Zusammen mit der nachfolgenden Reise SO110 stellen diese beiden Expeditionen einen Meilenstein in der deutschen Meeresforschung dar. Zum ersten Mal war es möglich, in internationaler Kooperation und in einem ausschließlich durch wissenschaftliche Fragestellungen bestimmten Forschungsprogramm, ein unbemanntes Tieftauchsystem (ROV) vom Forschungsschiff SONNE aus einzusetzen. Auf beiden Fahrten, SO109 und SO110, mußten technische Probleme mit dem Tiefseekabel behoben werden, die zu nicht unerheblichen Einbußen der tatsächlichen Einsatzzeit des Systems am Meeresboden führten. Trotzdem stehen am Ende beachtliche Erfolge. Der wissenschaftliche Erfolg besteht in der unvergleichlich besseren Dokumentation der Prozesse im Bereich der heißen und den kalten Quellen und der hochspezialisierten Ökosysteme und ihrer Funktionsweise, als dies mit herkömmlichen, geschleppten Systemen möglich war. Ebenso gelang durch die gezielte Probennahme, besonders der Ventfluide und der Sulfidschlote aus dem heißen Bereich der Phasentrennung, eine Sammlung einmaligen Materials, dessen Auswertung eine nachhaltige wissenschaftliche Bedeutung haben wird.

Der technische Erfolg besteht zum einen in dem Erreichen einer Rekordtauchtiefe des ROPOS Systems von 4.960 m (auf Reise SO110), bei dem alle Systeme einwandfrei funktionierten, zum anderen im Rekord des Dauereinsatzes von fast 30 Stunden, der die Überlegenheit und die größere Wirtschaftlichkeit des unbemannten Tieftauchsystems gegenüber

bemannten Tauchbooten dokumentiert. Für die deutsche Meeresforschung schließlich konnte überzeugend gezeigt werden, daß das FS SONNE mit seiner exzellenten Ausstattung und der wertvollen Erfahrung der Besatzung solche Einsätze technisch hervorragend bewältigen kann. Aus dem übereinstimmenden Urteil aller beteiligten nationalen und internationalen Arbeitsgruppen geht hervor, daß mit diesen ROPOS-Einsätzen während der Reisen SO109 und SO110 enorme Fortschritte erzielt wurde, die es nun auszubauen gilt.

Dieser Erfolg ist in erster Linie der Zusammenarbeit zahlreicher Stellen in Wissenschaft und Verwaltung zu verdanken und dem Willen, dieses Projekt zu realisieren. HYDROTRACE (SO109) wurde gemeinsam von der Technischen Universität Bergakademie Freiberg und dem Forschungszentrum GEOMAR, das Vorhaben SO-RO (SO110) vom Forschungszentrum GEOMAR konzipiert, koordiniert und durchgeführt. Die Finanzierung der Projekte erfolgte durch das Bundesministerium für Bildung, Wissenschaft, Forschung und Technologie, Bonn (Projektnummern 03G0109 und 03G0110) im Rahmen des Schwerpunktes Tiefseeforschung. Die Projektbegleitung erfolgte durch BEO Warnemünde. Für die Unterstützung, Abwicklung und die Flexibilität bei der Überwindung der technischen Probleme bedanken wir uns im Namen aller Beteiligten ganz besonders bei diesen Stellen und ihren Mitarbeiterinnen und Mitarbeitern. Finanzielle Unterstützung wurde den Projekten auch zuteil von kanadischer Seite durch das National Science and Engineering Council (NSERC) und von amerikanischer Seite durch die National Science Foundation (NSF). Ebenso leistete die Reedereigemeinschaft Forschungsschiffahrt (RF) materielle Unterstützung bei der Schaffung der technischen Voraussetzungen zur Aufnahme des ROPOS System an Bord des FS SONNE. An dieser Stelle danken wir der RF und ganz besonders Herrn Kapitän Henning Papenhagen und seiner Besatzung für den besonders engagierten und professionellen Einsatz sowie ihren Beitrag zur überaus angenehmen Arbeitsatmosphäre im Verlauf der beiden Reisen.

Das ROPOS System wurde ursprünglich mit Mitteln der kanadischen Regierung entwickelt und wird zur Zeit über die Canadian Scientific Submersible Facility (CSSF) in Montreal/Toronto gegen kommerzielle Charter der Forschung zur Verfügung gestellt. Ohne den enormen Einsatz des ROPOS-Teams, seinem Enthusiasmus und die Bereitschaft zur Zusammenarbeit mit der Besatzung des FS SONNE und den Wissenschaftlergruppen wäre dieser Erfolg nicht möglich gewesen.

1. Cruise Participants and Schedule

1.1 Scientists

1.1.1 Leg SO109-1 23 May - 5 June, Astoria/Oregon - Victoria/Canada

Bayer, Reinhold	Universität Heidelberg
Biebow, Nicole	GEOMAR Forschungszentrum, Kiel
Bleyer, Anke	GEOMAR Technologie GmbH, Kiel
Chin, Carol	Oregon State University, Corvallis
Collier, Robert	Oregon State University, Corvallis
Domeyer, Bettina	GEOMAR Forschungszentrum, Kiel
Elderfeld, Harry	University of Cambridge
Elvert, Marcus	GEOMAR Forschungszentrum, Kiel
Finke, Mark	TU Bergakademie Freiberg
Greinert, Jens	GEOMAR Forschungszentrum, Kiel
Jones, Nicola	University of Victoria
Kinsey, Susan	GEOMAR Forschungszentrum, Kiel
Klinkhammer, Gary	Oregon State University, Corvallis
Kunze, Rüdiger	GEOMAR Forschungszentrum, Kiel
Lammers, Stephan	GEOMAR Forschungszentrum, Kiel
Petersen, Asmus	GEOMAR Technologie GmbH, Kiel
Preißler, Heike	TU Bergakademie Freiberg
Rickert, Dirk	GEOMAR Forschungszentrum, Kiel
Schäfer, Markus	TU Bergakademie Freiberg
Schumann, Marcus	GEOMAR Forschungszentrum, Kiel
Schwarz, Ulrich	TU Bergakademie Freiberg
Soffregen, Paul	Oregon State University, Corvallis
Suess, Erwin	GEOMAR Forschungszentrum, Kiel,
	Chief Scientist
Uhlig, Stefan	TU Bergakademie Freiberg
Whiticar, Michael	University of Victoria

1.1.2 Leg SO109-2 6 - 25 June, Victoria/Canada - Astoria/Oregon

Bayer, Reinhold	Universität Heidelberg
Becker, Klaus-Peter	TU Bergakademie Freiberg
Bleyer, Anke	GEOMAR Technologie GmbH, Kiel
Chadwick, Bill	NOAA-PMEL, Newport
Embley, Robert	NOAA-PMEL, Newport, co-Chief Scientist
Hannington, Mark	Geological Survey of Canada, Ottawa
Herzig, Peter	TU Bergakademie Freiberg,
	Chief Scientist
Jonasson, Ian	Geological Survey of Canada, Ottawa
Lammers, Stephan	GEOMAR Forschungszentrum, Kiel
Linke, Peter	GEOMAR Forschungszentrum, Kiel
Massoth, Gary	NOAA-PMEL, Seattle
Masurenko, Christian	TU Bergakademie Freiberg
Perfit, Mike	University of Florida, Gainesville
Petersen, Sven	TU Bergakademie Freiberg
Summit, Melanie	University of Washington, Seattle
Tamburn, Keith	DTEC, Anmore
Tunnicliffe, Verena	University of Victoria

1.1.3 Leg SO109-3 26 June - 8 July, Astoria/Oregon - Victoria/Canada

Appel, Frank
Banfield, Robert
Barker, Dan
Bleyer, Anke
Buchholz, Peter
Butterfield, Dave
Chadwick, Bill
Cremer, Axel
Dählmann, Anke
Holland, Robert
Illmann, James
Junniper, Kim
Kuhn, Thomas
Linke, Peter

Meinig, Chris
Mirbach, Nikolaus von
Nakamura, Ko-ichi
Sahling, Heiko
Seifert, Thomas
Shepherd, Keith
Stalin, Scott
Summit, Melanie
Tamburri, Keith
Tunnicliffe, Verena
Winckler, Gisela

GEOMAR Technologie GmbH, Kiel
Canadian Scientific Submersible Facility
Canadian Scientific Submersible Facility
GEOMAR Technologie GmbH, Kiel
TU Bergakademie Freiberg
NOAA-PMEL, Seattle
NOAA-PMEL, Newport
BioLab
GEOMAR Forschungszentrum, Kiel
University of Victoria
SEA, Seattle
GEOTOP, Montreal
FU Berlin
**GEOMAR Forschungszentrum, Kiel,
Chief Scientist**
NOAA-PMEL, Seattle
GEOMAR Forschungszentrum, Kiel
Geological Survey of Japan, Higashi
GEOMAR Forschungszentrum, Kiel
TU Bergakademie Freiberg
Canadian Scientific Submersible Facility
NOAA-PMEL, Seattle
University of Washington, Seattle
DTEC, Anmore
University of Victoria
Universität Heidelberg

1.2 Participating Institutions

College of Ocean and Atmospheric Sciences Oregon State University Corvallis, OR 97331-4501 USA	DTEC Ltd. 127 Hemlock Drive Anmore, BC V3H4W9 Canada
FU Berlin Fachbereich Geowissenschaften, Rohstoff- und Umweltgeologie Malteserstr. 74-100 D-12249 Berlin Germany	Geological Survey of Canada 601 Booth Street Ottawa, Ontario K1A 0E8 Canada
Geological Survey of Japan 1-1-3 Higashi Tsukuba, Ibaraki 305 Japan	GEOMAR Forschungszentrum für marine Geowissenschaften Wischhofstr. 8 D-24148 Kiel Germany
GEOMAR Technologie GmbH Wischhofstr. 1-3 D-24148 Kiel Germany	GEOTOP Université du Québec à Montréal Case Postale 8888, succursale Centre-ville Montréal (Québec) H3C 3P8 Canada

Institut für Umweltphysik Universität Heidelberg Im Neuenheimer Feld 366 D-69120 Heidelberg Germany	NOAA-PMEL 2115 SE Oregon State Univ. Drive Newport, OR 97365-5258 USA
NOAA-PMEL 7600 Sand Point Way NE Seattle WA 95073 USA	Software Engineering Associates PO Box 25496 Seattle, WA 98125 USA
TU Bergakademie Freiberg Institut für Mineralogie Lehrstuhl für Lagerstättenlehre Brennhausgasse 14 D-09596 Freiberg Germany	University of Cambridge, Department of Earth Sciences Downing Street Cambridge CB2 3EQ United Kingdom
University of Florida Department of Geology Gainesville FL 32611 USA	University of Victoria Biology Department P.O. Box 1700 Victoria B.C. V8W 2Y2 Canada
University of Victoria Centre for Earth and Ocean Research P.O. Box 1700 Victoria, B.C. V8N 1Y2 Canada	University of Washington College of Oceanography Box 357940 Seattle WA 98195 USA

1.3 Ship's crew

Angermann, Rudolf
Behnisch, Holm
Bekaan, Steffen
Bethge, Hans
Duthel, Rainer
Gebhardt, Volkmar
Grund, Helmut
Hartwig, Karl-Heinz
Hentschel, Rainer
Hoffmann, Wolf-Hilmar
Kaiser, Reiner
Kiefer, Josef
Korte, Detlef
Krause, Nils
Ladewich, Norbert
Liebe, Thomas
Lindemann, Erhard
Martin, Andreas
Melsbach, Herbert
Müller, Werner
Naeve, Ingo
Papenhagen, Henning
Rossa, Georg
Sandersfeld, Uwe
Schlosser, Thomas
Schramme, Heinrich
Schrapel, Andreas
Slotta, Werner
Stängl, Günter
Stenzler, Joachim
Sturm, Wolfgang
Teske, Roland

Electronics Engineer
Able Seaman
Electrical Engineer
Motor-Man
Electronics Engineer
System Manager
Second Engineer
Boatswain
Second Cook
Electronics Engineer
Able Seaman
Motor-Man
First Mate
System Manager
First Mate
System Manager
Able Seaman
Chief Engineer
Able Seaman
Second Steward
Doctor
Master
Fitter
Second Engineer
Second Engineer
Second Steward
Able Seaman
Chief Steward
Able Seaman
Fitter
Radio Operator
Motor-Man

1.4 Summary of Activities of Participating Institutions

Freiberg University (Project Coordination)

A Hydrosweep survey of the volcano was completed to complement Seabeam mapping at Axial Volcano by NOAA. NOAA has repeatedly mapped the central Juan de Fuca on a 5-year cycle as a means of detecting major changes in bathymetry associated with new volcanic features. The most recent Seabeam survey was completed in 1991. Hydrosweep data collected during SO109-1, -2, and -3 will permit a detailed study of the bathymetry of the neo-volcanic zone and provide a new baseline for further studies of the volcanic and tectonic evolution of the volcano. The Hydrosweep surveys of the volcano will be prepared as a two map series (1:75,000 scale and 1:25,000 scale) for joint publication by the participants as a GSC Open File Report. Freiberg University and the Geological Survey of Canada will also conduct detailed studies of mineralization on Axial Volcano as part of an ongoing joint project on hydrothermal systems operating on shallow portions of the mid-ocean ridges. Axial Volcano is an important end-member in this study, owing to the relatively shallow depths of the caldera floor (ca. 1500 m). The pressure at the seafloor within the caldera is at the upper limit of conditions at which typical black smoker fluids start to boil. Samples of fluids from boiling vents allow to study the effects of high-temperature boiling on the distribution of gold, silver, and other major and trace elements. The partitioning of elements between the condensed vapour phase and residual liquids needs to be determined in the end-member fluids in order to compare the results with the concentration of those elements in the chimney substrates.

GEOMAR Kiel

EXPLOS surveys of the caldera and the North and South Rift Zones were used extensively to target transponder navigated CTD-casts in areas of both focussed and diffuse venting. A total of 18 CTD stations were run at locations inside and outside the caldera. Methane and nutrient analyses of water samples, done onboard, delineated the plume structure and spreading pattern. Sediments were cored from bathymetric basins around Axial Volcano as well as along a 150 km long transect from the Cascadia Basin to the flank of the Juan de Fuca Ridge. The purpose of the sediment sampling program was to detect episodes and the history of hydrothermal input from the ridge. Several intensive survey and sampling programs were carried out at the Cascadia Margin, with emphasis on the Second Accretionary Ridge. The programs included detailed bathymetric mapping with HYDROSWEET, CTD-casts, EXPLOS-surveys and sampling with the giant TV-grab. Shipboard analyses of methane in water samples documented extensive degassing of the Second Accretionary Ridge. Sampling of those areas with the TV-grab recovered carbonate-cemented sediments and fauna specific to cold seeps. Assemblages were kept alive for

experiments performed during the cruise onboard RV Sonne. Pore water extraction was done on all sediment cores, the short near-surface boxcores as well as the long kasten cores. The analyses performed on board (SiO_2 ; NH_4 , PO_4 , Alk; NO_3 ; ΣCO_2 , H_2S , Cl) provided evidence for active fluid discharge through sediments as the presence of gashydrates.

Gas hydrate sampling and preservation was a major successful task carried out at the Second Accretionary Ridge during SO109-1 and SO109-2; as was the collection and preservation of sediments and biota for biomarker studies. Of particular interest were samples from methane-dominated systems in order to determine biomarkers for methylophic activities.

University of Heidelberg

CTD-casts were carried out by R. Bayer and G. Winckler jointly with GEOMAR personnel on all legs of SO109. The main purpose was the collection of vent and ambient water samples for He-isotope analyses and other noble gases. G. Winckler showed previously that the cold vent fluids from the accretionary margin are highly enriched in ^4He from U-decay in content-derived accreted sediments. This contrasts sharply with the ^3He -enrichment in hydrothermal fluids from the spreading ridge. Hence, He-isotopic studies combined with total He and noble gas contents provide one of the most promising tracers in the water column for differentiation between volatile input from the ridge crest and the accreted margin. The anticipated He-signals would be correlated with all other anomalies (i. e. manganese, methane, temperature, turbidity, silice) as derived from the samples of the hydrocasts and CTD-recordings.

Geological Survey of Canada

The GSC (M. Hannington and I. Jonasson) continued its 12-year long investigation of the mineralogy and geochemistry of sulfide-sulfate-silica deposits in the three main vent fields of Axial Volcano, including both high-temperature vents and lower-temperature (baritic) peripheral zones to these fields. Samples of hydrothermal precipitates from the vents were taken to complement the water chemistry studies by NOAA (see Freiberg University). The GSC will also analyze basalt samples in collaboration with M. Perfit (U. Florida), who has been studying the petrogenesis of new lava flows at Axial Volcano since 1986.

NOAA Newport and Seattle

NOAA has been at the forefront of research on the impact of submarine volcanic eruptions and related hydrothermal activity on the chemistry of the oceans, and the long-term scientific objectives of the NOAA Vents Program closely parallel those of HYDROTRACE. NOAA has conducted long-term monitoring of the discharge of hot water from active vent sites along

the Juan de Fuca, and particularly at Axial Volcano. Major surface ship and submersible surveys of the caldera of Axial Volcano since 1984 have monitored the recent volcanic activity at the summit of the volcano and the distribution of plumes in the overlying water column (during SO109, the NOAA ship DISCOVERER was conducting concurrent plume surveys at Axial Volcano: E. Baker, Chief Scientist). NOAA's interests are focussed on the heat and metal output that are associated with volcanic eruptions and related dike intrusions and particularly the giant plumes of warm water that commonly develop as a result of the eruptions (megaplumes).

The NOAA team consisted of Bob Embley (Co-Chief Scientist), Bill Chadwick, and Gary Massoth. They contributed both scientific and technical resources to the SO109-2 cruise.

A long baseline transponder navigation system SeaScape (acquired for use with ROPOS in 1992) was used for navigation of the EXPLOS system and CTD surveys in the caldera, the North Rift Zone, South Rift Zone, and CoAxial Segment. The same system will be used for precise tracking of ROPOS and its cage during SO109-3. Ship positioning was achieved through an interface with the SeaScape navigation system.

A comprehensive database of all previous data from Axial Volcano was made available during the SO109-2 cruise through NOAA's ARCView GIS system. The database allows rapid retrieval and plotting of geological, geochemical, geophysical, biological, and other data and was first used extensively on the recent ALVIN/AlI dive series at CoAxial in July, 1995.

Extensive mapping by side scan sonar, towed camera, and submersible operations by NOAA in the 1980s was used as a baseline for studies of the volcanology of the Axial caldera. During SO109-2, the NOAA-GSC-Freiberg-U. Victoria team conducted detailed studies of recent volcanic and tectonic activity in the North Rift Zone, South Rift Zone, ASHES Field, and CASM site to monitor changes in flow distribution and morphology since the last major eruptions thought to have occurred between 1986 and 1988. EXPLOS surveys of the North and South Rift Zones also provided the opportunity to search for surface manifestations of recent seismic events in these areas. The opportunity to document the evolution of diffuse venting along the rifts and map the very young volcanic fissure eruptions (probably less than one decade old) was a high priority during the cruise. Additional surveys of the CoAxial Segment were undertaken to monitor changes since the last major eruption at that site in 1993.

NOAA deployed a small array of acoustic extensometer instruments on Axial's North Rift Zone near the caldera, to better establish the relationship between ongoing T-phase events, volcanic activity, hydrothermal venting, and biological responses. These instruments measure the distances between benchmarks on the seafloor to within 1 cm, and so can be used to monitor surface deformation caused by dike intrusion along the rift zone. This

experiment will complement the vertical deformation monitoring already underway in Axial's caldera (Fox, 1990).

The NOAA-PMEL chemical scanner (SUAVE) was successfully deployed by G. Massoth on the EXPLOS camera system in the South Rift Zone, North Rift Zone, ASHES Field, and CoAxial Segment. G. Massoth, who designed and built the SUAVE chemical scanner, has surveyed both high-temperature and diffuse vent sites on the Juan de Fuca Ridge, but the SUAVE has not been used at Axial. The scanner was modified from its original configuration (to fit ROPOS) and mounted on the top of the EXPLOS frame. During SO109-2, the instrument was deployed as a prospecting tool to detect chemical signatures of the diffuse venting, which is now more abundant in the caldera, as well as in the high-temperature plumes. The scanner recorded ultra low-level concentrations of H_2S , Mn, Fe^{2+} , and Fe^{3+} associated with low-temperature vent and water column anomalies. It was also equipped with CTD and transmissometer for real-time plume detection. Chemical data was recorded in remote-mode and down-loaded following retrieval of the EXPLOS system. When mounted on the ROV, the scanner sends real-time chemical data up the fiber optic cable, and the possibility exists for similar communication between SUAVE and EXPLOS, which would greatly improve the utility of this configuration.

Oregon State University, Corvallis

The main contribution to the project HYDROTRACE by OSU-participation was the availability of the ZAPS-system. The Zero Angle Photo-Spectrometer, developed by G. Klinkhammer at OSU, is capable of continuously recording the concentration of dissolved manganese. This signal, combined with transmissometer, temperature, conductivity and density recordings is used to delineate plumes in the water column and resolve their fine structure. The system is complementary to the SUAVE chemical scanner (G. Massoth) but is better able to detect Mn near the ambient background concentration, although is unable to detect Fe. The mode of deployment of ZAPS, as simultaneously towed and yo-yoed, allows to follow a plume once detected for an extended period of time and over considerable distance. The hydrothermal plumes generated from the ASHES-field in the caldera of Axial Volcano could thus be tracked southward. ZAPS-deployment on the margin failed to detect a Mn-signal in the vent plumes but revealed considerable transmissometer anomalies. These could not always unambiguously be correlated with vent plumes because of regional turbidity maxima which peeled off the continental slope and extended seaward at mid-water depths. R. Collier provided and deployed a short current meter at the western flank of the Second Accretionary Ridge. The purpose was to monitor the bottom currents which affect the methane plume emanating from the summit. Repeated hydrocasts at the mooring site provided time-series measurements of methane concentrations. M. Torres was responsible for collecting water samples from plume casts, ROPOS- and VESP-deployments as well as biota for REE-

analyses and other trace elements. It was previously shown that Li and B and their isotopes may be used as tracers for cold vent fluids as well as Ba and Li in carbonate skeletons of vent biota. M. Torres will attempt to expand and supplement the list of tracers for fluid venting, particularly from cold seeps, by looking at REE-element patterns.

University of Cambridge

H. Elderfield pursued the utility of Sr-isotopes in pore waters for the degree of hydrothermal interaction between the oceanic basement and the overlying sediment cover. This approach is analogous to that based on the dissolved Mg-distribution in which the basement acts as a sink and hence the Mg-depth concentration profiles are directly related to the degree of alteration. Since the Sr-isotope signature between seawater and basaltic basement is very large and the precision at which differences can be measured is very high it is expected that the Sr-isotope pattern might provide even more information than the Mg-pattern does. Pore waters from a transect of sediment cores over basement of different ages and depths provided the data base for this work. Shipboard analyses of Mg and Ca showed significantly different concentration gradients with depths that the Sr-isotope work, to be done at the shore-based laboratory at Cambridge University, appears highly promising.

University of Victoria

Biology department

V. Tunnicliffe conducted detailed surveys of vent fauna in the Axial caldera, on the North Rift and South Rift Zones, and at the HDV site on the CoAxial Segment. An EXPLOS survey and TV-Grab at the HDV site provided a critical time-series for monitoring the evolution, extent and diversity of hydrothermal communities that appeared after the 1993 eruption. The opportunity to link biological, chemical, and mineralogical features of the vents to volcanic and tectonic activity is considered a key element of future work in the ecology of Axial Volcano.

University of Victoria

Centre for Earth and Ocean Research

M. Whiticar has a long-standing interest in the marine methane cycle and his laboratory is particularly well-equipped to measure low concentrations in seawater and carry out high precision mass spectrometry on C- and H-isotopes of methane. The work has included bacterial methane utilisation, characterization of vent methane, and work on hydrate gases from the Cascadia convergent margin. During SO109 splits of all methane samples stripped from plume waters were conserved for shore-based isotope analyses at University of Victoria. the ship-board set up to detect low concentrations of methane in sediments proved particularly useful during SO109-1 because apparent lateral fluid flow in sediment sequences

could be detected by positive methane anomalies. Finally, M. Whiticar assisted in the collection and preservation of sediment and biota from methane-dominated vent systems in order to determine biomarkers for methylothermic activity.

University of Florida

M. Perfit was responsible for investigating the petrologic and geochemical characteristics of the lavas that were recovered and interpreting the morphology of the eruptions. He will complete microprobe analyses of glasses and coexisting mineral phases, major and trace element analyses of glasses and whole-rocks, and radiogenic isotope measurements (Sr, Nd, Pb) of selected samples. Volatile analyses of glasses will be determined in collaboration with J. Dixon at the University of Miami. The overall objectives are to decipher the petrogenetic history and relationships of lavas from Axial Seamount and its related rift zones. The data will also be used to constrain the degree to which a "hotspot" component has affected the chemistry of Axial magmas. Samples recovered from the recent flow on the North Rift Zone will provide information regarding the spatial distribution of mantle sources in the Axial-CoAxial region.

University of Washington

M. Summit, working with J. Baross, undertook detailed studies of the microbiology in vent materials, including waters, with a focus on the presence of hyperthermophilic bacteria. Microbiological studies are fast becoming the most significant new development in the deep sea research, and the extensive diffuse venting at Axial makes this an ideal site for future work in this field.

2. Geologic Setting of the Vent Fields

2.1 Juan de Fuca Ridge

by Peter Herzig and Mark Hennington

2.1.1 Background

Axial Volcano dominates the magmatic/hydrothermal budget of the central portion of the Juan de Fuca Ridge (6 cm/yr spreading rate). The Volcano rises 700 m above the mean level of the ridge crest and is the most magmatically robust and seismically active site between the Blanco Fracture Zone and the Cobb offset (Fig. 2). The Volcano is a product of intense volcanic activity from the Cobb-Eikelberg hotspot and represents a large mass excess on the ridge. Older Volcanoes that formed on or near the ridge axis are now found along the Cobb-Eickelberg chain to the west. Several Volcanoes east of Axial also formed on the ridge axis, but ended up on the Juan de Fuca Plate, rather than the Pacific Plate (Johnson and Embley, 1990).

Axial Volcano was initially mapped in the late 1970s (Delaney et al., 1981) and in greater detail with Seabeam by NOAA in the early 1980s. Following the discovery of active hydrothermal vents in the northern portion of the caldera in 1983 (CASM, 1985), a concentrated mapping and sampling program was carried out (Johnson and Embley, 1990). Results of this work are summarized in a special issue of the *Journal of Geophysical Research* (Vol. 95, B8). Camera tows, and submersible dives have revealed extensive areas of fresh lava and diffuse venting within the summit caldera and along extensional zones to the north and south of the caldera (North and South Rift Zones: Fig. 3). The distinctive summit caldera has a rectilinear outline which is oblique to the main tectonic fabric in the area, and Embley et al. (1990) suggest that the orientation of the caldera walls may be a manifestation of overlapping spreading centers represented by the North and South Rift Zones. Seismic monitoring of the area since 1991 using the SOSUS array has shown that more than 90% of the on-axis events of the Central Juan de Fuca (excluding the recent CoAxial dike injection) originated from the vicinity of Axial Volcano, with several seismic swarms centered over the summit area. The high level of seismicity on or near Axial Volcano has been recognized since the 1960's (Hammond and Walker, 1992), and Axial Volcano is the only site on the Juan de Fuca Ridge that has been geophysically monitored for such a long period (e.g., C. Fox's pressure gauge and rumblometer). Axial Volcano also has the distinction of being the first seafloor site that was instrumented during a diking event. Manifestations of volcanic and tectonic activity were observed directly in 1988 with a pressure gauge, current meter, and time-lapse camera (Fox, 1990). The caldera is also floored by very recent lava flows, some of which are young enough to onlap actively venting hydrothermal deposits (Johnson and Embley, 1990).

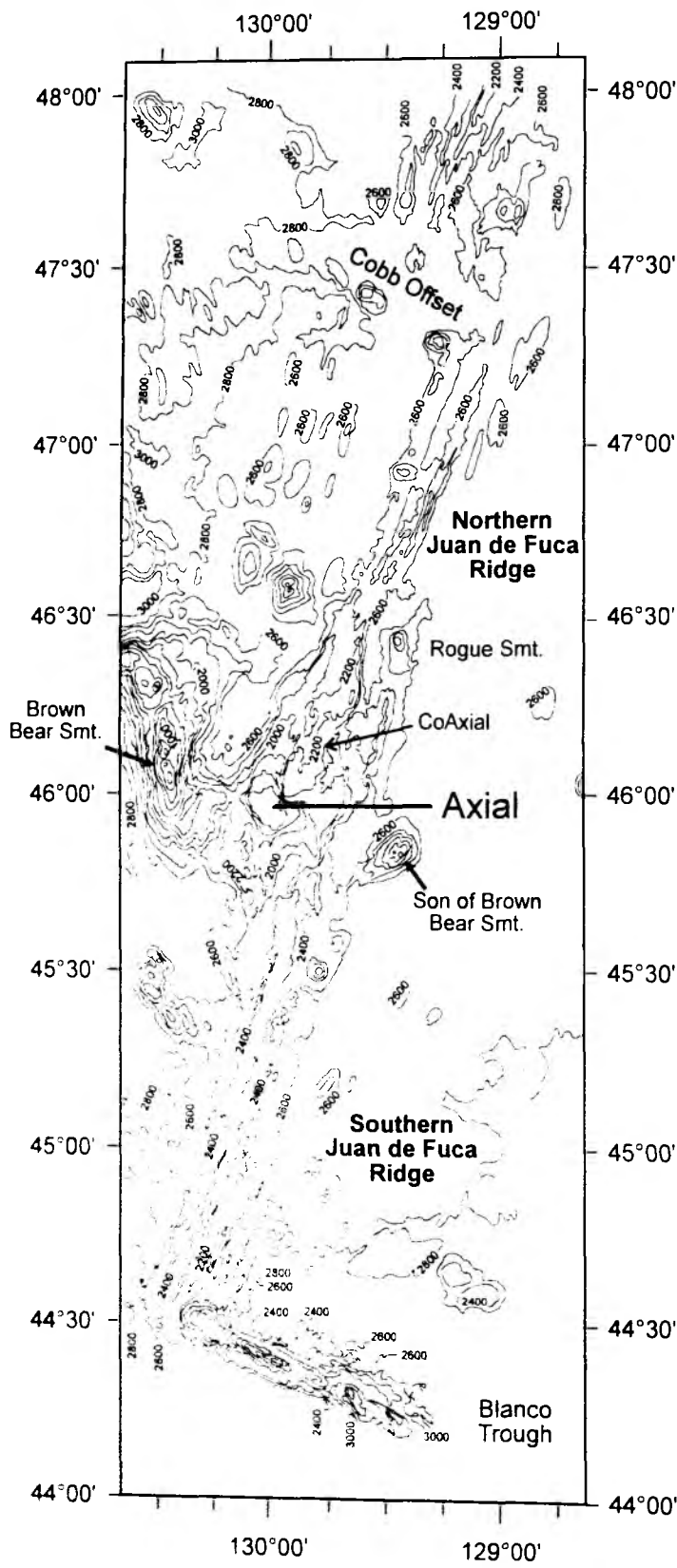


Fig. 2: Regional bathymetry of the Juan de Fuca Ridge showing the location of Axial Volcano, the CoAxial Segment, and adjacent seamounts (modified from Tivey & Johnson, 1990).

The summit caldera and adjacent rift zones are host to widespread diffuse hydrothermal flow and focussed venting in several locations. Hydrothermal venting and mineralization includes black and white smoker chimneys, and "snow-blower" vents charged with bacterial floc. Recent time-series measurements in the water-column also have revealed significant variability in light attenuation that may represent pulsing of the hydrothermal system. In addition, because of its shallow depth, the highest-temperature vents in the caldera are locally undergoing phase separation (Massoth et al., 1989; Butterfield et al., 1990). The influence of boiling on the hydrothermal fluids and their mineral precipitates is significant, and detailed studies of the active vents in the caldera have provided the first opportunity to study mineralizing processes in a deep-sea boiling hydrothermal system.

2.1.2 ASHES Vent Field

The ASHES Vent Field (Fig. 4) was discovered in 1985 by NOAA and investigated in detail in 1986 (NOAA-GSC-U. Victoria) when six high-temperature vents were mapped and sampled. The original group of investigators (which includes all of the Canadian/U.S. participants of SO109-2) studied the area with PISCES in 1983 and 1986, and with ALVIN in 1987, 1988 and most recently in 1995. B. Embley, W. Chadwick, and M. Perfit have studied the lavas in the vicinity of the vent field and have produced comprehensive maps of the entire caldera floor and walls. D. Butterfield has been analyzing hot vent waters and has developed an extensive time-series at ASHES. Hydrothermal precipitates have been studied by I. Jonasson, J. Franklin, and M. Hannington, with a focus on boiling vents and the nature of gold enrichment. V. Tunnicliffe has documented the vent biota.

An ALVIN dive in July 1995 at the ASHES Field revealed significant increases in the areal extent of venting, fluid fluxes, and temperature. One chimney had doubled in size since 1988. Also in that time, temperatures had increased by about 20°C on most of the high-temperature vents. A high of 348°C measured at Inferno vent is the exact temperature for subcritical phase separation (i.e., boiling) at 1,540 m water depth. Previously, these vents were at approximately 330°C and were boiling well below the seafloor. The most recent observations indicate that the boiling zone has ascended into the chimneys themselves, and video of at least one of the vents shows clear evidence of phase separation in a flame-like pattern where the vent fluids exit the chimney orifice.

A precise correlation between T-phase events and the recent increase in the heat output at ASHES has not been established, but one hypothesis is that the seismicity may represent small diking events and the release of strain caused by magma movement or deepening of fractures into the higher-temperature upflow zones of the hydrothermal system. The increase in temperatures and extent of hydrothermal activity in the ASHES Field could be a result of displacement of magma coupled with an increase in permeability caused by release of tectonic stress.

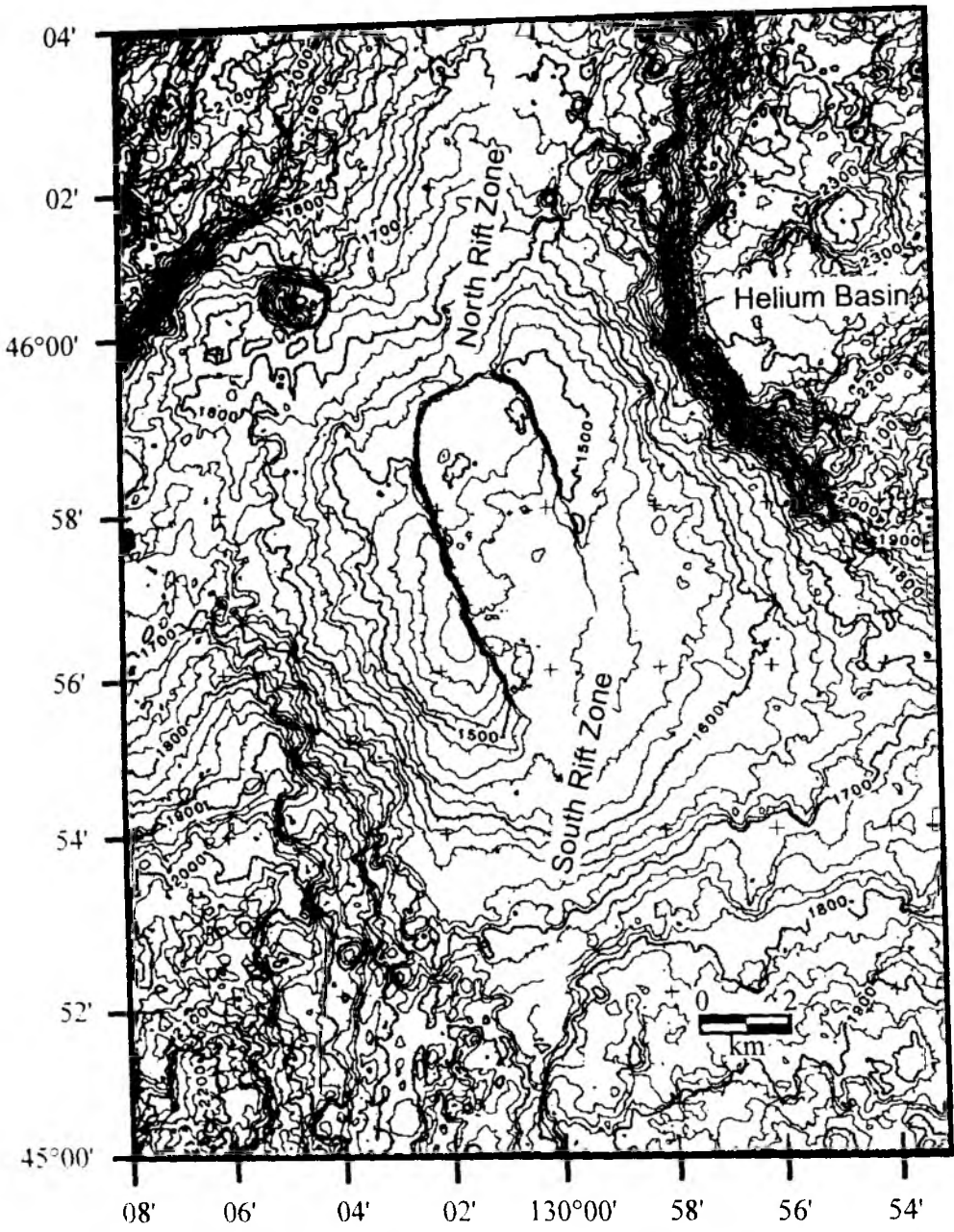


Fig. 3: Detailed bathymetry of Axial Volcano showing the location of the caldera wall, the North Rift Zone, the South Rift Zone and Helium Basin (25 m contour interval: from Embley et al., 1990).

2.1.3 CASM Site

The CASM Field (Fig. 4 and 5), at the northern end of the caldera, includes a number of warm-water vents occupying the main eruptive fissure, a large area of diffuse flow, and a small chimney complex to the east of the eruptive fissure. In 1983, this site was characterized by several large sphalerite-barite structures and low-temperature venting at a maximum temperature of about 30 °C. V. Tunnicliffe is the authority on the CASM Site, and this site was re-visited and sampled in 1988 by the NOAA-GSC-U. Victoria group (ALV2084).

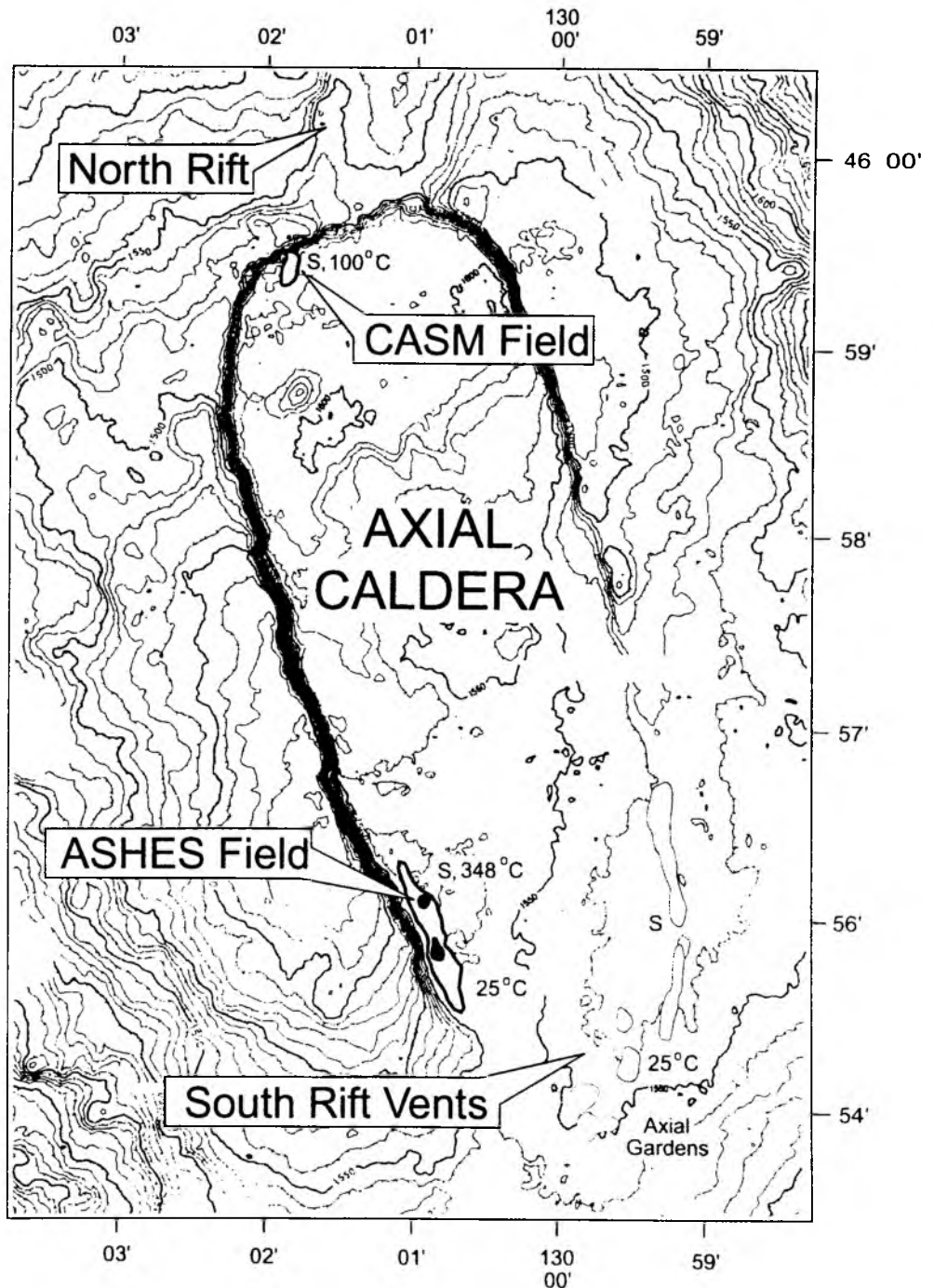


Fig 4: Detailed bathymetry of Axial caldera showing the location of the main vent fields (10 m contour interval: from Embley et al., 1990).

At that time, a barite-sphalerite chimney was venting water at 99 °C, suggesting reactivation of the site. However, the impact of the most recent hydrothermal and seismic activity in the caldera on vent fields at CASM was not established and was a principal target for investigation during SO109-2.

2.1.4 North Rift Zone

Extensive fissuring in a zone about 100-200 m wide extends for nearly 5 km north of the caldera rim (Fig. 3-5). The fissuring cuts the caldera wall and is continuous with the main fissure of the CASM Field. Recent camera tows in the North Rift Zone revealed fresh lava flows along much of its length, and these were investigated during SO109-2. Seismic events centered on the North Rift Zone were recorded as recently as May 1996, by shore-based NOAA investigators using the SOSUS array. These observations suggested that the North Rift Zone was active at the time of deployment of the ROV and EXPLOS camera system.

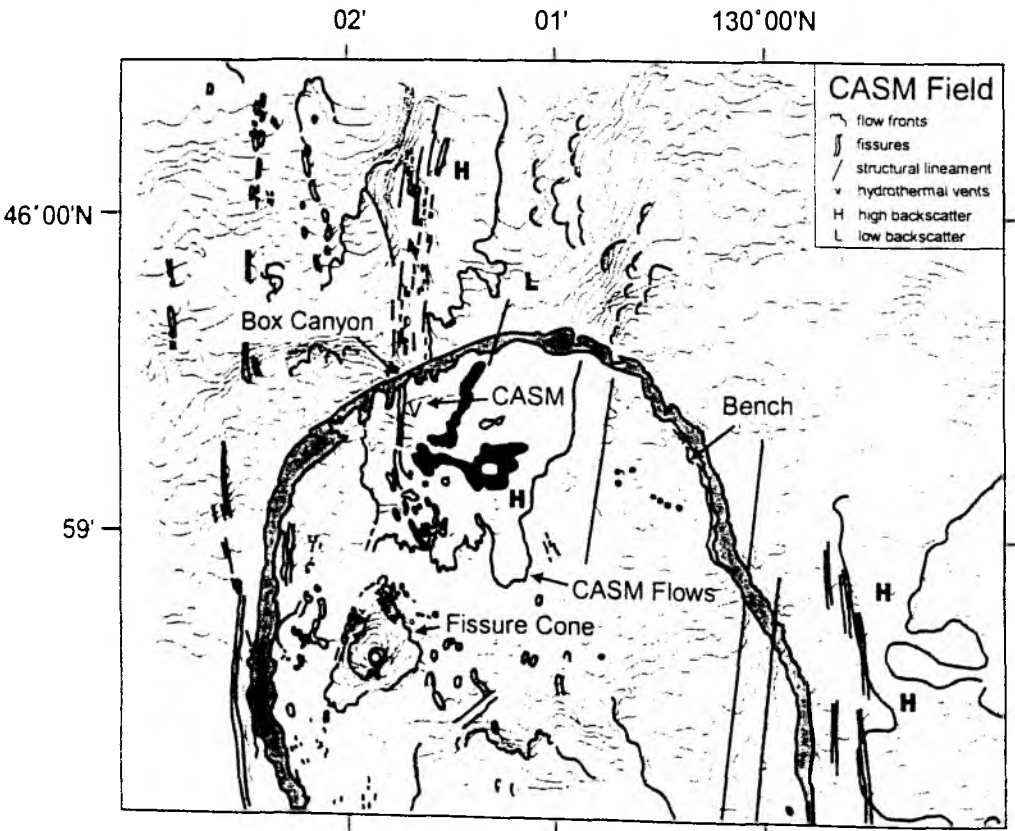


Fig. 5: Detailed bathymetry and geology of the north end of the Axial caldera in the vicinity of the CASM Field (5 m contour interval). Lava fronts are interpreted from acoustic backscatter; black areas represent areas of low backscatter (lava pond or lake). Modified from Embley et al. (1990).

2.1.5 South Rift Zone

The South Rift Zone (Fig. 3 and 4) is a series of en echelon fissures beginning at the southeastern rim of the caldera and extending down the south flank of the volcano. Embley et al. (1990) have shown that most of the recent post-caldera volcanism at Axial is associated with the South Rift Zone. Extension along the rift is accommodated by ridge-parallel faults and these are the likely sources for recent lava flows in this region. The eruption of a very large lava field east of the South Rift Zone may have contributed to the collapse of the summit crater (Applegate, 1990).

The distribution of low-temperature vents at the northern end of the South Rift (e.g., Axial Gardens) appears to delineate the southern margin of the caldera where it has been buried by lavas flows. CTD tow-yos over the upper South Rift Zone in July, 1994 (in response to an intense T-wave swarm in the area) measured a high attenuation value relative to signals recorded from that location in 1986. This site, because of its possible links with activity at the summit caldera, was investigated extensively during SO109-2. Seismic events were also recorded in the South Rift Zone during SO109-2 and suggest that the South Rift was also active during deployment of the ROV and EXPLOS camera system.

2.1.6 CoAxial Site

Between June 26 and July 10, 1993, prolonged seismic events along the CoAxial Segment (Fig. 6 and 2), north of Axial Volcano, were recorded by NOAA, indicating a major dike injection over a 40 km long strike-length of the ridge crest. Surveys of the area using ROPOS discovered new lava flows at the northern end of the dike swarm and discontinuous venting of low-temperature fluids (including bacteria) over a 22 km segment. This site was also examined during SO109-2, providing an important opportunity to examine the rapidly evolving nature of hydrothermal systems associated with short-lived crustal accretion events along the Central Juan de Fuca Ridge.

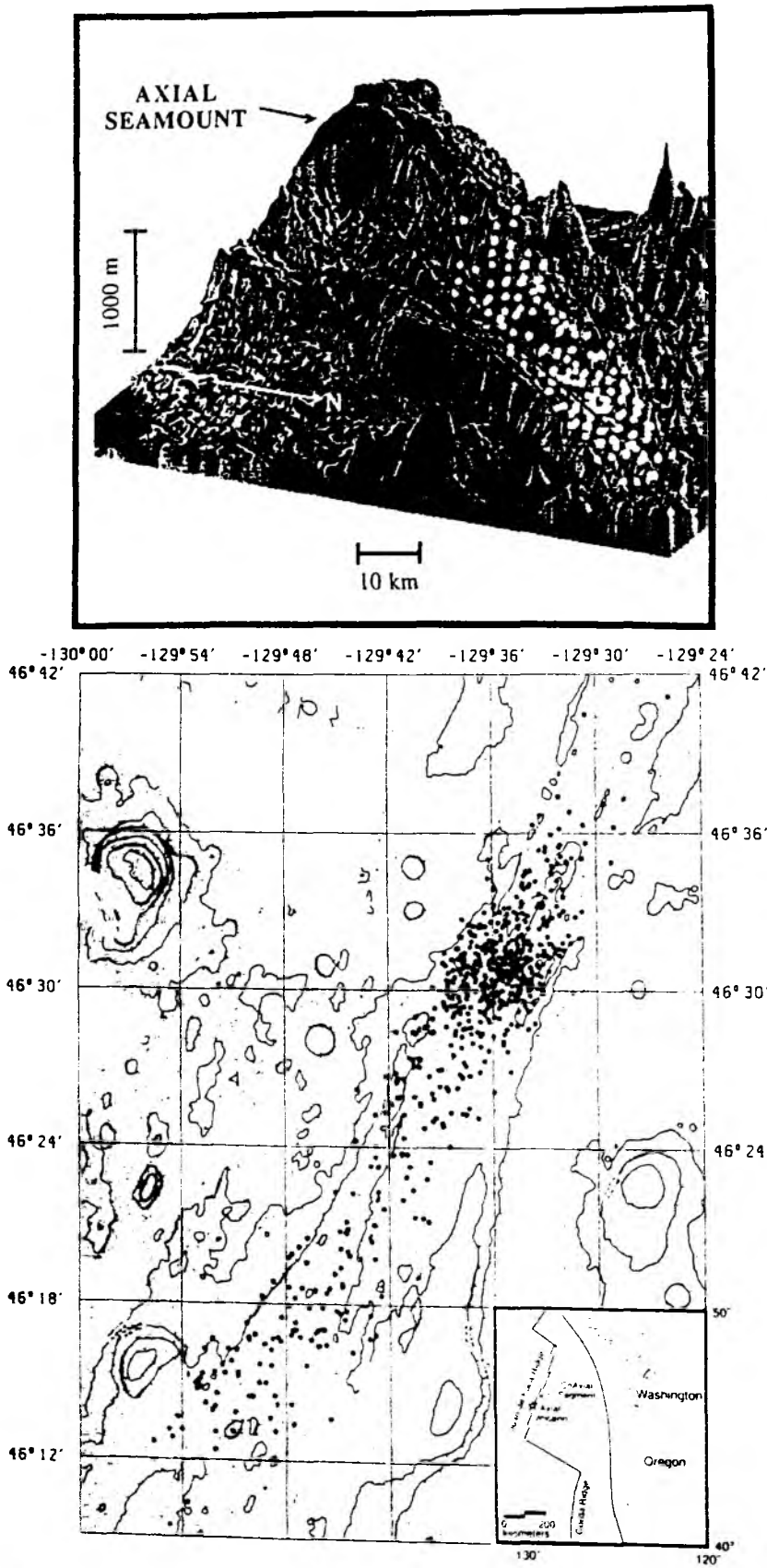


Fig. 6: Seismic events at the CoAxial segment northeast of Axial Seamount (Fox et al., 1995; Dziak et al., 1995).

References

- Applegate, B.T., 1990, Volcanic and structural morphology of the south flank of Axial Volcano, Juan de Fuca Ridge: Results from Sea MARC I side scan sonar survey: *Jour. Geophys. Research*, v. 95, p. 12765-12784.
- Butterfield, D.A., Massoth, G.J., McDuff, R.E., Lupton, J.E., and Lilley, M.D., 1990, Geochemistry of hydrothermal fluids from Axial Seamount Hydrothermal Emissions Study Vent Field, Juan de Fuca Ridge; Subfloor boiling and subsequent fluid-rock interaction: *Jour. Geophys. Research*, v. 95, p. 12895-12922.
- CASM II, 1985, Hydrothermal vents on an axis seamount of the Juan de Fuca Ridge: *Nature*, v. 313, p. 212-214.
- Delaney, J.R., Johnson, H.P., and Karsten, K.L., 1981, The Juan de Fuca Ridge hot-spot propagating ridge system: New tectonic, geochemical, and magnetic data: *Jour. Geophys. Research*, v. 86, p. 11747-11750.
- Dziak, R.P., Fox, C.G., and Schreiner, A.E., 1995, The June-July 1993 seismo-acoustic event at CoAxial segment, Juan de Fuca Ridge: Evidence for a lateral dike injection: *Geophys. Res. Lett.*, v. 22, p. 135-138.
- Embley, R.W., Murphy, K.W., and Fox, C.G., 1990, High-resolution studies of the summit of Axial Volcano: *Jour. Geophys. Research*, v. 95, p. 12785-12812.
- Fox, C.G., 1990, Evidence of active ground deformation on the mid-ocean ridge: Axial Seamount, Juan de Fuca Ridge, April-June 1988: *Jour. Geophys. Research*, v. 95, p. 12813-12822.
- Fox, C.G., Radford, W.E., Dziak, R.P., Lau, T.-K., Matsumoto, H. and Schreiner, A.E., 1995, Acoustic detection of a seafloor spreading episode on the Juan de Fuca Ridge using military hydrophone arrays: *Geophys. Res. Lett.*, v. 22, p. 131-134.
- Johnson, H.P., and Embley, R.W., 1990, Axial Seamount: An active ridge axis Volcano on the Central Juan de Fuca Ridge: *Jour. Geophys. Research*, v. 95, p. 12689-12696.
- Massoth, G.J., Butterfield, D.A., Lupton, J.E., McDuff, R.E., Lilley, M.D., and Jonasson, I.R., 1989, Submarine venting of phase-separated hydrothermal fluids at Axial Volcano, Juan de Fuca Ridge: *Nature*, v. 340, p. 702-705.

2.2 Cascadia Accretionary Margin

by Erwin Suess and Peter Linke

2.2.1 Background

The segment of the Cascadia convergent margin off Oregon is the first at which tectonic dewatering has been observed and documented (Kulm et al. 1986; Suess et al. 1985). Since this discovery it has become one of the classic sites for our understanding of fluid venting processes at active margins and the formation of accretionary complexes (Moore et al. 1990, Westbrook et al. 1994). The style of accretion alternates along this margin between thrust faults dipping towards the continent and those dipping towards the oceanic plate. The surface expression of accretion are several N-S trenching ridges of progressively older age towards the continental plate. Ponded sediment basins develop between the ridges. The detailed structure of the seaward-verging (dipping towards the oceanic plate) accretionary complex was established in numerous seismic and bathymetric surveys and provided the basis for targeting the Second Accretionary Ridge for detailed investigations during HYDROTRACE. From W to E the morpho-tectonic units of the convergent margin off central Oregon are (1) the proto-deformation zone immediately west of the first accretionary ridge; it is characterized by a seaward-facing scarp which rises 30-40 m above the sea floor of the oceanic plate. Here little evidence for surface expressions of fluid venting has been found; (2) the first accretionary ridge, which appears to be locally cut by a back-thrust; it is characterized by a very deep seaward facing flank with seaward shallow dipping rock out crops, sharp ridges, narrow canyons and precipitous scarps (Kulm et al. 1986). At the base of the scarp as well as along exposed strata in the canyons extensive biological communities indicate active fluid venting. However, by far the most vigorous fluid discharge has consistently been observed at the contact between the ponded basin fill and the projected outcrop of the back-thrust at the landward flank of the first ridge; (3) the Second Accretionary Ridge which is underlain by landward dipping reflectors which are locally folded and faulted. Slope deposits are not apparent on the ridge crest nor in the basins to the east and west of the ridge. Several ALVIN dives to this region have documented extensive biologic communities and diagenetic evidence for fluid venting on or near the top of all the accretionary ridges that are the topographic expressions of anticlines in the accretionary wedge (Moore et al., 1990). Carson et al. (1994) were able to show from Gloria images of the Second Accretionary Ridge that were corrected for topographic effects, that the projection of the main subsurface seepage zones correspond to regions of intrinsically high backscattering. This effect is proposed to be associated with enhanced diagenetic cementation (either carbonate, methane and/or H₂S hydrate) in the near surface sediments.

2.2.2 Second Accretionary Ridge

The Second Accretionary Ridge where the Gloria back-scatter intensity has the greatest magnitude in a roughly north south trending linear region some 2 - 3 km wide and more than 20 km long. (Fig. 7a) The ridge is cut by faults striking N15° E (Carson, Westbrook, Musgrave and Suess 1995), parallel to the topography of the ridge. Surface off-sets and the association of faults with growing folds indicate that some of the faults are active. Surface off-sets are thrusts which along with compressional folds suggest the Second Accretionary Ridge is currently undergoing shortening and uplift. The northern summit of the ridge correlates with a hydrogeologically active out-of-sequence thrust zone, with more extensive carbonate build up, vigorous seep activity, and a well-developed BSR. The northern summit was also targeted for drilling during ODP-Leg 146. The borehole observatory at Site 892 (CORK) was positioned on the westward slope of the ridge to study this out-of-sequence fault, where thermal anomalies indicated that active flow is currently occurring (Westbrook et al., 1994, Davis et al, 1995; Screaton et al., 1995). The fault outcrop (approx. 350 m west of the drill site) is marked by chemosynthetic clam communities and an accumulation of diagenetic carbonate (called „bioherm“ by Moore et al., 1991, although it is strictly not formed by biota like a coral reef). This is the region where most direct flux measurements at cold seeps have been attempted (Carson et al., 1990; Linke et al., 1994; Schlüter et al., 1993). The ridge to the south continues to show high back-scatter intensities but the topography becomes distinctly smoother than in the north. This is probably related to the absence or at least significant reduction of the rugged bioherm carbonates. The depth of the ridge crest deepens from 585 m in the north to 980 m in the south some 20 km away (Fig. 7b). Previous studies and surveys had been unable to document any evidence for active fluid venting along the ridge crest.

2.2.3 Bottom Simulating Reflector

A well-developed BSR underlies the crest of the Second Accretionary Ridge. It was the drilling target of Site 892 of ODP Leg 146 (Westbrook, Carson, Musgrave et. al. 1994; Westbrook, Carson, Musgrave, Suess et al. 1995). It extends down the seaward flow of the ridge and continues landward. Two major faults cut through the BSR causing a slight upward bulging of the reflector and surface off-sets. The fault nearest the ridge crest (water depth = 720 m) was intersected at 105 m bsf by drilling at Site 892. The drill hole also intersected the BSR at 73 m bsf. Active flow in the drill hole at Site 892 was indicated by geochemical anomalies in the pore water, by overpressure from a packer test, and by local temperature excursions (1.6° and 2.5°) above the linear geothermal gradient.

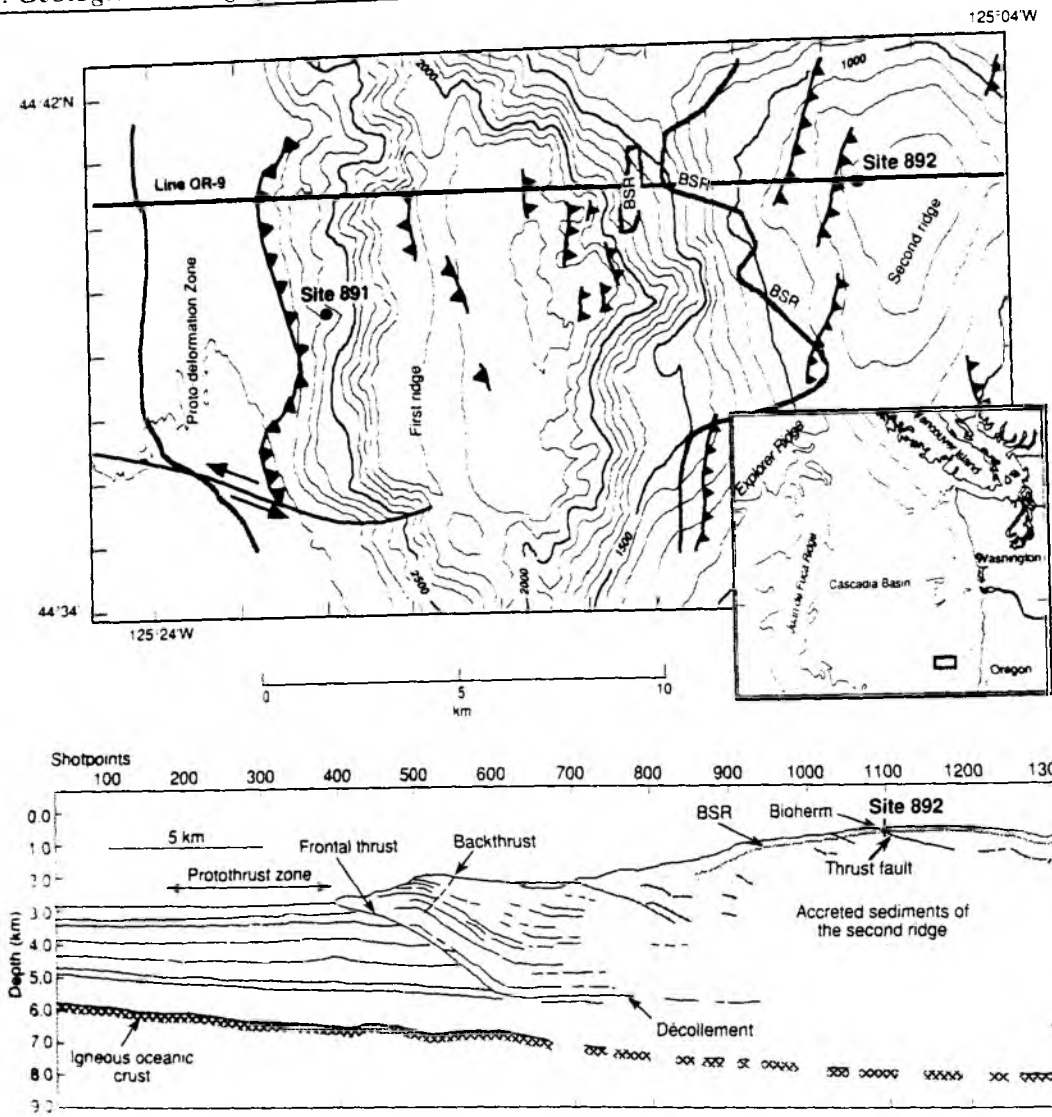


Fig 7 a) Position of Sites 891 and 892 and seismic line OR-9 off Oregon. The positions of thrust fault traces are indicated by heavy toothed lines. The seaward limits of the proto-deformation zone and of the BSR are shown by heavy gray lines. After MacKay et al. (1992)
b) Depth-converted migrated seismic-reflection section OR-9, showing flat-lying Cascadia Basin deposits (Shotpoints 43-150), the proto-deformation zone characterized by blind thrusts (Shotpoints 150-400), the first ridge of the lower slope underlain by a seaward-verging thrust fault (Shotpoints 400-600), and the second ridge (Shotpoints 725-1355). The position of Site 892 is indicated. The structural position of Site 891 was projected from the actual drilling location, 3 km south.

Macroscopic aggregates of gas hydrates were found in the upper 19 m bsf at Site 892 and were inferred to occur disseminated throughout the 73 m thick section above the BSR. Gas from the hydrate zone contained methane, ethane, hydrogen sulfide and carbon disulfide. The hydrates may contain all these species. Low sonic velocities (1.5 km/sec.) unequivocally show the presence of free gas below the BSR.

2.2.4 Bioherm Carbonate

Massive carbonate deposits (= bioherm) are scattered over the seaward flank of the Second Accretionary Ridge (Linke et al. 1994; Moore et al. 1994). They mark the surface trace of outcropping faults and their carbon originates exclusively from methane (Ritger et al. 1987). The volume of carbonate deposited suggests a long-term discharge of methane-rich fluids along fault zones which cut across the BSR. Drilling at Site 892, being spudded off the fault trace showed little diagenetic carbonate downhole and no massive bioherm - like deposits near the sea floor. Therefore the association of the blocky carbonates solely with active vents is quite convincing. The only detailed descriptions of carbonate mineralogies from the Second Accretionary Ridge come from downcore concretions and cements found during ODP-drilling (Kopf et al. 1995; Sample and Kopf, 1995). The mineralogy is highly variable consisting of aragonite, low- and high Mg-calcites and also dolomites. The C-isotope composition indicates fermentation carbonate (+20 ‰ PDB), a range of mixtures of organic derived carbonates (-5‰ to -22‰ PDB), and a few methane-derived carbonates (-28‰ to -52‰ PDB). The latter are restricted to shallow depths below the sea floor. The O-isotopes are consistent with low temperatures of formation for most carbonates with the exception of those few samples from fault zones. These show a ^{18}O -depletion consistent with temperatures of up to 100°C, invoking ascending warm fluids. No clear relationship between either pore water environment or tectonic and stratigraphic position and the carbonates could be found, although reconstruction of formation temperatures from $\delta^{18}\text{O}$ suggests a generally increasing temperature downhole with positive temperature spikes around fault zones. It is abundantly clear from the results of OSD Leg 146 that these carbonates are truly diagenetic and have formed well below the seafloor possibly influenced by fluid conduits along faults. Pure methane derived carbonates are rare among the diagenetic phases and hence they do not resemble the bioherm carbonates currently found at the surface of the ridge. This situation suggests that the bioherm carbonates are unique in that they are related to vigorous fluid venting, very likely triggered by gas hydrate decomposition and methane escape. The quantity of bioherm carbonates constitutes a record of long-term fluid escape, and the surface distribution is directly related to outcrops of subsurface fluid pathways.

References

- Carson, B, Erol, S., Paskevich and Holmes, M. L. (1994) Fluid expulsion sites on the Cascadia accretionary prism: Mapping diagenetic deposits with processed GLORIA imagery. *J. Geophys. Res.*, 99, 11959-11969.
- Carson, B., Westbrook, G.K., Musgrave, R.J. and Suess, E. (1995) *Proc. ODP, Sci. Results, 146 (Pt. 1): College Station, TX (Ocean Drilling Program).*

- Davis, E., Becker, K., Wang, K. and Carson, B. (1995) Long-term observations of pressure and temperature in Hole 892B, Cascadia accretionary prism. In: Westbrook, G.K., Carson, B. and Musgrave, B. (eds.) ODP, Scientific Results: College Station, TX, Ocean Drilling Program, p. 299-313.
- Kulm, L.D., Suess, E., Moore, J.C., Carson, B., Lewis, B.T., Ritger, S.D., Kadko, D.C., Thornburg, T.M., Embley, R.W., Rugh, W.D., Massoth, G.J., Langseth, M.G., Cochrane, G.R., and Scamman, R.L. (1986). Oregon margin subduction zone: Geological framework, fluid venting, biological communities, and carbonate lithification observed by deep submersible, *Science*, 231, 561-566.
- Linke, P., Suess, E., Torres, M., Martens, V., Rugh, W.D., Ziebis, W., and Kulm, L.D. (1994). *In situ* measurement of fluid flow from cold seeps at active continental margins. *Deep-Sea Res.*, 41, 721-739.
- Moore, J.C., Orange, D. and Kulm, L.D. (1990) Interrelationship of fluid venting and structural evolution: Alvin observations from the frontal accretionary prism, Oregon. *J. Geophys. Res.*, 95, 8795-8808.
- Schlüter, M., Linke, P. and Suess, E. (1993). Geochemistry and fluid flow observed at deep-sea boreholes (CORK) on the Cascadia accretionary wedge (ODP Sites 889 and 892). *EOS* 74 (43), 578.
- Screaton, E.J., Carson, B. and Lennon, G.P. (1995). Hydrogeologic properties of a thrust fault within the Oregon Accretionary Prism. *J. Geophys. Res.*, 100, B10, 20,025-20,035.
- Suess, E., Carson, B., Ritger, S.D., Moore, J.C., Kulm, L.D. and Cochrane, G.R. (1985). Biological communities at vent sites along the subduction zone off Oregon. In: Jones, M.L. (ed.), *The Hydrothermal Vents of the Eastern Pacific: An overview*. Bull. Biol. Soc. Washington, No. 6, 475-484.
- Westbrook, G.K., Carson, B., Musgrave, R.J., et al. (1994). Proc. ODP, College Station, TX, Ocean Drilling Program, Init. Repts. 146, Part I.

3. Leg SO109-1

3.1 Cruise objectives and Operations Background

by Erwin Suess

The distribution patterns of chemical tracers (CH_4 , $^3\text{He}/^4\text{He}$, Mn, Cu, Zn a. o.) in the oceans are essentially affected by the input from two different tectonic regimes. On the one hand are hydrothermal fluids which discharge at active riftzones and on the other hand are cold fluids from the dewatering of accretionary prisms. These two end-members and their inter-relationship have not been surveyed along the boundaries of the same lithospheric plate. Hence, Axial Volcano and the accretionary ridges off central Oregon were selected as two important sources emitting material from the boundaries of the Juan de Fuca plate. Also unknown are the distribution patterns of the dissolved and particulate transport into water column and sediments. An approach for the differentiation of the tracer from both vent systems are determining the C-isotopics of CH_4 or investigating the difference in the $^3\text{He}/^4\text{He}$ - and Mn/ CH_4 relationships. Also the heavy metals in water column and sediment provide diagnostic differences. The general objectives of the HYDROTRACE expedition are therefore to

- (1) determine the characteristics of the rift- and subduction-induced tracers;
- (2) identify the characteristic parameters for the proximal and distal vent areas;
- (3) estimate the supply from the two main vent systems;
- (4) trace the regional distribution pattern of tracers in the water column and in the sediment along a transect from the Juan de Fuca Ridge to the subduction zone.

The specific objectives of Leg SO109-1 were to first survey the Axial Volcano sites and the sites on the Second Accretionary Ridge. The purpose was to identify currently active point sources of hydrothermal and cold fluids respectively. The survey includes high-resolution mapping by the multibeam system HYDROSWEEP and, when sediments are present, by PARASOUND. Identification of active vents was to be accomplished by delineation and tracking of plume structures based on tracer anomalies such as temperature, methane, turbidity, manganese, silica, and helium isotopes. This was followed by coring sediments along a transect from the more distant Cascadia Basin towards Axial Volcano. The sediment cover at the coring sites was to be of different thickness, distance and age with respect to the oceanic basement and the active rift zones. The purpose was to detect episodes or variations of hydrothermal input as recorded by the hydrothermal components in the sediment. Also anomalies in dissolved Mg, Ca and Sr-isotopes in pore waters from sediments taken at various distances from the basement, were to be used as tracers for hydrothermal interaction. Finally, the surveying and mapping during Leg SO109-1 were in

preparation for ROPOS deployments on the following legs. In this context Leg SO109-1 was designed to address these specific objectives. High-resolution video-mapping by the EXPLOS-and TVG-systems combined with multibeam HYDROSWEEP surveys were conducted during this leg. Detailed sampling of all varieties of bioherm carbonates and their association with hydrates, methane escape structures, tension fractures, and fault outcrops were the major tasks during leg SO109-1. Work during SO109-1 included completion of the detailed multibeam bathymetry of the Second Accretionary Ridge with HYDROSWEEP. CTD-deployments and hydrocasts, EXPLOS-runs and TV-grab sampling were concentrated on active vent sites of this ridge. Quantification of biota at vent communities and their structure were equally important tasks as was the detection and distribution of plumes in the water column. Deployment of ZAPS and a near current meter gave some indication of the highly dynamic behaviour of these plumes. Sampling of gas hydrates as well as escaping methane became important tasks during Leg SO109-1. Deployment of the giant TV-grab and surveys by EXPLOS runs were the preferred operations for looking at gashydrates, whereas multiple hydrocasts with high vertical sample resolution near the seafloor was the approach taken to detect plumes from escaping methane and map their distribution.

3.2 Fahrtverlauf und Zusammenfassung der Ergebnisse

von Erwin Suess

Woche vom 24.5. - 30.5.1996

Am 24. Mai um 18:00 h Ortszeit verließ FS SONNE planmäßig und bei relativ kalten Temperaturen und verhangenem Himmel den Hafen von Astoria, Oregon. Vorausgegangen waren zwei Tage mit umfangreichen Ent- und Beladearbeiten sowie das Einrichten der Labore. Bei der 16 Stunden währenden Dampfzeit in das Untersuchungsgebiet des Juan de Fuca Rückens wurden die Analyse-systeme an Bord funktionstüchtig gemacht. Diese kamen alle zum Einsatz, als wir im Laufe des 25. 05. die erste Station im Cascadia Basin abarbeiteten. In der folgenden Nacht wurde mit Profilfahrten das engere Areal östlich des Axial Volcano erkundet. Die Aufzeichnungen mit PARASOUND ergaben eine Sedimentbedeckung unterschiedlicher Mächtigkeit die durch vulkanische Rücken bzw. Kegel in Unterbecken gegliedert war. Die bathymetrische Aufnahme ließ an Qualität zu wünschen übrig, da wir mit 12 Knoten fuhren sowie Wind und Seegang nicht immer optimale Bedingungen schufen.

Am 26.05. vormittags erreichten wir die Kaldera des Axial Volcano und begannen mit dem Einsatz des ZAPS (kontinuierliche Messung gelösten Mangans und Partikelverteilung) und der Kombination CTD Rosette im Bereich des hot vent Feldes ASHES. Wir konnten eine gut

entwickelte Austrittswolke (Plume) ca. 250 m über Grund mit allen Sensoren und Systemen registrieren und nach Süden zum Ausgang der Kaldera verfolgen. Bemerkenswert ist die deutliche Intensitätsentwicklung und feine Internstruktur der Wolke, aber ihre räumlich begrenzte Ausdehnung war unerwartet.

Danach setzten wir die Profillfahrten fort, um geeignete Sedimentbedeckung für die Kernentnahme festzulegen. Diese konnten im Laufe des 27.05. begonnen werden, allerdings nicht ohne die Erkenntnis, daß eine weiträumig verbreitete verfestigte Schicht nahe der Oberfläche den sonst so zuverlässig einzusetzenden Multicorer hier als wenig geeignet erscheinen ließ. Kastenlot und Kastengreifer allerdings erbrachten den erwarteten Kerngewinn und es konnte eine enorme Anzahl von Porenwasserproben extrahiert und analysiert werden. Am 28.05. begannen wir mit der Vermessung des Rogue Seamount nordöstlich des Axial Volcano, um eine geeignete Dredgeposition festzulegen. Im Laufe des Tages kam das Gerät dann auch zum Einsatz wurde aber, zum Bedauern aller, zuguter Letzt durch Nachgeben der Sollbruchstelle wieder entleert.

Inzwischen erreichte uns die Nachricht von NOAA/Newport, daß 3 Tage zuvor ein mittleres Beben im Zentrum der Kaldera am Axial Volcano registriert worden war. Wir fuhren erneut in das Gebiet und setzten das ZAPS-System auf der durchgegebenen Position ein, konnten aber keine Indizien für eine Megaplume feststellen. Die CTD-Einsätze allerdings zeigten in Fortsetzung des früher festgestellten Ausbreitungsmusters erneut signifikante Temperatur-, Trübe- und Methananomalien.

Nach abschließenden Vermessungen der Sedimentverteilung, wobei das PARASOUND-System Aufzeichnungen von hervorragender Qualität lieferte, beendeten wir am 29.05. die Sedimentbeprobung. Obwohl wir unmittelbar neben einer Rückenstruktur zweimal ein leeres Kastenlot an Deck holten, überdeckten bei Abschluß der Beprobung 4 Kastenlote (KAL) mit bis zu 6 m Kerngewinn, 2 Multicorer (MUCs) und 1 Kastengreifer (GKG) ein 88 sm langes Profil senkrecht zur Rückenachse. Die Sedimente mit Turbiditlagen und anderen Horizonten zur Korrelation untereinander sind hervorragend geeignet, um Hydrothermaleinträge bzw. Episoden verstärkter Aktivität am Juan de Fuca Rücken dokumentieren zu können. Gradienten der Mg+Ca- sowie der Cl-Gehalte im Porenwasser zeigten ein Muster, das auf Wechselwirkung zwischen der basaltischen Kruste, deren Alter, dem aufliegenden Sedimentpaket und dessen Mächtigkeit schließen lassen.

Mit Abschluß der ersten Woche beendeten wir die Arbeiten am Axial Volcano und erreichten am 30.05. um 07:00 h das Gebiet der Subduktionszone vor Oregon. Das Wetter hatte sich

inzwischen beruhigt und es herrschten angenehme, fast sommerliche Temperaturen bei glatter See.

Zweite Woche, 30.5. - 4.6.1996

Die zweite Hälfte der Reise war den Fluidaustritten, ihrer Biogeochemie und Verteilungsmuster von Tracern in der Wassersäule entlang der Subduktionszone vor Oregon gewidmet. Mit Ankunft im Arbeitsgebiet wurden am ersten Akkretionsrücken bei ca. 44°40'N und 2100 m Wassertiefe zwei Einsätze mit dem TV-Greifer an bekannten Fluidvents gefahren. Obwohl sogleich bei Bodenberührung die bei ALVIN-Tauchgängen abgeworfenen Gewichte gesichtet wurden, gelang in den canyonartigen Hangpartien die Beprobung nur einiger Karbonatkonkretionen, u.a. eines Fluidschlotes, sowie lebender Vent-Mollusken. Die erhoffte Beprobung einer gesamten Vent-Kolonie mit Sediment gelang nicht, obwohl auch am folgenden Tage (31.05.) noch zwei TVG-Einsätze darauf verwendet wurden. ZAPS- und CTD-Einsätze im frontalen Bereich des Akkretionskeiles ergaben moderate CH₄- und Trübungs-Anomalien in Bodennähe und um 1000 m Wassertiefe. Ihre Zuordnung zu Vent-Feldern war nicht eindeutig. Nachts wurde ein 6 km breiter Streifen des zweiten Akkretionsrückens vermessen, der bei dem 3. Fahrtabschnitt bearbeitet werden soll.

Vom 01.06. bis zum Ende der Reise konzentrierten sich die Untersuchungen auf den zweiten Akkretionsrücken. Mit einer bis 580 m aufragenden Gipfelhöhe aus 1000 m überdeckt dieser einen deutlich flacheren Bereich in der Wassersäule als der erste Rücken. An der Westflanke wurde die Bioherm Lokation beprobt, die das Ziel einer Bohrung des ODP-Legs 146 gewesen war. Bei einem TVG-Einsatz wurde das Bohrloch mit seiner kegelförmigen Eintrittsöffnung gesichtet. Je drei TVG-, ZAPS- und CTD-Einsätze an dieser Lokalität und an der östlichen Flanke des Rückens dokumentierten mehrere großräumige Vent-Strukturen in Form von Biohermen und intensiven in der Tiefenlage sehr eng begrenzten CH₄-Anomalien in der Wassersäule. Um eine eindeutige Zuordnung dieser Anomalien zu morphologischen Strukturen zu erhalten, wurde die Vermessung des Areals nach Osten bis an die Schelfkante in Wassertiefen von 300 m ausgedehnt.

Der wissenschaftliche Höhepunkt der Reise kam, wie häufig der Fall, am letzten Arbeitstag. Am 02.06. vormittags gelang die Beprobung einer durch Gashydrate zementierten und mit einer Vent-Vergesellschaftung belebten Sedimentpartie aus 625 m Wassertiefe von der westlichen Flanke des 2. Akkretionsrückens. Wir waren bestens vorbereitet, diesen Fund zu bergen, denn schon beim Hieven konnte bei ca. 400 m Wassertiefe eine Entgasung des Sediments im Inneren des Greifers durch die zugeschaltete TV-Kamera beobachtet werden. Die Intensität der Entgasung stieg mit abnehmender Wassertiefe und enorme Blasen eilten dem Greifer voraus und brachen durch die Oberfläche. Die große Menge des freiwerdenden

Gases deutete eher auf eine Hydratphase hin als auf sich ausdehnende Gase aus dem gelösten Zustand. Die Zusammensetzung des Hydrates war zu diesem Zeitpunkt nicht bekannt. Gewaltiger H_2S -Gestank kurz nach an Deck bringen des Gerätes jedoch machte ein Mischhydrat von CH_4 und H_2S wahrscheinlich. Alle an Deck Tätigen konnten durch vorbereitete Atemschutzmasken bei der Beprobung des TV-Greifens versorgt werden.

Das Sediment zeigte die bekannte Schaum-Textur, hervorgerufen durch die entweichenden Gase. Es wurden mehrere kurze Kerne für Porenwasseruntersuchungen entnommen sowie schließlich ein Stück festen Gashydrates geborgen. Ein weiterer TVG-Einsatz an der gleichen Stelle enthielt ebenfalls CH_4 und H_2S im Sediment, es wurden aber keine Anzeichen für Hydrate gefunden. Abgestorbene Vent-Organismen und Karbonatkonkretionen wurden in großer Zahl geborgen.

Auch die zweite Hälfte des letzten Tages ergab ein Rekordergebnis mit der Kartierung - basierend auf Daten von sechs CTD-Einsätzen- einer in nördlicher Richtung über dem Gipfel sich ausbreitenden Methanfahne. Hier wurde ein Gehalt von 1200 nL/L an Methan in der Wassersäule gemessen. Damit wurden um eine Größenordnung höhere Werte registriert als die für Plumes am Axial Volcano. Ein abschließender TVG-Einsatz am Gipfel des Akkretionsrückens zeigte mehrere ausgedehnte Vent-Felder, sowohl durch dichte Besiedlung gekennzeichnet als auch durch blockartige Karbonatstrukturen. Die Ergebnisse zeigen, daß dieser zweite Akkretionsrücken über weite Teile und über geraume Zeit erhebliche Mengen an Fluiden und Gasen emittiert hat und noch emittiert. Aktive Großstrukturen dieser Art, die durch entweichende Hydratgase aufrecht erhalten werden, sind bisher nicht bekannt gewesen.

Am 03.06. gegen 00:00 h Ortszeit verließ F.S. SONNE das Arbeitsgebiet in Richtung Vancouver Island bei ruhiger See, Nebel und angenehmen Temperaturen. Nebel hüllte uns ein über die gesamte Strecke bis zur Olympic Peninsula. Am 04.06. um 00:00 h erreichten wir den Eingang der Juan de Fuca Strait. Nach Lotsenübernahme machten wir um 07:30 h an der Pier Ogden Point im Hafen von Victoria fest.

3.3 Cruise Narrative and Summary of Results

by Erwin Suess

First week, 24 - 30 May 1996

On 24 May at 6 p.m. local time RV SONNE departed Astoria, Oregon as scheduled at unseasonably low temperatures and overcast skies. Prior to departure we had spent two days loading and unloading gear and equipping the laboratories. During the 16-hours transit to the Juan de Fuca Ridge the analytical systems were set up and sampling gear readied. On 25 May all systems were operational when we worked on coring the first station in the Cascadia Basin. The following night the sedimented flank east of Axial Volcano was surveyed. The PARASOUND records showed a sediment cover of different thickness that is divided into subbasins by volcanic ridges and cones which dot the eastern ridge flank. The multibeam bathymetric survey was of poor quality as we steamed 12 knts and wind and seas did not always provide optimal conditions for data recording.

In the morning of 26 May we reached the Axial Volcano's caldera and started a ZAPS survey (continuously recording dissolved manganese and particle distribution) and ran several hydrocasts in the area of the hot vent field ASHES. A well-developed plume, about 250 m above the seafloor, was recorded with all sensors and systems. The plume could be traced towards the south out of the caldera. The plume intensity was well developed, but its spacially limited extent was unexpected.

Continued PARASOUND profiling was used to determine a suitable sedimentary thickness for coring. On 27 May coring started, but not without discovering that the usually reliable multicorer was unsuitable to penetrate a wide-spread unusually indurated surface sediment encountered on the ridge flank. Box corer and kasten corer, however, succeeded in securing the expected core material on board. A tremendous number of porewater samples were obtained and analysed. On 28 May we began to survey the Rogue Seamount located to the northeast of the Axial Volcano to find a suitable dredge position. During the day the dredging operation appeared successful, but, to everybody's regret the weak link broke when bringing the dredge on board and the contents emptied.

NOAA/Newport informed us on 28 May that a medium earthquake had been registered in the center of the caldera at the Axial Volcano three days ago. We returned to the area and lowered the ZAPS system at the given position, but could not find any evidence for a megaplume as was hoped for. However, the hydrocast showed again significant anomalies in temperature, suspended matter and methane in continuation of the plume pattern detected earlier.

On 29 May sediment coring was completed after a final survey of the sediment distribution by the PARASOUND system which yielded records of excellent quality. Although we failed twice with box coring next to a buried ridge structure, in the end 4 kasten cores (KAL) with each up to 6 m recovery, 2 multicores (Mucs) and 1 box core (GKG) were recovered along a 88 n.m. profile perpendicular to the ridge axis. The sediment sequence showed turbidite layers and other horizons which could be readily correlated. The cores appeared perfectly suitable to document hydrothermal inputs or episodes of increased activity at the Juan de Fuca Ridge. Gradients of Mg+Ca and Cl contents in the pore water showed a pattern from which the interaction between the adjacent basaltic crust, the age, the overlying sediment package, and its thickness could be inferred.

At the end of the first week we completed work at the Axial Volcano and steamed towards the area of the subduction zone off central Oregon on 30 May at 7 a.m. During transit the weather stabilized with almost summerlike temperatures and calm seas.

Second week , 30 May - 4 June 1996

The second part of the cruise was devoted to the fluid vents at the Oregon accretionary margin, their biogeochemistry and distribution patterns of tracers in the water column. On arrival in the area two deployments of the TV-grab were carried out at the first accretionary ridge at 2100 m of water depth in the vicinity of known vent fields. Although we sighted the weights dropped during ALVIN dives, the canyon-like steep slope provided only a few carbonate concretions and living vent molluscs. We did not succeed in the expected sampling of a complete vent colony, although the next day (31 May) two more giant TV-grab deployments were carried out. ZAPS- and CTD-deployments in the frontal area of the accretionary wedge yielded moderate CH_4 and turbidity anomalies near the bottom and at around 1000 m of water depth. Their correlation with vent fields was not clear, however, at night the Second Accretionary Ridge was continued to be surveyed, since it was the target for the third leg.

From 6 June until the end of the cruise the investigations focussed on the Second Accretionary Ridge. This ridge rises to 580 m above the surrounding seafloor at 1000 m. On the western flank a bioherm was sampled which is thought to mark the out crop of fault. This fault was also the target of ODP Leg 146 drilling. The bore hole with its cone-shaped entry hole was sighted when deploying the giant TV-grab. At this location and at an eastern ridge flank three TVG-, ZAPS- and CTD-deployments were carried out. Each documented large-scale vent structures in the form of bioherms and intense, narrowly depth limited, CH_4 anomalies in the water column at 550 m of depth. The survey was extended to the eastern

ridge flank at water depths of 300 m in order to trace the origin of these anomalies to morphological structures.

As is often the case during expeditions the scientific highlight came on the last day (2 June). In the morning of that day at 625 m of water depth we successfully sampled sediment that was cemented by gas hydrates and contained a live vent assemblage of the TV-grab from the western flank of the Second Accretionary Ridge. We were prepared to recover this find as during heaving we could observe strong degassing inside the corer beginning at 400 m. The degassing intensity increased with decreasing water depth. Huge bubbles rose ahead of the corer and broke through the surface beside the ship. The great amount of gas released pointed to a hydrate phase as the source rather than to expanding dissolved gases. At the time the hydrate's composition was not known, but an enormous H_2S smell accompanying sediment recovery made a mixed hydrate of CH_4 and H_2S likely.

The sediment showed the known froth texture caused by escaping gas. Several short cores were subsampled for pore water analysis and finally a solid egg-size piece of gas hydrate was recovered. Another TV-grab deployment at the same location again yielded CH_4 - and H_2S -rich sediment, but no indications for hydrates were found. Dead vent organisms and carbonate concretions were recovered in great quantities.

Based on the results from six CTD deployments around the ridge crest a methane plume with contents as high as 1200 nl/L was located in the water column above the northern summit of the Second Accretionary Ridge. Thus, values of higher order of magnitude than those measured at the Axial Volcano were recorded. A final TV-grab deployment at the summit of the ridge showed several large active vent fields. They were characterized by dense colonies of benthic organisms and blocky carbonates. Our results document that the Second Accretionary Ridge has emitted and is still emitting considerable amounts of fluids and methane over a large area. Large active vent structures of this kind fuelled by gas hydrates have not been known until now.

On 3 June at midnight RV SONNE left the area and steamed north towards Vancouver Island. The sea was calm and the air foggy and pleasant temperatures prevailed throughout the transit. On 4 June at midnight we reached the entrance to the Juan de Fuca Strait, and, after taking on the pilot, tied up at Odgen Point Pier in Victoria, Canada at 7.30 a.m. the same day.

3.4 Results

3.4.1 Water Column Program

by Reinhold Bayer, Carol Chin, Robert Collier, Gary Klinkhammer, Stephan Lammers, Paul Stoffregen

Introduction

The water column sampling team applied CTD and ZAPS instruments to survey the water column for tracers of fluid venting -- hydrothermal fluids at Axial Seamount and cold seep fluids at the Oregon Margin subduction zone complex. While these are well-established analytical tools for remotely locating, characterizing, and sampling hydrothermal plumes, the cold seep environment represented a new application of these techniques.

ZAPS instrument package

The ZAPS Sled is an open framework of 2 inch Type 316 stainless steel pipe. It stands 36 inches wide, 36 inches tall, and is 7 feet long with a tapered bow 16 inches wide. This frame hangs from the towing cable by an adjustable, three-point chain bridle to ensure that the sled attains a forward facing, level attitude in the water. The two vertical sides of the sled aft of its center of gravity have three-eighths inch Lexan polycarbonate panels attached to serve as rudder vanes and give the structure hydrodynamic stability while being towed at 1 to 2 knots through the water.

The central instrument on the sled is a SeaBird 911 plus CTD, sampling at 24 Hz, fitted with modular temperature and conductivity sensors and a Paroscientific Digiquartz pressure sensor. Six analog instruments are interfaced through the SeaBird CTD underwater unit:

- A SeaTech transmissometer to measure 660 nm wavelength beam attenuation through a 25 cm seawater path.
- A Chelsea Aquatracka Mk III fluorometer operating as a nephelometer at 420 nm to measure light scattered at 90 degrees to the incident light beam.
- A SeaTech turbidity sensor, which measures backscattered light at 650 nm.
- A SeaPoint turbidity sensor, another measure of backscattered light which extends the detection range at higher suspended matter concentrations.
- A Zero-Angle Photon Spectrometer. ZAPS is an experimental instrument that uses solid-state chemistry with analog fluorescence signal detection to measure the concentration of dissolved manganese in seawater.
- A SIMRAD Mesotech Systems Model 807 echo sounder/altimeter used to determine the sled's height off the bottom within a 300 meter range.

Also included on the ZAPS sled is a rosette which will accommodate a dozen 1.5-liter Niskin bottles for collecting seawater samples for laboratory measurements of methane and trace

metals. The rosette was fitted with six water bottles during this cruise. The bottles can be tripped any time using the software without interrupting the incoming data stream. An attitude module indicates the sled's heading, pitch, and roll.

Ship and sled positions are monitored during the ZAPS operations and this navigational information merged with the geochemical data. This system includes a Garmin MRN 100 Satellite Receiver that is interfaced to a 486DX4-100 MHz computer. This computer runs a proprietary SLED navigation program developed at OSU. The computer plots the ship's position and trackline in real time and compares this with target positions to aid in navigating ZAPS over the bottom.

ZAPS is a fixed filter fiber optic spectrometer that can be deployed as a chemical sensor or fluorometer. ZAPS has an operating range between 200 and 900 nm. ZAPS and the ZAPS pump are digitally controlled from the ship. The major operating parameters of flash rate, offset, averaging, flash intensity, PMT bias voltage, and pump rate can be changed at any time during the deployment. This capability is particularly useful when making measurements at high PMT sensitivity. It is possible, for example, to keep the detector turned off in the photic zone then turn up the sensitivity once the package moves into deeper water.

Three different ZAPS measurements were made during the cruise. Dissolved manganese was determined by attaching chemical cartridges in-line with the bifurcated fiber-optic assembly that makes up the lightguide system in ZAPS. Water was pumped through these cartridges at a rate of 30 mL/min using a specially designed magnetically-coupled gear pump built at OSU. The sample stream was irradiated at 250 nm and monitored at 370 nm and variations in this signal with depth were calibrated against dissolved manganese concentrations. Fluorescent dissolved organic matter (FDOM) was determined by removing the chemical cartridges and pump from ZAPS and irradiating the water column at 320 nm while monitoring fluorescence at 420 nm. These wavelengths are known to be sensitive to the amount of humic-type organic matter that is part of the pool of dissolved organic matter (DOM) in sea water. UV fluorescence was determined in a manner similar to FDOM -- the filters over the flash lamp and photomultiplier tube were replaced with a 250 narrow-band interference filter and a broad band filter with a 300 nm cutoff and 355 nm transmission maximum.

CTD Instrument Package

The CTD instrumentation was the new GEOMAR Sea-Bird CTD / Rosette system. This included a Sea-Bird 911 plus CTD, SeaTech light transmissometer (same as on the ZAPS sled), altimeter, and bottom trigger. The rosette system was a Sea-Bird Model 32 12-position

rosette pylon with 10-L Niskin-type water sample bottles. Sampling depths were selected based on the downcast data and tripped on the upcast. Sample data was post-processed using the recommended set of Sea-Bird utilities. We noticed that the transmissometer calibration coefficients in the seasoftware file were incorrect with respect to the most recent calibration records. The calculated mid-water transmissions were over 93% and the data should be reprocessed after the cruise using corrected calibrations.

Water samples collected by various participants in SO109-1 included Helium isotopes and Tritium (Bayer), Methane and Methane isotopes (Lammers and Whiticar), nutrients (Suess), Total Dissolvable Manganese (TDM, Collier) and other trace elements (Collier, Herzig). Methane and nutrients were measured onboard, analyses of the other tracers will be performed onshore.

Station description

ZAPS and CTD/rosette operations began with a background station taken approximately 200 km east of the Juan de Fuca Ridge (JdFR). Both packages worked well during this test and water samples were collected from the rosette.

Table 1: ZAPS Stations

ZAPS #	Stn. no.	deg:min.sec		date	time UTC Start/End	depth m	Bottom site
		N	W				
1	1-2	45:29.28	128:02.05	May 25 1996	21:33	2849	Bkgrnd
2	3-1	45:55.99	130:00.80	May 26 1996	16:19/S	1535	Axial
		45:54.18	129:54.18		18:58/E	1536	
3	6-1	45:55.80	129:59.33	May 27 1996	00:05/S	1533	Axial
		45:54.59	129:58.66		03:28/E	1563	
4	18-1	45:57.78	129:59.97	May 29 1996	07:57	1545	Axial
5	18-2	45:55.51	130:01.55	May 29 1996	10:10	1445	Axial
6	28-1	44:40.44	125:17.61	May 31 1996	09:48/S	2023	Margin
		44:40.61	125:17.49		13:55/E	2096	
7	32-1	44:40.27	125:03.62	Jun 1 1996	05:13/S	958	Bioherm
		44:39.61	125:04.04		07:29/E	899	
8	33-1	44:40.52	125:07.33	Jun 1 1996	08:26/S	676	Bioherm
		44:40.11	125:07.89		10:49/E	773	
9	38-1	44:40.20	125:04.48	Jun 2 1996	06:04	766	Bioherm

The first half of the cruise focused on Axial Seamount -- an active ridge axis volcano on the central Juan de Fuca Ridge with several vent fields including high- and low-temperature

vents. We sampled plumes derived from vents at the southern end of the caldera including the only known high-temperature vents at the "ASHES" vent field. Four deployments of the ZAPS instrument package were completed in the vicinity (Table 1). Two of these were drift-yos (3-1, 6-1), and the others were vertical profiles (18-1, 18-2). Station 18-1 was located within the caldera in response to a seismic event detected several days earlier by NOAA/PMEL scientists using the US Navy's SOSUS array (pers. comm. C. Fox and R. Embley). We collected 5 CTD/Rosette profiles at Axial (Table 2), sampling a range of hydrothermal plumes localized by the ZAPS tows.

Table 2: CTD Stations

CTD #	Stn. no.	deg:min.sec		date	upcast time UTC	depth m	Bottom Site
		N	W				
1	1-1	45:28.94	128:01.90	May 25 1996	20:06:06	2843	Bkgrnd
2	4-1	45:55.86	130:00.78	May 26 1996	20:20:27	1540	Axial
3	5-1	45:53.55	129:58.55	May 26 1996	22:46:55	1667	Axial
4	7-1	45:53.99	129:45.95	May 27 1996	05:36:53	2132	Axial
5	19-1	45:55.60	130:00.51	May 29 1996	11:55:37	1539	Axial
6	20-1	45:55.19	129:59.02	May 29 1996	14:08:23	1529	Axial
7	26-1	44:40.58	125:17.48	May 30 1996	23:46:18	2049	Margin
8	29-1	44:40.79	125:18.02	May 31 1996	15:09:03	2347	Margin
9	34-1	44:40.52	125:07.38	Jun 01 1996	11:26:34	661	Bioherm
10	35-1	44:40.27	125:03.80	Jun 01 1996	13:12:37	890	Bioherm
11	37-1	44:40.25	125:04.53	Jun 02 1996	04:19:00	740	Bioherm
12	42-1	44:39.88	125:06.68	Jun 02 1996	17:47:50	742	Bioherm
13	44-1	44:41.18	125:05.67	Jun 03 1996	01:28:01	702	Bioherm
14	45-1	44:40.31	125:05.74	Jun 03 1996	02:46:42	600	Bioherm

The Oregon Margin subduction zone cold seeps were sampled during the second half of the cruise. Two sites were sampled: the first (referred to as "Margin" in Tables 1,2) was located at the base of the slope at the cold seep vents previously sampled by Alvin. The second site was located upslope to the east on the second pressure ridge of the complex near the "Bioherm" vent site. We conducted one ZAPS drift-yo at the Margin site (28-1) and three lowerings at the Bioherm site (32-1, 33-1, 38-1; Table 1). We collected two CTD/Rosette profiles at the Margin site (Table 2) and six lowerings at the Bioherm site in search of the source of a remarkable methane plume sampled by the Rosette (see data report section by Lammers and Whiticar).

Preliminary results

Results from the ZAPS chemical sensor and filter fluorometer. Small to moderate manganese plumes were found associated with the turbidity signals over Axial Seamount. Normal "background" levels of dissolved manganese in this area are about 0.3 nmol/L. Dissolved Mn levels in the plumes over Axial were only on the order of 1 nM. Reports of total dissolvable manganese (TDM) in these plumes are in excess of 10 nM suggesting that most of the Mn in these plumes may be particulate and not reactive to the ZAPS spectrometer. It will be possible to determine this relationship as TDM samples were collected during the cruise.

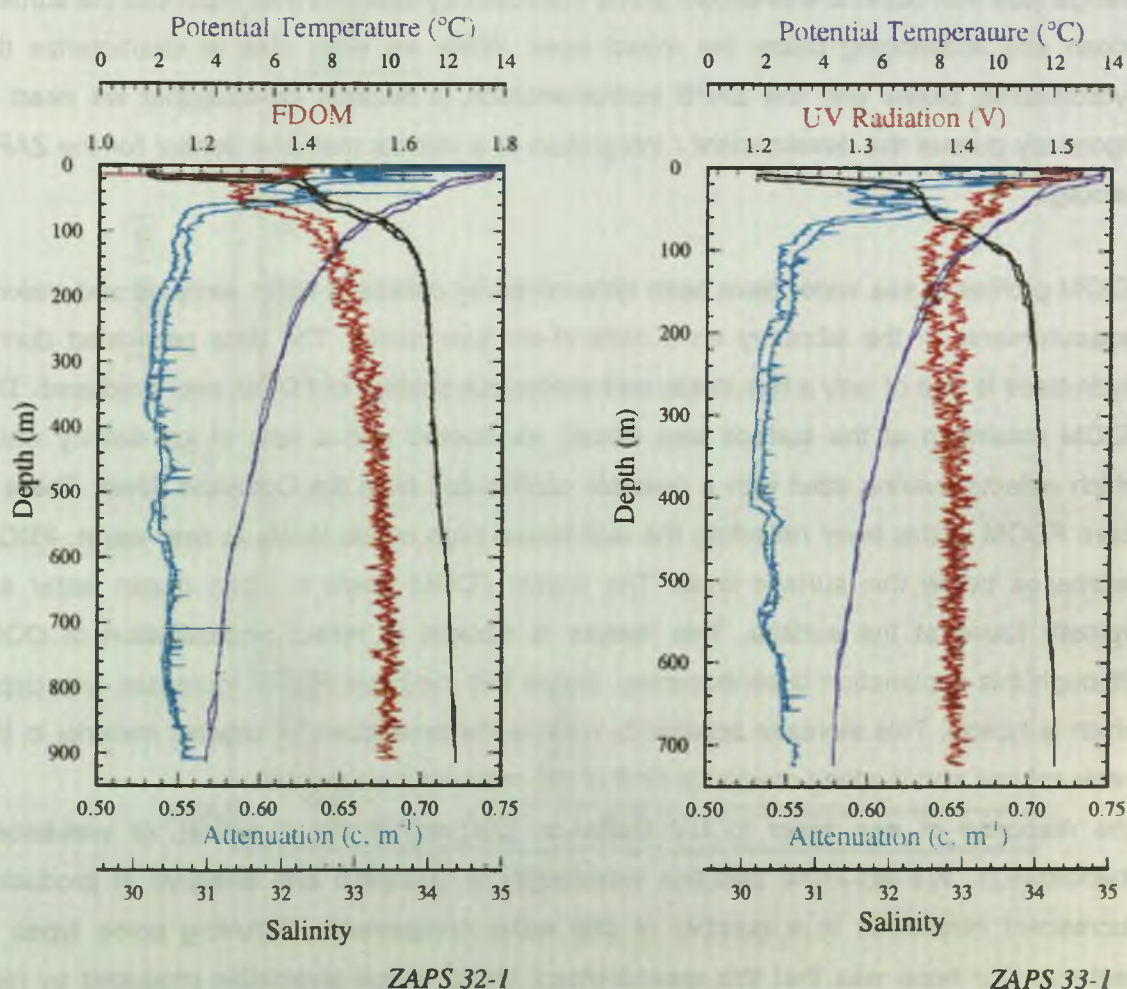


Fig. 8: ZAPS vertical casts near the Bioherm site. Both plots include potential temperature, light attenuation, salinity and ZAPS output. The left-hand panel ZAPS signal represents fluorescent dissolved organic matter (FDOM). This was determined by removing the chemical cartridges and pump from ZAPS and irradiating the water column at 320 nm while monitoring fluorescence at 420 nm. These wavelengths are known to be sensitive to the amount of humic-type organic matter that is part of the pool of dissolved organic matter (DOM) in sea water. UV fluorescence (right panel) was determined in a manner similar to FDOM -- the filters over the flash lamp and photomultiplier tube were replaced with a 250 narrow-band interference filter and a broad band filter with a 300 nm cutoff and 355 nm transmission maximum.

Mn maxima overlap with the turbidity plumes but the shape of the Mn anomalies are quite different with Mn signals often extending further up into the water column than the clouds of particles. This is consistent with what has been observed in other areas and is apparently related to the fractionation of plume parameters during evolution of fluids from the sea floor and/or subsequent dispersion in buoyant and non-buoyant plumes. The ZAPS probe was used to produce profiles of dissolved Mn, UV radiation, and FDOM at the two "Bioherm" sites (Fig. 8). None of these profiles produced anomalies at the depth of the methane maximum (550 m), although these profiles are consistent with what we know about the biogeochemistry associated with these measurements. The distribution of dissolved manganese with depth is well-known and is controlled by dust and river input into the surface ocean and scavenging below the mixed layer. While we were able to characterize the hydrothermal plume with the ZAPS instrumentation, it became obvious that we need to vigorously pursue the development / integration of a remote methane sensor for the ZAPS package.

FDOM profiles in sea water have been determined by collecting water samples and making measurements in the labratory on a state-of-art fluorometer. The data generated during Hydrotrace is one of only a few *in situ* and continuous profiles of FDOM ever produced. The FDOM maximum at the surface was closely associated with a lens of low-salinity water which reflects riverine input with a possible contribution from the Columbia River. There is more FDOM in this layer reflecting the well-known high humic levels in river water. FDOM decreases below this surface layer. The lowest FDOM levels in open ocean water are typically found at the surface. This feature is thought to reflect photooxidation of DOM, although this explanation is controversial. Below this minimum FDOM increases with depth which is typical. This increase apparently reflects the breakdown of organic material in the water column and the long residence time of this material in sea water.

The response of sea water to UV excitation (250 nm) is not a typical, or well-known phenomenon. We do know that this wavelength is energetic and effective at producing fluorescent responses in a number of sea water components, including some types of bacteria. Our hope was that this measurement would reveal anomalies produced by high levels of bacteria associated with the methane plume. We did not see such an anomaly but the profile of UV radiation seems to make sense if such signals are indicative of the size of bacterial populations, i.e. levels are high in the mixed layer and at the top of the sub-surface turbidity maximum with fairly increasing levels below. There is a subtle break in the UV radiation profile at 400 meters, where the waters become more turbid.

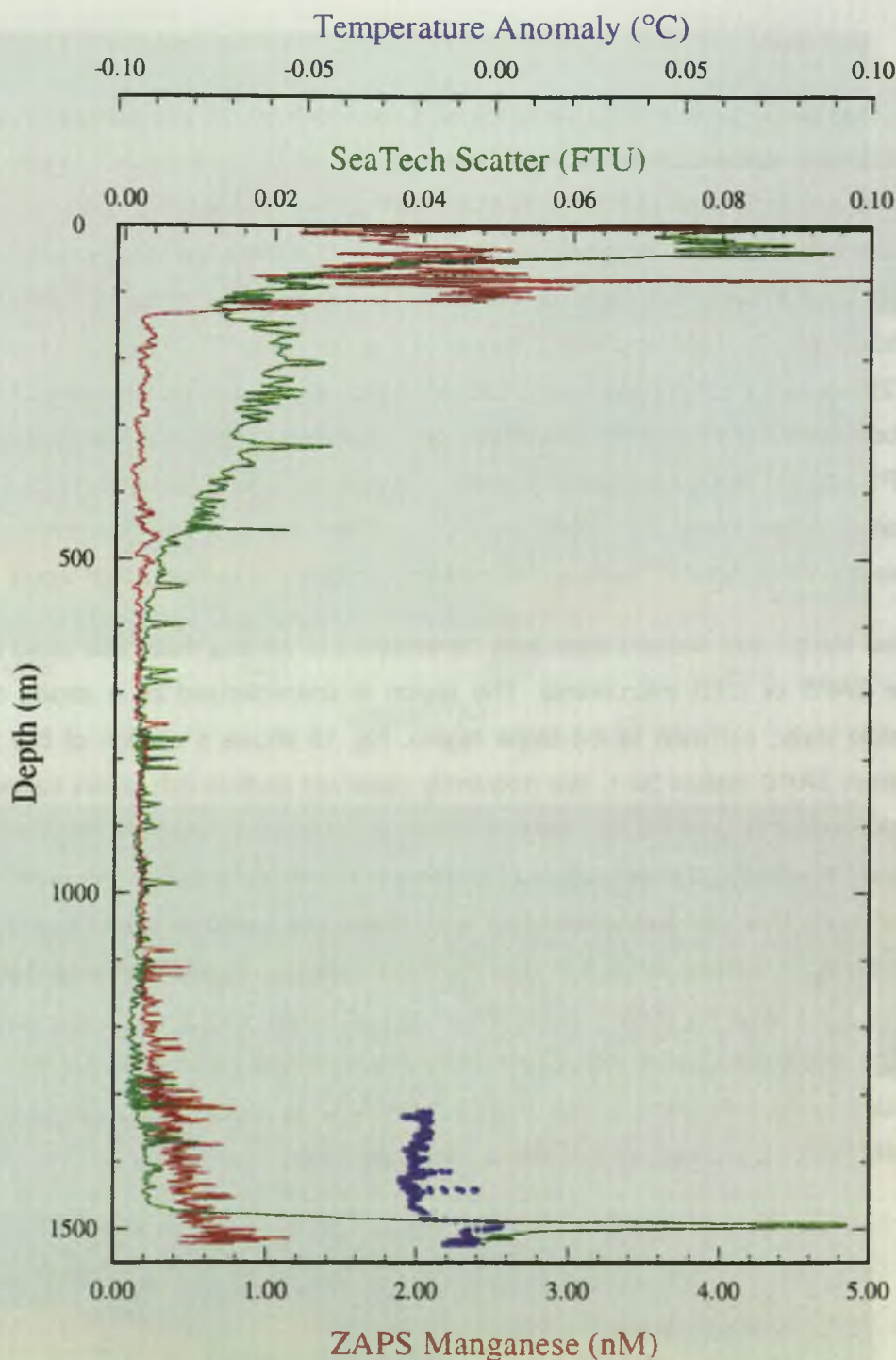


Fig. 9: Vertical profile of backscattered light (SeaTech) related to particulate matter concentration, temperature anomaly (see caption of Fig. 12 for calculation), and dissolved manganese. Dissolved manganese was determined by attaching chemical cartridges in-line with the bifurcated fiber-optic assembly that makes up the lightguide system in ZAPS. Water was pumped through these cartridges at a rate of 30 ml/min using a specially designed magnetically-coupled gear pump built at OSU. The sample stream was irradiated at 250 nm and monitored at 370 nm and variations in this signal with depth were calibrated against dissolved manganese concentrations.

Preliminary plots of a vertical lowering and two sections of plume tracers at the Axial Seamount site are shown in Fig. 9-13. The data clearly demonstrate the plumes which were similar to previous observations by NOAA investigators. The distributions suggest that both the fluids from the ASHES high-temperature vent field and the low temperature field at "Axial Gardens" were being advected to the south at the time of sampling, although we had insufficient time to complete a full survey of the site. The CTD profiles (4-1, 19-1, 20-1; Fig. 12) focused on sampling the hydothermal plumes at, and downstream of the ASHES and Axial Gardens vent fields. Essentially no indications of hydrothermal tracers were seen at ZAPS station 18-1 (in the caldera near the location of recent seismicity) nor at station 18-2, located to the SW of the ASHES field. The CTD casts 5-1 and 7-1 were located to the east-southeast of the vent fields and showed no evidence of hydrothermal inputs.

The first Margin site showed essentially no evidence of venting fluids that could be detected by the ZAPS or CTD instruments. The region is characterized by a strong near-bottom nepheloid layer, common to the slope region. Fig. 13 shows a section of this particle-rich layer from ZAPS station 33-1. We frequently observed particle-rich layers between 1000 m and 400 m depth which are inferred to originate at the slope/pycnocline contact. The shallow "Bioherm" site showed even stronger heterogeneity in water masses and particulate matter "layers" such that up- and down-casts were frequently quite different. Again, we did not observe any consistent tracers of fluid injection from the remote sampling ZAPS or CTD. However, we carefully collected water column samples with the rosette and shipboard methane analyses (Lammers) demonstrated a dramatic plume above the ridge. We continued to sample these plume depths intensively to locate the origin of the methane anomaly (Table 2) -- in all, six CTDs were collected here.

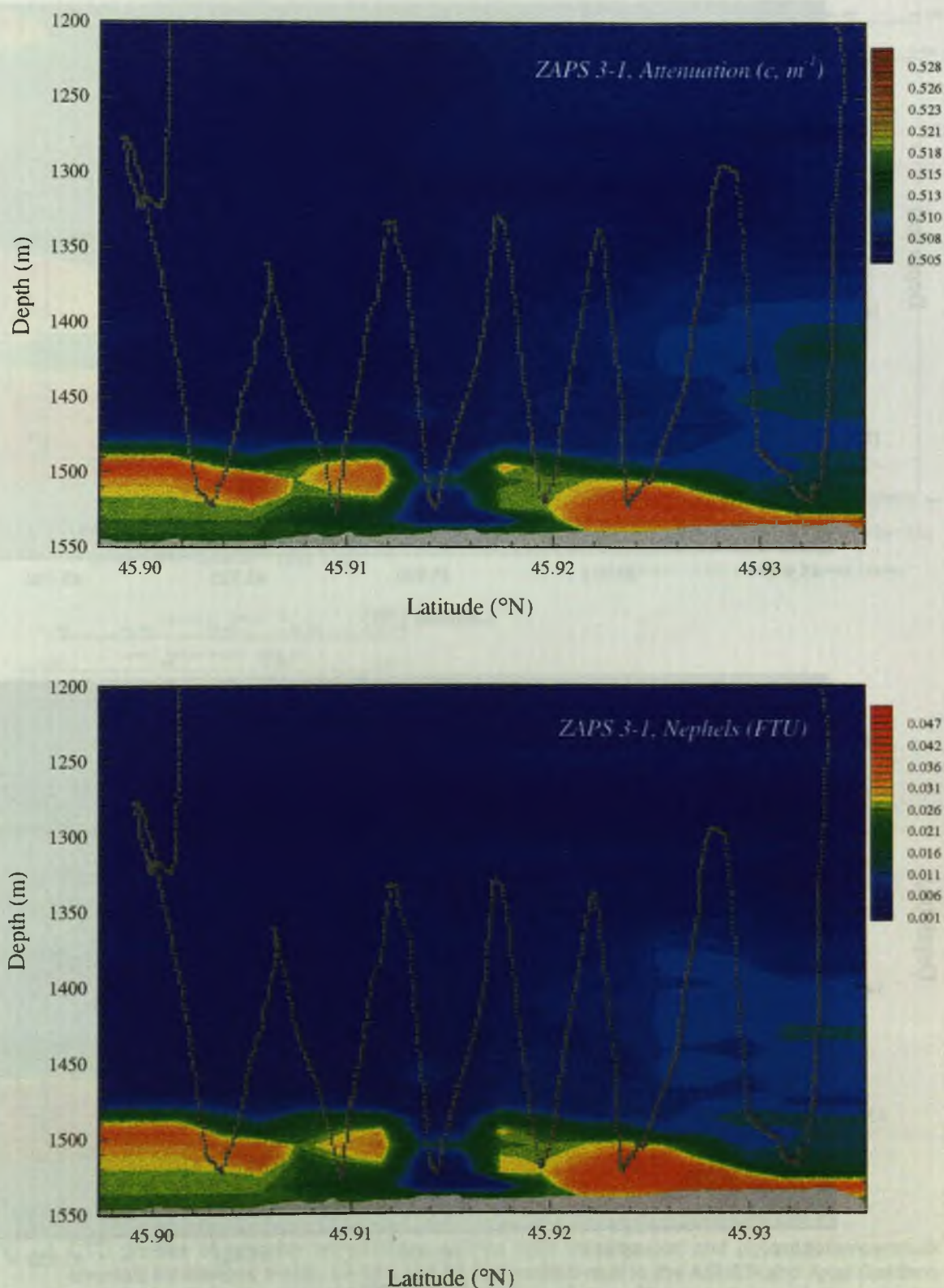


Fig. 10: Vertical sections of light attenuation (SeaTech transmissometer) and nephelometer output (Chelsea Instruments) at ZAPS tow 3-1 -- both related to particulate matter concentrations in the hydrothermal plume. The beginning of the cast (right-hand side of the plate) was located in the center of the ASHES vent field and the tow proceeded south-southeast. In this case, both particle sensors are nearly perfectly correlated.

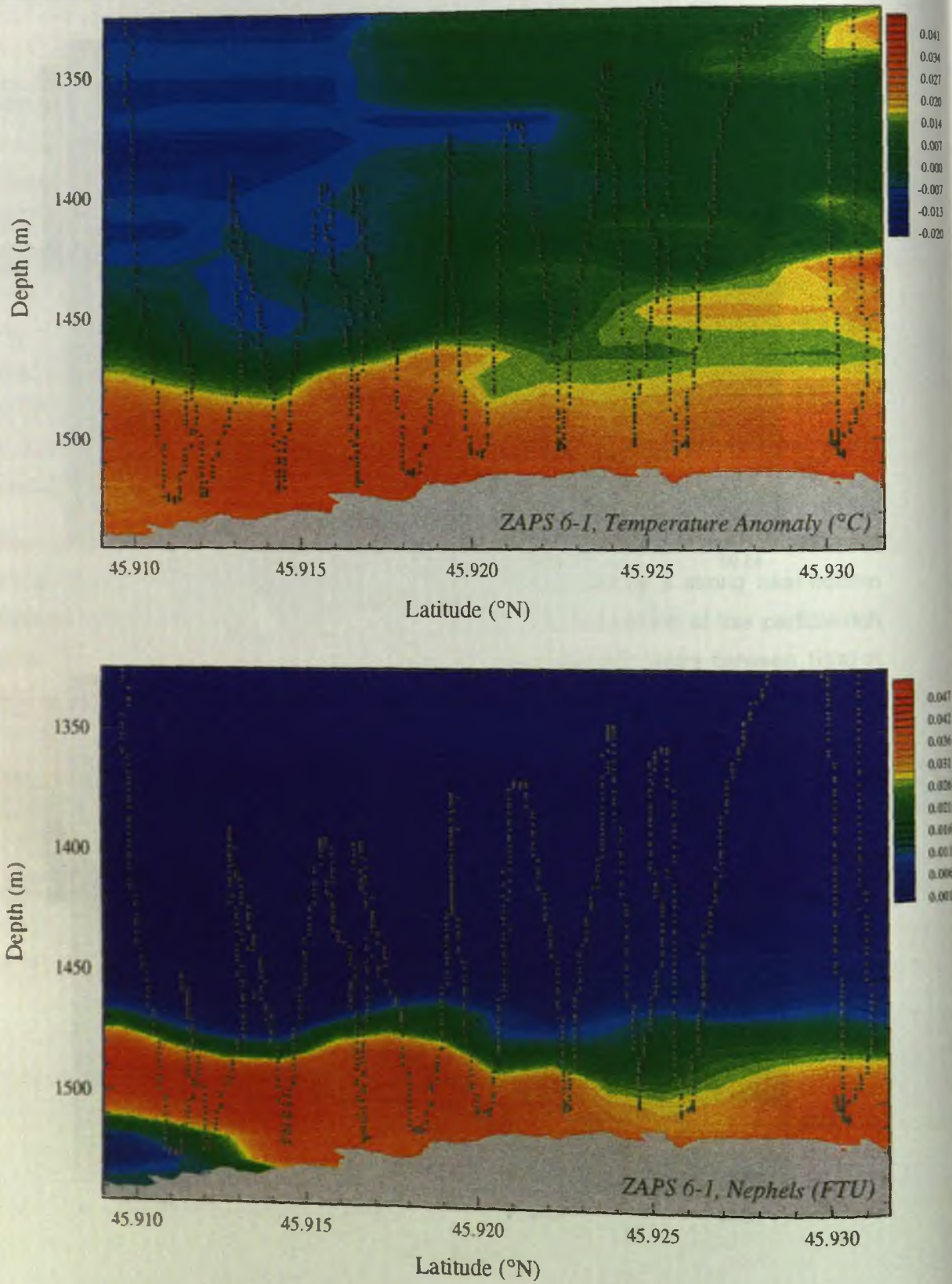


Fig. 11: Vertical sections of temperature anomaly (Sea-Bird CTD) and nephelometer output at Axial Seamount. The tow began near the Axial Gardens low-temperature field and proceeded to the south-southeast.

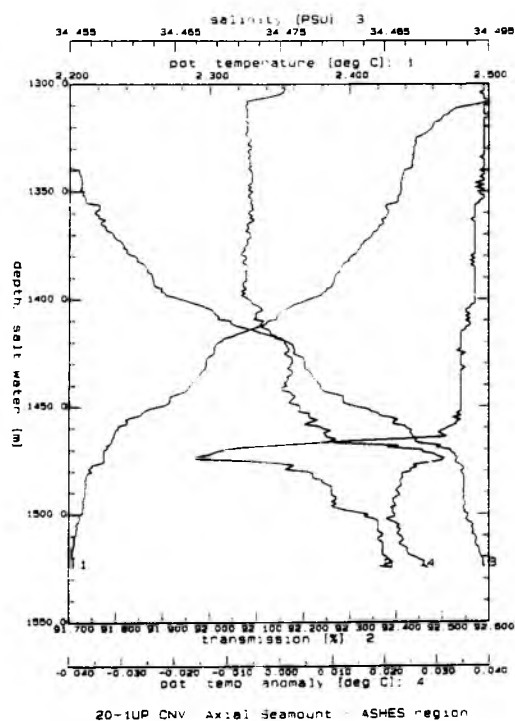
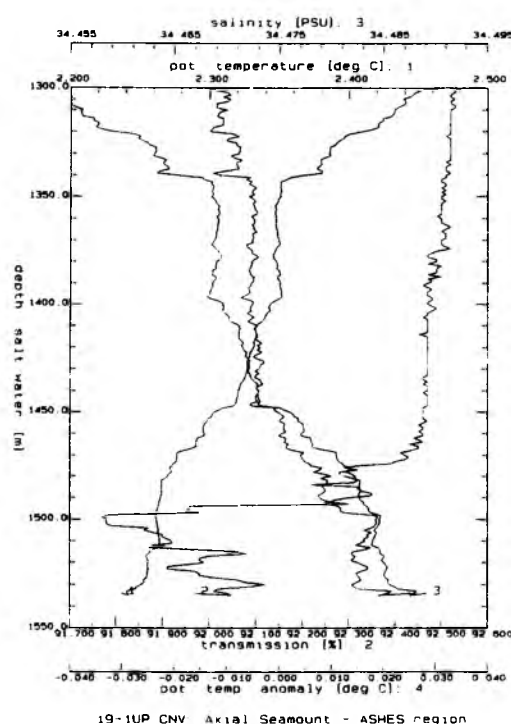
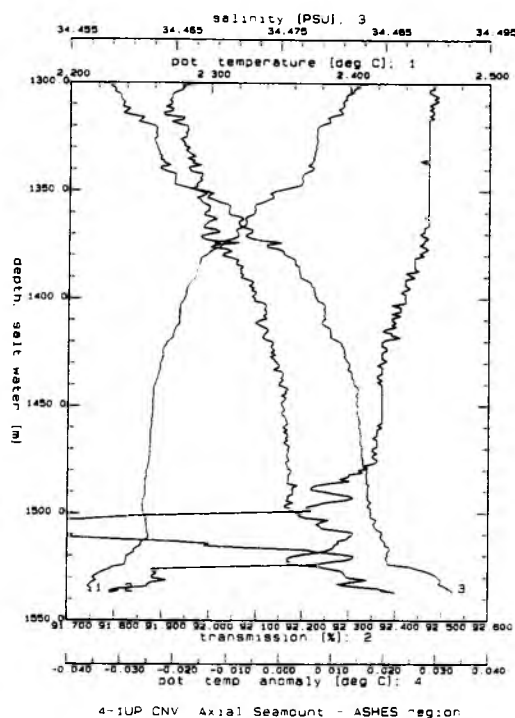


Fig. 12: CTD profiles of potential temperature, salinity, light transmission and potential temperature anomaly for stations 4-1(a), 19-1(b) and 20-1(c) located next to the ASHES and Axial Gardens vent fields. Only the data below 1500 m depth is shown. The calculation of the potential temperature anomaly is based on the deviation from the linear correlation of potential temperature and salinity as observed at station 4-1 in the depth range between ca. 1200 m and 1500 m ($q = 242.64^\circ - 6.9711^\circ/\text{PSU} \cdot \text{S}$). As clearly visible in all profiles, local minima of light transmission centered between 1460 m and 1540 m depth indicate the presence of a vent plume layer with a mean thickness of about 40 m. A potential temperature anomaly of about $+0.02^\circ\text{C}$ was calculated for this layer. The plume was also characterized by its methane content clearly elevated above the background signal.

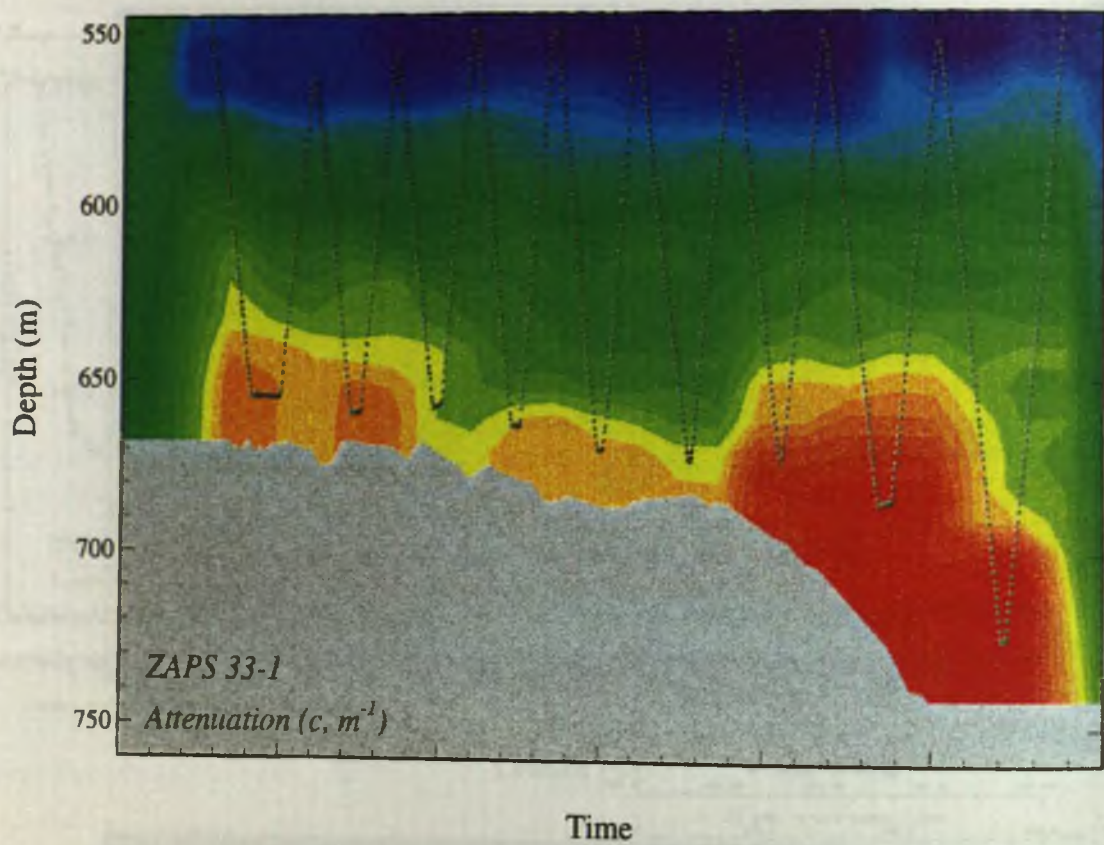


Fig. 13: Vertical section of light attenuation (SeaTech Transmissometer) at the Bioherm vent site. This is representative of the near-bottom nepheloid layer seen in all casts at this site. The depth of the 20 m-thick methane anomaly (Lammers) was variously located between 580 m and 520 m in the water column and did not correlate significantly with any of the water column tracers.

3.4.2 Methane Analyses on Hydrocast Samples

by Stephan Lammers, Michal J. Whiticar and Nicola Jones

Introduction

Measurements of dissolved methane in the water column, accompanied by the ZAPS surveys for tracers of fluid venting, served as an immediate indicator of either hydrothermal or cold vent activity in the main target areas of the SO109-1 expedition, i.e. the Axial seamount and the Oregon subduction margin. Water samples, mostly from the near-bottom section, were taken from the hydrocast rosette and immediately degassed by vacuum-ultrasonication and analysed by GC as a quick reference for vent influence and best choice of coring sites. Additionally, samples were taken for high precision shore analyses of CH_4 and $\delta^{13}\text{CH}_4$ by helium stripping and GC/GC-MS determination.

Methods

Two techniques were applied for the determination of dissolved methane in water samples taken during SO109-1 cruise.

On board analyses were performed using a vacuum-ultrasonication degassing method (Schmitt et al., 1991, Lammers & Suess, 1994) and subsequent determination with a Shimadzu GC 14A gas-chromatograph.

This technique yields 70% with 5% standard deviation of measurements (subject to modification after the SO109-2 and helium-stripping calibration). This simple and easy-to-handle method has the advantage of a higher sensitivity compared to normal head-space techniques and allows for the results from 1 hydrocast (max. 12 samples) within 3 hours after recovery.

On shore high precision analyses of CH_4 and $\delta^{13}\text{CH}_4$ are performed at the Department of Biogeochemistry of the University of Victoria using a total yield helium stripping technique and GC/GC-MS determination. This method yields 100% of the dissolved methane with standard deviations of less than 2%, mostly determined by the gas-chromatography. The results of this precise technique will replace the data achieved on board and also be used for an improved calibration of the vacuum-ultrasonic method.

Preliminary Results

During SO109-1 expedition a total of 148 samples from 13 hydrocasts were analysed for dissolved methane. 5 hydrocasts were run at the Axial seamount area and 8 around the "Bioherm" stations at the Oregon margin. The immediate determination of dissolved methane from hydrocasts again was proven a valuable tool for fluid expulsions as other venting indications were only small to moderate in the Axial region and did not coincide with

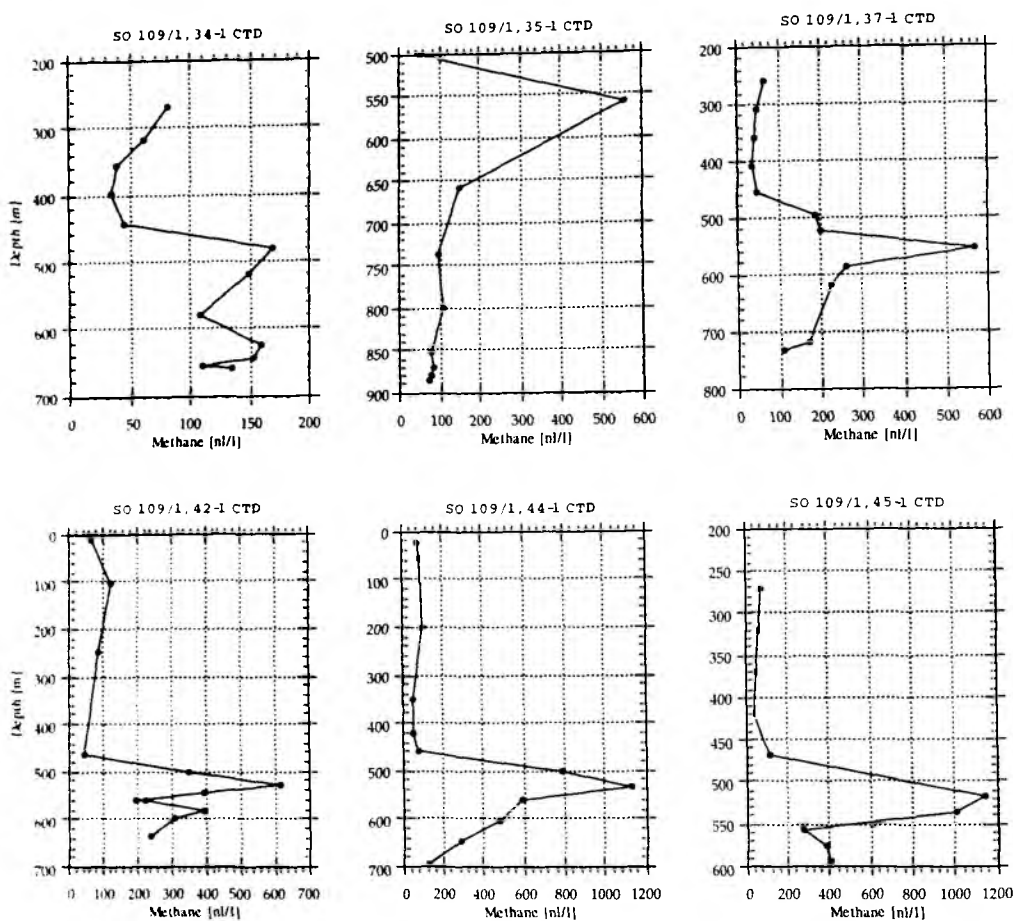


Fig. 14: Methane profiles at the Axial Seamount.

the methane anomalies at the "Bioherm" stations. The results are summarized in Fig. 14-16 and show generally an unexpected low to moderate venting of fluids enriched in methane, while signals of cold venting around the "Bioherm" stations were found up to an order of magnitude higher.

Axial Seamount Region

Bottom near methane maxima ranged between 32 nl/l at station 7-1 at the E-slope of the seamount and 225 nl/l at station 4-1 at the hydrothermally active "Ashes" vent field (Fig. 14). For comparison, station 7-1 SE of "Ashes" in its bottom near section shows only slight deviations from values of 5-8 nl/l above 1500 m depth, which is the normal background concentration in this part of the NE Pacific. To the S of "Ashes" (stations 19-1 and 20-1), plume maxima of 150 nl/l appeared at slightly different depths, which may be attributed to thermohaline buoyancy.

Oregon Margin - Vent Field

Hydrocasts at the Oregon vent site did not show remarkably elevated methane concentrations (Fig. 15). At the easternmost station 29-1 the methane maximum of 66 nI/l at 1600 m most likely reflects terrestrial influences from the continental slope (Collier, pers. comm.).

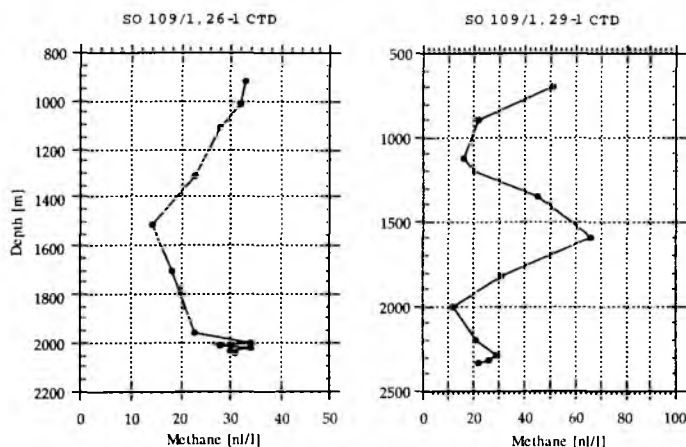


Fig. 15: Methane profiles at the Oregon vent site.

"Bioherm" Area

After the initial detection of a significant 150 nI/l double-peak anomaly below 400 m depth at station 34-1, the further survey revealed spectacular methane anomalies at the top and NE flank of a 400 m elevation (Fig. 16). The profiles show methane maxima between 500 and 1200 nI/l at depths of 520-560 m. This indicates the occurrence of a widespread methane plume supplied by bottom sources probably on the top of this morphological feature. TV guided grab deployments in the area recovered anaerobic, gas-rich sediments and gas hydrates. It remains a task for the SO109-3 leg to completely map this methane plume and to approach the source.

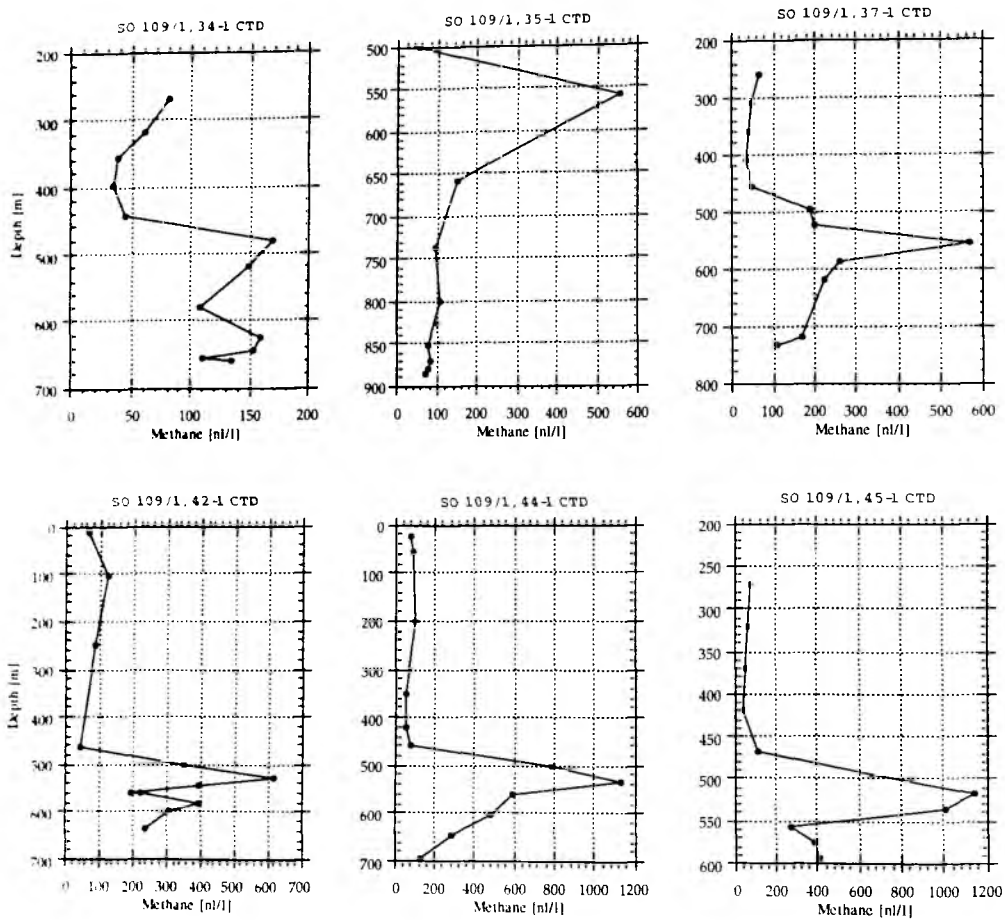


Fig. 16: Methane profiles at the 'Bioherm' stations.

References

Schmitt, M., Faber, E., Botz, R. and Stoffers, P. (1991). Extraction of methane from seawater using ultrasonic vacuum degassing. *Anal. Chem.*, 63: 529-531.

Lammers, S. and Suess, E. (1994). An improved head-space analysis method for methane in seawater. *Mar. Chem.*, 47: 115-125.

3.4.3 Hydrosweep and Parasound Seafloor Mapping

by Jens Greinert, Rüdiger Kunze, Stephan Uhlig, Ulrich Schwarz, Mark Finke, Heike Preißler and Markus Schäfer

During Leg SO109-1 the 3 working areas Axial Volcano, Rogue Seamount and Oregon margin as well as the Astoria Canyon as a potential future working area were swathmapped by Hydrosweep and shallow sub-bottom profiling was conducted by using Parasound (Fig. 17). The objectives of these surveys were to obtain a bathymetric overview of the working areas and to get a basis for the selection of the sediment and water column stations.

System configuration and data processing

The **HYDROSWEEP** system (HS) installed on RV SONNE (HYDROSWEEP DS, Krupp Atlas Elektronik GmbH) uses a field of 59 acoustic beams at a frequency of 15.5 kHz and an angle of 90 degrees, allowing a swathwidth that is twice the water depth. The accuracy of the system is approximately 1% of the water depth. The calibration of the sound velocity can be performed automatically, a preset sound velocity profile or, like here, a depth-constant sound velocity (1480 m/s; SO108).

For the storage of the data magnetic tapes were used and maps were processed on a workstation. The raw data were preprocessed with the MB-System Software of the Lamont-Doherty Earth Observatory and displayed using the GMT software. Data obtained on the Juan de Fuca Ridge were effected by high swell and steaming velocities (> 10 kn) and show artefacts even after careful reduction of the slant beams. Data from the Rogue seamount and the Oregon Margin are specially in the more shallow regions of good quality and could be reduced without problems.

The sediment echosounder **PARASOUND** (PS; Krupp Atlas Elektronik GmbH) is used to obtain geological and sediment property informations of the upper layers of the seafloor. The penetration depth is significantly influenced by the sediment properties and reached up to 50 meters in the well defined turbidic layers on the eastern flank of the Juan de Fuca Ridge. The principle of the frequency radiation is based on the interference of two adjacent, high energy frequencies (18 to 23.5 kHz) and results in a very narrow (4°), parametric beam of 2.5 to 5.5 kHz (here 4 kHz). The quality of the record is determined by the morphology and properties of the sediment. With slope inclinations of more than 2° or very rough topography most of the pulse energy is reflected to the sides and its information content is lost.

By using the **PARADIGMA** system (**PARA**sound **DIGI**talisierungs- und **Mehr**kanal-**Aus**werte-system) the Parasound signals could be digital recorded, stored and printed together with other ship's data.

Mapping Areas

The first mapping area is situated on the Juan de Fuca plate, in a near-axis position to the Juan de Fuca ridge (Fig. 17). It includes the eastern flank of Axial Seamount, the central and northern parts of the Son of Brown Bear Seamount and two basins to the west and east of this seamount (Fig. 19, 20).

A second mapping area, about 56 km to the north, covers the Rogue Seamount. The mapping was conducted as a pre site survey for basalt sampling (Fig. 23).

On the continental slope off the Oregon coast, parts of the Oregon Margin were mapped (Fig. 24, 25) for systematic vent sampling purposes. There are two coast-parallel ridge structures atop of the accretionary prism, reaching a minimal water depth of 570 m.

A next bathymetric profile was measured on the foot of the continental slope, following the Astoria Canyon (Fig. 28). It was the last station of the leg SO109-1 on the transit to Victoria.

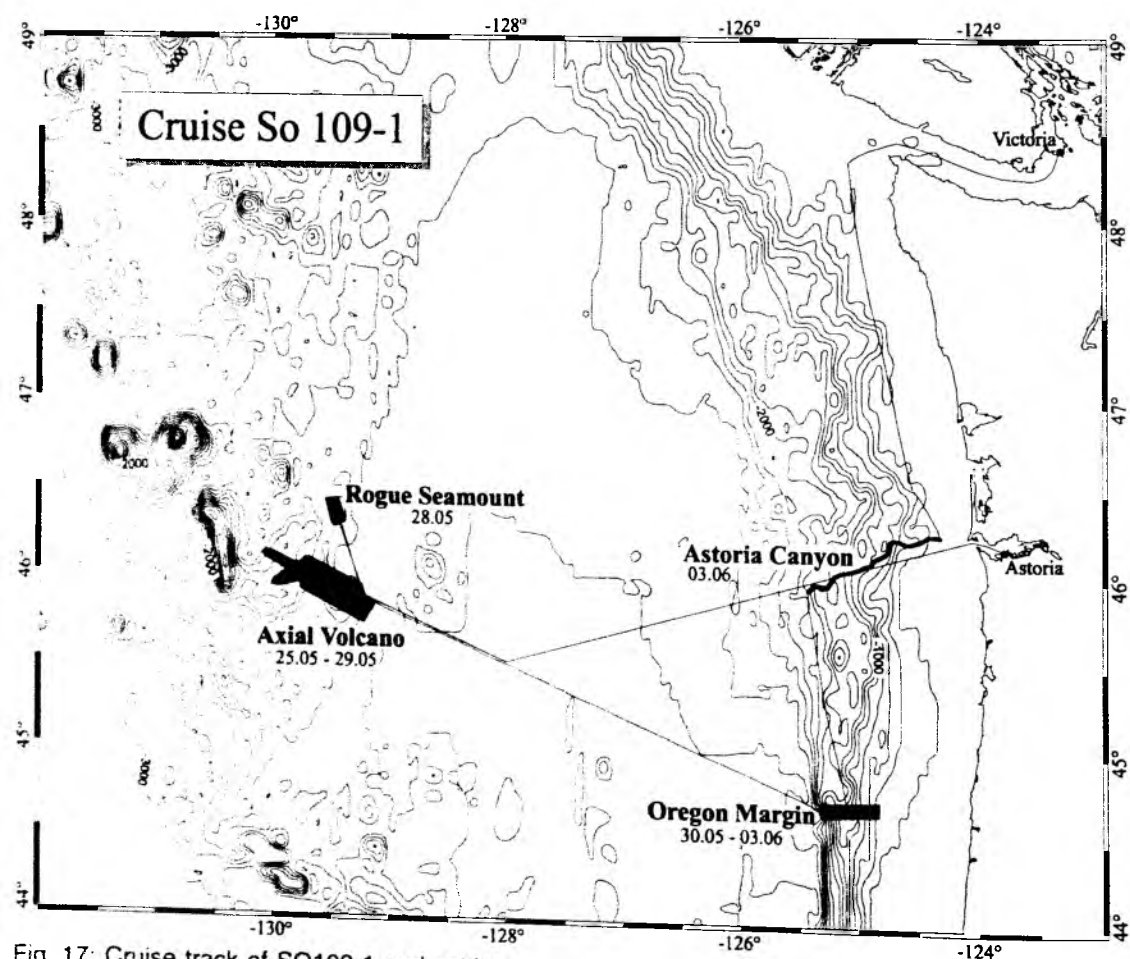


Fig. 17: Cruise track of SO109-1 and setting of working areas including Axial and Rogue seamounts, Oregon Margin, and Astoria Canyon.

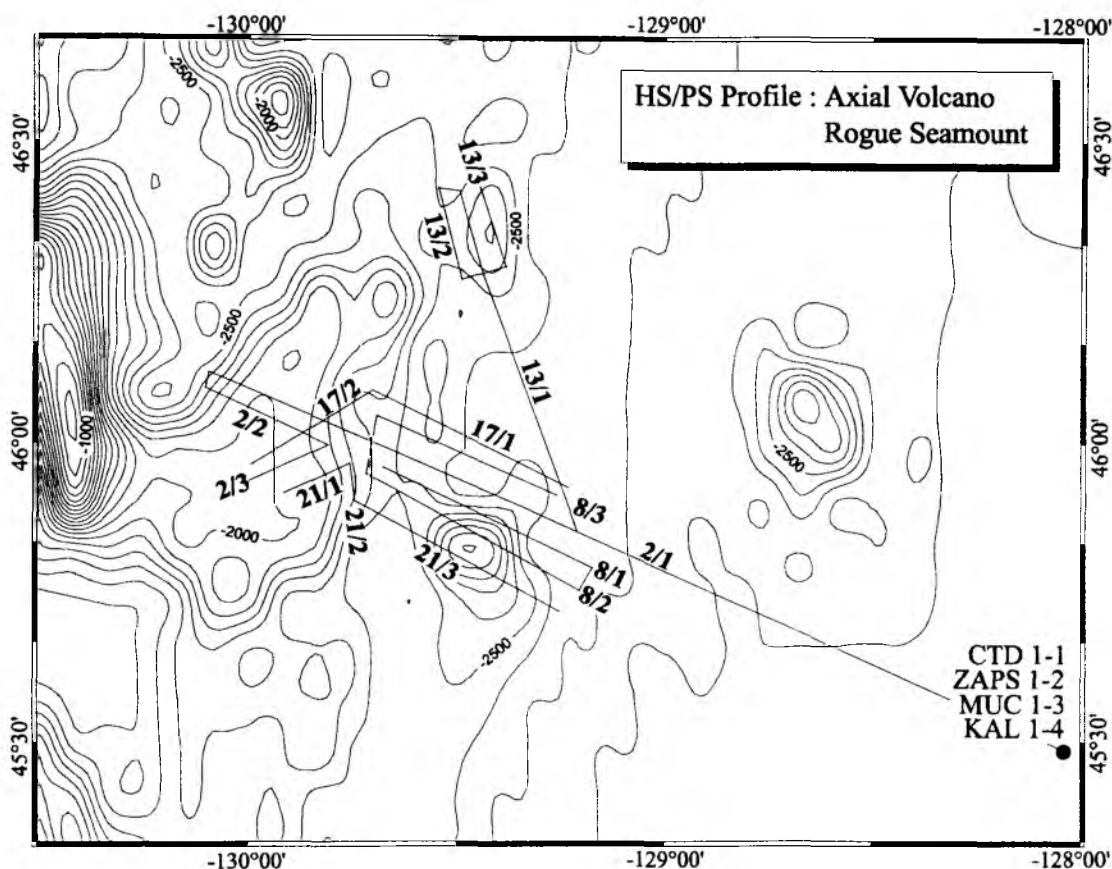


Fig. 18: Location of Hydrosweep and Parasound profiles 2/1 through 13/3 and of stations 1-1 through 1-4 to the E of Juan de Fuca ridge.

Axial Seamount

During the night from May 25 to 26 the Hydrosweep and Parasound profiles (HS/PS) 2/1 to 2/3 were mapped. Target were the two basins easterly and westerly of the Son of Brown Bear Seamount (Fig. 18).

Well bedded sediments could be resolved up to 50 m depth bsf. Along profile 2/1, a transition between more lithified sediments with a lower Parasound penetration depth situated towards SE, to softer and well bedded sediments to the NW was observed. The coordinates of this transition are approx. 45_48.024' N / 129_402.497' W (Fig. 21). This lithological change represents probably a transition between coarser, distinctly terrigenous influenced sediments to the SE and mainly finer turbiditic sediments to the NW. That is in accordance to the sediment samples of box cores 10-2, 11-1, and 12-1.

NE of the outlined lithological transition, Parasound records often show broad updoming structures which partly penetrate the sediment surface (Fig. 21). During the N and S parallel profile cruises 8/1 and 8/3 across the NE-SW striking basins, similar updoming patterns of Parasound profiles were observed, which correlate spatially well with respective structures of

profile 2/1. This profile revealed a N-S strike and a wall-like structure of these updomings, which were traced during a N-S "search cruise" (not declared as a station).

They probably represent either convection related centers of seawater recharge or potential focussed upflow zones of deep fluids. Accordingly, they were particularly densely sampled during nine sedimentologic stations (Fig. 20). However, the sampling proved to be not always successful. Otherwise, the wall-like appearance could be indicative of either dyke-like basaltic intrusions or tilted lithified sediments.

In steeply sloped areas of the Juan de Fuca ridge no interpretable Parasound data were recorded. The Hydrosweep records of the Axial Volcano area yielded worse data, compared to profile cruises 13/1 to 13/8 (8 kn speed) across the Rogue Smt. The W part of the mapped area comprises the water sampling stations indicated in Figure 22.

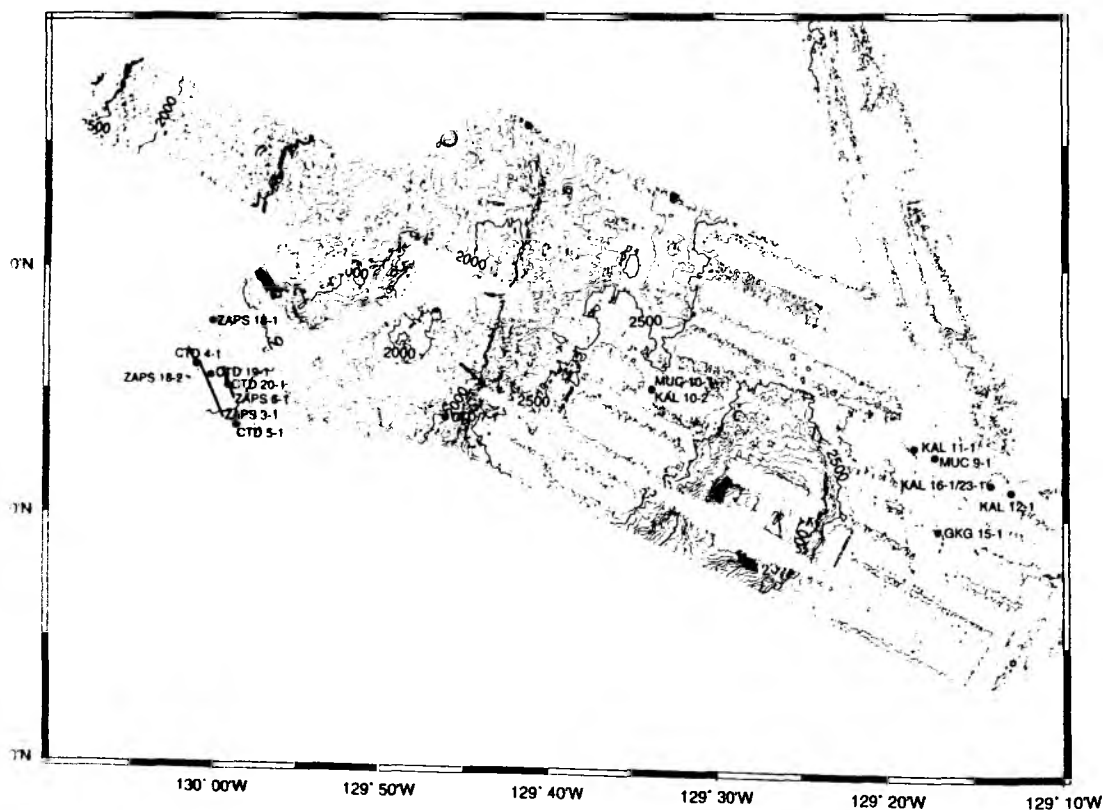


Fig. 19: Area of Axial Volcano with sampling stations in the caldera and the basins to the E. Black circles indicate stationary sampling methods. Lines indicate tracks of towed sampling facilities (ZAPS).

Rogue Seamount: Seamounts at the border between the Juan de Fuca plate and the Juan de Fuca ridge

The Axial Seamount is situated at the intersection between the NW striking Cobb-Eickelberg seamount chain and the NNE oriented Juan de Fuca ridge. This submarine volcano is regarded as the latest product of the Cobb hot spot (Johnson & Embley 1990), according to the high magma production, compared to normal ridge segments, and to the age

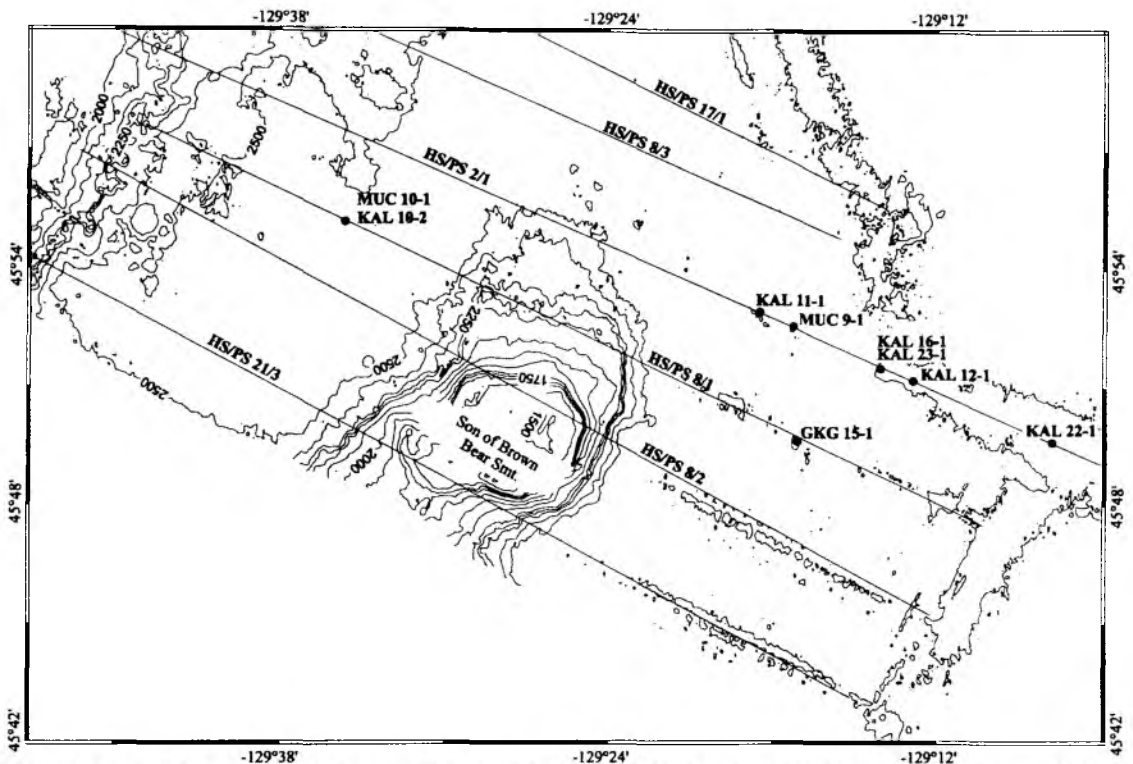


Fig. 20: Locations of sediment sampling stations to the West and East of the Son of Brown Bear Smt. and their setting on the HS/PS profiles 2/1 and 8/1.

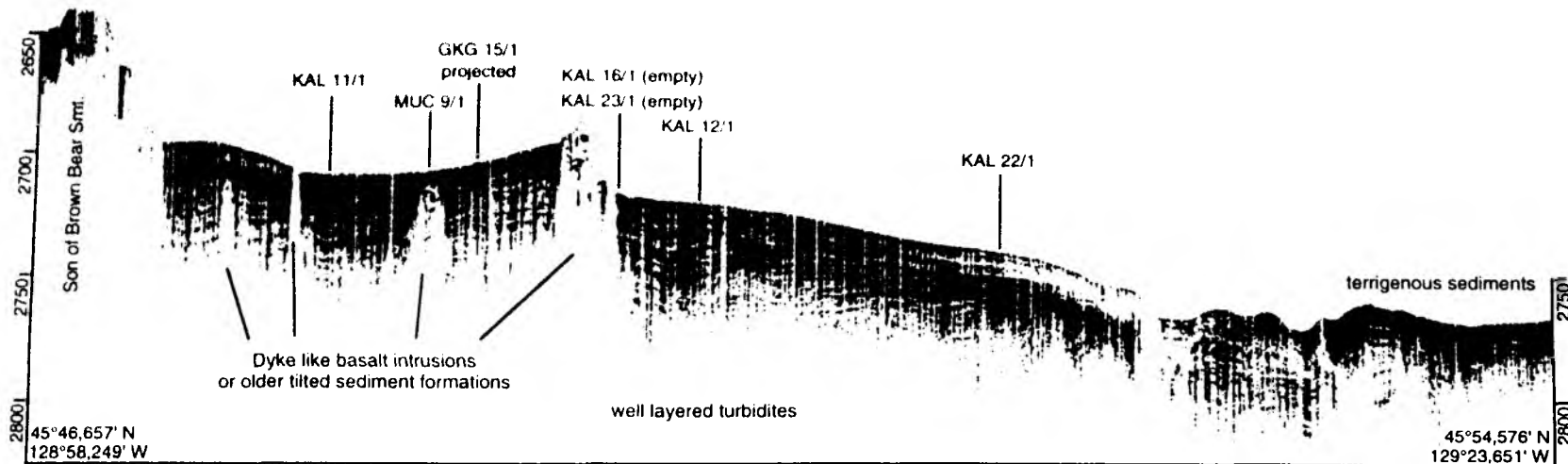
progression of this seamount chain (Desonie & Duncan 1990). Probably, the Axial Smt. marks the recent position of the Cobb hot spot. However, the geochemistry of Axial Smt. lavas is closer to N-MORB (Desonie & Duncan 1990, Rhodes et al. 1990).

Davis & Karsten (1986) and Desonie & Duncan (1990) related this phenomenon to the on-axis position of the Axial Smt. In accordance with the low lithospheric thickness below the ridge axis, they suppose a mode of magma generation characterized by relatively low pressures and high melting rates. Otherwise, Rhodes et al. (1990) suppose a thermal anomaly in the upper mantle rather than a geochemical heterogeneity to cause magma generation. Further, more dilution or mixing of hot spot related enriched magmas by depleted ridge magmas appears to be a possible mechanism.

The Juan de Fuca ridge (half spreading rate: 3 cm/a; Riddihough et al. 1984) is moving itself at a rate of approx. 2 cm/a to the W (Davis & Karsten 1986). Accordingly, the difference between the ages of a respective intraplate volcano and the hosting oceanic lithosphere increases in the same direction along the Cobb-Eickelberg seamount chain on the Pacific plate. Equally, the alkalinity of respective seamount lavas increases together with the distinctiveness of OIB-type geochemical signatures (Desonie & Duncan 1990). This particular applies to the lavas of the approx. 9 Ma Eickelberg Smt., which is just 2 to 3 Ma younger than its lithospheric base.

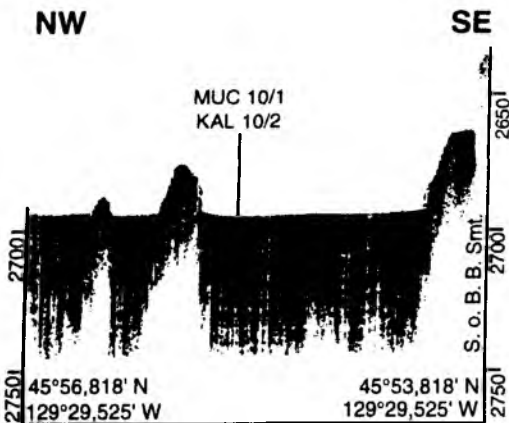
SE

NW



Parasound cross section : Station 2/1

a.



Parasound cross section : Station 8/1

b.

a.) Section of the HS/PS cross section 2/1 : Terrigenous sediments overlay well layered turbidites in the SE. At the NW end of the section the steep escarpment represents the onset of the slope of the Son of Brown Bear Seamount. Light colored, diapire-like structures which intrude the sediment layers may represent basalt intrusions or tilted older sediment formations. These structures could induce seawater convection through overlaying sediments. Positions of the gravity and box cores are indicated on the profile (station GKG 15/1 is projected).

b.) Section of the HS/PS cross section 8/1 : The basin between Juan de Fuca Ridge and S.o.B. Bear Smt. shows similar sediment structures to the ones we found E' of the S.o.B. Bear Smt..

On the Juan de Fuca plate, with the Son of Brown Bear, Rogue and Jinja seamounts, there exist only very few submarine volcanos, which could be related to the Cobb hot spot. If they were generated at an on-axis position, they must be older than the currently on-axis situated Axial Seamount. Otherwise, they might be related to a very recent near-axis volcanism. By analogy to the older seamounts of this chain, hosted by the Pacific plate, their lavas could be generated at lower melting rates, at a lower dilution by MOR-magmas, and could show a more complex history of fractionation, accordingly.

To check this assumption, first the morphology of the Rogue seamount was completely mapped during profile cruises 13-1 to 13-3 (Fig. 18, 23). Rogue Smt. is situated approx. 18 km perpendicular to the spreading axis. Assuming a constant half spreading rate of 3 cm/a, the oceanic lithosphere beneath the Rogue Smt. should be 0,6 to 1,0 Ma. old. The same applies to seamounts Son of Brown Bear and Jinja.

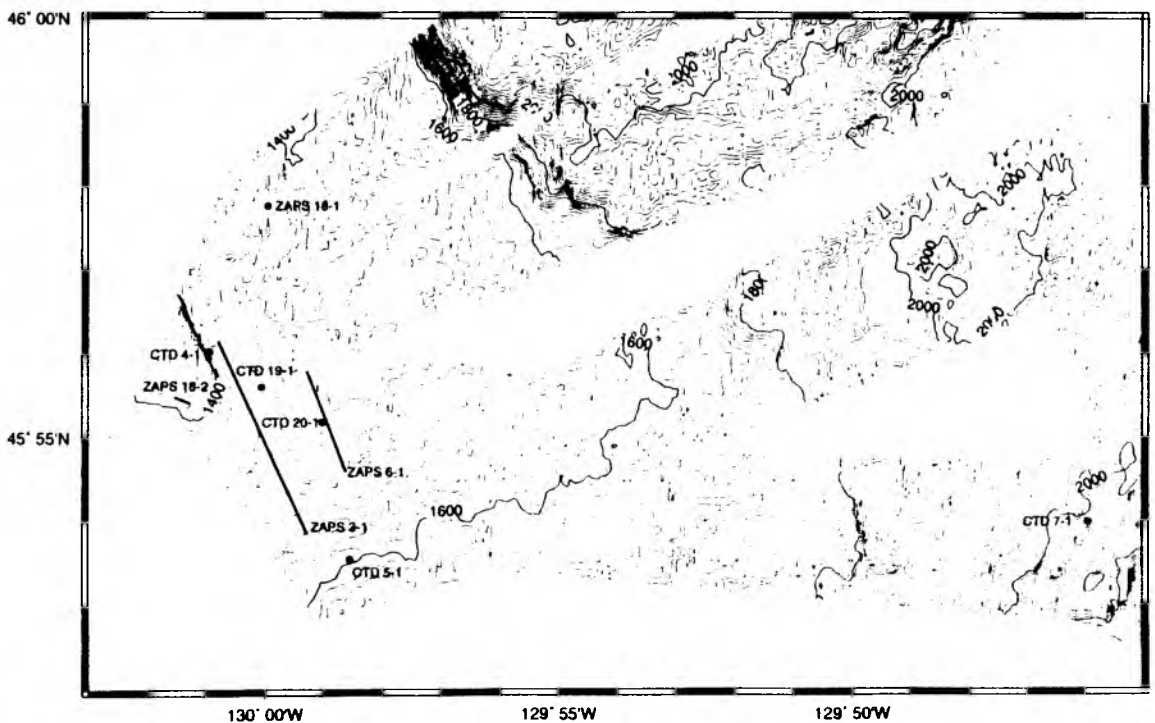


Fig. 22: Locations of water sampling to the East of Axial Volcano caldera. Black circles indicate stationary sampling methods. Lines indicate tracks of towed sampling facilities (ZAPS).

The bathymetric survey revealed for the base of the seamount an average water depth of 2650 m. The volcanic complex comprises a central cone and three smaller parasitic cones at least (Fig. 23). The base of the volcanic structure is oval shaped and NNW oriented, comprising an area of approx. 15 x 10 km. The respective cones display a nearly circular shape. The top of the central cone arises to 1820 m water depth. This top is situated on a

plateau, bordered by moderately dipping flanks, except the steeply inclined NNW flank. At the base of this NNW flank, there are sitting two parasitic cones with tops at 2360 and 2540 m, respectively. The third parasitic cone observed is situated at the SE margin of the oval complex, with the top lying at 2100 m water depth.

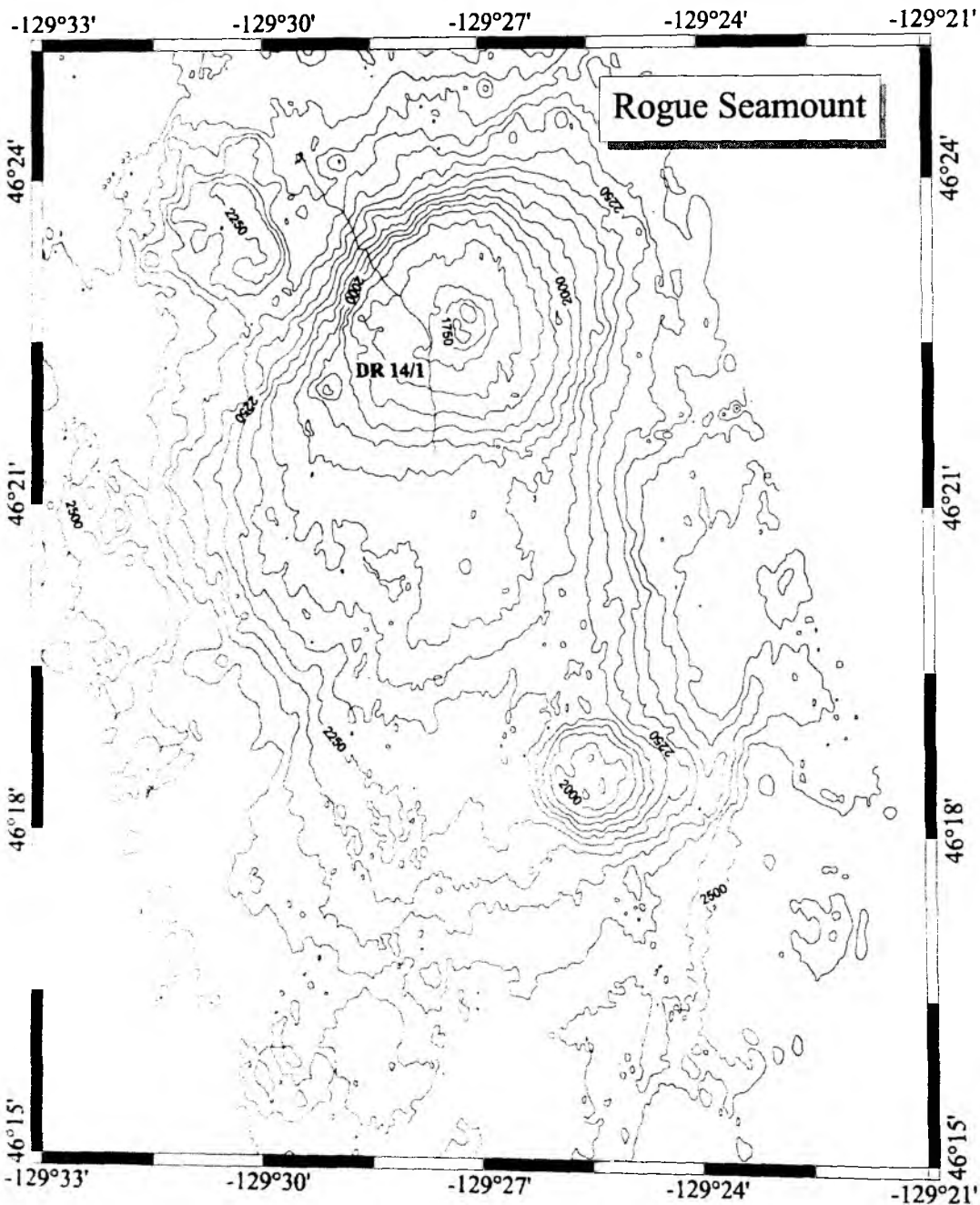


Fig. 23: Bathymetric map of Rogue Smt. with track of dredge 14-1.

The seamounts on both sides of the Axial seamount resp. the Juan de Fuca Ridge are differentiated in two morphological groups (compare to Sea Beam bathymetry of Embley et al. 1990). Brown Bear Smt. on the Pacific plate and Son of Brown Bear Smt. on the Juan de Fuca plate both display an elongate shape, oriented subparallel to the strike of the ridge

axis. Further, both seamounts are arranged symmetrical to the ridge axis, resp. to the Axial Smt. The latter has an elongate shape as well. These features might indicate, that Brown Bear Smt. and its smaller son on the Juan de Fuca plate, were - alike the Axial Smt. - generated primarily as comprehensive on-axis volcanic structure.

At Axial Smt., a linear stress field, as typical for spreading centre settings, is superimposed by a radial stress field, characteristic for oceanic intraplate volcanoes in turn (Embley et al. 1990). The volumetric bulk of lava erupts along two, about 70 km long rift zones to the N and S of Axial Smt. Their strike is strongly determined by the strike of the spreading centre.

According to the bathymetric data of Embley et al. (1990), Jinja Smt. and Newport volcano (situated 8 km NE of Jinja), both display a circular shape, pointing to the predominance of radial stress fields with no indications of linear stress components. Rogue Smt. shows an oval shape, however. As it strikes at an angle of 45° to the ridge axis, a genetic relation to the Juan de Fuca ridge seems improbable. Furthermore, the existence of a central and parasitic cones point to a mode of eruption distinctly differing from rift related submarine volcanism. It is suggested, that Rogue, Jinja, and Newport volcanic structures were generated in a near-axis setting, but outside of the ridge tectonic regime.

From the above follows the intriguing question, whether the apparent relationship between the tectonic setting and the morphology of the volcanic structures is significant, and if so, whether it is reflected in the geochemistry of lavas. By analogy to the geochemical

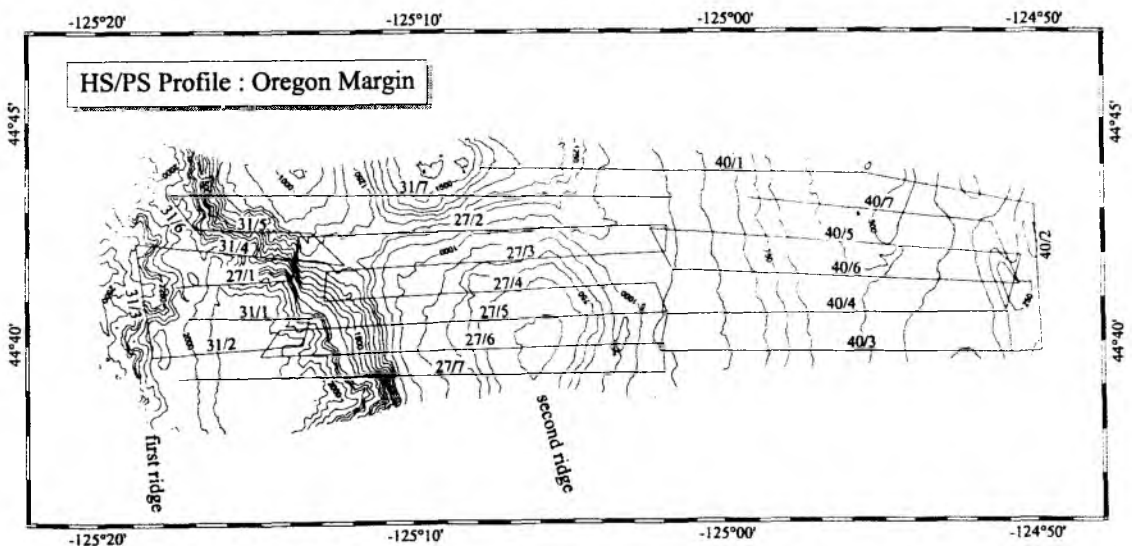


Fig. 24: Hydrosweep and Parasound profiles 27/1 through 40/7 crossing the First and Second Ridges on the Oregon Margin accretionary prism.

development of lavas of the Cobb-Eickelberg seamount chain (Davis & Karsten 1986, Desonie & Duncan 1990), the off-ridge seamounts of the Juan de Fuca plate should display a distinctly lower degree of dilution by magmas derived from depleted sources. The primary

magmas should be generated at significantly lower melting rates compared to Axial Smt. and Son of Brown Bear lavas. Accordingly, incompatible trace element concentrations and ratios

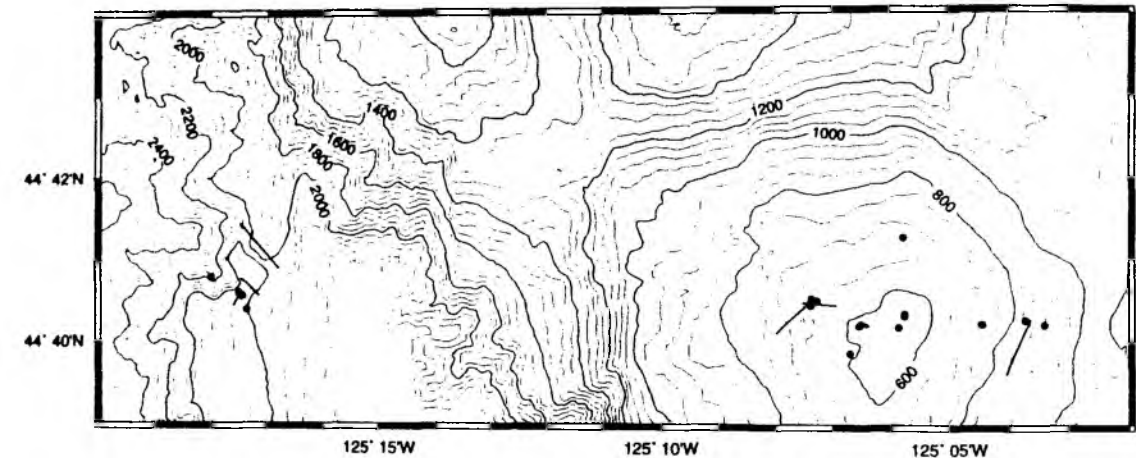


Fig. 25: Setting and Bathymetry of the two working areas on the Oregon Margin.

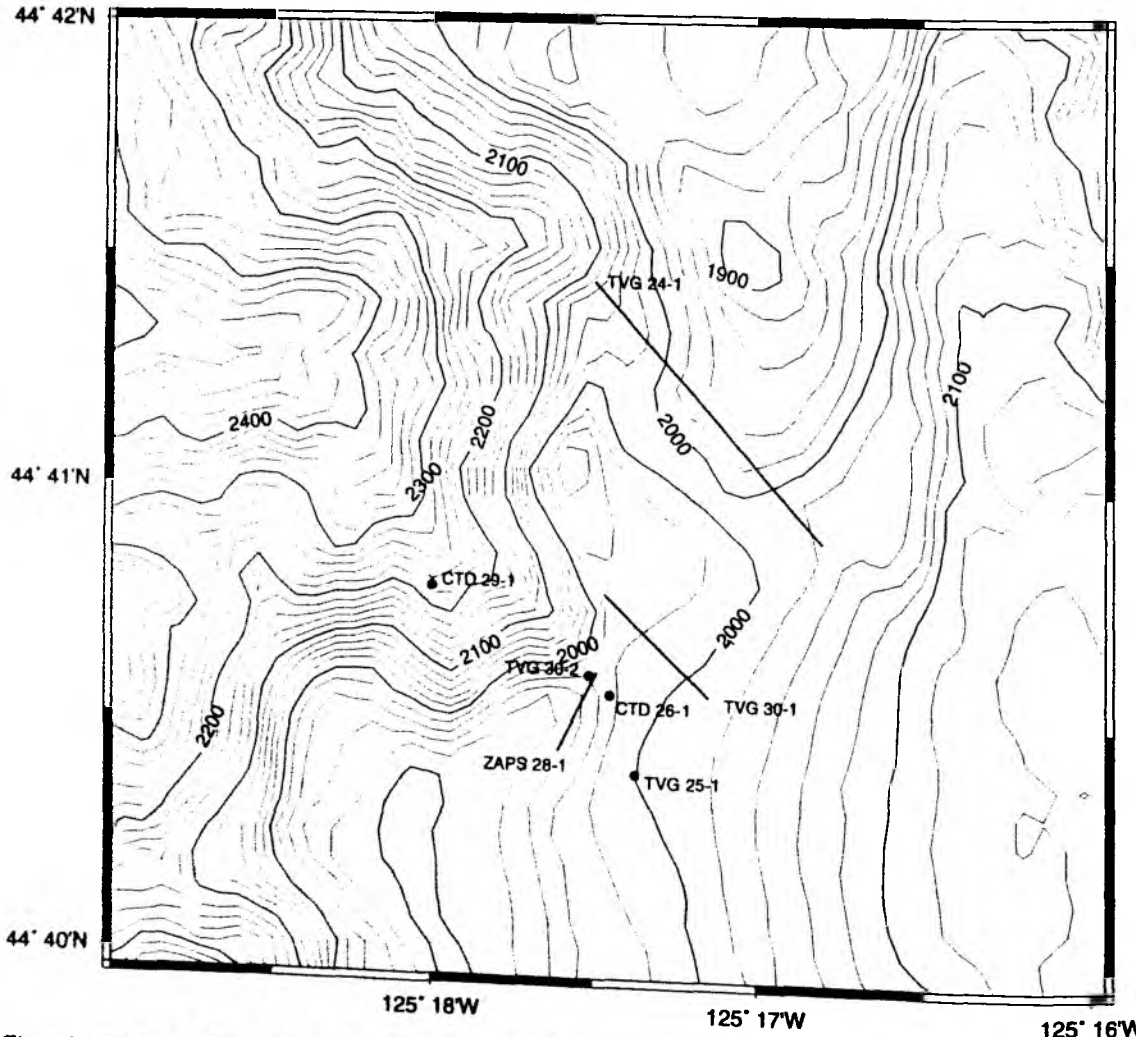


Fig. 26: Working area on the First Ridge with location of sampling stations: lines indicate towing tracks of TV-grab and the ZAPS-profile 28-1.

as well as radiogenic isotope ratios should display signatures typical for enriched magma sources.

This assumption makes systematic sampling of Juan de Fuca plate hosted seamounts worthwhile. A detailed sampling is lacking yet. During cruise SO109-1 sampling by dredging at the NW flank of Rogue Smt. was attempted. The safety cable had been broken resulting in an empty dredge, however.

Oregon Margin

Bathymetric mapping in the area of the Oregon margin included the First, Second and the W foothills of the Third Ridge of the Oregon accretionary prism (Fig. 24).

The First, most westward ridge, arises from 2500 to 2040 m water depth, forming the westward outline of a shallow southward extended basin. On the steep NW scarpe of this basin, a canyon-like structure is situated, which was chosen for the first working area (Fig. 25, 26).

The Second Ridge arises up to a water depth of 480 m. Due to the supposed outcropping of gas hydrates at the ridge surface numerous TV grab stations were deployed (Fig. 25, 27). The sediments of the Second Ridge are probably of Pliocene age (Westbrook et al. 1994). According to the structural dynamics of accretionary prisms, they are older than the sediments composing the First Ridge. The steep morphology and rough bottom surface inhibited deeply penetrating Parasound records. So, neither the landward dipping of layers nor the BSR outcrop at the top of the Second Ridge, as described by Westbrook et al. (1994), could be observed.

Astoria Canyon

Target of the Hydrosweep records in the valley bottom area of the Astoria Canyon was the location of fault zones, striking parallel to the slope of the Oregon Margin. These cause identifiable lateral displacements or otherwise related modifications of the canyon morphology. Such fault zones are preferred dewatering pathways of the accretionary prism. Their surficial reflection could be enhanced vent activities.

As the transit route to Victoria yielded just one profile, no reliable indications of faulting could be gained. However, the Hydrosweep profile (Fig. 28) may represent a foundation for further spatially adjoining bathymetric investigations.

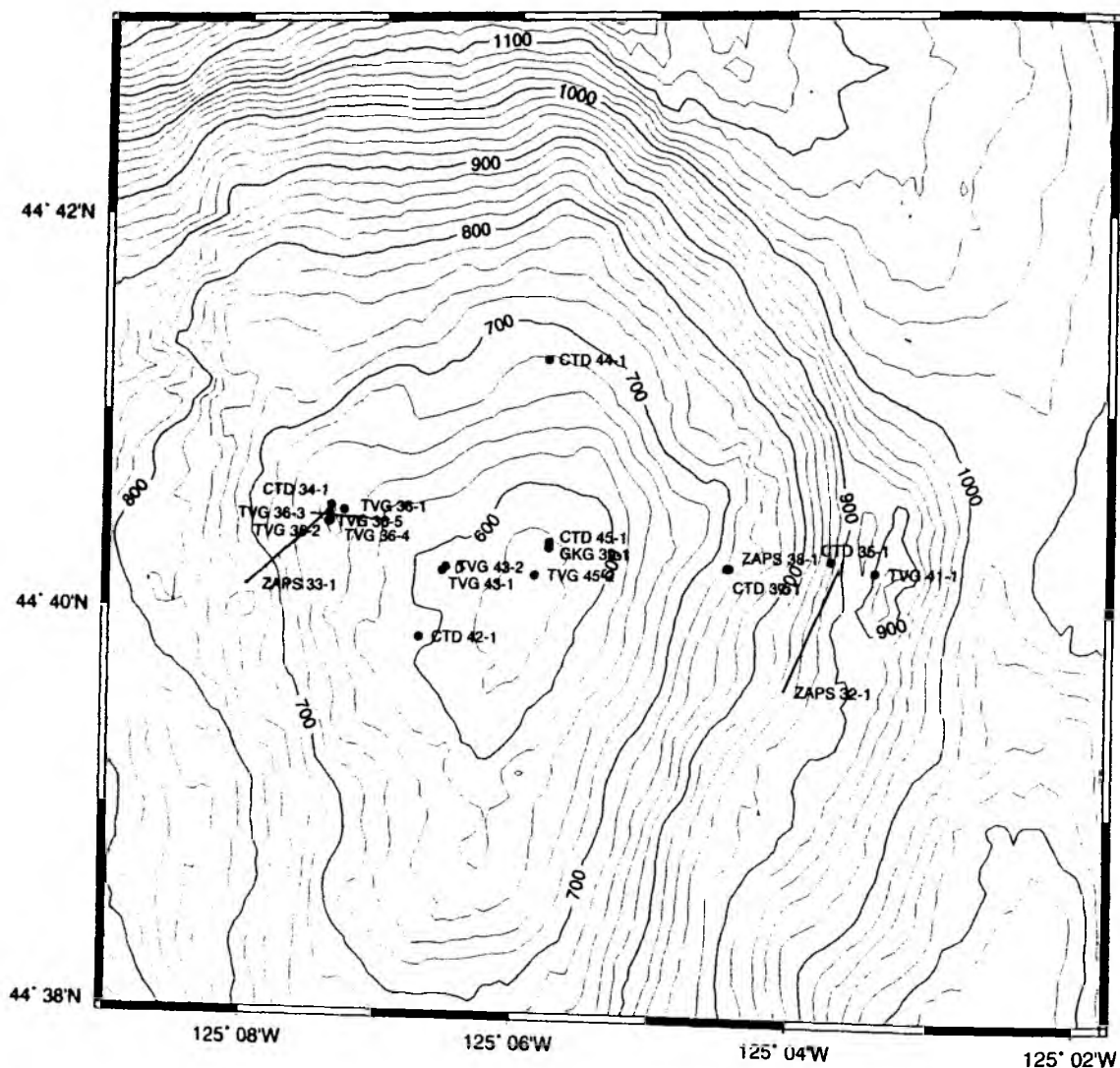


Fig. 27: Working area on the Second Ridge with location of sampling stations: lines indicate towing track of TV-grab 36-3 and ZAPS-profiles.

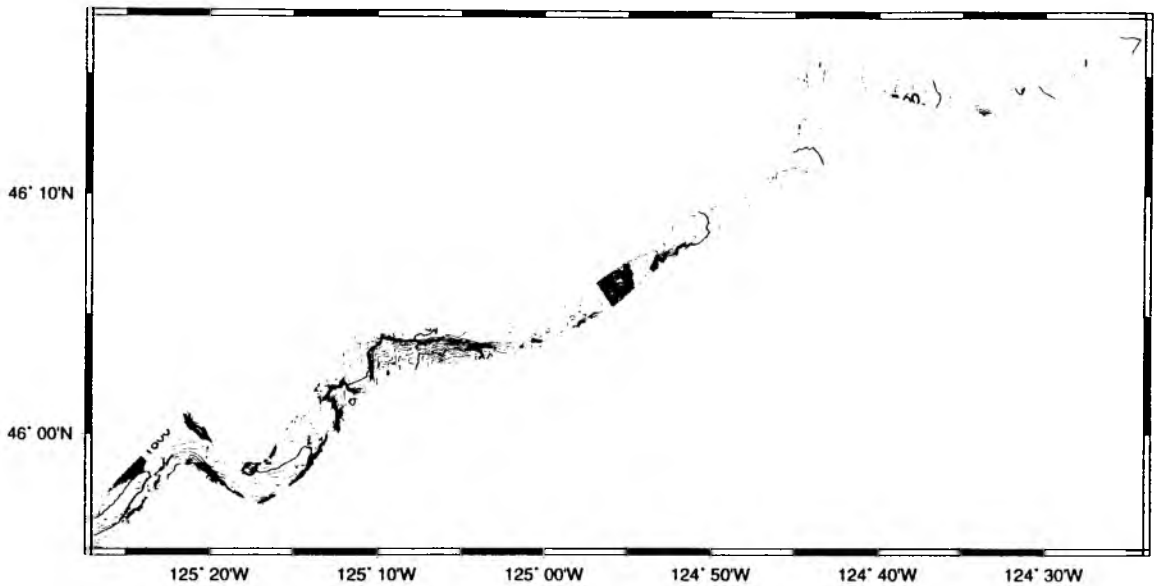


Fig. 28: Cruise track in the Astoria Canyon area and bathymetry.

References

- Davis, E.E. & J.L. Karsten (1986): On the cause of the asymmetric distribution of seamounts about the Juan de Fuca ridge: ridge-crest motion over a heterogeneous athenosphere. *Earth Planet. Sci. Lett.* 79, pp. 385-396.
- Desonie, D.L. & R.A. Duncan (1990): The Cobb-Eickelberg seamount chain: hotspot volcanism with mid-ocean ridge basalt affinity. *J. Geophys. Res.* 95, pp. 12697-12711.
- Embley, R.W., K.M. Murphy, C.G. Fox (1990): High-resolution studies of the summit of Axial Volcano. *J. Geophys. Res.* 95, pp. 12785-12812.
- Johnson, H.P. & R.W. Embley (1990): Axial Seamount: An active ridge axis volcano on the central Juan de Fuca ridge. *J. Geophys. Res.* 95, pp. 12689-12696.
- Rhodes, J.M., C. Morgan, R.A. Liias (1990): Geochemistry of Axial Seamount lavas: magmatic relationship between the Cobb hotspot and the Juan de Fuca ridge. *J. Geophys. Res.* 89, pp. 12713-12733.
- Riddihough, R.P. (1984): Recent movements of the Juan de Fuca plate system. *J. Geophys. Res.* 89, pp. 6980-6994.
- Westbrook, G.K., B. Carson, R.J. Musgrave et al. (1994): Site 892, *Proc. ODP Init. Repts. Vol 146 Part I*, pp. 301-305.

3.4.4 Sediment Sampling and Sedimentology

by Nicole Biebow, Mark Finke, Jens Greinert, Susann Kinsey, Heike Preissler and Marcus Schäfer

During RV Sonne cruise SO109-1 sediment sampling was carried out along the eastern flank of the Juan de Fuca Ridge and at the Oregon subduction zone. The main objective of sediment sampling along the Juan de Fuca Ridge was to determine the effects of hydrothermal fluid venting on sediment chemistry.

Sampling at the Oregon subduction zone area was carried out in potential vent areas to clarify vent phenomena.

Table 3: Sediment sampling during SO109-1 cruise.

(n = number of tubes, N = nutrients in porewater, M1 = methane (syringe), M2 = methane (bags), M3 = methane (fabric bag), PP = physical properties, T = trace elements, L = lipids, D = dinoflagellate cysts, A = archive; numbers indicate number of tubes/number of samples.

Stat. No.	Instr.	n	Core length (cm)	N	pH	M1	M2	M3	PP	T	L	D	A
1-3	MUC	6	23-30	1/15 1/15	1/22	-/-	1/5	-/-	1/22	-/-	-/-	1/6	1/23
1-4	KAL	1	444	24	24	14	7	-/-	23	14	8	-/-	-/-
9-1	MUC	0	-/-	-/-	-/-	-/-	-/-	-/-	-/-	-/-	-/-	-/-	-/-
1 bag + suspension samples													
10-1	MUC	0	-/-	-/-	-/-	-/-	-/-	-/-	-/-	-/-	-/-	-/-	-/-
10-2	KAL	1	369	24	24	24	10	-/-	20	10	9	-/-	-/-
11-1	KAL	1	462	34	34	15	-/-	9	23	17	8	-/-	-/-
12-1	KAL	1	447	27	27	11	-/-	10	25	13	11	-/-	-/-
14-1	DR	0	-/-	-/-	-/-	-/-	-/-	-/-	-/-	-/-	-/-	-/-	-/-
15-1	GKG	1	32	10	10	-/-	-/-	-/-	8	3	-/-	1	-/-
16-1	KAL	0	-/-	-/-	-/-	-/-	-/-	-/-	-/-	-/-	-/-	-/-	-/-
22-1	KAL	1	603	26	26	12	12	10	13	18	12	-/-	-/-
Additional from the set of weight: 5 porewater + pH samples													
23-1	KAL	0	0	-/-	-/-	-/-	-/-	-/-	-/-	-/-	-/-	-/-	-/-
24-1	TVG	0	-/-	-/-	-/-	-/-	-/-	-/-	-/-	-/-	-/-	-/-	-/-
25-1	TVG	0	0	3	3	4	2	-/-	-/-	3	-/-	-/-	-/-
All clams, sediment > 63µm. 1 bag unconsolidated sediment + H ₂ S													
30-1	TVG	0	-/-	-/-	-/-	-/-	-/-	-/-	-/-	-/-	-/-	-/-	-/-
30-2	TVG	4	25-29	1/16	1/16	-/-	-/-	-/-	1/10	1	2	-/-	-/-
36-1	TVG	3	19-25	1/14 1/11	1/14 1/11	-/-	-/-	4	-/-	1	1	-/-	-/-
36-2	TVG	2	28-30	1/12	1/12	-/-	-/-	-/-	-/-	1	1	-/-	-/-
36-3	TVG	0	-/-	-/-	-/-	-/-	-/-	-/-	-/-	-/-	-/-	-/-	-/-
36-4	TVG	1	34	1/13	1/13	2	9	2	-/-	1	-/-	-/-	-/-
36-5	TVG	1	22	1/9	1/9	2	1	4	-/-	1	-/-	-/-	-/-
39-1	GKG	0	-/-	-/-	-/-	-/-	-/-	-/-	-/-	-/-	-/-	-/-	-/-
41-1	TVG	0	0	3	3	2	2	2	-/-	2	-/-	-/-	-/-
43-1	TVG	2	19-21	1/9 1/8	1/9 1/8	3	4	4	-/-	2	4	-/-	-/-
All clams													
43-2	TVG	1	20	1/9	1/9	2	5	4	-/-	2	2	-/-	-/-
45-2	TVG	0	0	5	5	2	4	2	-/-	1	-/-	-/-	-/-

Sediment was sampled with 3 multicorers (MUC), 2 box corers (GKG) , 7 kasten corers (KAL) and 10 TV-grabs (TVG). Number of samples and sample types are documented in Table 3. Apart from the samples for geochemical investigations, which were processed directly on board, samples for the determination of physical properties are of special interest. Water content and density will be determined from this samples at the GEOMAR laboratory. These samples will also be used for TOC and carbonate analyses. Additional samples from each core were taken as archive samples for several investigations at GEOMAR. Sample records were drawn up from every station and will be archived at GEOMAR.

Along the eastern flank of the **Juan de Fuca Ridge** intense geological sampling was carried out with MUC, GKG and KAL spanning water depths between 2600 and 2800 m. Fig. 29 shows the general lithology of the sediment cores and gives an impression of the facies distribution.

The surface and subsurface sediments of KAL 1-4 consist of gray diatom-bearing muds. Several turbidity sequences, which consist of terrigenous mud with dark gray sandy silts at the bottom, are following below. The carbonate content of the sediments increases with increasing depth and gray nannofossil muds were observed.

Sediments of KAL 10-2 are also characterized by several turbidity sequences containing sandy silts at their bottom. The upper meter of this core consists of gray terrigenous muds followed by nannofossil muds below.

The sediment cores KAL 11-1 and 12-1 contain several turbidity sequences, of which the grain size increases from top to base. The turbidity sequences are build of terrigenous muds with dark gray sandy to silty layers at the bottom.

Surface and subsurface sediments of GKG 15-1 are dark brown diatom oozes, changing into diatom bearing muds with increasing depth. The base of this core consists of greenish gray foraminifera- and nannofossil bearing muds.

Sediment core KAL 22-1 provided 620 cm of sediment and is the longest core achieved during SO109-1 cruise. Sediments of this core are carbonate rich and consist of foraminifera bearing muds in the upper part changing into greenish gray nannoplankton muds with increasing depth (see Appendix 2).

In the **Oregon subduction zone** study area only TV-grabs were used for geological sampling, because it is the best device for sediment sampling and sampling of specific hard rocks in vent areas.

TV-grabs 30-2 to 41-1 were dropped near vent sites, but did not contain any living bivalves, though a rich fauna of already dead vent organisms, like *Calytogenia* spp., *Solemya* spp. and pogonophorans. Several carbonate precipitates, which were covered by vent organisms and metal sulfids were sampled. The sediments of TV-grabs 30-2 to 41-1 consist of gray terrigenous muds.

Juan de Fuca Ridge

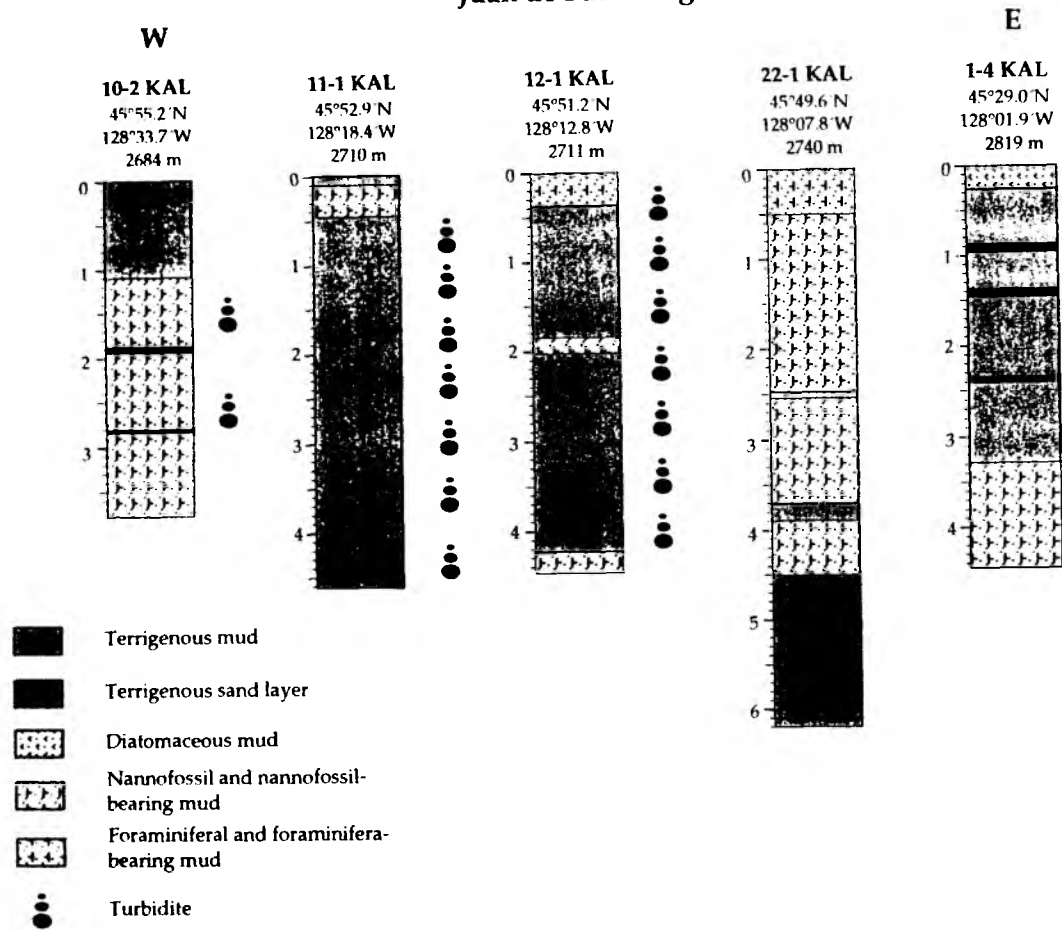


Fig. 29: Lithological composition of the sediment cores

TV-grab 43-1 was the first device during SO109-1 cruise which was dropped at a active vent site. Several gas bubbles were observed already during heaving of this device. An intense smell of H_2S made a sampling with gasmasks neccessary.

The TV-grab contained gas hydrates of which one sample was taken. Several living clams of the genus *Calypptogena* were sampled. All individuals were of the same size, which indicates that these organisms settled at this vent site at the same time.

Few bivalves of the genus *Solemya* were observed and sampled. TV-grab 43-1 contained also carbonate precipitates and metal sulfids.

TV-grabs 43-2 and 45-2 were also characterized by a slight smell of H_2S , although living bivalves were not observed. Several dead species of the genus *Calypptogena* and *Solemya* were sampled. Several fragments of mudstones, carbonate precipitates and metal sulfids were collected.

3.4.5 Pore water studies

by Dirk Rickert, Harry Elderfield, Anke Bleyer, Bettina Domeyer and Stephan Lammers

Introduction

Pore waters were sampled from cores taken on the eastern flank of the Juan de Fuca Ridge in order to study hydrothermal circulation through mid-ocean ridge flanks. The hydrothermal circulation at flanks is driven by heat from the cooling lithosphere which is transferred ultimately to sea water by a combination of conduction and advection, although the relative importance of the two processes is unknown.

The main aim of the work was to evaluate the mode of heat transport and advective velocity using chemical gradients in pore waters using the approach of Wheat and Mottl (1994). Mg is a key variable as it is known to be extracted from sea water by reaction with basalt. Other pore water constituents are important for determining other aspects of the circulation of sea water through the sediments and for evaluating diagenetic processes. Samples were also taken for laboratory studies of $^{87}\text{Sr}/^{86}\text{Sr}$ ratios of the pore waters in order to evaluate low temperature extraction of Sr from oceanic crust which provides a means to balance the oceanic Sr isotope budget (Elderfield and Schultz, 1996).

Hemipelagic sediments are, in general, characterized by rapid burial of organic matter with the consequence that pore waters are enriched in the products of organic matter metabolization which may be used to evaluate the redox status of sediments. A second objective of the pore water programme was, therefore, to evaluate organic matter metabolization within the sediments through concentrations of "nutrient species".

The sediments in this region are deposited in an area characterized by significant basement outcrop and buried ridges which form ponded basins. From work at about 2°N of the study area, it has been estimated that sediment cover is typically 30-100 m along the crest of ridges and 200-600 m in the adjoining basement troughs (Davis et al., 1989; Wheat and Mottl, 1994). Because of rapid turbidite sedimentation from the North American margin, the ridge flank becomes more rapidly sealed to advection than at most ocean ridge settings (Davis et al., 1992).

Samples

Sediment samples were taken from the cores listed in Table 4 using syringes inserted into the core. Immediately it was retrieved and transferred to the geology laboratory on board R.V. SONNE. Pore waters were extracted at 4 °C in the cold room of the ship using a polypropylene squeezer pressurised by argon and samples were filterered on line through 0.4 mm cellulose acetate membrane filters.

The analytical techniques used on board to measure the various dissolved constituents are listed in Table 5. Concentrations of dissolved nitrate, phosphate, silicate and ammonia were

determined using an autoanalyser working with standard photometric procedures. pH electrodes were used for the determination of pH and alkalinity and were calibrated using buffers prepared in artificial seawater (Dickson, 1993). BIS and 2-Aminopyridine were used as buffers in the neutral pH range (pH 7 to 9). Ca and Mg were determined by EGTA/EDTA titrations and chloride by Mohr titration. Some samples from cores 109-36-2A, 109-43-1A and B had very high H₂S concentrations and it is thought that this underestimated Cl determinations.

Table 4: Cores analysed for porewater chemistry

Station/core	Lat. (N)	Long. (W)	water depth (m)
109-1-3 MUC	45°29.084'	129°02.050'	2850
109-1-4 KAL	45°29.022'	129°01.866'	2819
109-10-2 KAL	45°55.192'	129°33.656'	2684
109-11-1-KAL	45°52.934'	129°18.378'	2710
109-12-1 KAL	45°51.182'	129°12.935'	2711
109-15-1 GKG	45°49.618'	129°17.029'	2705
109-22-1-KAL	45°49.628'	129°07.805'	2740
109-30-1-TVG	44°40.780'	125°17.470'	2091
109-36-1A/B-TVG	44°40.770'	125°07.110'	690
109-36-2A/B-TVG	44°40.470'	125°06.720'	649
109-36-4-TVG	44°40.460'	125°07.170'	678
109-36-5-TVG	44°40.420'	125°07.090'	667
109-43-1A/B-TVG	44°40.350'	125°06.180'	625
109-43-2-TVG	44°40.170'	125°06.530'	619

The length of the cores, the number of samples taken from each core and the types of analyses performed onboard are shown in Table 6. Subsamples were also taken for shore-based analysis of ⁸⁷Sr/⁸⁶Sr ratios. In addition to pore water sampling, sediment samples were taken for porosity and smear slides (see Section 3.4.4) and for methane analysis (see Section 3.4.2).

Results

Results are listed in Appendix 3-6 and depth profiles of chemical constituents of the pore waters are illustrated in Figures 30-32.

Multicorer (MUC)/Box Corer (GKG) (Fig. 30)

The multicorer core 109-1-3 shows silicate concentration increasing as a consequence of diagenesis from bottom water values of about 200 mM to a constant value of just in excess

Table 5: Techniques used for pore water analysis

Constituent	Method	Reference
Alkalinity	2-point titration	Van der Berg and Rogers (1987)
pH	2-point titration	Van der Berg and Rogers (1987)
Ammonium	spectrophotometry	Grasshof et al. (1983)
Calcium	EDTA titration	Gieskes et al (1991)
Magnesium	EGTA titration	Gieskes et al (1991)
Phosphate	autoanalyser	Grasshof et al. (1983)
Silicate	autoanalyser	Grasshof et al. (1983)
Nitrate	autoanalyser	Grasshof et al. (1983)
Chloride	Mohr (AgNO ₃)titration	Gieskes et al (1991)
Hydrogen sulphide	spectrophotometry	Grasshof et al. (1983)

of 400 mM below 4.5 cm. Nitrate decreases as a result of denitrification to zero at the base of the core (defining the onset of suboxic conditions) and > 2 mM of ammonia are detected below about 8 cm. Phosphate increases slightly and alkalinity by about 0.6 mM. All these changes are associated with the oxidation of organic matter. There are no detectable changes in either Mg or Ca.

The box core 109-15-1 shows an upper suboxic (denitrification) 15 cm layer where phosphate increases and nitrate decreases. Ammonia concentrations are not zero in this layer but do increase below it.

Table 6: Number of samples taken from each core and types of analyses performed

Core	length of core (cm)	no. of samples	analyses*
109-1-3 MUC	22	16	S P N O N M C A p
109-1-4 KAL	430	23	S P N O N M C A p
109-10-2 KAL	365	24	S P N O N M C A p
109-11-1 KAL	460	34	S P N O N M C A p
109-12-1 KAL	450	29	S P N O N M C A p Cl
109-15-1 GKG	21	10	S P N O N M C A p
109-22-1 KAL	600	30	S P N O N M C A p
109-30-1 TVG	18	13	S P N O N A p
109-36-1A/B TVG	24	11 + 12	S P N O N A p
109-36-2A/B TVG	20	9 + 9	S P N O N A p H
109-36-4 TVG	34	13	S P N O N A p M C
109-36-5 TVG	22	9	S P N O N A p
109-43-1A/B TVG	21	9 + 8	S P N (A) p M H Cl
109-43-2 TVG	22	9	S P N O N A p

*S=SiO₂, P=PO₄, NO=NO₃, N=NH₄, M=Mg, C=Ca, A=alkalinity, p=pH, Cl=Cl, H=H₂S

Kastencorer (KAL) (Fig. 31)

Core 109-1-4 KAL was taken at the same site as 109-1-3 MUC and shows evidence of increasing dissolved metabolite concentrations of diagenetic origin. Phosphate increases to 60 mM and ammonia to 150 mM (but the DN/DP ratio of about 2.5 is much lower than that for marine organic matter). Nitrate is close to zero as expected (but erratic), but interestingly increases below 250 cm. There is a corresponding small but significant decrease in silicate to values below 300 mM. Alkalinity is low throughout the core. Mg concentrations show a very slight decrease with depth.

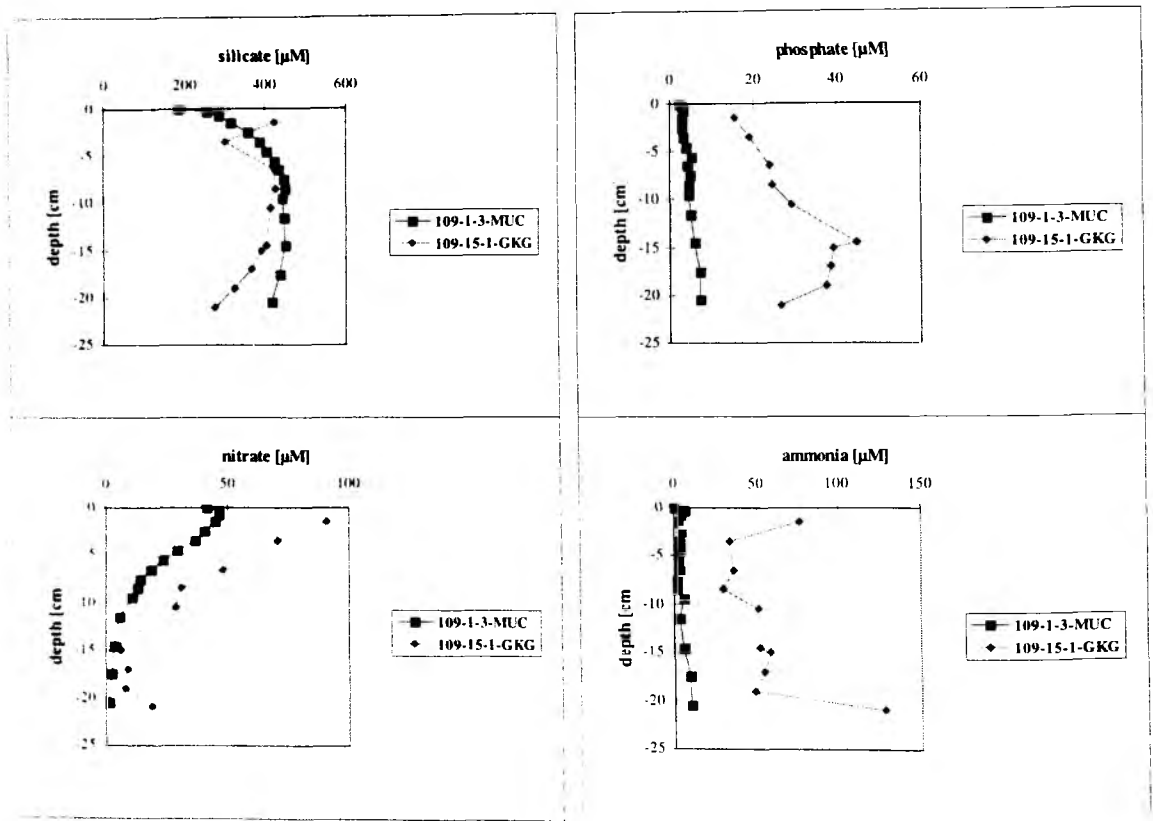


Fig. 30: Profiles of geochemical analyses on multicorer (MUC) and box corer (GKG) sediment pore waters

The pore waters at Core 109-10-2 KAL are characterised by rather constant concentrations of silicate, phosphate and nitrate upon which are seen small peaks of elevated concentrations. These may be associated with the presence of turbidite layers throughout the core. Ammonia increases regularly with depth. There are no detectable changes in Mg. At Core 109-11-1-KAL is evidence of denitrification within the upper 50 cm of the sediment at this site, which is surprising as, visually, the sediment appeared similar to the other cores. With the exception of ammonia, depth profiles of the metabolites tend to show "noisy" profiles which may be a reflection of turbidite layers within the sediments. Magnesium shows a small but significant decrease in concentration with depth.

As with the previous there is some evidence of denitrification at the core top of 109-12-1 KAL but values fall to zero below 200 cm. This core shows the strongest Mg depletion of about 8 % from sea water values to about 50 mM at the base of the core. This is evidence of extraction of Mg by reaction of basement fluids with the oceanic crust. Chloride shows a small increase in concentration with depth at this site.

Phosphate and nitrate are low in pore waters from Core 109-22-1-KAL. Silicate shows a small decrease from a maximum of about 400 mM which is typical for all sites cored. Mg shows a small decrease with depth.

TV grabs (Fig. 32)

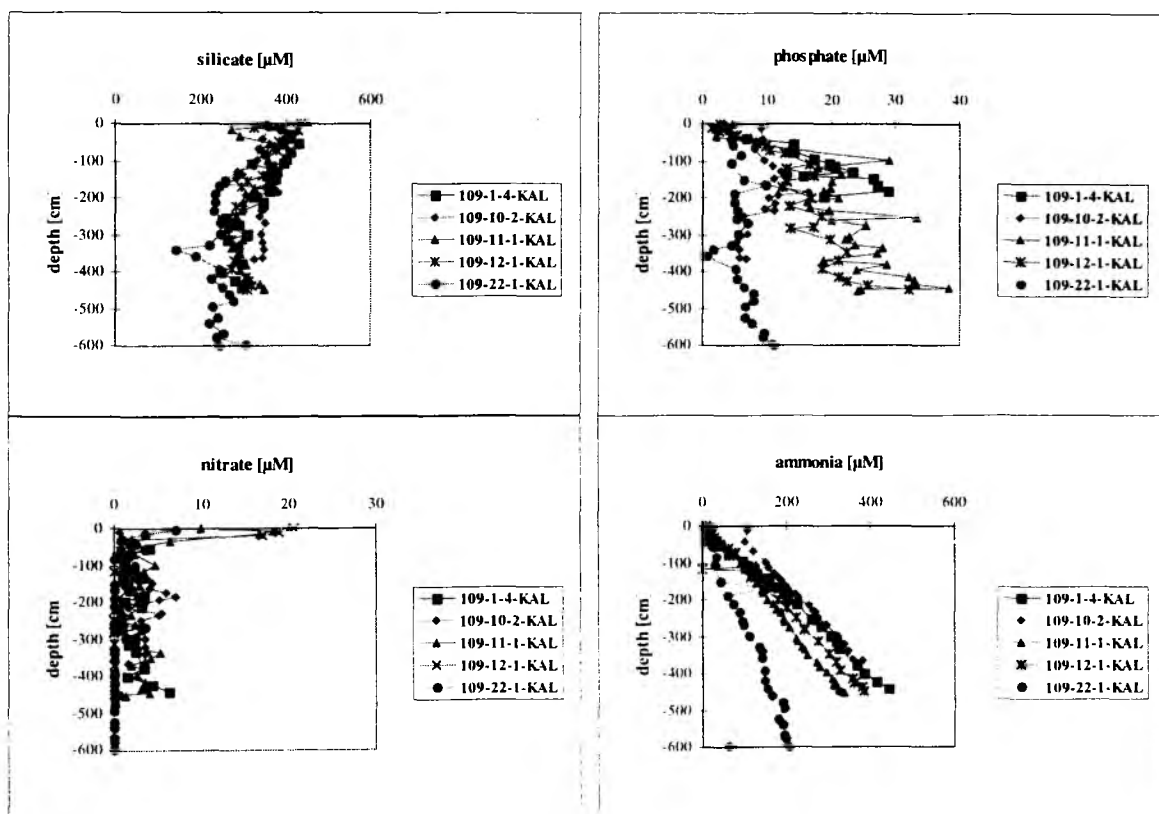


Fig. 31: Profiles of geochemical analyses on kastencorer (KAL) sediment pore waters

Surface sediments taken with a TV grab and cored with multicorer tubes reflect the upper 30 cm of sediments at these sites. Silicate concentrations reach highest values (500 mM) at depth in core 109-30-1-TVG. All other cores show more or less Si increases with a maximum at about 20 cm depth with concentrations of just in excess of 300 μM and Si decrease below. Nitrate decreases close to zero at the base of the cores as a result of denitrification in deeper suboxic layers. Surprisingly high and constant values were obtained in core 109-36-2B. Nitrate was not measured in cores of high H₂S values. Ammonia increases regularly with depth throughout the cores and shows highest concentrations in core 109-G 43-1 A. A corresponding increase in alkalinity, pH and H₂S profiles is recorded. Core 109-43-1B shows

the same relationship between high H_2S concentrations and high values for alkalinity. Low values for alkalinity were recorded in core 109-36-2A regardless of very high H_2S concentrations (up to 20 mM). Increasing ammonia and H_2S concentrations up to 18 mM in core 109-43-1A indicate typical anoxic conditions. Greater solubilities of silica tests as a consequence of pH increasing from 7.8 up to 8.4 causes a strong gradient in silicate profile between 9 and 15 cm. Phosphate concentrations tend to increase with depth throughout the cores but often show "noisy" profiles.

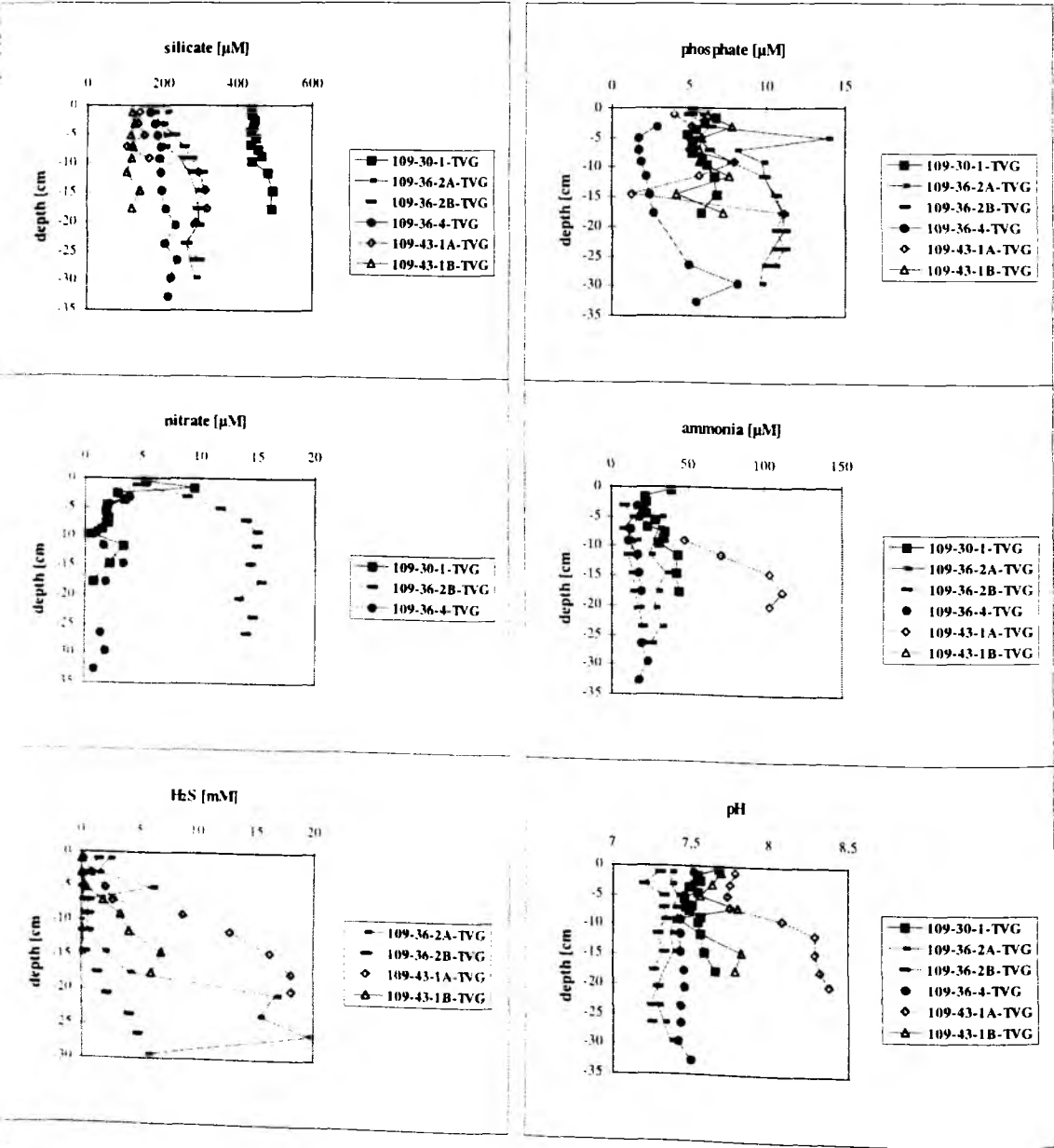


Fig. 32: Profiles of geochemical analyses on TV grab (TVG) sediment pore waters

Discussion

Evidence for basement flow

Mg concentrations in some of the cores were indistinguishable from normal seawater values over the length of the cores. This indicates either that there is no fluid flow from the basement or that there is flow and the concentration of basement fluids is similar to that of seawater. In other cores, Mg profiles show small but significant decreases with depth. This shows that seawater is flowing vertically through the sediment. The core with the largest Mg depletion also shows a small enrichment in Cl. This is due in part to the influence of glacial seawater (up to 4% higher Mg and Cl) and in part to hydration of the oceanic crust.

Further chemical and isotopic analyses will constrain the extent of reactions between basement and sea water and the rates of fluid advection in this region.

Evidence for organic matter diagenesis

All cores show metabolite profiles typical of oxic, suboxic and anoxic diagenesis. This is best seen by means of nitrate and ammonia profiles through (i) an increase in concentration with depth indicating oxidation of organic matter by oxygen, (ii) a decrease with depth, indicating oxidation by nitrate, and (iii) zero nitrate and increasing ammonia, indicating anoxic conditions. In general, the depths of the zones are about 0-2 cm, 2-15 cm and >15 cm but there are complications in this interpretation, principally the presence of ammonia in higher sections of some cores.

Silicate profiles of *109-1-3 MUC*, *109-15-1 GKG* and *TV grab cores* are typical in showing an increase from bottom water values to a constant value of about 200-400 mM below which concentration remain approximately constant. Atypically the silicate profiles of all kasten cores show a decrease from bottom water values of 350-450 mM to values of 250-350 mM at the top.

The metabolite stoichiometry seen in the pore water profiles is also of interest. In the short core *109-1-3 MUC* the DN/DP of about 15 is typical for marine organic matter but in core *109-15-1 GKG* DN/DP is about 2 and significant amounts of ammonia are present. Although it may be inferred from Si data that the sediment surface was collected intact in *109-1-3 MUC* (bottom water Si is about 180 mM and that in the core top was 184 mM) the maximum porewater nitrate is only about 35 mM. In contrast, in *109-15-1 GKG*, maximum nitrate values (66 mM) are slightly higher than for oxic oxidation of organic matter (for example, oxidation of $C_{106}N_{16}P_1$ by $138 O_2$ yields 23 mM plus bottom water NO_3 of 38 mM = 61 mM) but the evidence from Si profile is that the core surface was not collected. Comparison with SCO_2 should address this problem.

The role of turbidites

In several of the pore water profiles there is evidence of small maxima imposed upon otherwise smooth curves of changing concentration with depth. A good example of this is seen in the nitrate and phosphate data from core 109-10-2 KAL. Visually, the sediment cores are characterised by the presence of turbidite layers (some of which appear to be associated with redox fronts) and this may offer an explanation for the pore water anomalies. However, it will first be necessary to make detailed comparison of such anomalies with information from the core logs.

References

- Davis, E.E., Chapman, D.S., Forster, C.B. and H. Villinger, 1989. Heat-flow correlated with buried basement topography on the Juan de Fuca Ridge flank. *Nature*, 342, 533-537.
- Davis, E.E., Chapman, D.S., Mottl, M.J., Bentkowski, W.J., Dadey, K., Forster, C., Harris, R., Nagihara, S., Rohr, K., Wheat, G. and M. Whitarcar, 1992. Flank flux: an experiment to study the nature of hydrothermal circulation in the young oceanic crust. *Can. J. Earth. Sci.*, 29, 925-952.
- Dickson, A.G., 1993. pH buffers for sea water media based on the total hydrogen ion concentration scale. *Deep Sea Res.* 40, 107-118.
- Elderfield, H. and A. Schultz, 1996. Thermal and chemical fluxes at mid ocean ridges and the chemical composition of the ocean. *Ann. Rev. Earth. Planet. Sci.*, 44.
- Gieskes, J.M., Gamo, T. and H. Brumsack, 1991. Chemical methods for interstitial water analyses on Joides Resolution. Ocean Drill. Program, Texas A&M Univ., College station.
- Grasshof, M., Ehrhardt, K. and K. Kremling, 1983. *Methods of seawater analysis*, 2nd edition, Verlag Chemie, Weinheim, 419pp.
- Van der Berg, C. and H. Rogers, 1987. Determination of alkalinities of estuarine waters by a two-point potentiometric titration. *Mar. Chem.* 20, 219-226.
- Wheat, C.G. and M.J. Mottl, 1994. Hydrothermal circulation, Juan de Fuca Ridge eastern flank: factors controlling basement composition. *J. Geophys. Res.*, 99, 3067-3080.

3.4.6 Biomarker sampling

by Marcus Elvert

Introduction

The methanotrophic activity of bacteria plays a significant role within the diagenetic processes of sediments and in symbioses with eukaryotic organisms. Symbiotic associations between methanotrophic bacteria and mussels have been reported to occur at a number of deep-sea hydrocarbon seep communities.

The cycling of carbon by the bacterial activities of methanotrophic processes are associated with isotope effects. Essentially these are kinetic isotope effects (KIE's), that result in partial partitioning (fractionation) of the ^{12}C and the ^{13}C isotope due to differences in physico-chemical characteristics, such as diffusion velocities and bond strengths. The magnitude and extent of these isotope fractionation processes are reliable, predictable and diagnostic indicators for the biological pathways involved, and record characteristic carbon isotope signatures in the reactants and products involved during microbial diagenesis.

The methanotrophic activity leaves specific biomarker molecules behind. Typically they show very negative $\delta^{13}\text{C}$ -values up to -90‰. It seems that especially molecules like isoprenoids, hopanoids, and steroids are distinct biomarkers of methanotrophic processes. The analysis of these biomarkers will be made by coupled gas chromatography-mass spectrometry (GC-MS). After structural identification the individual biomarkers are analysed for their specific $^{13}\text{C}/^{12}\text{C}$ ratio by gas-chromatography-combustion-isotope ratio mass spectrometry (GC-C-IRMS). The isotopic measurements will be made using identical columns and operating conditions.

Sampling methods

On the cruise Sonne 109-1 we obtained a large number of samples on a transect vertical to the Juan de Fuca Ridge as well as in the area of the Oregon Margin. The sampling in the area of the Juan de Fuca Ridge took place with a KAL (gravity corer) and at the Oregon Margin with a TVG (TV-Grab). All samples were frozen immediately after collection and stored at -20°C till analysis.

The primary goal of the sampling was to obtain clams, especially *Calyptogena*, which frequently live in symbiotic association with methanotrophic bacteria. These clams could provide an extract enriched in specific biomarkers. At the Oregon Margin (TVG 43-1) we recovered numerous *Calyptogena* which probably harbour methanotrophic bacteria in their gills. For the support of this thesis we took additional samples of the sediment surrounding the clams. Furthermore we collected other clam specimens (*Solemya*, TVG 25-1 and 41-1). The research of specific biomarkers within the tissue of these mussels may provide a hint for a similar symbiotic association as for *Calyptogena*.

Table 7: Sample list Juan de Fuca Ridge

Date	Station	Sampling tool	Depth [cm]	Coordinates	Water depth HS [m]
26. May	001-4	KAL	38-40 129-131 193-195 250-252 300-302 351-353 392-394 427-429	45°29.022'N, 128°01.866'W	2819
27. May	010-2	KAL	95-97 134-137 184-187 191-194 197-199 234-237 257-260 310-313 338-341	45°55.192'N, 129°33.656'W	2684
28. May	011-1	KAL	56-59 134-137 190-193 233-236 287-290 349-352 414-417 452-455	45°52.934'N, 129°18.378'W	2710
28. May	012-1	KAL	0-3 17-19 29-31 59-61 110-112 155-157 200-202 249-251 313-315 370-372 439-441	45°51.182'N, 129°12.835	2711
29. May	022-1	KAL	79-82 103-106 148-151 164-166 186-188 249-251 298-301 364-366 419-421 477-479 520-522 574-576	45°49.628'N, 129°07.805'W	2740

Table 8: Sample list Oregon Margin

Date	Station	Sampling tool	Recovered samples	Coordinates	Water depth HS [m] (beginning/end)
30. May	025-1	TVG	1 Sediment sample Mussels: 3 Solemya Mussel shales: Solemya Calypthogena Pogonophore	44°40.609'N, 125°17.609'W	2025/2068
31. May	030-2	TVG	1 Sediment sample (Depth ca. 0-5 cm) 1 Sediment sample (Depth ca. 10-15 cm)	44°40.601'N, 125°17.518'W	2247/2124
01. June	036-1	TVG	1 Sediment sample	44°40.495'N, 125°07.268'W	690/682
01. June	036-4	TVG	1 Sediment sample 2 Gashydrate samples	44°40.443'N, 125°07.368'W	649/675
02. June	041-1	TVG	1 Sediment sample Mussels: 3 Solemya 1 Worm	44°40.207'N, 125°03.396'W	847/1026
02. June	043-1	TVG	4 Sediment samples Mussels: 9 Calypthogena (sprayed with H ₂ O) 12 Calypthogena (not sprayed with H ₂ O)	44°40.195'N, 125°06.538'W	625/637
02. June	043-2	TVG	2 Sediment samples	44°40.213'N, 125°06.505'W	619/705

3.5 Appendix

Appendix 1: Station list

SO109-1 Juan de Fuca Ridge

Date 1996	Stat. No Instr.	Begin (UTC)	at seafloor	End (UTC)	Latitude N° Longitude W°	Water depth (m)	Recov. (m)	Remarks
25. Mai	1/1 CTD	16:50	18:03	19:30	45°28.900' 128°01.900'	2851		Test
25. Mai	1/2 ZAPS	20:11		22:55	45°29.280' / 45°29.010' 128°02.048' / 128°01.950'	2848/ 2850		
25. Mai	1/3 MUC+TS	23:17	00:11	01:18	45°29.084' 128°02.050'	2850	0.23 - 0.30	6 liner TS no data
26. Mai	1/4 KAL	01:50	00:24	03:41	45°29.022' 128°01.866'	2819	4.42	
26. Mai	2/1 HS/PS	04:19		12:15	45°29.028' / 46°07.091' 128°01.885' / 130°05.701'	2852/ 2501		
26. Mai	2/2 HS/PS	13:04		14:15	46°05.549' / 45°59.798' 130°06.211' / 129°48.629'	2428/ 2061		
26. Mai	2/3 HS/PS	14:15		15:00	45°59.798' / 45°56.237' 129°48.629' / 130°00.017'	2061/ 1551		
26. Mai	3/1 ZAPS	15:18		18:57	45°56.146' / 45°53.850' 130°00.790' / 129°59.280'	1555/ 1601		
26. Mai	4/1 CTD	19:34	20:18	21:09	45°55.890' / 45°56.030' 130°00.810' / 130°00.940'	1534/ 1512		at seafloor is max depth
26. Mai	5/1 CTD	22:06	22:45	23:40	45°53.500' / 45°53.550' 129°58.470' / 129°58.550'	1684/ 1682		last coordinates are max. depth
27. Mai	6/1 ZAPS	00:05		03:28	45°55.795' / 45°54.594' 129°59.330' / 129°58.662'	1533		
27. Mai	7/1 CTD	04:52	05:35	06:41	45°50.930' / 45°53.990' 129°46.000' / 129°45.95'	2129/ 2139		last coordinates are max. depth
27. Mai	8/1 HS/PS	07:22		09:20	45°57.631' / 45°47.503' 129°40.904' / 129°10.288'	2391/ 2720		
27. Mai	8/2 HS/PS	09:36		12:07	45°45.217' / 45°56.965' 129°12.216' / 129°43.272'	2711/ 2067		
27. Mai	8/3 HS/PS	12:47		14:25	46°02.736' / 45°54.796' 129°02.747' / 129°54.796'	2159/ 2711		
27. Mai	9/1 MUC	15:03	15:57	17:00	45°52.598' 129°17.186'	2711		two bag samples (suspension)
27. Mai	10/1 MUC	18:40	19:31	20:46	45°55.205' 129°33.661'	2683	none	
27. Mai	10/2 KAL	20:59	21:51	23:02	45°55.192' 129°33.656'	2684	3.69	
28. Mai	11/1 KAL	00:48	01:41	02:43	45°52.934' 129°18.378'	2710	4.62	
28. Mai	12/1 KAL	04:10	04:58	06:11	45°51.182' 129°12.835'	2711	4.47	
28. Mai	13/1 HS/PS	08:55		10:00	46°16.810' 129°26.301'	2492		
28. Mai	13/2 HS/PS	10:20		11:29	46°25.495' 129°32.811'	2657		
28. Mai	13/3 HS/PS	12:00		13:02	46°17.572' 129°23.130'	2640		
28. Mai	14/1 DR	13:40	14:36	18:10	46°24.190' / 46°21.630' 129°29.428' / 129°28.103'	2530/ 2077	none	exceeded weak link
28. Mai	15/1 GKG	22:06	22:55	23:51	45°49.618' 129°17.029'	2705	0.36	
29. Mai	16/1 KAL	00:49	01:34	03:04	45°51.480' 129°13.980'	2703	none	penetration and flaps closed
29. Mai	17/1 HS/PS	03:15		05:20	45°55.571' / 46°05.263' 129°13.899' / 129°42.245'	2726		
29. Mai	17/2 HS/PS	05:45		06:38	46°03.992' / 45°57.835' 129°48.263' / 129°59.800'	2257/ 1540		
29. Mai	8/1 ZAPS	06:55		08:46	45°57.760' / 45°57.780' 129°59.950' / 129°59.960'	1545/ 1545		
29. Mai	18/2 ZAPS	09:23		10:58	45°55.491' / 45°55.410' 130°01.530' / 130°01.240'	1449/ 1435		

Date 1996	Stat. No Instr.	Begin (UTC)	at seafloor	End (UTC)	Latitude N° Longitude W°	Water depth (m)	Recov. (m)	Remarks
29. Mai	19/1 CTD	11:13	11:50	12:45	45°55.580' / 45°55.610' 130°00.550' / 130°00.580'	1548/ 1551		
29. Mai	20/1 CTD	13:33	14:07	15:21	45°55.160' / 45°55.180' 129°59.000' / 129°59.020'	1544/ 1542		last coordinates are max. depth
29. Mai	21/1 HS/PS	15:26		16:02	45°54.967' / 45°57.982' 129°55.181' / 129°45.545'	1638/ 2042		
29. Mai	21/2 HS/PS	16:02		16:20	45°57.982' / 45°54.485' 129°45.545' / 129°44.923'	2042/ 2127		
29. Mai	21/3 HS/PS	16:21		18:15	45°54.274' / 45°43.109' 129°44.901' / 129°15.155'	2239/ 2703		
29. Mai	22/1 KAL	19:10	20:03	21:05	45°49.628' 129°07.805'	2740	5.7	Top KAL ca. 50 cm bsf
29. Mai	23/1 KAL	22:20	23:16	00:24	45°51.469' 129°13.958'	2718	none	penetration and flaps open

SO109-1 Oregon Vent

Date 1996	Stat. No Instr.	Begin (UTC)	at seafloor	End (UTC)	Latitude N° Longitude W°	Water depth HS (m)	Recov. (m)	Remarks
30. Mai	24/1 TV-G	14:55	15:20	16:30	44°40.900' / 44°41.450' 125°16.800' / 125°17.500'	2100/ 1980		not dropped
30. Mai	25/1 TV-G	18:38	20:35	21:48	44°40.520' / 44°40.390' 125°17.610' / 125°17.370'	2025/ 2068		some sed., shells, precipitates
30. Mai	26/1 CTD	22:51	23:40	00:40	44°40.560' / 44°40.560' 125°17.510' / 125°17.450'	2048/ 2063		
31. Mai	27/1 HS/PS	01:05		01:25	44°41.332' / 44°41.449' 125°17.574' / 125°13.926'	2145/ 1793		
31. Mai	27/2 HS/PS	01:35		02:42	44°42.434' / 44°42.647' 125°13.693' / 125°01.864'	1271/ 1080		
31. Mai	27/3 HS/PS	02:49		03:52	44°42.049' / 44°41.656' 125°01.906' / 125°12.802'	1082/ 1402		
31. Mai	27/4 HS/PS	04:00		05:00	44°40.985' / 44°41.344' 125°12.882' / 125°02.233'	1671/ 1081		
31. Mai	27/5 HS/PS	05:10		06:25	44°40.683' / 44°40.346' 125°01.865' / 125°14.305'	1041/ 2255		
31. Mai	27/6 HS/PS	06:34		07:53	44°39.751' / 44°39.457' 125°14.930' / 125°01.750'	2283/ 1076		
31. Mai	27/7 HS/PS	08:00		09:24	44°39.296' / 44°39.250' 125°02.655' / 125°17.500'	1100/ 2034		
31. Mai	28/1 ZAPS	09:48	11:20	13:55	44°40.440' / 44°40.608' 125°17.612' / 125°17.490'	2023/ 2096		
31. Mai	29/1 CTD	14:24	15:16	16:27	44°40.760' / 44°40.790' 125°18.030' / 125°18.000'	2293/ 2296		
31. Mai	30/1 TV-G	17:06	17:49	20:08	44°40.780' / 44°40.560' 125°17.470' / 125°17.150'	2091/ 2103		not dropped
31. Mai	30/2 TV-G	20:23	21:11	00:14	44°40.770' / 44°40.180' 125°17.760' / 125°17.030'	2247/ 2124		dropped at 44°40.6014/ 125°17.5176
01. Jun	31/1 HS/PS	00:47		01:08	44°40.605' / 44°40.597' 125°17.233' / 125°13.368'	2086/ 1931		
01. Jun	31/2 HS/PS	01:17		01:44	44°39.983' / 44°39.749' 125°13.575' / 125°18.316'	2144/ 2094		
01. Jun	31/3 HS/PS	01:44		02:04	44°39.749' / 44°42.290' 125°18.316' / 125°18.850'	2094/ 2511		
01. Jun	31/4 HS/PS	02:04		02:36	44°42.290' / 44°41.781' 125°18.850' / 125°12.225'	2511/ 1377		
01. Jun	31/5 HS/PS	02:46		03:08	44°42.516' / 44°42.605' 125°13.292' / 125°16.968'	1251/ 1909		
01. Jun	31/6 HS/PS	03:08		03:15	44°42.605' / 44°43.391' 125°16.968' / 125°17.789'	1909/ 1971		
01. Jun	31/7	03:15		04:41	44°43.391' / 44°43.270'	1971/		

Date 1996	Stat. No Instr.	Begin (UTC)	at seafloor (UTC)	End (UTC)	Latitude N° Longitude W°	Water depth HS (m)	Recov. (m)	Remarks
	HS/PS				125°17.789' / 125°01.696'	1051		
01. Jun	32/1 ZAPS	05:13	05:52	07:29	44°40.270' / 44°39.610' 125°03.620' / 125°04.040'	958/899		Bioherm II
01. Jun	33/1 ZAPS	08:26	09:06	10:49	44°40.520' / 44°40.110' 125°07.330' / 125°07.890'	676/773		Bioherm I
01. Jun	34/1 CTD	11:05	11:26	11:52	44°40.500' / 44°40.520' 125°07.350' / 125°07.360'	677/673		
01. Jun	35/1 CTD	12:45	13:13	13:52	44°40.300' / 44°40.260' 125°03.750' / 125°03.710'	896/919		
01. Jun	36/1 TV-G	14:49	15:09	16:33	44°40.770' / 44°40.740' 125°07.110' / 125°06.410'	690/668		dropped at 44°40.4948/ 125°07.2682'
01. Jun	36/2 TV-G	16:53	17:18	18:11	44°40.470' / 44°40.370' 125°06.720' / 125°07.290'	649/675		dropped at 44°40.4331/ 125°07.3816
01. Jun	36/3 TV-G	18:22	18:54	21:25	44°40.440' / 44°40.470' 125°06.930' / 125°07.520'	651/682		not dropped
01. Jun	36/4 TV-G	21:58	22:30	23:38	44°40.460' / 44°40.400' 125°07.170' / 125°07.110'	678/668		dropped at 44°40.4425/ 125°07.3684'
01. Jun	36/5 TV-G	23:40	00:03	03:36	44°40.420' / 44°40.760' 125°07.090' / 125°07.380'	667/686		dropped at 44°40.4781/ 125°07.3739'
02. Jun	37/1 CTD	04:00	04:18	04:52	44°40.240' / 44°40.220' 125°04.500' / 125°04.440'	765/771		
02. Jun	38/1 ZAPS	05:30	06:04	06:36	44°40.200' / 44°40.220' 125°04.460' / 125°04.460'	767/767		
02. Jun	39/1 GKG	07:01	07:30	07:30	44°40.314' 125°05.751	610	none	
02. Jun	40/1 HS/PS	08:13	08:37	09:37	44°43.958' / 44°43.085' 125°07.913' / 124°50.119'	1539/294		
02. Jun	40/2 HS/PS	09:37	09:51	09:51	44°43.085' / 44°41.215' 124°50.119' / 124°49.923'	294/280		
02. Jun	40/3 HS/PS	10:05	10:59	10:59	44°39.776' / 44°39.809' 124°50.473' / 125°02.110'	275/1063		
02. Jun	40/4 HS/PS	11:09	12:00	12:00	44°40.643' / 44°40.673' 125°01.865' / 124°51.042'	1042/337		
02. Jun	40/5 HS/PS	13:20	14:13	14:13	44°41.655' / 44°41.299' 125°01.679' / 124°50.617'	1057/254		
02. Jun	40/6 HS/PS	12:15	13:10	13:10	44°41.939' / 44°42.567' 124°50.544' / 125°02.403'	290/1114		
02. Jun	40/7 HS/PS	14:25	15:02	15:02	44°42.678' / 44°43.256' 124°51.452' / 124°59.268'	396/814		
02. Jun	41/1 TV-G	15:32	15:58	16:56	44°40.430' / 44°40.160' 125°03.910' / 125°02.890'	847/1026		dropped at 44°40.2071/ 125°03.3960'
02. Jun	42/1 CTD	17:06	17:48	18:24	44°39.940' / 44°39.860' 125°06.680' / 125°06.700'	641/644		
02. Jun	43/1 TVG	18:32	19:01	20:31	44°40.350' / 44°40.440' 125°06.180' / 125°06.410'	625/637	H ₂ S	dropped at 44°40.1950/ 125°06.5383'
02. Jun	43/2 TVG	21:03	21:32	00:44	44°40.170' / 44°40.900' 125°06.530' / 125°07.330'	619/705		dropped at 44°40.2131/ 125°06.5047'
03. Jun	44/1 CTD	01:18	01:27	02:09	44°41.240' / 44°41.270' 125°05.710' / 125°05.770'	712/712		
03. Jun	45/1 CTD	02:31	02:46	03:19	44°40.300' / 44°40.340' 125°05.750' / 125°05.750'	605/606		
03. Jun	45/2 TV-G	03:37	03:57	05:59	44°40.450' / 44°40.110' 125°05.640' / 125°05.760'	619/599	H ₂ S	dropped at 44°40.1745/ 125°05.8523'
03. Jun	46/1 HS/PS	12:40	19:02	19:02	45°57.818' / 46°15.857' 125°24.098' / 124°19.262'	2044/132		Astoria Canyon

Appendix 2: Lithological composition of the sediment cores

15-1 (GKG)

Estern Juan de Fuca Ridge

SO-109-1

Recovery: 0.32 m

45° 49.6'N, 129° 17.0'W

Water depth:2705 m

Depth in core (m)	Lithology	Struct	Colour	Description	Age
0			10YR2/1	0-9 cm: diatomaceous mud, very dark brown	
			10YR3/1	9-19 cm: diatom-bearing mud, dark brown, laminated	
			5GY5/3	19-32 cm: foraminiferal and nannofossil-bearing mud, greenish gray	
1					
2					
3					
4					
5					



1-4 (KAL)

Eastern Juan de Fuca Ridge

SO-109-1

Recovery: 4.44 m

45° 29.0'N, 128° 01.9'W Water depth: 2819 m

Lithology		Struct.	Colour	Description	Age
0			5Y5/1	0-25 cm: diatomaceous mud, gray with dark olive gray streaks (5Y3/2)	
			5Y5/1	25-87 cm: terrigenous mud, gray	
			5Y4/1	87-93 cm: sandy silt, very dark gray	
			5Y5/1	93-138 cm: terrigenous mud, gray 116-120 cm: silty layer, gray (2.5YN5/1)	
			5Y3/1	138-145 cm: sandy silt, very dark gray	
			5Y5/1	145-234 cm: terrigenous mud, gray 215-230 cm: sand lenses, very dark gray (5Y3/1) 220 cm and 239 cm: foraminiferal rich layers 225-234 cm: dark gray layers (5Y4/1)	
			5Y4/1	234-240 cm: sandy silt, very dark gray	
			5Y5/1	240-280 cm: terrigenous mud, gray	
			5Y5/1	280-319 cm: terrigenous mud, gray with black streaks (5Y2.5/1)	
			5Y5/1	319-444 cm: nannofossil mud, gray 319-323 cm: silty layers, very dark gray (5Y3/1) 327-329 cm: silty layers, very dark gray (5Y3/1) 337-338 cm: silty layers, very dark gray (5Y3/1) 370 cm and 379 cm: black streaks (5Y2.5/1)	
1					
2					
3					
4					
5					

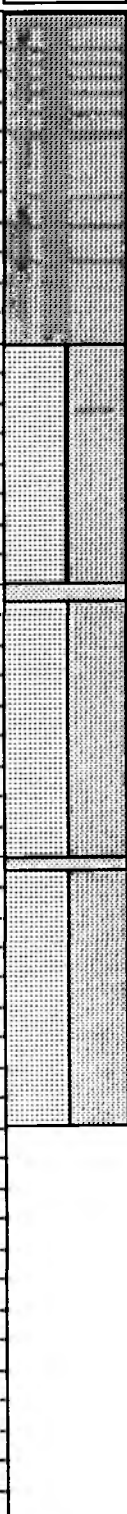

10-2 (KAL)

Estern Juan de Fuca Ridge

SO-109-1

Recovery: 3.69 m

45° 55.2'N, 129° 33.7'W Water depth: 2684 m

	Lithology	Struct.	Colour	Description	Age
0			5Y5/1	0-110 cm: terrigenous mud, gray 14-15 cm: mud lenses, greenish gray (5GY5/1) 20-21 cm: mud lenses, greenish gray (5GY5/1) 74 cm: mud lens, greenish gray (5GY5/1)	
1			5Y5/1	110-189 cm: nannofossil mud, gray 123 cm and 133 cm: foraminiferal mud, olive gray (5Y5/2)	
			5Y3/1	189-195 cm: sandy silt, very dark gray	
2			5Y5/1	195-280 cm: nannofossil mud, gray 235-237 cm: foraminiferal mud, olive gray (5Y5/2)	
			5Y3/1	280-282 cm: sandy silt, very dark gray	
3			5Y5/1	282-369 cm: nannofossil mud, gray 335 cm, 340 cm, 344 cm: foraminiferal mud, olive gray (5Y5/2) 335-344 cm: black lenses (5Y2.5/1)	
4					
5					

11-1 (KAL)

Eastern Juan de Fuca Ridge

SO-109-1

Recovery: 4.61 m

45° 52.9'N, 129° 18.4'W Water depth: 2710 m

	Lithology	Struct.	Colour	Description	Age
0			5Y3/2	0-10 cm: terrigenous mud, dark olive gray	
			5Y5/1	10-44 cm: nanntofossil-bearing silty mud, gray	
				44-78 cm: terrigenous mud, dark gray	
				64-70 cm: foraminiferal-bearing, nanntofossil mud, olive gray (5Y5/2)	
				77-78 cm: sandy silt, very dark gray (5Y3/1)	
				78-86 cm: terrigenous mud, dark gray	
				85-86 cm: sandy silt, very dark gray (5Y3/1)	
		▲	5Y4/1	86-102 cm: terrigenous mud, dark gray	
				101-102 cm: sandy silt, very dark gray (5Y3/1)	
		▲	5Y4/1	102-116 cm: terrigenous mud, dark gray	
				115-116 cm: sandy silt, very dark gray (5Y3/1)	
		▲	5Y4/1	116-129 cm: terrigenous mud, dark gray	
				128-129 cm: sandy silt, very dark gray (5Y3/1)	
1		▲	5Y4/1	129-151 cm: terrigenous mud, dark gray	
				150-151 cm: sandy silt, very dark gray (5Y3/1)	
		▲	5Y4/1	151-160 cm: terrigenous mud, dark gray	
				159-160 cm: sandy silt, very dark gray (5Y3/1)	
		▲	5Y4/1	160-174 cm: terrigenous mud, dark gray	
				173-174 cm: sandy silt, very dark gray (5Y3/1)	
		▲	5Y4/1	174-193 cm: terrigenous mud, dark gray	
				192-193 cm: sandy silt, very dark gray (5Y3/1)	
		▲	5Y4/1	193-210 cm: terrigenous mud, dark gray	
				209-210 cm: sandy silt, very dark gray (5Y3/1)	
		▲	5Y4/1	210-218 cm: terrigenous mud, dark gray	
				217-218 cm: sandy silt, very dark gray (5Y3/1)	
		▲	5Y4/1	218-232 cm: terrigenous mud, dark gray	
				231-232 cm: sandy silt, very dark gray (5Y3/1)	
		▲	5Y4/1	232-243 cm: terrigenous mud, dark gray	
				242-243 cm: sandy silt, very dark gray (5Y3/1)	
		▲	5Y4/1	243-258 cm: terrigenous mud, dark gray	
				257-258 cm: sandy silt, very dark gray (5Y3/1)	
		▲	5Y4/1	258-276 cm: terrigenous mud, dark gray	
				275-276 cm: sandy silt, very dark gray (5Y3/1)	
		▲	5Y4/1	276-284 cm: terrigenous mud, dark gray	
				283-284 cm: sandy silt, very dark gray (5Y3/1)	
		▲	5Y4/1	284-291 cm: terrigenous mud, dark gray	
				290-291 cm: sandy silt, very dark gray (5Y3/1)	
		▲	5Y4/1	291-307 cm: terrigenous mud, dark gray	
				306-307 cm: sandy silt, very dark gray (5Y3/1)	
		▲	5Y4/1	307-317 cm: terrigenous mud, dark gray	
				316-317 cm: sandy silt, very dark gray (5Y3/1)	
		▲	5Y4/1	317-325 cm: terrigenous mud, dark gray	
				324-325 cm: sandy silt, very dark gray (5Y3/1)	
2		▲	5Y4/1	325-336 cm: terrigenous mud, dark gray	
				335-336 cm: sandy silt, very dark gray (5Y3/1)	
		▲	5Y4/1	336-348 cm: terrigenous mud, dark gray	
				347-348 cm: sandy silt, very dark gray (5Y3/1)	
		▲	5Y4/1	348-354 cm: terrigenous mud, dark gray	
				353-354 cm: sandy silt, very dark gray (5Y3/1)	
		▲	5Y4/1	354-366 cm: terrigenous mud, dark gray	
				365-366 cm: sandy silt, very dark gray (5Y3/1)	
		▲	5Y4/1	366-382 cm: terrigenous mud, dark gray	
				381-382 cm: sandy silt, very dark gray (5Y3/1)	
		▲	5Y4/1	382-390 cm: terrigenous mud, dark gray	
				389-390 cm: sandy silt, very dark gray (5Y3/1)	
		▲	5Y4/1	390-404 cm: terrigenous mud, dark gray	
				403-404 cm: sandy silt, very dark gray (5Y3/1)	
		▲	5Y4/1	404-413 cm: terrigenous mud, dark gray	
				412-413 cm: sandy silt, very dark gray (5Y3/1)	
		▲	5Y5/1	413-421 cm: terrigenous mud, dark gray	
				421-430 cm: terrigenous mud, gray	
		▲	5Y4/1	430 cm: silty mud, gray	
				430-444 cm: terrigenous mud, dark gray	
				443-444 cm: sandy silt, very dark gray (5Y3/1)	
		▲	5Y4/1	444-461 cm: terrigenous mud, dark gray	
				460-461 cm: sandy silt, very dark gray (5Y3/1)	
3					
4					
5					

12-1 (KAL)

Eastern Juan de Fuca Ridge

SO-109-1

Recovery: 4.47 m

45° 51.2'N, 129° 12.8'W Water depth:2711 m

	Lithology	Struct.	Colour	Description	Age
0			5Y4/1	0-22 cm: foraminiferal-bearing terrigenous mud, dark gray 21-22 cm: olive layer (5Y4/3)	
		▲	5Y4/1	22-37 cm: foraminiferal-bearing terrigenous mud, dark gray 36-37 cm: sandy silt, very dark gray (5Y3/1)	
		▲	5Y4/1	37-47 cm: terrigenous mud, dark gray 40 cm: nannofossil mud, olive gray (5Y5/2)	
		▲	5Y4/1	46-47 cm: sandy silt, very dark gray (5Y3/1)	
		▲	5Y4/1	47-55 cm: terrigenous mud, dark gray 49 cm: nannofossil mud, olive gray (5Y5/2)	
		▲	5Y4/1	54-55 cm: sandy silt, very dark gray (5Y3/1)	
		▲	5Y4/1	55-63 cm: terrigenous mud, dark gray 59-60 cm: nannofossil mud, olive gray (5Y5/2)	
		▲	5Y4/1	62-63 cm: sandy silt, very dark gray (5Y3/1)	
		▲	5Y4/1	63-73 cm: terrigenous mud, dark gray 72-73 cm: sandy silt, very dark gray (5Y3/1)	
1		▲	5Y4/1	73-92 cm: terrigenous mud, dark gray 91-92 cm: sandy silt, very dark gray (5Y3/1)	
		▲	5Y4/1	92-109 cm: terrigenous mud, dark gray 100 cm: nannofossil mud, olive gray (5Y5/2)	
		▲	5Y4/1	108-109 cm: sandy silt, very dark gray (5Y3/1)	
		▲	5Y4/1	109-118 cm: terrigenous mud, dark gray 117-118 cm: sandy silt, very dark gray (5Y3/1)	
		▲	5Y4/1	118-134 cm: terrigenous mud, dark gray 128-134 cm: foraminiferal-bearing nannofossil mud (5Y4/2)	
		▲	5Y4/1	134-167 cm: terrigenous mud, dark gray 157-159 cm: nannofossil mud, olive gray (5Y5/2)	
			5Y4/1	166-167 cm: sandy silt, very dark gray (5Y3/1)	
		==	5Y4/1	167-184 cm: terrigenous mud, dark gray 170-172 cm: nannofossil mud, olive gray (5Y5/2)	
		==	5Y5/1	180-184 cm: laminated mud, gray (5Y5/1)	
2		==	5Y5/1	184-202 cm: nannofossil mud, gray 197-202 cm: laminated mud, gray (5Y5/1)	
		==	5Y5/1	202-210 cm: terrigenous mud, gray 209-210 cm: sandy silt, very dark gray (5Y3/1)	
		==	5Y5/1	210-220 cm: terrigenous mud, gray 219-220 cm: sandy silt, very dark gray (5Y3/1)	
		==	5Y5/1	220-236 cm: terrigenous mud, gray 235-236 cm: sandy silt, very dark gray (5Y3/1)	
		▲	5Y4/1	236-253 cm: terrigenous mud, dark gray 252-253 cm: sandy silt, very dark gray (5Y3/1)	
		▲	5Y4/1	253-266 cm: terrigenous mud, dark gray 256-266 cm: sandy silt, very dark gray (5Y3/1)	
		▲	5Y4/1	266-278 cm: terrigenous mud, dark gray 277-278 cm: sandy silt, very dark gray (5Y3/1)	
		▲	5Y4/1	278-288 cm: terrigenous mud, dark gray 287-288 cm: sandy silt, very dark gray (5Y3/1)	
3		▲	5Y4/1	288-310 cm: terrigenous mud, dark gray 296-304 cm: terrigenous mud, gray (5Y5/1)	
		▲	5Y4/1	309-310 cm: sandy silt, very dark gray (5Y3/1)	
		▲	5Y4/1	310-340 cm: terrigenous mud, dark gray 330-334 cm: mud lenses 339-340 cm: sandy silt, very dark gray (5Y3/1)	
		▲	5Y4/1	340-352 cm: terrigenous mud, dark gray 351-352 cm: sandy silt, very dark gray (5Y3/1)	
		▲	5Y4/1	352-364 cm: terrigenous mud, dark gray 363-364 cm: sandy silt, very dark gray (5Y3/1)	
		▲	5Y4/1	364-374 cm: terrigenous mud, dark gray 373-374 cm: sandy silt, very dark gray (5Y3/1)	
		▲	5Y4/1	374-384 cm: terrigenous mud, dark gray 383-384 cm: sandy silt, very dark gray (5Y3/1)	
4		▲	5Y4/1	384-398 cm: terrigenous mud, dark gray 397-398 cm: sandy silt, very dark gray (5Y3/1)	
			5Y4/1	398-412 cm: terrigenous mud, dark gray 407 cm and 411 cm: mud layers, gray (5Y5/1)	
		==	5Y4/1	412-423 cm: terrigenous mud, dark gray 420-423 cm: laminated	
			5GY5/1	423-447 cm: nannofossil-bearing mud, greenish gray with black mud lenses	
5					

22-1 (KAL)		Eastern Juan de Fuca Ridge		SO-109-1
Recovery: 6.20 m		45° 49.6' N, 129° 07.8' W		Water depth: 2740 m
Lithology	Struct	Colour	Description	Age
		SGY4	0-50 cm laminar lateral bearing mud, greenish gray	
		SGY4	50-186 cm laminar lateral and non-laminar bearing mud, dark greenish gray 156-177 cm black streaks 170-186 cm bioturbated	
		SGY4	186-247 cm non-laminar mud, greenish gray 183-207 black streaks 208-217 dark gray (SY4/1) 218-224 dark gray (SY4/1) 224-247 dark greenish gray (SGY4/1)	
		SY4/1	247-256 cm laminar mud, dark gray	
		SGY4	256-304 cm non-laminar bearing mud, greenish gray 273-280 dark layers	
		SGY4	304-340 cm non-laminar mud, greenish gray	
		SY4/1	340-370 cm non-laminar mud, gray	
		SGY4	370-380 cm laminar mud, greenish gray	
		SGY4	380-414 cm non-laminar mud, greenish gray 383-391 cm black streaks 402 cm light gray	
		SGY4	414-446 cm non-laminar mud, greenish gray 420 cm light gray 446-448 cm black streaks	
		SGY4	446-450 cm non-laminar mud, dark greenish gray	
		SGY4	450-530 cm laminar mud, dark greenish gray 480-481 cm non-laminar bearing mud, dark greenish gray (SGY4/1)	

22-1 (KAL)		Eastern Juan de Fuca Ridge		SO-109-1
Recovery: 6.20 m		45° 49.6' N, 129° 07.8' W		Water depth: 2740 m
Lithology	Struct	Color	Description	Age
		SGY4	530-549 cm laminar mud, dark greenish gray	
		SGY4	549-603 cm laminar mud, dark greenish gray 560 cm, 570 cm, 579 cm: denser layers, dark greenish gray (SGY4/1)	
		SY4/1	603-620 cm laminar mud, dark gray	

Appendix 3 Geochemical data of multicorer (MUC) and box corer (GKG) sediments

109-1-3-MUC

depth (cm)	SiO ₂ [µM]	NO ₃ [µM]	NH ₄ [µM]	PO ₄ [µM]	N/P	Mg [mM]	Ca [mM]	TA [mM/kg]	pH
0	184.64	41.26	0.00	2.4	36.4	54.1	10.7	2.54	7.46
-0.25	255.36	46.14	6.29	2.76	33.4	54.1	10.5	2.54	7.46
-0.75	283.88	45.92	3.92	3.24	27.9	55	10.2	2.63	7.46
-1.5	312.44	44.50	2.73	2.96	28.7	53.9	10.5	2.50	7.41
-2.5	355.92	40.33	4.15	2.92	26.2	55	10.7	2.54	7.39
-3.5	385.64	36.17	3.44	3.4	19.2	54.3	10.4	2.63	7.28
-4.5	402.24	28.99	3.32	3.8	13.6	54.3	10.2	2.50	7.28
-5.5	420.72	22.85	2.14	5.04	8.1	54	10.6	2.67	7.28
-6.5	432.28	18.03	3.08	4.36	7.3	54.4	10.5	2.74	7.33
-7.5	446.52	13.70	1.90	4.8	5.5	54.2	10.7	2.77	7.39
-8.5	447.56	12.88	1.66	4.64	5.1	54.6	10.6	2.80	7.35
-9.5	443.28	10.58	5.69	4.68	3.4	54.9	10.4	2.80	7.31
-11.5	443.6	5.37	3.56	4.88	1.7	54.8	10.3	2.83	7.37
-14.5	449.08	3.12	5.81	5.8	0.9	53.5	11	2.94	7.41
-17.5	435.36	1.97	8.66	7.28	0.5	54	10.6	3.13	8.4
-20.5	413.8	1.37	10.20	7.04	0.2	54.7	10.7	3.17	8.25

109-15-1-GKG

depth (cm)	SiO ₂ [μM]	NO ₃ [μM]	NH ₄ [μM]	PO ₄ [μM]	N/P	Mg [mM]	TA [mM/kg]	pH
-1,5	421,58	90,75	76,88	15,68	10,3	53,9	2,50	7,51
-3,5	299,44	70,58	33,69	19,20	6,2	54,7	2,49	7,60
-6,5	422,14	47,57	36,07	23,84	3,3	54,1	2,49	7,64
-8,5	426,08	30,91	29,90	24,80	2,4	54,7	2,53	7,62
-10,5	412,26	28,50	51,25	29,28	1,1	54,2	2,53	7,56
-14,5	401,3	4,38	51,73	44,80	0,2	53,4	2,57	7,60
-15	388,92	6,14	58,37	39,36	0,4	53,9	2,53	7,58
-17	365,86	8,77	54,10	38,72	0,4	53,7	2,67	7,86
-19	323,08	7,67	48,88	37,60	0,7	53,6	2,64	7,86
-21	272,42	18,41	128,13	26,56	0,7	53,8		7,90

Appendix 4 Geochemical data of Kastencorer (KAL) sediments**109-1-4-KAL**

depth (cm)	SiO ₂ [μM]	NO ₃ [μM]	NH ₄ [μM]	PO ₄ [μM]	N/P	Mg [mM]	Ca [mM]	TA [mM/kg]	pH
-37	406,36	1,97	31,56	6,80	4,9	54,7	11,0	2,58	8,33
-54	429,04	4,06	43,66	14,20	3,4	55,5	10,6	2,62	8,17
-74	411,02	0,27	63,29	14,16	4,5	55,9	10,4	2,93	7,86
-96	400,74	1,18	94,50	17,28	5,5	54,6	10,5	2,91	7,71
-107	393,90	1,12	101,97	19,68	5,2	54,9	10,3	2,62	7,84
-115	362,90	1,32	122,67	20,56	6,0	54,6	10,5		7,95
-127	376,06	0,99	127,48	23,28	5,5	55,2	10,0	2,46	7,86
-138	353,60	0,90	150,67	15,68	9,7	55,2	10,0		7,93
-148	373,06	1,51	158,15	26,56	6,0	54,6	10,6	2,65	7,75
-167	361,68	1,82	178,67	27,20	6,6	55,4	10,2	2,91	7,75
-181	360,63	3,40	191,87	28,80	6,8	55,6	10,3	2,65	8,04
-198	327,89	1,10	199,02	18,80	10,6	55,4	10,2	2,65	7,84
-211	345,55	3,10	222,69	29,00	7,8	55,0	10,0	2,46	7,71
-237									7,82
-254	258,60	0,27	260,41	26,00	10,0	55,3	9,7	3,33	7,70
-273	288,80	0,82	280,58	51,00	5,5	54,6	10,2	3,00	7,60
-297	307,80	2,19	306,09	36,80	8,4	55,0	9,8	3,22	7,71
-315	261,20	1,64	316,77	21,80	14,6	55,2	9,6		7,66
-332	283,80	2,47	323,29	39,20	8,3	53,9	10,3	3,12	7,75
-357						54,9	10,0	3,18	7,62
-379	294,00	3,29	366,60	39,20	9,4	55,6	9,8	3,38	7,46
-399	245,80	1,37	382,61	34,40	11,2	53,8	9,9	3,38	7,57
-423	277,80	4,38	411,68	55,20	7,5	53,9	9,8	3,15	7,57
-440	296,00	6,30	443,12	51,40	8,7	53,3	9,8	3,08	7,81

109-10-2-KAL

depth (cm)	SiO ₂ [μM]	NO ₃ [μM]	NH ₄ [μM]	PO ₄ [μM]	N/P	Mg [mM]	Ca [mM]	TA [mM/kg]	pH
-12,5	361,44	0,66	107,25	9,12	11,8	53,5		4,12	8,00
-41,5	344,00	1,75	102,98	9,44	11,1	53,7		4,15	7,96
-66,5	335,52	1,10	120,54	8,16	14,9			4,62	7,87
-98,5	331,84	2,41	149,49	9,60	15,8	53,5	10,5	4,47	7,90
-112,5	325,12	1,75	158,50	10,88	14,7	53,7		4,58	7,74
-126,5	286,72	2,63	171,32	12,16	14,3	53,7		5,05	7,81
-136,5	296,00	3,73	176,06	13,28	13,5	53,8		5,05	7,68
-147,5	280,96	4,38	185,55	11,20	17,0	53,5		5,12	7,65
-160,5	260,64	3,95	197,89	9,60	21,0	53,7		5,25	7,70
-172,5	349,28	5,92	204,06	12,48	16,8	53,9		5,28	7,79
-185,5	379,20	7,01	219,25	16,48	13,7	53,8		5,31	7,68
-191,5	304,96	5,04	224,94	11,84	19,4	53,4	9,9	5,31	7,90
-198,5	319,68	3,51	226,84	10,24	22,5	53,9		5,36	7,76
-215,5	343,36	1,53	252,47	11,36	22,4	53,5		5,38	7,76
-230,5	348,00	5,48	263,38	9,60	28,0	53,3		5,63	7,74
-235,5	341,92	5,04	267,65	11,20	24,3	54,0		5,66	7,74
-249,5	337,28	3,07	276,67	6,40	43,7			5,69	7,76
-269,5	352,16	2,85	296,13	7,20	41,5			5,88	7,79
-281,5						53,7			7,85
-299,5	340,16	3,51	320,33	7,04	46,0	53,3	11,0	6,34	7,68
-320,5	343,84	3,51	336,94	5,44	62,6	53,6	11,0	6,54	7,70
-340,5	348,16	3,51	348,80	5,76	61,2	53,8		6,67	7,68
-360,5	343,68	3,51	358,29	5,76	62,8	53,7		6,79	7,65
-365	324,48	1,53	379,65	6,88	55,4	53,7	10,8	6,74	7,78

109-11-1-KAL

depth (cm)	SiO ₂ [μM]	NO ₃ [μM]	NH ₄ [μM]	PO ₄ [μM]	N/P	Mg [mM]	Ca [mM]	TA [mM/kg]	pH
0	451,2	9,86	6,17	4,64	3,5		10,4	2,59	7,72
-7,5	378,24	18,19	10,91	3,04	9,6	54,2	10,3	2,68	7,79
-16,5	273,6	16,66	18,03	2,24	15,5	53		2,9	8
-32,5	292	6,36	18,98	2,24	11,3	53		3	8,36
-52,5	361,44	1,97	30,85	8,48	3,9	54,1	10,3	3,05	7,85
-66,5	342,56	2,19	60,74	13,44	4,7	53,9	10,5	3,46	7,64
-96,5	357,28	4,60	92,06	29,12	3,3	54,1		3,06	7,72
-116,5	373,44	3,29	101,56	17,92	5,9	53,7		3,44	7,75
-136,5	376,48	3,07	114,84	21,6	5,5	53,7		3,67	7,66
-156,5	371,68	2,85	127,69	20,16	6,5	53,7		2,3	7,62
-174,5	325,44	3,29	140,94	19,84	7,3	53,4		3,86	7,81
-182,5	377,6	2,63	145,69	18,88	7,9	52,8		4,28	7,64
-200,5	326,56	2,63	155,66	21,12	7,5	53,6		4,28	7,45
-210,5	298,88	0,66	167,99	16,32	10,3	53,2		4,38	7,57
-225,5	298,72	0,88	177,49	16,64	10,7	53,2		4,14	7,58
-235,5	295,68	1,97	185,55	19,68	9,5	52,8		4,03	7,93
-254,5	283,68	1,10	192,67	33,28	5,8	53	10,7	4,23	7,57
-261,5	265,12	2,41	195,52	20,16	9,8	52,7		4,33	7,53
-276,5	273,92	3,07	205,48	25,44		53,3		4,41	7,45
-307,5	308,48	2,41	222,57	22,88	9,8	52,7		4,49	7,53
-312,5	299,52	2,41	224,94	22,24	10,2			4,57	7,55
-326,5	287,04	3,73	235,38	23,68	10,1	52,8		4,65	7,49
-337,5	271,2	5,26	241,08	28	8,8	52,8	10,3	4,72	7,6
-350,5	292,16	4,16	250,09	27,2	9,3	52,9		4,78	7,57
-369,5	279,2	1,97	272,40	18,88		51,7		4,84	7,53
-380,5	304	3,29	278,57	28,64		51,3		5,36	7,4
-395,5	293,44	2,63	295,18	24,06		51,5	9,1	5,42	7,53
-416,5	309,76	3,51	308,94	32		52		5,48	7,41
-421,5	314,24	3,29	314,16	32,96		51,9		5,53	7,49
-428,5	300,48	3,51	311,79	32,96		51,8		5,57	7,41
-434,5	338,24	3,07	315,58	33,12		51,4	10,4	5,62	7,57
-444,5	347,68	3,95	325,55	38,24		52,3		5,66	7,45
-450	348,8	0,88	332,19	24,64		52		5,7	7,49
-453,5		1,32	339,31	24,16		51,6		6,22	7,6

109-12-1-KAL

depth (cm)	SiO ₂ [μM]	NO ₃ [μM]	NH ₄ [μM]	PO ₄ [μM]	N/P	Mg [mM]	Ca [mM]	TA [mM/kg]	pH	Cl [mM]
-1,5	435,52	20,60	9,97	2,88	10,6	53,9		2,48	7,85	542,2
-10,5	326,08	18,85	20,88	1,44	27,6			2,55	8,4	542,2
-17,5	429,76	16,88	18,03	2,56	13,6	54,1		2,73	7,92	540,5
-29,5	405,76	1,53	30,37	5,28	6,0	53,9		3,12	8,14	
-49,5	383,68	0,88	43,18	8,32	5,3	53,7		3,43	7,85	540,5
-60,5	372,48	0,88	61,69	9,76	6,4	53,2		3,31	7,76	542,2
-73,5	376,48	1,53	80,20	10,56	7,7	53,2		3,47	7,74	540,5
-80,5	348	1,32	74,98	12,8	6,0	53,3		3,71	7,68	540,5
-110,5	319,2	1,97	116,74	16,64	7,1	53		3,93	7,67	542,2
-116,5						52,9		3,85	7,67	543,9
-120,5	360,16	3,07	118,64	13,12	9,3	53		4,05	7,79	
-138,5	343,36	2,19	114,84	17,28	6,8	52,9		4,34	7,76	543,9
-155,5	308,64	1,53	134,30	12,96	10,5	52,7		4,51	7,72	544,8
-171,5	295,36	1,32	143,32	12,48			10,4	4,76	7,7	
-200,5	316	0,00	180,81	16,96	10,7	52,4		4,59	7,7	543,9
-222,5	283,52	0,00	201,21	13,44	15,0	52,1	10,3	4,68	7,94	
-249,5	281,92	0,00	222,09	18,56	12,0	52		4,94	7,79	543,9
-277,5	262,72	0,00	242,50	17,28	14,0	52,9		5,27	7,79	
-282	257,92	0,00	243,45	13,6	17,9	51,5		5,36	7,76	546,5
-313,5	270,88	0,00	274,77	19,84		51,4		5,45	7,78	
-346,5	289,12	0,00	300,87	22,56	13,3	50,7		5,78	7,74	
-370,5	279,84	0,00	317,96	21,28	14,9	50,6	9,8	6,15	7,74	545,7
-392,5	272,64	0,00	329,34	18,56	17,7	50,5		6,33	7,7	
-414,5	305,76	0,00	356,87	21,28	16,8	50,5	9,9	6,11	7,68	
-426,5	312,64	0,00	361,61	22,4		50,7	9,7	6,35	7,65	545,7
-439,5	319,52	0,00	380,60	25,76		49,7		6,35	7,68	545,7
-450	308,64	0,00	383,44	32,16		50,3	9,9	6,5	7,63	546,5

109-22-1-KAL

depth (cm)	SiO ₂ [μM]	NO ₃ [μM]	NH ₄ [μM]	PO ₄ [μM]	N/P	Mg [mM]	Ca [mM]	TA [mM/kg]	pH
-3,5	354,4	7,01	21,83	3,36	8,6	54		2,63	8
-16,5	387,68	3,51	19,46	3,84	6,0	54,1		2,50	
-28,5	413,6	0,88	18,51	4,8	4,0	54,3		2,45	7,82
-41,5	395,36	2,41	10,91	4,48	3,0	54,1		2,80	7,9
-57,5	392,64	3,51	21,36	4,64	5,4	54,3		2,80	7,85
-81,5	351,36	0,00	31,80	5,92	5,4	53,9		3,23	7,86
-105,5	318,4	2,19	29,42	4,48	7,1	54,2		3,13	7,86
-149,5	255,52	0,00	43,18	6,4	6,7	54,3		3,32	7,73
-165,5	242,88	0,00	160,40	9,92	16,2	53,5		4,02	7,78
-188,5	233,6	0,00	60,27	4,96		54,3		3,14	7,8
-210,5	232,32	0,00	72,13	4,96	14,5	53,6		3,37	7,75
-235,5	229,6	0,88	87,32	5,28	16,7	53,9		3,63	7,8
-255,5	250,08	0,00	93,96	5,44	17,3	53,5		3,44	7,67
-266,5	245,92	3,51	98,23	7,04		53,8		3,57	7,77
-299,5	247,04	1,32	112,47	5,6	20,3	53,4		3,74	7,75
-329,5	219,68	0,00	134,30	4,48	30,0	53,4		3,57	7,67
-340,5	140	0,00	142,37	1,76	80,9	52,8		2,88	7,8
-359,5	188	0,00	139,52	0,64	218,0	52,7		3,44	7,77
-393,5	241,28	0,00	146,16	5,12	28,5	53,3		4,14	7,65
-420,5	223,2	0,00	149,01	5,28		53		4,17	7,75
-442,5	249,28	0,00	155,66	6,4	24,3	53,1		4,32	7,71
-459,5	264,48	0,00	163,72	7,84	20,9	53,6		4,32	7,75
-478,5	275,52	0,00	191,72	7,84	24,5	53,4		4,32	7,78
-495,5	226,24	0,00	193,15	6,72	28,7	53		4,37	7,88
-524,5	240,16	0,00	181,76	6,72		52,7		4,17	7,88
-539,5	218,4	0,00	188,87	7,68		52,6		4,60	8,12
-564,5	251,2	0,00	193,15	9,6		52,8		4,40	7,84
-575,5	237,44	0,00	196,94	9,44		53,2		4,40	7,93
-596,5	305,28	0,00	62,17	10,88		53,7		3,10	7,78
-600	242,56	0,00	203,59	11,04		52,8		4,30	7,8

Appendix 5 Geochemical data of TV grab (TVG) sediments

109-30-1-TVG

depth (cm)	SiO ₂ [μM]	NO ₃ [μM]	NH ₄ [μM]	PO ₄ [μM]	N/P	TA [mM/kg]	pH
-0,5	436,21	5,21	39,03	5,16	8,6	2,73	7,68
-1,5	437,96	9,43	21,71	6,76	4,6	2,67	7,54
-2,5	444,4	2,74	22,54	5,96	4,2	2,67	7,56
-3,5	442,65	3,40	21,00	5,44	4,5	2,64	7,48
-4,5	435,62	1,81	22,42	4,88	5,0	2,64	7,54
-5,5	448,5	1,70	27,88	5,16	5,7	2,7	7,45
-6,5	436,79	1,97	22,78	5,2	4,8	2,7	7,5
-7,5	454,94	1,97	34,52	5,2	7,0	2,67	7,48
-8,5	464,31	1,37	33,58	5,8	6,0	2,76	7,56
-9,5	439,72	0,55	30,49	6,2	5,0	2,76	7,54
-11,5	480,71	3,23	42,83	6,68	6,9	2,87	7,56
-14,5	495,93	2,08	41,64	6,84	6,4	2,93	7,58
-17,5	490,66	0,66	43,42	5,72	7,7	2,91	7,65

109-36-1A-TVG

depth (cm)	SiO ₂ [μM]	NO ₃ [μM]	NH ₄ [μM]	PO ₄ [μM]	N/P	TA [mM/kg]	pH
-1,5	213,13	2,90	12,69	5,52	2,8	2,5	7,65
-3,5	210,2	9,70	16,25	4,96	5,2	2,52	7,67
-4,5	216,05	5,97	15,54	4,84	4,4	2,57	7,75
-5,5	214,3	4,60	15,54	4,84	4,2	2,44	7,9
-6,5	222,49	6,14	15,30	4,4	4,9	2,52	7,65
-7,5	218,4	2,41	16,85	5,4	3,6	2,54	7,65
-8,5	228,94	5,59	19,58	5,72	4,4	2,55	7,67
-9,5	218,98	2,30	18,63	6,72	3,1	2,57	
-11,5	249,43	1,97	19,69	6,92	3,1	2,69	7,69
-14,5	254,7	1,32	23,73	9,12	2,7	2,65	7,58
-17,5	292,17	4,44	30,73	16,32	2,2	2,86	7,62
-20,5	270,51	1,04	22,42	8,16	2,9	2,5	7,65
-23,5	247,09	4,16	18,63	7,4	3,1	2,5	7,64

109-36-1B-TVG

depth (cm)	SiO ₂ [μM]	NO ₃ [μM]	NH ₄ [μM]	PO ₄ [μM]	N/P	TA [mM/kg]	pH
-1,5	179,75					2,41	7,39
-3,5	206,69	6,96	8,42	5,52	2,8	2,48	7,39
-4,5	234,21	8,49	15,19	15,4	1,5	2,41	7,51
-5,5	218,98	3,29	8,30	5,08	2,3	2,54	7,52
-6,5	245,33	7,07	15,90	14,76	1,6	2,54	7,56
-7,5	221,32	2,79	10,68	5,72	2,4	2,22	7,62
-8,5	218,4	2,52	13,76	6	2,7	2,57	7,49
-9,5	232,45	2,41	15,19	5,84	3,0	2,28	7,54
-11,5	238,89	2,19	17,44	7,84	2,5	2,12	7,51
-14,5	249,43	1,59	19,81	7,2	3,0	2,54	7,49
-17,5	255,28	2,30	22,54	6,64	3,7	2,58	7,41

109-36-2A-TVG

depth (cm)	SiO ₂ [μM]	NO ₃ [μM]	NH ₄ [μM]	PO ₄ [μM]	N/P	TA [mM/kg]	pH	H ₂ S [μM]
-1	207,55			5,76		2,52	7,37	2,37
-3	199,32			6,4		2,69	7,37	1,43
-5	204,61		32,51	13,84		2,72	7,41	5,99
-7	204,02		31,08	8,04		2,78	7,39	0,49
-9	246,94		28,35	9,72		2,75	7,39	0,49
-11,5	269,87		24,68	9,88		2,5	7,37	0,49
-14,5	291,63		35,59	10,48		2,78	7,39	1,97
-17,5	298,09		29,66	11				4,11
-20,5	296,92		27,76	11,08		2,86	7,28	16,74
-23,5	262,23		32,39	10,36		2,86	7,28	15,26
-26,5	275,16		25,74	9,76		2,75	7,32	19,56
-29,5	286,92			9,6		2,62	7,36	5,59

109-36-2B-TVG

depth (cm)	SiO ₂ [μM]	NO ₃ [μM]	NH ₄ [μM]	PO ₄ [μM]	N/P	TA [mM/kg]	pH	H ₂ S [mM]
-1	174,03	4,44		4,96	0,9	2,48	7,3	1,39
-3	193,44	8,77	8,42	6,4	2,7	2,65	7,19	0,51
-5	231,07	11,67	15,19	5,64	4,8	2,81	7,32	0,11
-7	255,76	13,97	8,30	6,32	3,5	2,83	7,32	0,18
-9	275,75	14,91	15,90	7,8	3,9	2,81	7,34	0,31
-11,5	308,09	14,85	10,68	9,8	2,6	2,88	7,28	0,11
-14,5	309,26	14,30	13,76	10,64	2,6	2,86	7,32	0,18
-17,5	294,56	15,23	15,19	11,04	2,8	2,69	7,26	1,25
-20,5	288,1	13,32	17,44	10,64	2,9	2,86	7,28	1,99
-23,5	260,46	14,52	19,81	11,08		2,88	7,24	4
-26,5	295,74	13,92	22,54	10,48	3,5	2,91	7,24	4,74

109-36-4-TVG

depth (cm)	SiO ₂ [μM]	NO ₃ [μM]	NH ₄ [μM]	PO ₄ [μM]	N/P	TA [mM/kg]	pH	Mg [mM]	Ca [mM]
-1	164,13					2,65	7,52	53,76	10,4
-3	179,21	3,78	16,85	2,92	7,1	2,54	7,51	53,43	10,5
-5	185,42	1,86	18,15	1,72	11,6	2,58	7,45	53,12	10,6
-7	193,41	1,75	12,10	1,72	8,1	2,62	7,45	53,6	10,6
-9	192,52	0,93	10,68	1,84	6,3	2,54	7,43	53,42	10,7
-11,5	196,07	1,53	16,85	2,2	8,4	2,62	7,43	53,81	10,4
-14,5	198,73	3,23	17,44	2,4	8,6	2,54	7,43	53,39	10,3
-17,5	206,71	1,75	18,75	2,68	7,6	2,62	7,45	53,14	10,7
-20,5	235,1					2,88	7,45	52,83	11
-23,5	204,94					2,62	7,43	53,26	10,8
-26,5	235,99	1,26	19,10	4,92	4,1	2,75	7,43	52,79	11
-29,5	221,8	1,70	23,13	8,12		2,69	7,41	53,04	10,6
-32,5	212,93	0,71	17,32	5,4		2,62	7,49	53,2	10,5

109-36-5-TVG

depth (cm)	SiO ₂ [μM]	NO ₃ [μM]	NH ₄ [μM]	PO ₄ [μM]	N/P	TA [mM/kg]	pH
-1	235,1	5,04	8,19	5,56		2,45	7,54
-3	223,57	4,38	8,42	4,96	2,6	2,41	7,54
-5	212,93	2,14	13,05	4,44	3,4	2,43	7,67
-7	212,93	1,10	12,69	4,04	3,4	2,5	7,65
-9	250,19	1,97	18,98	7,16	2,9	2,67	7,65
-11,5	251,96	2,14	19,58	3,24	6,7	2,47	7,65
-14,5	273,25	3,07	30,02	11,56	2,9	2,67	7,58
-17,5	283,01	2,52	25,86	7,4	3,8	2,7	7,65
-20,5	298,98	1,32	26,46	3,56		3,33	7,58

109-43-1A-TVG

depth (cm)	SiO ₂ [μM]	NO ₃ [μM]	NH ₄ [μM]	PO ₄ [μM]	N/P	TA [mM/kg]	pH	H ₂ S [mM]
-1	139,2			4,08		2,84	7,78	0,09
-3	136			5,2		5,75	7,75	0,86
-5	151,6			5,06		2,66	7,73	2,07
-7	106,9			5,06		12,04	7,75	2,72
-9	163,5		47,78	7,98		17,95	8,08	8,74
-11,5	297		71,75	5,64		24,38	8,29	12,8
-14,5	318		102,62	1,28		31,64	8,29	16,19
-17,5	319,8		111,08	11,08		34,94	8,32	18,02
-20	290,8		103,31			31,53	8,38	18,06

109-43-1B-TVG

depth (cm)	SiO ₂ [μM]	NO ₃ [μM]	NH ₄ [μM]	PO ₄ [μM]	N/P	TA [mM/kg]	pH	H ₂ S [mM]
-1	119,4			6,24		7,69	7,78	0,04
-3	125,6			7,8		7,64	7,75	0,03
-5	115,3			5,84		7,56	7,73	0,3
-7	121,5			5,64		7,8	7,75	1,78
-9	119,44			5,64		7,41	8,08	3,33
-11,5	105,94			7,6		7,56	8,29	4,12
-14,5	142,15			4,2		7,82	8,29	6,86
-17,5	119,4			7,2		7,78	8,32	6

109-43-2-TVG

depth (cm)	SiO ₂ [µM]	NO ₃ [µM]	NH ₄ [µM]	PO ₄ [µM]	N/P	TA [mM/kg]	pH
-1	134,8	7,07	18,27	3,76	6,7	2,35	7,52
-3	141,1	3,40	10,56	5	2,8	2,32	7,6
-5	149,7	0,99	10,68	7,04	1,7	2,32	7,64
-7	160,1	1,21	11,51	5,04	2,5	2,32	7,73
-9	169,2	1,53	13,05	6,32	2,3	2,37	7,64
-11,5	187,5	2,14	18,03	8	2,5	2,24	7,67
-14,5	209,9					2,35	7,71
-17,5	220,3	1,10	19,81	7,8	2,7	2,32	7,77
-20,5	224,2	1,75	21,36	6,84	3,4	2,3	7,84

Appendix 6 Nutrient data of CTD stations SO109-1

109-1-1-CTD

depth (dbar)	SiO ₂ [µM]	NO ₃ [µM]	PO ₄ [µM]	N/P
-45	1,65	3,84	0,75	5,1
-497	80,2	45,69	2,85	16,0
-1005	129,25	47,81	3	15,9
-1409	146,5	47,61	2,8	17,0
-1511	156,95	47,61	3,3	14,4
-1606	156,95	46,72	3,2	14,6
-2020	166,8	45,62	2,95	15,5
-2021	173,55	45,07	2,8	16,1
-2325	183,35	44,66	2,65	16,9
-2630	177,9	44,05	2,65	16,6
-2880	155,55	43,63	2,5	17,5

109-4-1-CTD

depth (dbar)	SiO ₂ [µM]	NO ₃ [µM]	PO ₄ [µM]	N/P
-1200	134,55	51,85	3,6	14,4
-1250	138,05	51,65	3,45	15,0
-1300	140,4	51,79	3,6	14,4
-1350	146,25	51,24	3,4	15,1
-1380	157,05	51,38	3,45	14,9
-1410	144,15	51,17	3,45	14,8
-1440	150	51,38	3,6	14,3
-1470	155,55	51,65	3,9	13,2
-1500	157,2	51,03	3,25	15,7
-1525	166,55	50,76	3,65	13,9
-1535	166	48,50	3,2	15,2

109-5-1-CTD

depth (dbar)	SiO ₂ [µM]	NO ₃ [µM]	PO ₄ [µM]	N/P
-1096	151,05	50,28	4,05	12,4
-1147	149,5	50,21	4	12,6
-1197	155,8	50,48	4,75	10,6
-1247	162,4	50,55	3,9	13,0
-1296	155,6	50,21	4,15	12,1
-1347	149,3	49,94	3,75	13,3
-1394	155,75	49,53	3,65	13,6
-1447	154,5	48,98	4	12,2
-1504	155,65	49,11	3,9	12,6
-1553	152,45	49,18	3,65	13,5
-1632	148,6	48,02	3,9	12,3

109-7-1-CTD

depth (dbar)	SiO ₂ [µM]	NO ₃ [µM]	PO ₄ [µM]	N/P
-1102	133	46,37	2,8	16,6
-1202	145,4	46,17	2,85	16,2
-1300	148,95	45,90	2,75	16,7
-1400	152,15	45,35	2,8	16,2
-1500	152,9	45,28	2,95	15,3
-1600	154,85	44,39	2,7	16,4
-1697	161,15	44,39	2,65	16,8
-1798	162,2	43,70	2,3	19,0
-1898	161,55	43,43	2,3	18,9
-1987	166,9	43,09	2,3	18,7
-2078	171,1	42,74	2,2	19,4
-2126	172,55	42,81	2,1	20,4

109-19-1-CTD

depth (dbar)	SiO ₂ [µM]	NO ₃ [µM]	PO ₄ [µM]	N/P
-1296	154,1	46,72	4,05	11,5
-1336	153,25	46,58	3,95	11,8
-1375	156,6	46,44	4	11,6
-1403	153,1	46,37	3,95	11,7
-1433	157,8	46,58	4,1	11,4
-1453	160,05	45,83	3,95	11,6
-1474	159,55	45,69	4,05	11,3
-1494	156,05	45,69	4,1	11,1
-1504	156,35	45,69	4	11,4
-1514	158,2	45,83	4,3	10,7
-1524	159,2	45,76	4,1	11,2
-1534	161,8	45,83	4,2	10,9

109-20-1-CTD

depth (dbar)	SiO ₂ [µM]	NO ₃ [µM]	PO ₄ [µM]	N/P
-1306	153,98	46,37	3,9	11,9
-1355	153,98	45,90	4	11,5
-1405	155,92	45,90	3,55	12,9
-1435	157,86	45,42	3,85	11,8
-1455	156,57	44,87	3,7	12,1
-1465	161,1	45,28	3,75	12,1
-1475	159,8	44,73	3,95	11,3
-1484	159,16	44,59	3,75	11,9
-1495	162,39	44,94	3,8	11,8
-1506	162,39	44,66	3,75	11,9
-1515	163,04	45,14	3,75	12,0
-1524	155,28	44,87	3,9	11,5

109-26-1-CTD

depth (dbar)	SiO ₂ [μM]	NO ₃ [μM]	PO ₄ [μM]	N/P
-912	128,7	46,24	4,1	11,3
-1011	131,6	46,58	4,15	11,2
-1111	136,45	46,58	4	11,6
-1309	143,55	46,44	10,8	4,3
-1507	167,35	46,03	8,4	5,5
-1706	156,5	44,73	3,85	11,6
-1954	162,5	43,36	3,55	12,2
-2004	166,95	42,95	3,5	12,3
-2014	166,65	43,16	3,5	12,3
-2024	170,3	43,02	3,45	12,5
-2034	170,3	43,22	3,35	12,9
-2044	166,05	40,89	2,15	19,0

109-29-1-CTD

depth (dbar)	SiO ₂ [μM]	NO ₃ [μM]	PO ₄ [μM]	N/P
-700	115,35	45,62	4,15	11,0
-898	123,4	45,69	3,8	12,0
-1123	127,4	45,48	3,85	11,8
-1200	136,05	45,83	3,7	12,4
-1351	146,55	45,62	3,55	12,9
-1600	157,55	44,80	3,35	13,4
-1817	166,5	44,53	3,5	12,7
-2002	172	43,43	3,25	13,4
-2201	174,1	43,16	3	14,4
-2291	174,8	42,74	3,2	13,4
-2322	176,7	43,02	3	14,3
-2342	178,9	41,03	2,5	16,4

109-34-1-CTD

depth (dbar)	SiO ₂ [μM]	NO ₃ [μM]	PO ₄ [μM]	N/P
-268	50,95	36,85	2,85	12,9
-317	62,25	39,25	3,25	12,1
-357	64,45	40,07	4,2	9,5
-396	70	40,89	4	10,2
-441	79,55	42,33	4	10,6
-481	85,8	43,29	4	10,8
-520	93,1	43,98	4,15	10,6
-580	102,4	44,80	4,25	10,5
-624	110,15	45,00	4	11,3
-644	104,75	44,59	3,8	11,7
-654	43,1	29,11	2,7	10,8
-659	101,45	43,09	3	14,4

109-35-1-CTD

depth (dbar)	SiO ₂ [μM]	NO ₃ [μM]	PO ₄ [μM]	N/P
-260	55,55	35,62	3,4	10,5
-357	66,85	39,39	3,75	10,5
-445	75,85	41,31	4,35	9,5
-500	83,35	42,95	4,55	9,4
-559	92,7	43,98	4,35	10,1
-659	97,4	44,59	4,8	9,3
-738	103,65	44,87	4,45	10,1
-802	107,25	45,07	4,45	10,1
-851	108,7	45,28	4,5	10,1
-871	111,05	45,35	4,65	9,8
-881	116,95	45,83	4,6	10,0
-885	120,1	45,55	4,3	10,6

109-37-1-CTD

depth (dbar)	SiO ₂ [μM]	NO ₃ [μM]	PO ₄ [μM]	N/P
-260	58,24	32,77	3,68	8,9
-309	60,64	35,40	3,8	9,3
-358	69,56	38,58	4,24	9,1
-408	76,24	39,18	4,16	9,4
-457	80,16	40,33	4,36	9,3
-495	83,88	41,10	4,4	9,3
-524	87,44	41,92	4,52	9,3
-554	94,68	42,52	4,56	9,3
-589	100,36	43,07	4,2	10,3
-619	99,44	42,80	4,28	10,0
-720	104,72	44,33	4,2	10,6
-734	102,96	43,02	3,32	13,0

109-42-1-CTD

depth (dbar)	SiO ₂ [μM]	NO ₃ [μM]	PO ₄ [μM]	N/P
-11	4,08	0,00	0,88	0,0
-103	29,72	20,50	3,04	6,7
-249	49,96	29,70	3,52	8,4
-461	78,56	37,92	4,4	8,6
-501	85,88	38,91	4,48	8,7
-526	87,4	39,68	4,48	8,9
-543	89,4	40,83	4,68	8,7
-559	96,16	40,83	4,72	8,6
-559	93,72	40,61	4,72	8,6
-579	97,24	41,37	4,68	8,8
-599	100	42,47	4,6	9,2
-637	104,4	41,87	4,4	9,5

4. Leg SO109-2

4.1 Cruise Objectives

by Peter Herzig and Mark Hannington

Axial Volcano is the dominant volcanic feature on the Juan de Fuca Ridge and is the site of several important active hydrothermal fields. The Volcano is located 250 nm from the Oregon coast, at a water depth of 1,500 m, and easily accessible to manned and remotely-operated submersibles (Fig. 33). The summit and the caldera of the Volcano (Fig. 34) has been the focus of intensive research by American and Canadian geoscientists following a series of undersea volcanic eruptions between 1986 and 1993. Continuous monitoring of earthquakes on the Volcano suggests that it is still active. The recent eruptions north of Axial, as well as ongoing high-temperature hydrothermal venting, have made this site an important long-term observatory for investigations of volcanic-hydrothermal processes, boiling hydrothermal systems, and metal inputs into the oceans. Because of its well-characterized biological communities, Axial Volcano is also considered to be unique for the study and long-term monitoring of faunal successions and their response to changing hydrothermal activity.

Five major research expeditions to Axial Volcano have been conducted by NOAA and GSC scientists using the manned submersibles PISCES IV and ALVIN (Jour. Geophysical Research, Special Volume, 95, B8). In 1993, the Canadian remotely-operated vehicle ROPOS was deployed near Axial Volcano to investigate the effects of a major diking event on the CoAxial segment (Fig. 35). This cruise provided the first detailed documentation of the early history of a new hydrothermal field (Geophysical Research Letters, Special Vol. 22). The present study was designed to characterize the detailed relationships between recent volcanic and tectonic events and hydrothermal fluxes in the vicinity of Axial Volcano for comparison with other sources of trace elements within the Juan de Fuca Plate (e.g., Oregon Margin, Fig. 33).

During cruise SO109-2, a joint research team from the University of Freiberg, GEOMAR (Kiel), the University of Heidelberg, the Geological Survey of Canada, the National Oceanic and Atmospheric Administration (NOAA), and the Universities of Victoria, Washington and Florida conducted a detailed survey of the present state of the Volcano and its associated hydrothermal activity. This collaborative project led to the first deployment and testing of Canada's deep submergence vehicle ROPOS (Remotely Operated Platform for Ocean Sciences) from R/V SONNE during SO109-3.

The principal scientific objective of the cruise was to document ongoing tectonic and volcanic activity at Axial Volcano and to monitor the changing hydrothermal fluxes. The volcanic-hydrothermal system at Axial is dynamic, and the presently active venting is intensifying.

Observations made during SO109-2 were designed to determine whether recent volcanic and tectonic events in the caldera could be responsible for the rejuvenation of the hydrothermal system. In addition to mapping and sampling in the caldera, the near and far

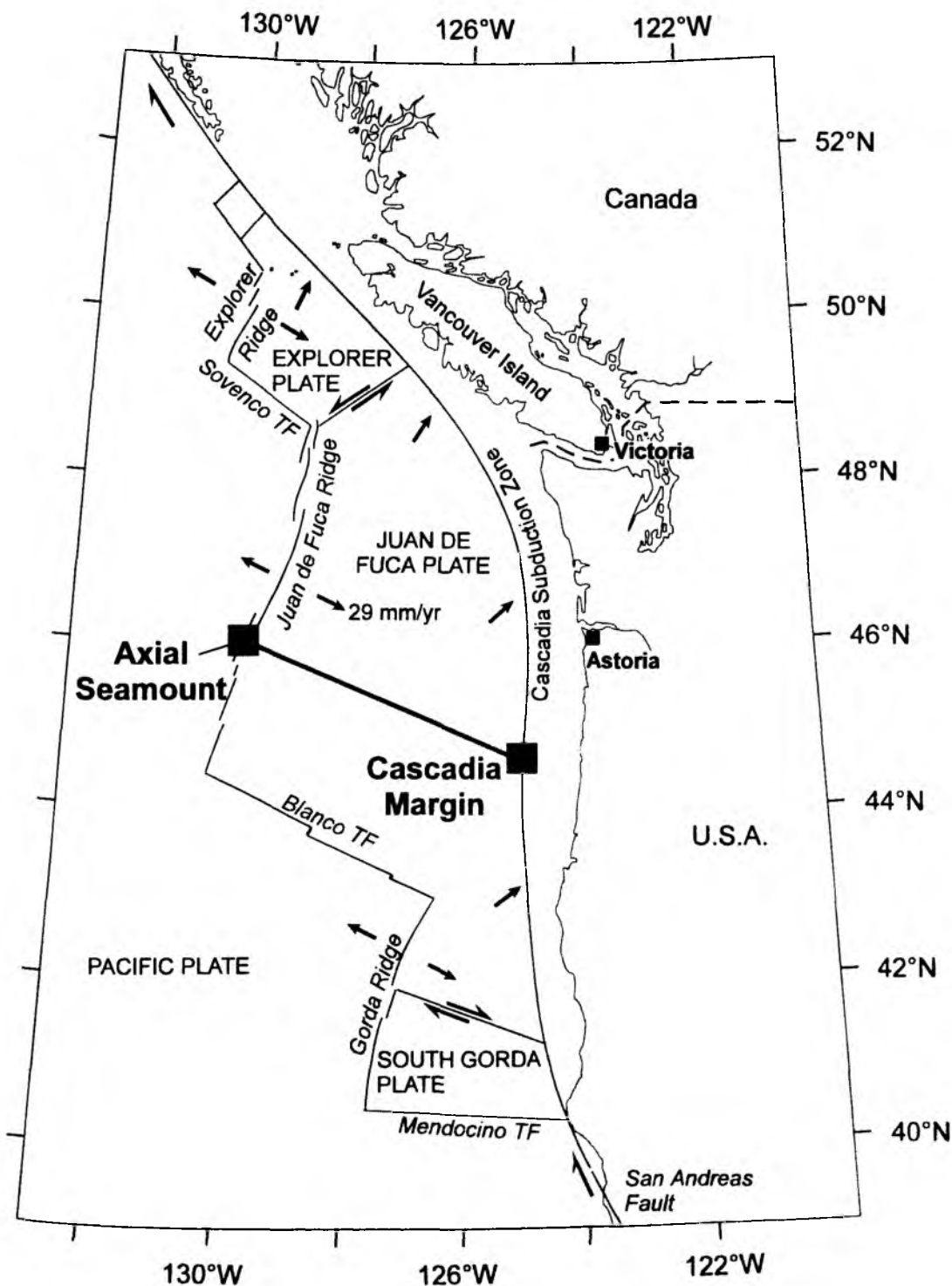


Fig. 33: Location of Axial Seamount at the Juan de Fuca Ridge and the Cascadia Margin in the NE-Pacific.

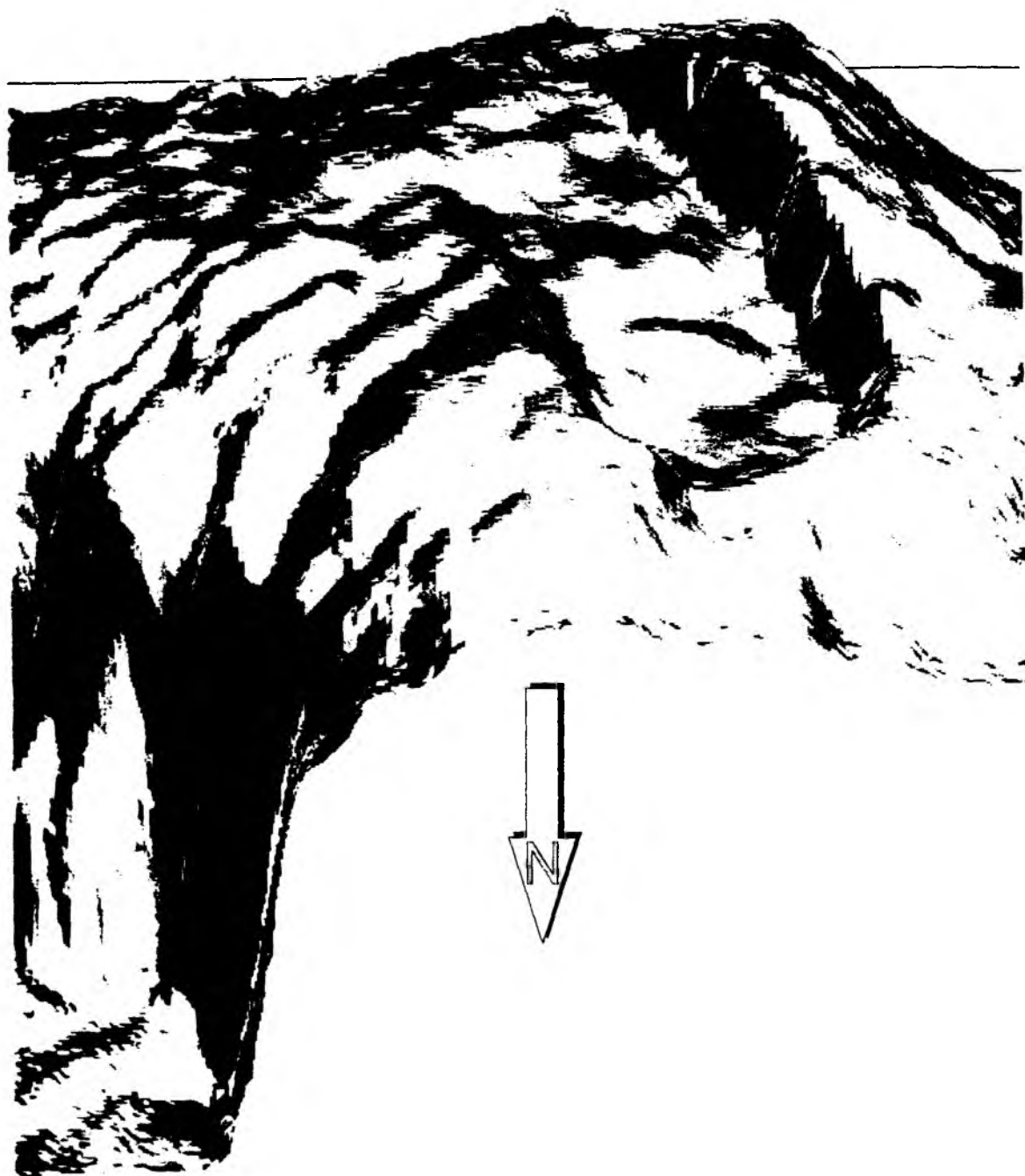


Fig. 34: Three-dimensional view of the summit and the caldera (25 km^2) of Axial Seamount based on Hydrosweep bathymetry collected during cruises SO109-1 and SO109-2.

field element dispersion from high- and low-temperature sources was examined in order to document the temporal and spatial variations in the physical and chemical characteristics of the water column above the Volcano. Axial Volcano is a complex magmatic system which also affects ridge-crest tectonism and hydrothermal activity north and south of the volcanic center, and these areas were targeted for additional investigation. Monitoring of the state of the Volcano and the present hydrothermal fluxes was accomplished by (i) detailed mapping and sampling of the ASHES and CASM hydrothermal vent fields in the caldera, (ii) investigations of several sites of recent eruptions and ongoing seismic activity in the North

and South Rift Zones (including areas with events recorded between April and June of 1996), (iii) detailed sampling of flows

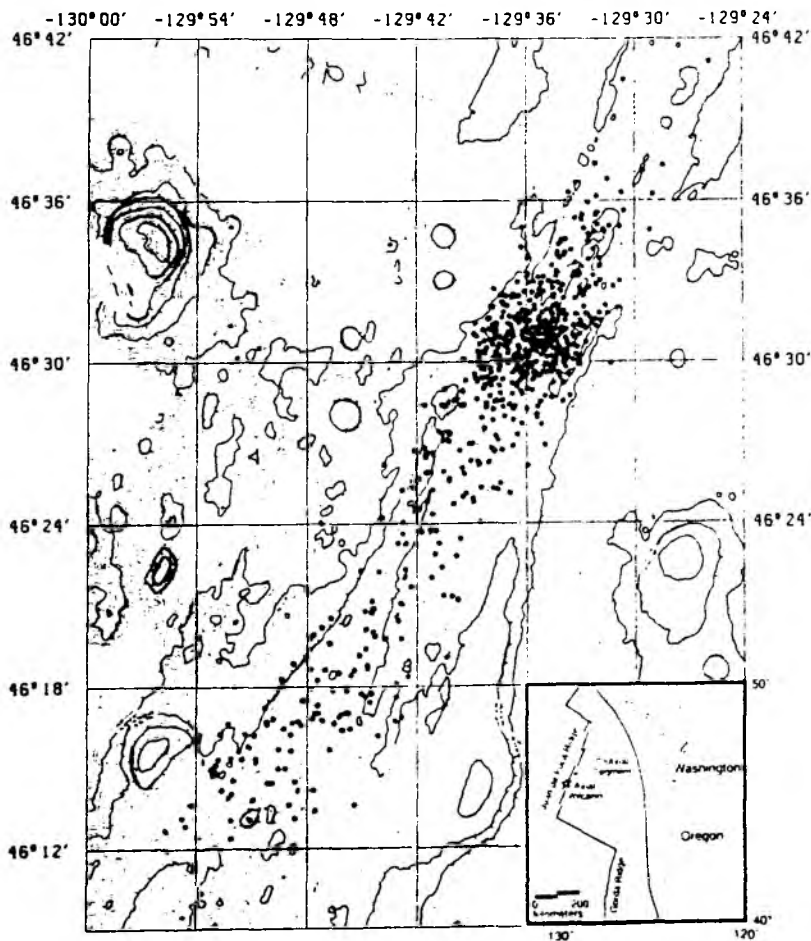
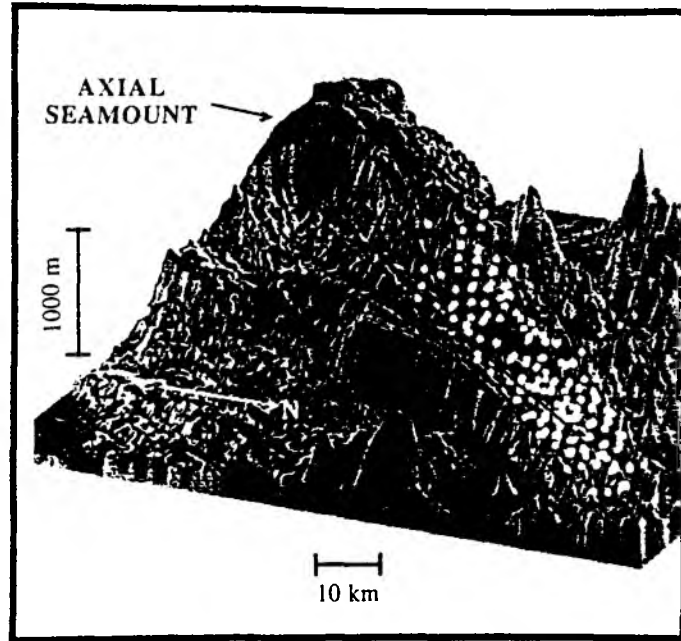


Fig. 35: Seismic events at the CoAxial segment northeast of Axial Seamount (Fox et al., 1995; Dziak et al., 1995).

from recent volcanic eruptions in the caldera (CASM) and in the North and South Rift Zones, (iv) monitoring of hydrothermal activity associated with volcanic eruptions and dike intrusions recorded in 1993 on the CoAxial Segment, (v) extensive hydrocast surveys of the caldera and adjacent rift zones, including navigated-CTD's over the active vent sites, (vi) sediment sampling in nearby basins, and (vii) placement of a long-term monitoring device to measure ongoing extension in the North Rift Zone (e.g., NOAA extensometer array).

The operations during SO109-2 were a prelude to detailed mapping and sampling of the vent sites using ROPOS. Several key targets for ROPOS dives during SO109-3 were identified, including new vents in the ASHES and CASM Fields and areas of diffuse hydrothermal flow at both the North Rift and South Rift Zones.

4.2 Cruise Narrative and Summary of Results

by Peter Herzig

The first Leg of the HYDROTRACE cruise (SO109-1) ended in Victoria/Vancouver Island on June 4, 1996. On June 5, the R/V SONNE was boarded by the shipboard scientific party of Leg SO109-2. The Canadian remotely operated vehicle ROPOS, the hydraulic unit, and a ROPOS service container were also taken on board. During SO109-2, the Hepburn winch for ROPOS was under repair in Victoria in preparation for diving operations during Leg SO109-3. After the scientific equipment was loaded and the installation of all systems completed, R/V SONNE left port on June 8 at 10:06 local time heading for Axial Volcano (46° N, 130° W).

On arrival at Axial on June 9 at 13:38, an array of five transponders was deployed and calibrated in the North Rift Zone. Sediment sampling by box corer in bathymetric basins NW and SE of Axial Seamount, as well as in the Helium Basin to the NE, was carried out in order to determine the extent of hydrothermal signatures recorded in distal sediments. The box corer in the Helium Basin recovered two distinct layers of volcanic ash (about 2-3 cm and > 90 cm thick), separated by a thin layer of pelagic sediment and topped by 5 cm of pelagic sediment. Radiometric dating of those layers will help to unravel the depositional history at this site. A CTD with 12 Niskin water samplers (10 l) was used to map the hydrothermal plume above Axial Volcano in three dimensions. A total of 18 CTD stations was carried out at locations inside and outside the caldera. Two CTD stations close to the ASHES Vent Field were transponder-navigated and sampled the near-field fluids. Shipboard methane analyses have shown values up to 680 nM CH₄, potential temperature anomalies up to 0.4°C, as well as distinct anomalies in light transmission, all about 10 to 20 m above bottom. Thermophile (> 55°C) and hyperthermophile (> 90°C) microorganisms were cultivated onboard from vent

plume samples collected with the CTD/rosette system. This is the first time that the presence of thermophile and hyperthermophile bacteria has been demonstrated in a hydrothermal plume. Similar bacteria were also cultured from samples of sphalerite and barite and in samples of gut from *Paralvinellid* worms collected with the TV-grab from active chimneys in the caldera. DNA analyses and epifluorescence microscopy will further characterize these bacteria.

A mapping program using SONNE's Hydrosweep system and Differential GPS (DGPS) was carried out to survey the area of Axial Volcano including the North and South Rift Zones. A total of 53 Hydrosweep profiles was compiled to generate a bathymetric map with 10 m contour intervals as well as a separate map for the caldera, encompassing the CASM and ASHES Fields, the South Rift Zone (5 m contour interval), and the North Rift Zone (5 m contour intervals). The bathymetry provides an important baseline for ongoing monitoring of volcanic and tectonic activity at Axial and complements existing Sea Beam bathymetric maps of the neovolcanic zone completed by NOAA in 1991. The Hydrosweep maps will be published jointly by the principal investigators as an Open File Report of the Geological Survey of Canada.

The North Rift Zone was investigated with the EXPLOS TV/camera sled system which is run on a 8,000 m fiber optic cable and rated to a water depth of 5,000 m. EXPLOS was navigated using the transponder net. A zig-zag tow along the North Rift Zone indicated abundant fissure- and fracture-controlled diffuse hydrothermal activity, marked by the presence of bacterial mats and hydrothermal fauna. A second camera tow was performed to investigate hydrothermally active areas in greater detail, and a deployment of the TV-controlled grab sampled a young lava flow observed during the camera runs. The grab recovered a large, 350 kg pillow, partly covered with fresh glass. In an attempt to measure horizontal extensions of the seafloor related to dike intrusions, five acoustic extensometer instruments were deployed in a line across the North Rift Zone at 100-200 m spacings. These instruments are battery powered and calibrated to measure baseline distances up to about 1 km with an accuracy of about 1 mm. The instruments can make one measurement per day for a year. The data are stored in a data unit which will be recovered together with the instruments in summer 1997. After operations at the North Rift Zone, three of the five transponders were released.

A deployment of the EXPLOS system in the South Rift Zone mapped additional areas of hydrothermal activity. NOAA's chemical scanner SUAVE (Submersible System Used to Assess Vented Emissions) was fitted at sea for use on the EXPLOS frame and has measured temporally coherent anomalies in temperature, light scattering, dissolved Mn, and H₂S. For each parameter measured, isolated anomalies were found. The scanner was run in an unattended monitoring mode at low sensitivity with detection limits of 20 nmol/l Mn,

35nmol/l Fe, and 40nmol/l H₂S. The thermochemical anomalies (Mn/heat(=Q), Fe/Q, and H₂S/Q) at the South Rift Zone are characteristic of diffuse fluid venting.

The CASM Hydrothermal Field in the northern part of the Axial Seamount caldera was sampled extensively with the TV-grab. The first deployment recovered 300 kg of basaltic material with some Fe-staining and pyrite as well as pyrrhotite occurring in vesicles. The second grab recovered 150 kg of basaltic sheet flows with distinct sulfide mineralization, anhydrite in cavities, and abundant vent fauna. The occurrence of sphalerite and chalcopryite on the underside of broken sheet flows and the fact that tube worms observed during sampling were growing from the surface down into lava cavities and collapse pits indicates hydrothermal fluid flow beneath the lava surface. The presence of chalcopryite in the mineral assemblage points to fluid temperatures of more than 300°C. Fluid inclusion analyses of coexisting anhydrite will constrain the fluid temperatures. Compared to earlier observations by PISCES IV and ALVIN, the main eruptive fissure at CASM appears to have been hydrothermally reactivated after a period of relative quiescence. Further deployments of the TV-grab at CASM recovered about 100 kg of massive barite with some associated sulfides, abundant vent fauna, and 500 kg of weakly altered basalt. The barite is part of the CASM chimneys which were located with the TV-grab during several crossings of the main fissure zone.

Reactivation of hydrothermal activity was also observed in the ASHES Vent Field. In 1986, ALVIN temperature measurements indicated that the Inferno chimneys were venting at about 330°C. Repeat measurements in 1995 showed that the fluid temperatures had increased by about 20° to 348°C. At a water depth of about 1,500 m (equal 150 bars or 15 mPa), these fluids cross the two-phase boundary of seawater and start to boil, as observed at Inferno during ALVIN diving. A major task of the forthcoming ROPOS dives will be to sample boiling fluids and associated precipitates from the same vent to document the impact of boiling on the fractionation of metals and sulfur isotopes. A transponder net consisting of three transponders was installed at ASHES in preparation for EXPLOS and ROPOS diving. Sampling with the TV-grab in the vicinity of Virgin Mound recovered about 100 kg of massive sulfides consisting of pyrite, marcasite, sphalerite, and chalcopryite, together with abundant tube worms, sulfide worms, and other vent fauna. Some of the samples represent small sulfide mounds of about 50 cm in diameter and 30 cm in height showing distinct high-temperature fluid channels lined with chalcopryite. This hydrothermal area was not known previously and likely represents a new vent that has grown during the recent thermal intensification of the field. In order to preserve the active chimneys at ASHES for time-series measurements and sampling by ROPOS during Leg SO109-3, further TV-grabs were avoided. However, a camera tow just east of the chimney field revealed new areas of venting, extensively covered by white bacterial mats with abundant tube worms and

spider crabs indicative of diffuse hydrothermal flow. Several small active vents were photographed.

The CoAxial Segment, which was the site of a major eruption just north of Axial in 1993, was surveyed using EXPLOS and SUAVE. A traverse along the main eruptive fissure up to the HDV (High Diffuse Venting) site indicted several areas of diffuse hydrothermal fluid flow and associated biological activity. Both vent specific fauna and bacterial mats were found, but their extent appears to have diminished dramatically since 1993, owing to the cooling of the lava flows and the collapse of low-temperature circulation. During one survey, the SUAVE system detected 6-8 distinct thermal and chemical anomalies, although no visible indications of active venting were observed during this tow. The $\text{H}_2\text{S}/\text{Q}$ value determined by SUAVE for CoAxial (5.3 nmol/J) is similar to the value measured in 1995 (3.8 nmol/J) but much lower than the pulse of high $\text{H}_2\text{S}/\text{Q}$ (32 nmol/J) that immediately followed the dike intrusion associated with the 1993 eruption. A TV-grab at the HDV site successfully sampled vent fauna, but the sample was washed out during heaving of the grab.

On June 22, R/V SONNE started an intense three-day work program at the Cascadia Margin (90nm off-shore Astoria). Four transponders were deployed and calibrated in preparation for ROPOS dives at this site during SO109-3. However, DGPS was not available on the second and third day of operations due to a failure in the ship's INMARSAT system. The aim of the Cascadia Margin program was to observe and sample cold seeps and associated fauna located at a bioherm in this area during Leg SO109-1 and on previous ALVIN dives. Work during SO109-2 included detailed bathymetric mapping with Hydrosweep, CTD/rosette sampler depolyments, EXPLOS runs, and sampling with the TV-grab. Shipboard analyses of water samples have revealed methane concentrations up to 4,700 nl/l and clearly documented extensive degassing at the seafloor. However, tides and currents appear to significantly affect the distribution pattern of plumes in this environment. H_2S is an important constituent of gas hydrates ($\text{CH}_4 + \text{H}_2\text{S}$), and abundant sulfidic muds were sampled during Leg SO109-2. The SUAVE scanner was mounted on the EXPLOS system in an experiment to map H_2S in the water column. However, no anomalous values were observed, suggesting that insufficient heat is available to support a buoyant plume of H_2S . Several EXPLOS runs were successful in delineating areas with abundant cold seep fauna, often located in bathymetric depressions similar to collapse pits. Sampling of those areas with the TV-grab recovered indurated sediments and limestone as well as abundant cold seep fauna. Degassing of H_2S was obvious during heaving of one of the grabs, and precautions were taken to avoid any hazards resulting from H_2S degassing on deck (personnel wearing gas masks). The content of this grab consisted of spectacular samples of indurated sediments, with complex degassing channels similar to small chimneys, and abundant fauna specific to cold seeps.

On June 25, at 05:24 local time, the R/V SONNE departed the Cascadia Margin for Astoria/Oregon. Leg SO109-2 ended at 15:00, when the ship was tied up at the pier of Astoria. After exchange of personal and loading of equipment and supplies, the ship departed for Victoria on June 26. On June 27, the ROPOS winch, with 3,000 m of fiber optic cable, was loaded and testing was carried out in preparation for ROPOS dives at Axial Volcano during Leg SO109-3.

4.3 Operations Background

Deployment of Transponders

Three existing transponders on site at the CoAxial Segment were also used to locate and navigate the EXPLOS/SUAVE surveys in the North Rift Zone.

Three transponder nets were used during Leg SO109-2. The first net was deployed at the North Rift Zone. The second covered the Axial caldera and the upper South Rift Zone. Net three was deployed at Cascadia Margin. Transponder nets were used to navigate camera tows, most TV-grabs and few CTD's.

CTD Casts and Related Studies

A total of 18 CTD casts and tow-yo's has been deployed at Axial Seamount and detected maximum methane concentrations of 680 n/l CH₄ near the ASHES Vent Field. Methane plumes are stable with time but maximum concentrations are generally between 100 to 150 n/l CH₄. For the first time hyperthermophylic microorganisms have been cultured from a vent plume (ASHES). Background CTD measurements were conducted around the Axial caldera. Nine CTD casts and tows in the bioherm area at Cascadia Margin found a highly variable methane distribution in space and time with extremely high CH₄ concentraions up to 4,700 n/l.

Sediment Sampling

Three box corer were deployed in sedimented basins around the Axial caldera to complement the sediment sampling conducted during SO109-1. Stations 53 GKG and 55 GKG retrieved beige carbonate clay/ooze on top of a glauconitic sand sized sediment from basins to the NW and SE of the Axial caldera. The sediments in the Helium Basin were sampled during station 58 GKG and recovered layered basaltic glass with interbedded pelagic mud horizons. TV-Grabs

Nine TV-grabs were conducted at the hydrothermal sites within the Axial caldera. Eight attempts at the CASM Field recovered fresh basalt, massive sulfides and massive barite crusts from the main fissure or the vicinity of the lamphere spire. A black smoker sulfide

assemblage was recovered during a single TV-grab at the ASHES hydrothermal field. One TV-grab was performed at each of the North Rift Zone and the South Rift Zone and they both recovered fresh glassy basalt. An attempt to recover vent fauna at the HDV site on the CoAxial Segment failed. Six TV-grabs deployed at the Cascadia Margin recovered abundant carbonate blocks and sediment with large amounts of vent fauna.

EXPLOS Camera Surveys

Eight camera tows were conducted at different working areas. The North and the South Rift Zone were mapped and surveyed during 5 camera runs and found diffuse venting especially in the South Rift Zone. A single camera tow was carried out in the vicinity of the ASHES Vent Field. Additional camera tows were also conducted at the CoAxial Segment and at the Cascadia Margin.

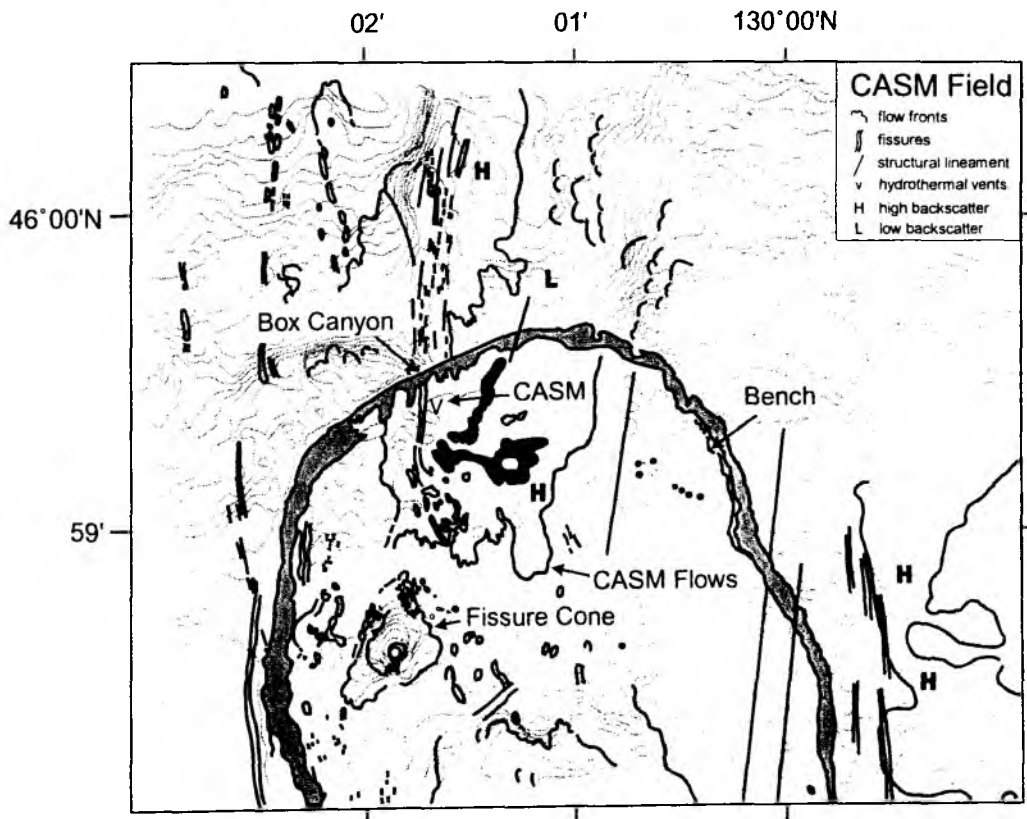


Fig. 36: Detailed bathymetry and geology of the north end of the Axial caldera in the vicinity of the CASM Field (5 m contour interval). Lava fronts are interpreted from acoustic backscatter; black areas represent areas of low backscatter (lava pond or lake). Modified from Embley et al. (1990).

Acknowledgements

Principal funding for the SO-109 HYDROTRACE project was provided by the German Ministry for Research and Technology, Bonn (BMBF Grant No. 03G0109A) to Freiberg University of Mining and Technology. Funding for the operation of ROPOS was provided by

Natural Resources Canada (Geological Survey of Canada). Additional operational costs for ROPOS were provided by the Natural Sciences and Engineering Research Council of Canada via a grant to University of Victoria. Logistical support for navigation, water sampling, and plume mapping was provided by the National Oceanic and Atmospheric Administration through NOAA (Newport and Seattle). Additional support for this research was provided by the U.S. Department of Interior's Mineral Institute Program, Generic Mineral Technology Center for Marine Minerals (MMTC) Grant No. G1135128-9711. We thank Master H. Papenhagen and the officers and crew of the R/V SONNE for their assistance and cooperation during research activities at Axial Volcano.

4.4 Results

4.4.1 Explos Camera Tows

by Bob Embley

Introduction

The caldera and upper rift zones of Axial Volcano were surveyed extensively with Seabeam, Sea MARC I (deep-towed 30 kHz sidescan), towed cameras, and submersibles in the 1980s (CASM, 1985, Embley et al., 1990, Zonenshain et al., 1989). Additional camera surveys (unpub. data) were made from the NOAA Ship DISCOVERER on the North Rift Zone in 1991 and 1994. These data revealed extensive areas of fresh lava and diffuse venting on the upper (shallowest) portions of the rift zones, including "snow-blower" type bacterial vents (Embley et al., 1990). Axial Volcano is the only site on the Juan de Fuca Ridge that has been geophysically monitored over a long period of time. Manifestations of a probable diking event were directly observed in 1988 with a pressure gauge, current meter, and time-lapse camera (Fox, 1990), so it has the distinction of being the first seafloor site that was instrumented during a diking event. The present-day high level of tectonic/magmatic activity on the summit of Axial Volcano also is indicated by frequent earthquake swarms that have been recorded on the NOAA T-wave monitoring system since 1991.

The EXPLOS program during R/V SONNE cruise 109-2 was designed to characterize the present state of the hydrothermal systems on the summit of Axial Volcano and to provide a baseline for future volcanic/hydrothermal perturbations.

North Rift Zone

EXPLOS 56

General

This tow (Fig. 37) was planned to survey the North Rift Zone of Axial Volcano from the northern caldera rim northward about 8 km. Of particular interest was to investigate whether

there had been any new eruptions and/or hydrothermal activity since the earlier surveys. The NOAA Newport T-phase group had reported several earthquake swarms in this area in the month preceeding Leg 109-2, providing special impetus to the resurvey. The NOAA long-baseline navigation was used together with the SONNE short-baseline system. The EXPLOS reached bottom at 20:15 (UTC) on 10-06-96 and made two cross-axis lines

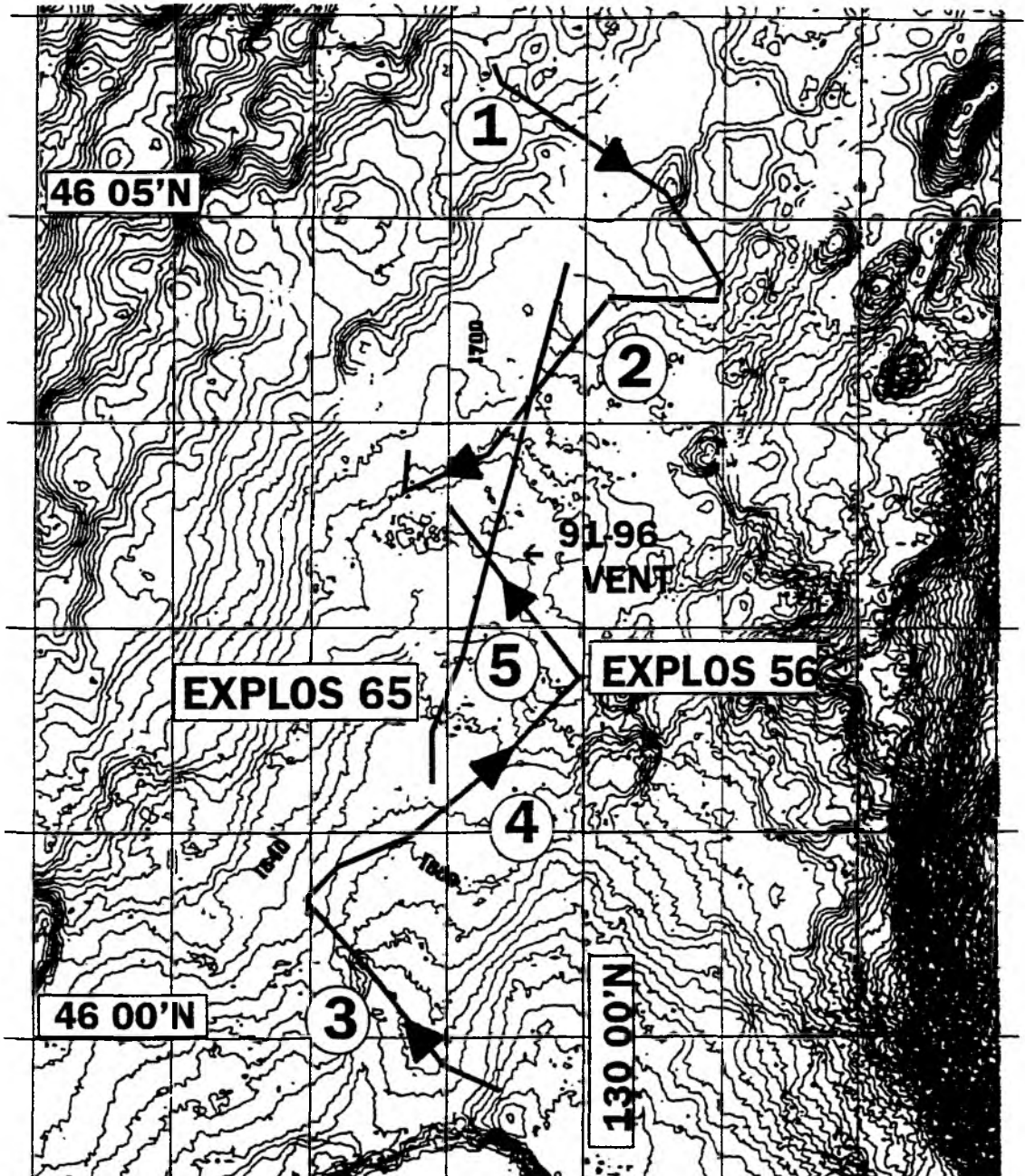


Fig. 37: Location of EXPLOS tows 56 and 65 on the upper North Rift Zone of Axial Volcano (north rim of caldera at bottom of map). Bathymetry is from NOAA SeaBeam data base (not corrected for sound velocity). Contours at 10 m intervals. Numbers in circles are traverse lines of EXPLOS tow 56 in sequence that they occurred (tow was in two parts, first part began north and second part began south). The 91-96 vent refers to vent site imaged on NOAA camera tows in 1991 and the 1996 EXPLOS tows.

(sections "1" and "2" on Fig. 37) before it started back to the surface at 00:37 in order to replace the failed relay transponder. The tow was restarted from the south because of a shift in the wind. It reached bottom again at 02:48 on 11-06-96 and crossed the axis of the NRZ three more times (section "3", "4", and "5" on Fig. 37) before terminating at 07:37.

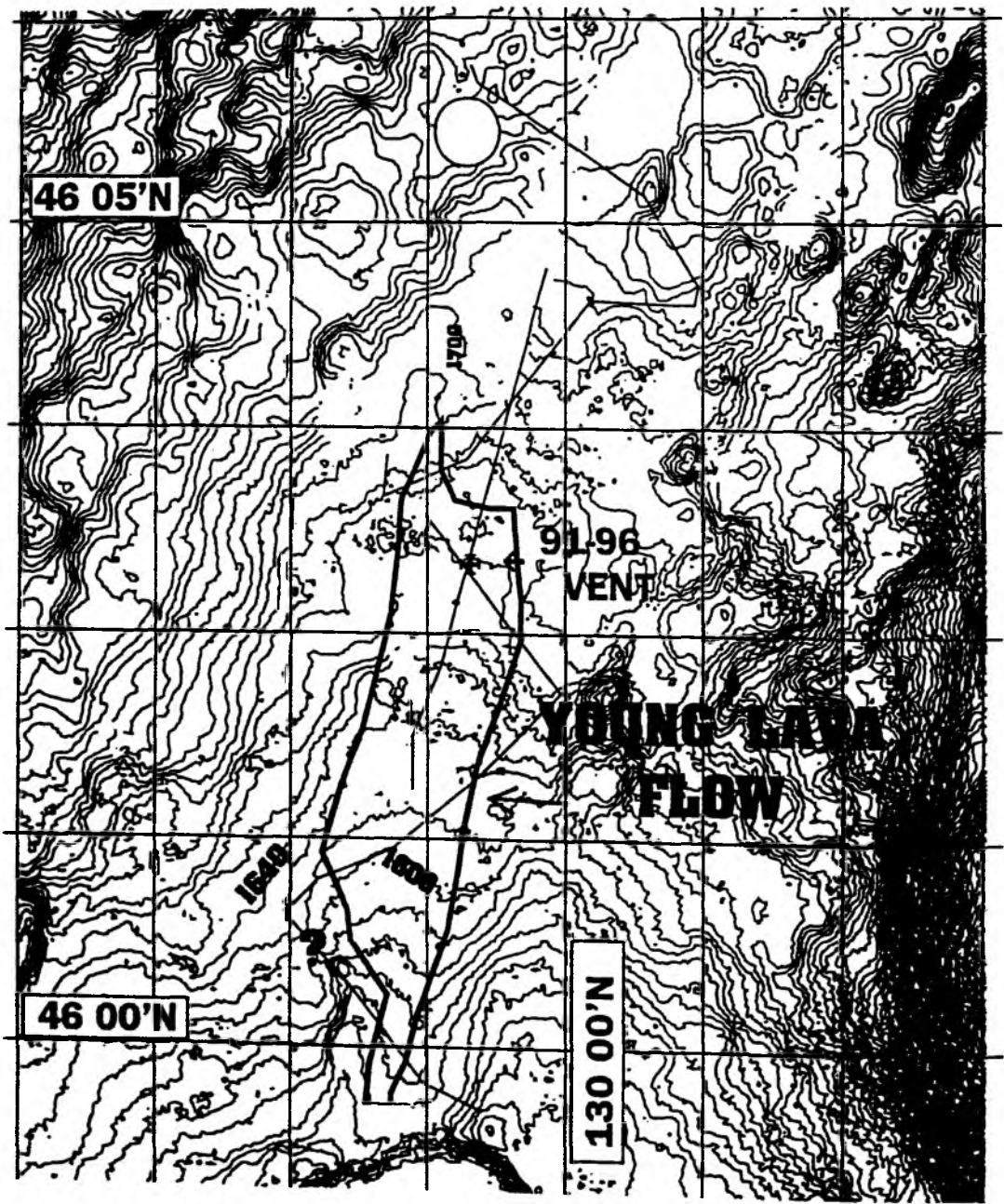


Fig. 38: Preliminary map of youngest lava flow on North Rift Zone of Axial Volcano. Boundaries taken from review of EXPLOS video tapes. (EXPLOS tows 56 + 65, see Fig. 37) There is uncertainty in exact location in some of boundaries, particularly the SW boundary near caldera (marked by "?").

Results

An extensive area of young lavas was mapped out from near the caldera rim to about 46°03' N (Fig. 38). The lava consists predominantly of glassy sheet flows with a light sediment coating. Obvious tectonic fissures were rare or absent within this zone. The sheet flows vary between flat ropy/lineated, jumbled chaotic, and lobate forms.

The central portion nearest the probable eruptive fissure contained extensive drain pits and lava spires.

North of its northern extent at about 46°03' N and to the east and west of the boundaries of the young flow, the lava flows are clearly older; they do not have a vitreous luster, and are covered with a thin coating of sediments. The higher rim of the caldera crossed at the beginning of the second part of the tow (line 3 at the SE corner of the tow track, Fig. 37) was surfaced with even older, heavily sedimented lavas. A distinctive dark colored sediment (fragmented volcanic glass and/or manganiferous sediment?) was intermixed with lighter sediment in this area. The only distinct area of hydrothermal venting found on EXPLOS 56 was located very near the vent site imaged during a NOAA camera tow in 1991 (marked as "91-96" vent on Fig. 37). Both the 1991 and 1996 towed camera video clearly show colonies of clams, bacterial mats, and tubeworms amongst young jumbled sheet flows. A probable hydrothermal temperature anomaly was detected at 23:57 at the mid-point of line 2 (Fig. 37), but no indication of active venting was observed on the video.

EXPLOS 65

General

EXPLOS 65 was planned as an along-axis tow to map the extent of venting only approximately defined by EXPLOS 56. The tow was made in a SW-NE direction and crossed over Lines 5 and 2 of EXPLOS 56 where temperature anomalies and/or biologic indicators of active venting were observed. It reached bottom at 22:48 on 12-06-96, and left bottom at 01:58 on 13-06-96. Both the NOAA long-baseline and SONNE short baseline navigation systems were used. The EXPLOS CTD was operational.

Results

The camera traversed through the young lava flow the entire time until 00:38, when it passed over the northern contact with older lavas. Several probable hydrothermal temperature anomalies were detected at 01:00 and 01:15 but no obvious hydrothermal indicators were seen on the video. The vent found on EXPLOS 56 was traversed at 00:10 to 00:15, but surprisingly, no distinct temperature anomaly was seen on the EXPLOS CTD at this location.

Summary of Results from North Rift Zone Tows

The youngest lava flow on the upper portion of the North Rift Zone was clearly delineated within a long baseline transponder reference frame during EXPLOS 56 and 65. The only clearly defined diffuse vent was found very close to the location of a vent located in 1991

during a NOAA camera tow. Based on crossings of it on the 1996 tows, it is approximately 50 to 100 m in diameter and is confined to pressure ridges of jumbled sheet flow in the youngest lava flow of the North Rift Zone. No other biologically active vents have been found on either Leg 109-2 or the earlier DISCOVERER camera tows so it now appears probable that this is the only substantive vent area remaining from the volcanic event that erupted the young lavas.

There were no indications of recent bacterial blooms over the North Rift Zone in the EXPLOS tow data. Experience from the 1993 CoAxial dike injection and the mid-1980's southern Juan de Fuca (Cleft segment) suggests that had such an event occurred within the past year in conjunction with the earthquake swarms over the summit of Axial Volcano, fallout from the bacterial bloom would have been clearly visible both in the water column as high turbidity layers on CTDs and on the seafloor in the form of small "drifts" and very turbid water.

The data from the Leg 109-2 EXPLOS tows over the North Rift Zone of Axial Volcano provide an important baseline for future magmatic/hydrothermal event detection and should allow researchers to more clearly determine the volcanic, tectonic, and biologic effects of an event in the future.

Caldera and Upper South Rift Zone

EXPLOS 79

General

EXPLOS 79 was planned as a resurvey of several vents that were located on PISCES IV and ALVIN dives made in the 1980s on the uppermost South Rift Zone where it lies within the caldera of Axial Volcano east of the ASHES Vent Field (Fig. 39). The southernmost target was the Axial Gardens vent field (marked 'AG' on Fig. 39) which had been discovered and sampled on ALVIN dives 1925 and 1928. The remaining targets were several vent areas observed on PISCES dive 1730. These lay along a trend parallel to the southeastern extension of the east wall of the caldera.

EXPLOS 79 reached bottom at 23:18 on 23-06-96 and left bottom on 04:30 on 24-06-96. Data from EXPLOS CTD and the NOAA SUAVE chemical scanner were recorded during this tow. Long-baseline navigation was used for the tow.

Results

The primary finding of EXPLOS 79 was the discovery of almost continuous diffuse venting along a 1.5 km path on the eastern side of the caldera. The most extensive and biologically productive of these vents was passed over at 02:00-02:04 (marked "SONNE Vent" on Fig. 39) in an area of (apparently) older pillow lavas. The SONNE Vent was characterized by densely packed "bushes" of tubeworms, clusters of clams in pockets between the pillow lavas, bacterial mats, and hydrothermal sediments. No clearly-defined high-temperature

deposits were observed, although a small chimney-like feature was passed over at 01:44 just south of the SONNE Vent.

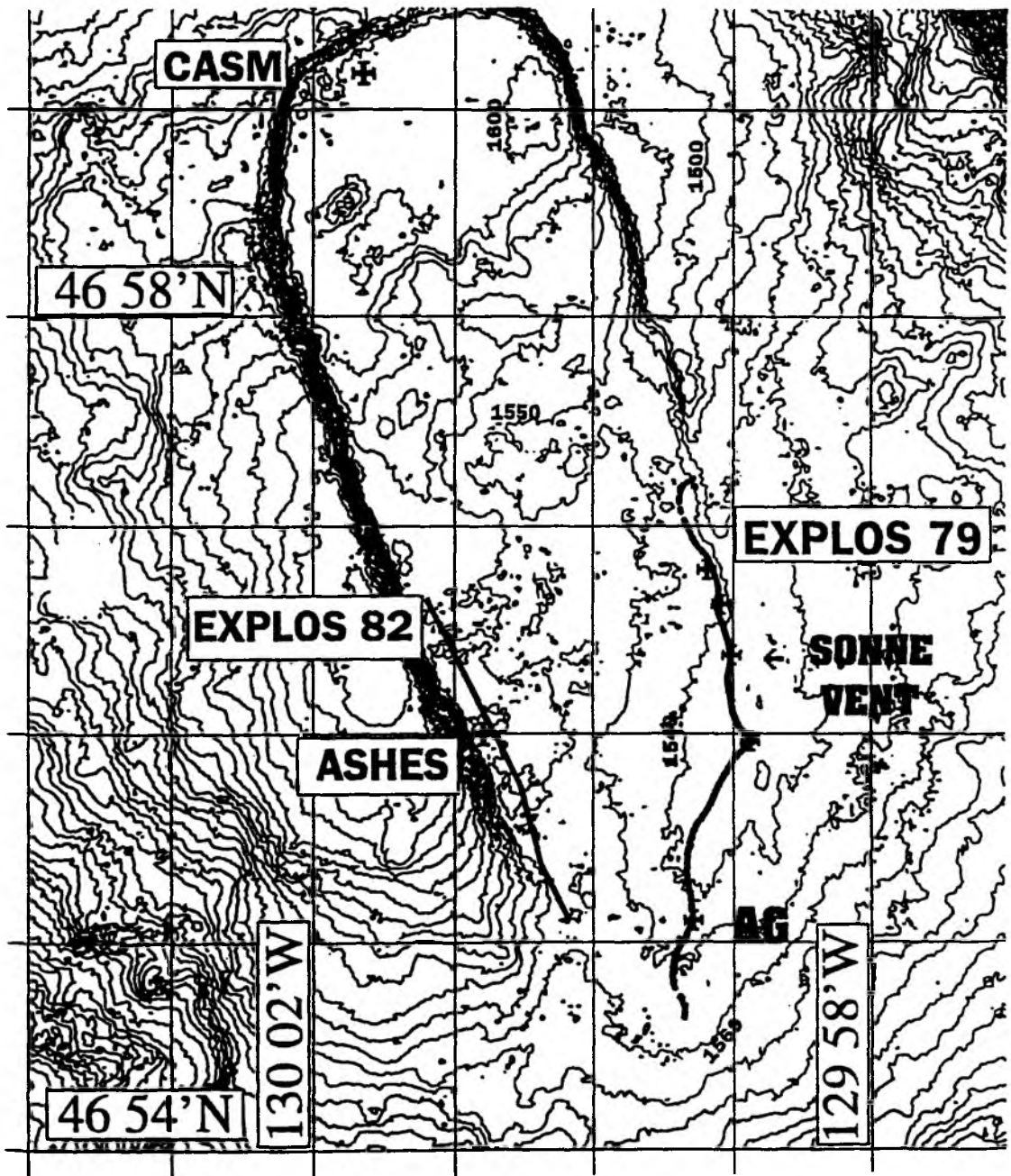


Fig. 39: Location of EXPLOS tows 79 and 82 in the southern Axial Caldera. Vents are marked by crosses. 'AG' is location of Axial Gardens vent site discovered in 1980 (Embley et al., 1990).

After passing over the SONNE Vent from east to west, no additional venting was observed until 02:45 as the EXPLOS moved west and then back to the north. Hydrothermal signs (bright sediment pockets, clams) were again observed at 02:49. At this point, the EXPLOS was turned onto a line oriented on a NW trend connecting the SONNE Vent with the location of the new vent. Semi-continuous signs of venting were observed along the EXPLOS track along this trend until about 03:30. EXPLOS continued NW until about 04:14 when it turned

NE toward the wall until the tow was terminated at 04:30. The SUAVE detected some chemical anomalies over the vents found on EXPLOS 79 (see section on SUAVE results for details).

EXPLOS 82

This tow (Fig. 39) was planned to survey the present extent and type of venting along the caldera floor south of and north of the ASHES Vent Field. It reached bottom at 23:29 on 16-06-96 about 2 km SE of the ASHES Vent Field and left bottom at about 02:09 on 17-06-96 about 1 km NW of the ASHES Vent. The first part of the tow (until 23:56) traversed the heavily sedimented older lavas on the west wall of the caldera. The remainder of the tow traversed the caldera floor along a line parallel to the wall. Hydrothermal sediment was observed within the interstices of the young lobate sheet and pillow lavas semi-continuously from about 00:10 until about 01:30. Tubeworms and possible anhydrite deposits were passed over at 01:08 to 01:11. The tow confirmed that the high-temperature ASHES Field still retains a NW-SE-oriented (wall parallel) halo of lower-temperature diffuse venting characterized by extensive Fe-Si precipitates.

Summary of Results from Caldera and Upper South Rift Zone

Togegther with the GTVA stations in the CASM area, the Leg 109-2 EXPLOS tows in the southern portion of the caldera and on the northern extension of the South Rift Zone of Axial Volcano show that the caldera retains extensive areas of diffuse venting. The EXPLOS 79 tow revealed extensive areas of venting along the eastern side of the caldera, some of which had not been imaged during the 1980's surveys. It is also now clear that the venting on this side of the caldera lies along a well-defined line of the same orientation as the caldera wall. This suggests that at least some of the vents on the east side of the caldera may be at least partly controlled by normal faults now partially buried beneath young lava flows.

Floc Site

EXPLOS 84

EXPLOS 84 was planned to image the Floc area lying within the Axial valley of the CoAxial Segment of the Juan de Fuca Ridge NE of Axial Volcano. During the 1993 dike injection/eruption event, this area had been the site of an extensive burst of diffuse venting that was associated with a spectacular bacterial bloom. Repeat visits in 1994 and 1995 with ALVIN recorded the continued shrinkage of the venting along a NE-SW trending fissure system cutting through pre-1993 lavas between 46°16' and 46°19' N. One goal of the HYDROTRACE leg 109-2 expedition was to characterize the state of venting at this site in 1996. The tow was planned to image several previously marked sites along a SE-SW track and reached bottom at the southernmost target at 17:13 on 17-06-96. Unfortunately, wind and wave conditions prevented the positioning of the EXPLOS at the two southern sites. A

portion of the northern site (HDV) was imaged during the latter portion of the tow but no active vents were located, and a severe surging of the camera into the bottom created turbid conditions which made visibility very poor in the vicinity of the vent. The tow was terminated at 00:52 on 18-06-96. The SUAVE was mounted on the EXPLOS during tow and did detect some anomalies over the site (see section on SUAVE results for details).

Concluding Comments

Axial Volcano has been the most volcanically robust segment of the Juan de Fuca/Gorda Ridge system over the past million years. Observations of perturbations in the volcanic and hydrothermal systems of Axial Volcano made during the 80's and 90's and the high level of seismicity seen on the T-wave monitoring system since 1991 strongly imply that there will be continued events with observable/measurable geologic, chemical, and biologic manifestations in the next decade. The EXPLOS tows over Axial Volcano during Leg 109-2 provide an important baseline for future magmatic/hydrothermal episodes at this site.

4.4.2 Hydrothermal Venting and Sulfide Deposits

by Ian Jonasson, Mark Hannington and Peter Herzig

Introduction

Detailed mapping and sampling was carried out within the caldera of Axial Volcano and along the North and South Rift Zones. Low-level hydrothermal activity is found in several areas throughout the caldera, but sulfide deposits have been sampled only in the ASHES and CASM Fields. Minor occurrences of Fe-oxide and silica deposits (hydrothermal sediments and small, delicate chimneys) are commonly associated with the diffuse venting, bacterial mats, and tube worm colonies. In areas of very recent eruptions (e.g., CoAxial site), the Fe-oxide deposits appear to be products of the biologically mediated interaction of hot lava and ambient seawater. These sediments generally disappear a few years after the eruption leaving residual aluminosilicates.

The principal objective of the sulfide sampling was to establish the present state of hydrothermal activity on the volcano and to identify precise dive targets for work with ROPOS during SO109-3.

ASHES Field

The ASHES Vent Field is a large area of discontinuous, patchy low-temperature venting, covering an area of 1,200 m x 200 m. The northern part of the field is punctuated by five higher-temperature vents (Inferno, Hell, Mushroom, Hillock, and Virgin Mound) in a small area of about 80 m x 80 m. Active low-temperature discharge also occurs along the caldera wall, adjacent to the high-temperature vents (Embley et al., 1990; Hammond, 1990).

Contrasting permeabilities between different lava types in the vent field appear to control the locations of the vents (e.g., Hammond, 1990).

Shipboard observations during SO109-2, and earlier observations from ALVIN in July 1995, indicate potentially dramatic increases in the intensity of hydrothermal upflow at ASHES. One EXPLOS camera tow (82 EXPLOS) at the margins of the ASHES Field revealed that the size of the field had expanded up to 40 m outward in conjunction with an increase in the temperature of hydrothermal upflow. Although the main upflow zone, close to the caldera wall, is well-established, the recent seismic activity and increase in hydrothermal temperatures appear to be associated with new cracking events at the margins of the field. New tube worm colonies are present east of the main field, and a new black smoker chimney at the northeast corner of the field was recovered during 81 GTVA. This sample comprises nearly 50% chalcopyrite, with multiple chalcopyrite-lined orifices, indicative of high-temperature venting. The intact portions of the chimney closely resemble sulfides collected from the Inferno chimney in 1988 and from Hell Vent 1995. In 1995, the highest-temperature vents at Inferno were boiling at 348°C, and the new vents may also be close to the two-phase boundary for seawater. Samples of the highest-temperature vents at ASHES have provided critical new insights into the behaviour of phase-separated fluids in seafloor hydrothermal systems (see SO109-3). The relationship between boiling and non-boiling vents and the impact of high-temperature boiling on mineral deposition will be investigated further by detailed mineralogical and chemical studies of chimney samples collected by ROPOS.

CASM Field

The CASM Field, at the northern end of the caldera, includes a number of warm-water vents occupying the main eruptive fissure, a large area of diffuse flow to the east of the eruptive fissure, and a small chimney complex. The vents in the main fissure occur at open fractures in basalt on the bottom of the fissure and in fractured sheet flows along its east wall (see 61 GTVA). The vents are populated by extensive bacterial mats, and several diffuse vents through the fractures in the basalt are inhabited by tube worms in mound-like colonies up to a meter in diameter. Similar venting was observed at this site in 1983, but hydrothermal fluids emanating from the fractures were less than 35°C (CASM II, 1985). More vigorous venting observed during 61 GTVA and 69 GTVA suggest a recent dramatic increase in temperature.

A small sulfide deposit adjacent to the main fissure occurs in an area of older, but still glassy lavas, about 20-25 m to the east. The Lamphere chimneys, which comprise the bulk of the deposit, were first described in 1983 (CASM II, 1985). The chimney complex is 10-15 m in diameter and 7-10 m high and is surrounded by broken lava flows abutting the lower portions of the chimneys.

One attempt to sample the Lamphere chimneys (90 GTVA) started about 50-75 m to the east of the main fissure and encountered additional areas of diffuse venting and tube worms (as well as a dive weight, probably belonging to the Russian submersible). This part of the caldera is not well-mapped, and the easternmost extent of diffuse venting observed during 90 GTVA may be the same area described by the Russians in 1988 (Lisitsyn et al., 1988).

North Rift Zone

The North Rift Zone is occupied by fresh lavas which are clearly visible in contact with older pillow lavas. Diffuse venting was observed in two EXPLOS/SUAVE camera-tows (56 EXPLOS and 65 EXPLOS), coincident with several small temperature anomalies. Earlier camera tows over the North Rift encountered patches of yellow hydrothermal sediment, but sulfides were not previously reported from this site (Embley et al., 1990). A TV-grab in an area of recent flows recovered fresh, glassy pillow basalt (99 GTVA).

South Rift Zone

Large areas of diffuse venting in the South Rift Zone (discontinuous zones over 1 km of the rift zone) were examined during one EXPLOS/SUAVE camera-tow (79 EXPL). The diffuse venting is associated with extensive collapsed pits in fresh, sheet-like lava flows. The main vent field at Axial Gardens is youthful and does not appear to be associated with sulfide mineralization, although hydrothermal deposits have been photographed at two locations in the South Rift (Embley et al., 1990). Fe-silica gel deposits are widespread, but a pyrite chimney described by Embley et al. (1990) could not be located. Small temperature and chemical anomalies above the largest tube worm field (30-50 m diameter) indicate mainly low-temperature upflow. However, the size of the temperature and tracer anomalies detected by SUAVE was much smaller than expected. This result may indicate that the tube worms occupying the diffuse vents are effectively trapping the heat and chemical constituents in the hydrothermal fluids. A TV-grab in this area (60 GTVA) recovered fresh basalt with local Fe-staining.

CoAxial Segment

Camera-tow (84 EXPLOS) and TV-grab operations at the nearby CoAxial eruption site were carried out for detailed time-series studies of volcanic, hydrothermal, and biological evolution following the 1993 eruption. A TV-grab sampling and mapping survey of the HDV site in the Floc Vent Field revealed that a vibrant biological community developed after the 1993 eruption had dramatically decreased in size, owing to the collapse of low-temperature hydrothermal upflow. No hydrothermal precipitates were reported from this site, although locally abundant yellow hydrothermal sediment was found shortly after the eruption (Embley et al., 1995). An attempt to recover samples from the vent communities using the TV-grab was not successful.

Sampling

A TV-grab close to the ASHES Field recovered a new black smoker chimney at the northeast corner of the field. Intact pieces of a small chalcopyrite-rich mound were retrieved in 81 GTVA. The location of the sample is in an area where venting was not previously observed. During 81 GTVA, the grab passed near the Mushroom and Hillock vents and made several crossings of the Crack Vents. However, it was considered imperative that as much as possible of the original vent structures be preserved by avoiding dredging or TV-

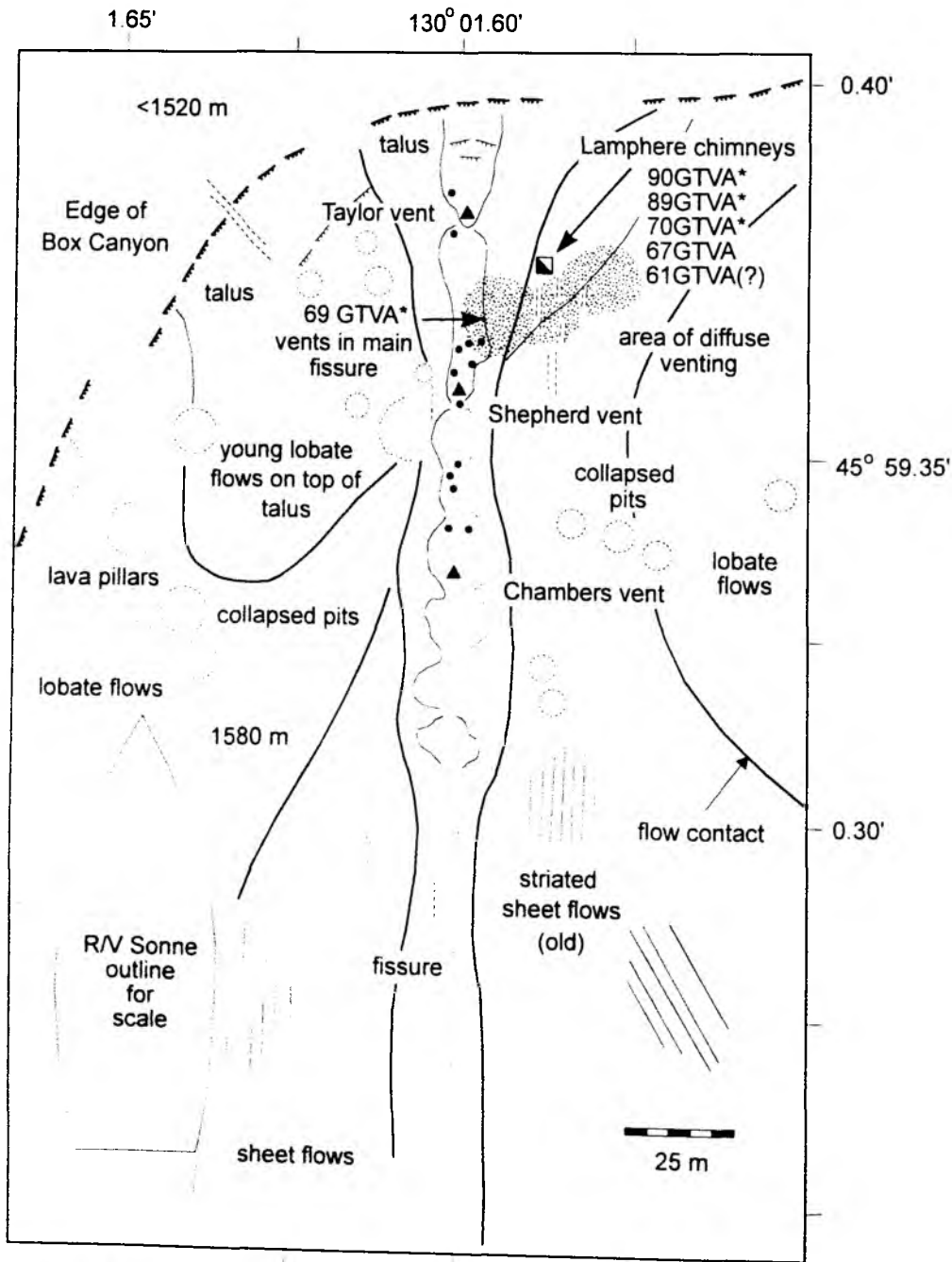


Fig. 40: Sketch of the CASM hydrothermal field showing the location of the main fissure and the different sites.

grab operations in the center of the field. Sampling was carried out with due care and regard to sensitive biological communities. The small anhydrite vent (Virgin Mound) originally targeted could not be located.

Eight TV-grabs were attempted in the CASM Field, both in the main fissure and at the nearby Lamphere chimneys. Precise location of the grabs was limited by the resolution of the short-baseline navigation of the ship. Approximate GPS locations for the grabs at the time of sampling are noted in the station lists. Locations for the 6 grab sites plot within a 50 m diameter circle, centered on the Lamphere chimneys (Fig. 40). The main area of venting is about 25-30 m south of the talus pile at the base of the caldera wall. During each grab, the chimneys were located by repeated crossings of the main fissure zone in the area of most abundant low-temperature venting, tube worm colonies, and bacterial mats. The chimneys are situated 25 m ENE of the most vigorous hydrothermal vents in the main fissure. During 89 GTVA and 90 GTVA (at the Lamphere chimneys), two large blocks of the Lamphere chimneys were knocked off the structure (one recovered), from the live Pagoda-shaped chimney and from the taller main spire. Venting at these chimneys may have been reactivated during sampling. Several attempts to sample the larger spire complex adjacent to the Pagoda structure were unsuccessful, although the upper portion of the tallest chimney was broken off during the last TV-grab at this site.

61 GTVA CASM Field

During a survey of the CASM Field, the TV-grab was used to sample close to a tube worm-covered wall within or close to the main fissure. The grab landed on fresh broken sheet flows covered by thick bacterial mats. Up to 500 kg of fresh basalt was recovered, together with abundant sulfide worms, limpets, and detached tube worms. These rocks are notably different from the broken sheet flows in the vicinity of the Lamphere site and may have been located up to 20 m from the chimneys (possibly within or adjacent to the main fissure: see chapter on Petrology).

67 GTVA CASM Field

An attempt to grab the Lamphere chimneys successfully placed the grab on top of one of the chimney structures, but the grab would not close.

69 GTVA CASM Field

A second survey of diffuse venting in the main fissure located vigorous flow, abundant tube worm colonies, and bacterial mats at the bottom of the fissure. A successful grab of 750 kg recovered 250 kg massive sphalerite and pyrite and 500 kg of jumbled sheet flows. Examination of the samples revealed that sulfides were actively forming beneath the broken sheet and lobate flows in the main fissure.

70 GTVA CASM Field

An attempt to recover sulfides in an area of diffuse venting on fresh lavas in the vicinity of the Lamphere chimneys recovered 300 kg of fresh basalt with glassy surfaces. Tube worms originally collected in the grab were washed out.

81 GTVA ASHES Field

During a search for Virgin Mound, to retrieve altered basalt beneath the anhydrite crust, new venting was discovered ENE of the ASHES Field. A small black smoker chimney complex (50 kg) was recovered largely intact.

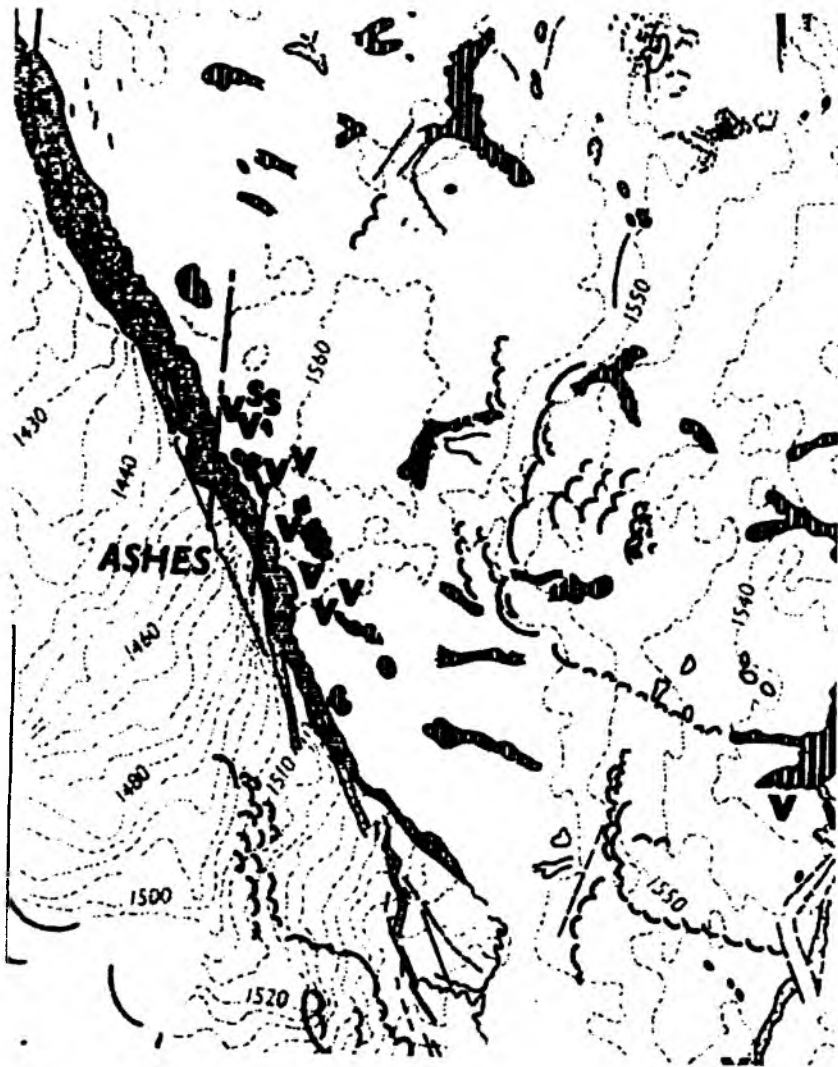


Fig. 41: Detailed bathymetry and geology of the west wall of the Axial caldera in the vicinity of the ASHES Vent Field (5 m contour interval). Lava fronts are interpreted from acoustic backscatter, black areas represent areas of low backscatter (lava pond or lake). Modified from Embley et al. (1990).

85 GTVA CASM Field

Another grab in the vicinity of the Lamphere chimneys recovered 300 kg of fresh basalt.

86 GTVA CASM Field

During a second successful approach to the Lamphere chimneys, the grab hit at least one structure. Several small pieces of barite were recovered together with 250 kg of fresh basalt.

89 GTVA CASM Field

Another attempt to sample the Lamphere chimneys recovered 100 kg of massive barite crust from the active Pagoda structure at the edge of the main sulfide edifice. The barite crusts were knocked off the chimney and recovered along with 500 kg of basalt. The removal of a flange or cap on the Pagoda chimney may have produced a new low-temperature vent at this site.

90 GTVA CASM Field

During a final attempt to sample the Lamphere chimneys, the grab was successfully positioned over the tallest spire. A large piece from the top of the spire (up to 1 m in length) was knocked off, but could not be recovered.

Results**ASHES Vent Field, ENE of Virgin Mound**

During a search for Virgin Mound, the TV-grab was used to make a series of traverses of the northeast corner of the ASHES Field (Fig. 41). One traverse (approximately 20 m ENE of Virgin Mound) revealed a low, squat chimney structure (0.5 m high) surrounded by reflective material of apparent hydrothermal origin. The chimney is thought to be a new vent in the ASHES Field (Fig. 42). The chimney sat on smooth flat sheet flows surrounded by abundant flocculent sediment and was easily detached from its base. The chimney broke into three pieces of approximately 20 kg each. The interior of friable material broke into hundreds of smaller pieces and sand-sized debris.

The grab recovered approximately 50 kg of sulfides (Fig. 43). The collection consists of 3 large intact fragments that preserve the chimney cross-section, a few dozen (0.2 to 0.5 kg) fragments of various zones, several hundred small pieces and two bags of mixed sulfide sand and gravel. The different materials are labeled according to the designations listed below (e.g., mineral type or zones) and packaged as separate samples or groups of samples.

Sample Groups

81 GTVA-1	Basalt chips (200 mg)
81 GTVA-2	Largest chimney fragment (15-20 kg)
81 GTVA-3	Large chimney fragment (8-10 kg)
81 GTVA-4	Large chimney fragment (10-12 kg)
81 GTVA-5	Sphalerite-rich outer portion of chimney (several 1 kg pieces)

81 GTVA-6	Chalcopyrite-rich core of chimney (10 small pieces)
81 GTVA-7	Wurtzite-bearing material from interior of chimney (6 small pieces)
81 GTVA-8	Miscellaneous chimney fragments (sorted as indicated below)
81 GTVA-9	Miscellaneous chimney samples for geochemistry (as indicated below)
81 GTVA-10A	Miscellaneous chimney fragments (1 kg sand-sized debris to TUBAF)
81 GTVA-10B	Miscellaneous chimney fragments (1 kg sand-sized debris to TUBAF)

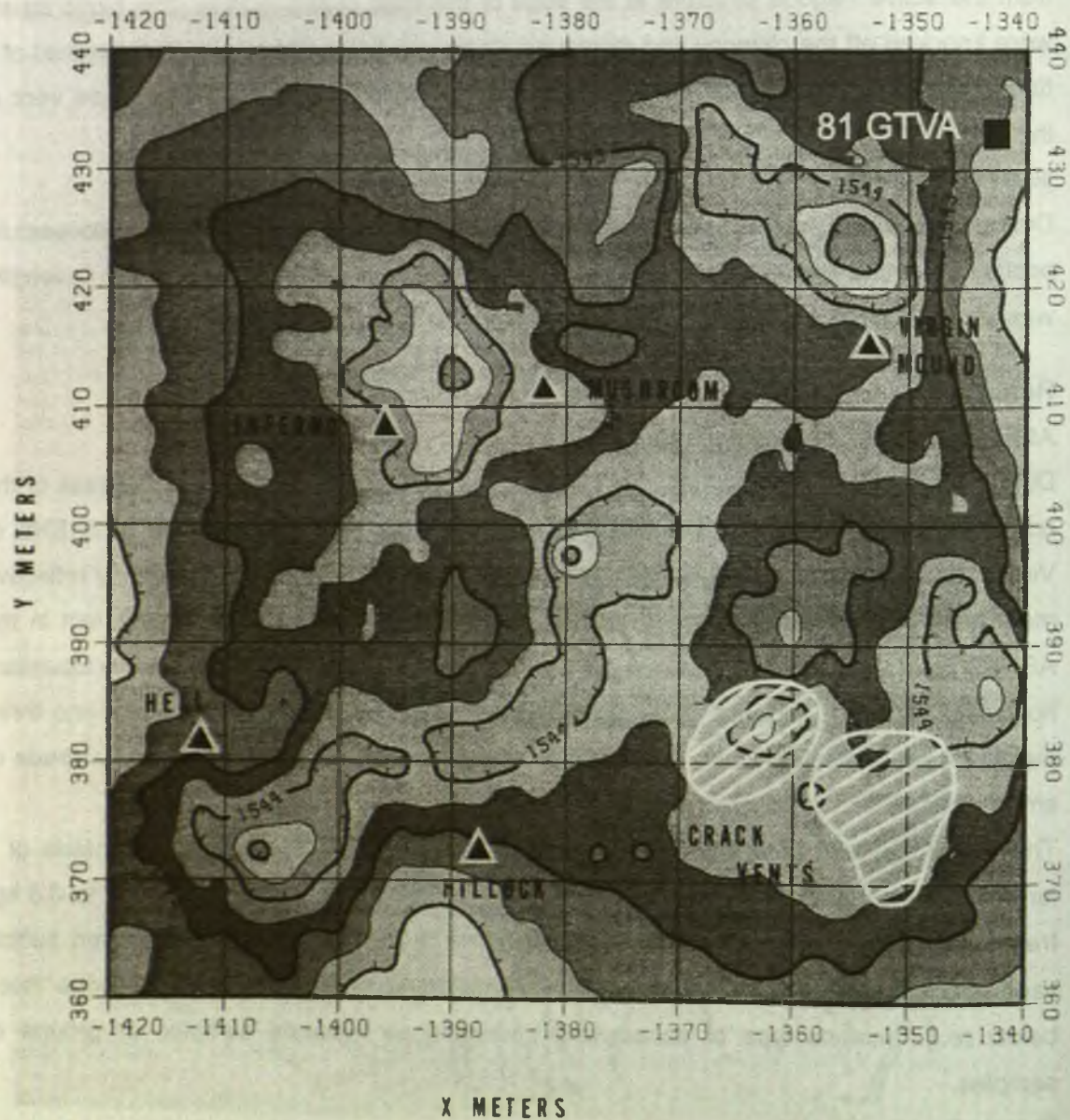


Fig. 42: Location of active vents in the ASHES Field and site of the new black smoker chimney recovered in 81-GTVA (modified from Hammond 1990).



Fig. 43a: Plate of photographs showing samples of Cu-rich sulfides from 81-GTVA.



Fig. 43b: Plate of photographs showing samples of Cu-rich sulfides from 81-GTVA.

General Description

Composition:

The recovered chimney fragments are composed of approx. 50% chalcopyrite, 30% sphalerite, and 10% pyrite/marcasite by volume. The remainder consists of anhydrite, thin outer marcasite crusts, minor silica, and organic material. The intact structures contain 50% pore and void space by volume.

Morphology:

The small vent complex was approximately 40 x 40 x 40 cm and blocky in shape (Fig. 44). At least three of the small orifices and chimneys on top of the structure are lined by chalcopyrite \pm wurtzite and would have been venting black smoke. The interior of the structure resembles a large bee-hive, probably originally constructed of sphalerite but later replaced by fine-grained chalcopyrite which fills the interior of the chimney as soft, friable masses (> 60% void space). The remnants of sphalerite ribbing are apparent in some of the larger chimney fragments. Very little anhydrite occurs in the interior of the chimney and is restricted to a few cm-sized cavities, together with fine, disseminated grains of chalcopyrite. The anhydrite clots may be relict features, left behind during high-temperature replacement in the interior of the chimney.

The porous interior of the chimney is encased in a harder carapace or outer shell of dark brown to black sphalerite up to 20 cm in thickness. The nature of the induration in the outer sphalerite crust is not immediately apparent and may reflect infilling by silica or pyrite. The sphalerite shell is enclosed by more porous, dendritic sphalerite (brown), pyrite, and minor anhydrite (< 5%). The entire edifice is encased by mm thick crusts or rinds of fine-grained, biogenic (?) marcasite \pm pyrite. The surface of the crust is rough and granular in some places and notably smooth or burnished in others. The smooth surfaces are typically associated with the presence of sulfide worms and may be coated by worm casings and mucus material. Silicified bacterial filaments and fronds are preserved on the undersides of the marcasite crusts.

The chalcopyrite-lined orifices or spigots of the black smokers on top of the edifice were 2 to 5 cm in diameter, and may have supported small chimneys at the surface of the edifice. The chalcopyrite-lined fluid channels (10-20 cm in length) can be traced through the larger fragments and are surrounded by bee-hive like material that makes up the bulk of the edifice (Fig. 44). Small (cm-sized) smoker tips protrude from the outer carapace where the channelways exit the structure. The individual orifices reflect the gross mineralogical zonation of the larger structure; polished chalcopyrite lining the interior of the pipe (2-10 mm thick), an intermediate zone of hard, dark brown to black sphalerite. A thin marcasite wall (up to 1 cm) separates the chalcopyrite-lined channelways from the rest of the bee-hive

structure. These may be the remnants of outer marcasite crusts on earlier black smoker chimneys that have been overgrown by the bee-hive structure. The marcasite crusts are not present at the smoker tips on top of the edifice. Delicate, networks of discontinuous channelways lined by fine-grained chalcopyrite, occur in the interior of the structure beneath the main orifices and adjacent to larger channelways throughout the edifice. A few crystals of black hexagonal wurtzite are always present where the coarsest crystals of chalcopyrite are found.

Sample Descriptions and Distribution

81 GTVA-1 consists of 200 mg of basalt chips collected by M. Perfit. Half of the chips are unaltered and likely unrelated to the chimney collected. The remaining chips consisted of glass flakes adhering to the sulfides or as the substrate for worm tubes.

81 GTVA-2 is the largest of the chimney fragments (15-20 kg) and consists of a series of coalesced fluid conduits that have boundaries marked by crusts or zones of radial marcasite-pyrite. These are interpreted to be the recrystallized remnants of outer marcasite walls associated with earlier chimney structures overgrown by the sulfide edifice. Remnants of dark sphalerite outer zones (1-3 cm thick) in the porous core of the structure are also interpreted to be part of the earlier chimney morphologies and indicate that the main edifice is constructed of coalesced spires. Chalcopyrite is the dominant mineral in zones of 10-15 cm diameter and locally replaces earlier zones of sphalerite and pyrite-marcasite. This chalcopyrite likely marks the fluid channelways feeding smoker tips at the top of the edifice. The entire edifice is encased in lighter brown, indurated sphalerite which overgrew the earlier chimneys (see photos) and now is coated by a 1-3 mm thick skin of marcasite. The outer surface is bulbous and hummocky, with small protuberances of sphalerite (possibly incipient outgrowths that may have become new black smoker vents). There is an overall ribbed-texture, similar to that of sphalerite-rich bee-hives.

(Sample Distribution: TUBAF)

81 GTVA-3 (8-10 kg) is similar to but smaller than 81-GTVA-2. The morphology and mineralogy of the sample is the same, although coarse-grained wurtzite is visible within the fluid conduits. The largest conduit is 5 cm in diameter (Fig. 43b). Anhydrite is notable within friable patches of pyrite and within the porous, fine-grained chalcopyrite in the interior of the sample.

(Sample Distribution: GSC)

81 GTVA-4 is the same as above (10-12 kg).

(Sample Distribution: TUBAF)

81 GTVA-5 is a collection of five, 1 kg pieces of the outer hard sphalerite carapace surrounding the central complex of chalcopyrite conduits. Bee-hive ribbing is apparent and is marked by pyrite-marcasite dendrites. These samples have well-developed, outer marcasite crusts (1-3 mm thick), and locally preserve older, recrystallized pyrite-marcasite chimney walls in their interiors.

(Sample Distribution: TUBAF 3, B,C,D; GSC 1, E, NOAA 1, A)

81 GTVA-6 is a collection of 10 pieces of chalcopyrite conduit material. Typically, these are 1 cm thick annuli (2-5 cm orifices) of chalcopyrite surrounded by outer zones of hard sphalerite (2-4 cm thick). There is evidence of small-scale fluid break-outs through these walls. Some marcasite crust material is present on thicker pieces, derived from the base of smoker tips.

(Sample Distribution: TUBAF 8, B to H; GSC 1, E, NOAA 1, A)

81 GTVA-7 is a collection of 6 small pieces of wurtzite-rich inner vent materials. The crystals of wurtzite, sphalerite, and chalcopyrite in these samples are notably coarse-grained, and suitable for picking for $\delta^{34}\text{S}$ and detailed trace element analyses.

(Sample Distribution: TUBAF 4, A, B,C,D; GSC 2, E)

81 GTVA-8 consists of several bags of small, broken pieces sorted into mineral types as follows: 8A-sphalerite; 8B-porous, chalcopyrite interior; 8C-marcasite crusts; 8D-chalcopyrite-lined conduits; 8E-porous chalcopyrite + pyrite interior; 8F-pyrite+marcasite ribbing or walls from the interior of the edifice.

(Sample Distribution: TUBAF)

81 GTVA-9 is a selection of small pieces of different zones for polished thin sections and detailed chemical analysis at the GSC. This sample set represent a channel sample across the structure that will provide an estimate of the bulk composition of the edifice.

(Sample Distribution: GSC)

81 GTVA-10A and B are two bags of miscellaneous, sand-sized, debris from the broken chimney structure.

(Sample Distribution: TUBAF 1; GSC 1)

Inferences

The small black smoker vent samples in 81 GTVA is thought to be a new, previously undocumented chimney structure at the northeast corner of the ASHES Field. The highly-polished chalcopyrite linings of the orifice are typical of high-temperature black smoker vents. Similar black smoker activity was previously known only at the Inferno chimney

(Harvey-Kelley et al., 1988). The apparent recent growth of this structure may be related to the increase in high-temperature upflow documented in the field in 1994-95. The absence of abundant sulfide worms on the structure gives the impression that the biological community associated with this vent was once much more vibrant. This may indicate that the chimney is part of a waning high-temperature vent.

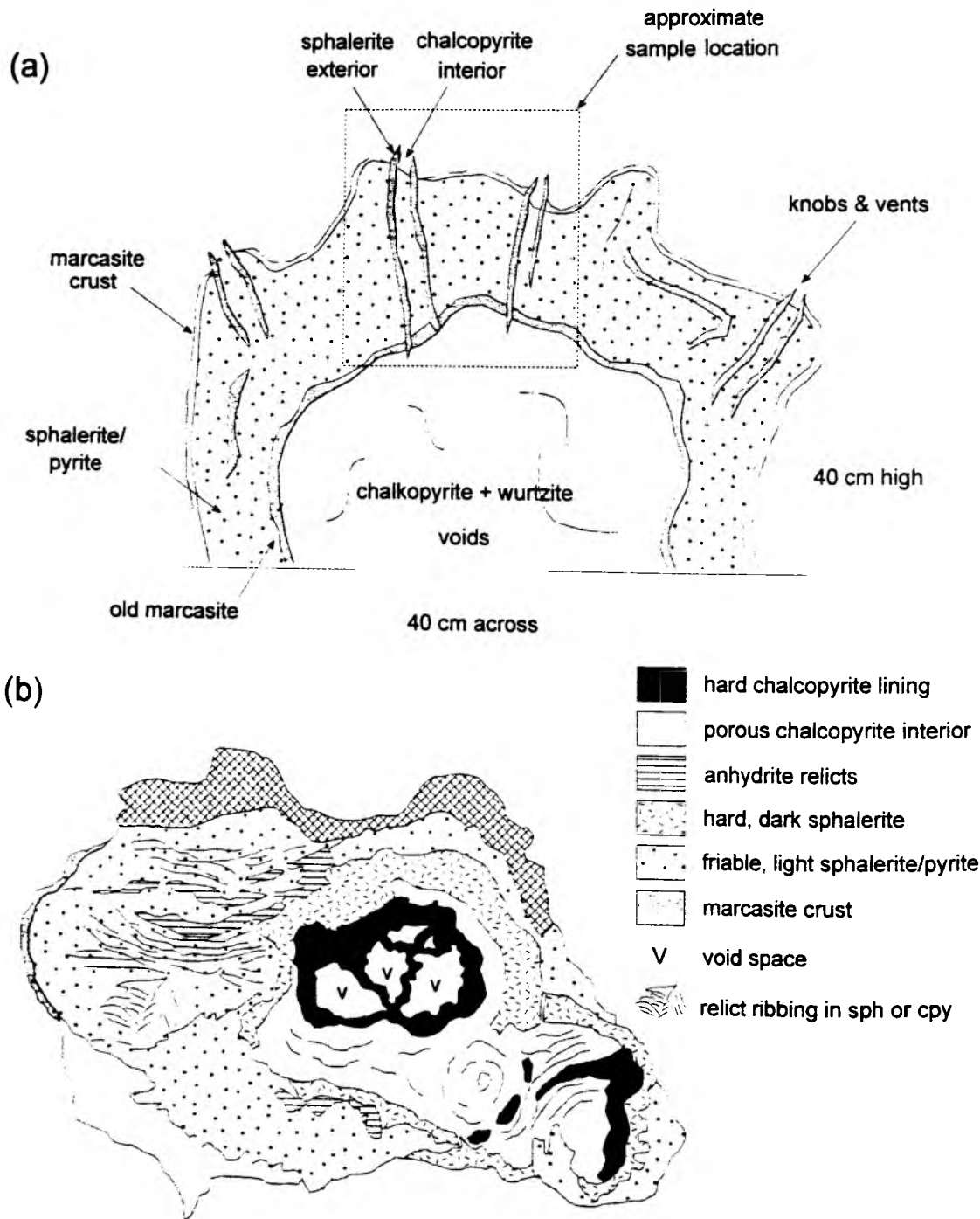


Fig. 44: Sketch of typical mineral zonation in Cu-rich samples from 81 GTVA

CASM Main Fissure

The central part of the CASM Field within and east of the main fissure is an area of diffuse venting marked by widespread tube worm colonies, clams, and bacterial mats (Figs. 35, 36 and 45). No obvious signs of venting water were noted during 69-GTVA, although vigorous venting of clear fluids was noted on two separate occasions at the same location during crossings of the main fissure in subsequent TV-grabs. The sampling target was a ledge of well-formed, flat and lobate lava adjacent to the east wall at the bottom of the main fissure (approx. 7-10 m deep) where the most vibrant biological communities were observed. The margins of the flow lobes are fringed by bacterial mats, which creates a striking contrast in the video. Some massive sulfides have formed locally as crusts on top of the lavas (Figs. 46 and 47). However, most of the sulfides occur beneath the surface and are deposited on the undersides of the fractured sheet flows. The undersides of the sheets are host to communities of sulfide worms, enveloped by white mucus. Tube worms and limpets occur along the fractures in the sheet flows and are concentrated in areas where fluids leak out between slabs of broken sheet flow. Brecciated fragments of basalt and abundant glass chips (mainly very fresh glass) occur between the broken slabs and are locally cemented by pyritic sulfides (basalt-sulfide breccias). A thin film of pyrite or marcasite coats most of the exposed surfaces on the undersides of the broken sheets.

The grab recovered ca. 250 kg or more of sulfides and 500 kg of basalt blocks, intermixed with abundant sulfide worms, limpets, worm tubes, and mucus. The loose material was discarded after limited sampling of biology by Verena Tunnicliffe. All samples were packaged and distributed as indicated below.

Sample Groups

- 69 GTVA-1 Fresh basalt - well-preserved, thick glass rinds
- 69 GTVA-2 Slightly altered and brecciated basalt, bleached and with minor pyritization
- 69 GTVA-3 "Highly" altered basalt with rinds and fracture filling/coatings of anhydrite and sulfides
- 69 GTVA-4 Basalt-sulfide-sulfate breccias; basalt clasts in a matrix of fine-grained pyrite anhydrite
- 69 GTVA-5 Massive sulfides; dominantly sphalerite, wurtzite, and pyrite with minor chalcopyrite
- 69 GTVA-6 Miscellaneous; bacterial ooze, secondary minerals, etc. (see below)
- 69 GTVA-7 Large specimen (20 kg) of broken sheet or lobate flow with encrustation of sulfide breccia
- 69 GTVA-8 Large specimen (20 kg) of broken sheet or lobate flow with encrustation of sulfide breccia

General Descriptions

Massive Sulfides:

The massive sulfide comprise mainly Zn-rich assemblages. They include massive dendritic sphalerite and sphalerite-cemented worm-tubes. Both types are found on the undersides of large slabs of broken sheet flow, and distinction between the sub-types is mainly for classification purposes.

(A) Pale brown, masses of dendritic sphalerite, with sweeping arrays of sphalerite dendrites ranging from cm's to dm's in length. Individual dendrites comprise interlocking fans of fine-grained sphalerite, with individual crystals, blades, or needles of sphalerite commonly only few hundred microns in width. The massive dendritic sphalerite is impregnated with fine-grained anhydrite, which fills most of the open spaces. The sphalerite dendrites are overgrown variably by darker sphalerite and black, hexagonal crystals of wurtzite. Chalcopyrite is present locally as disseminated grains. Overall fabric of the massive sphalerite gives a ribbed appearance (0.1 to 0.5 cm ribs) similar to that observed in beehive structures. However, the massive dendritic sphalerite is found underplating large slabs of broken sheet flows and appear to have formed in the near subsurface in open spaces between sheets and breccias. The sulfides are mainly flat-lying (i.e., lateral growth of dendrites along undersides of sheet flows) and locally cement brecciated basalt between the larger slabs.

(Sample Distribution: TUBAF 12; GSC 3; NOAA 1; UF 1)

(B) A second sub-class of massive sulfides consists of sphalerite/wurtzite that has rapidly overgrown clumps of tube worms and limpets. Massive to dendritic, pale brown sphalerite cements the worm tubes and limpets, and black sphalerite and wurtzite infills later cavities (including the fossilized worm tubes). Rare 0.1 mm grains of chalcopyrite are also present with wurtzite in the late cavities.

(Sample Distribution: TUBAF 5; GSC 2; NOAA 1; UF 1)

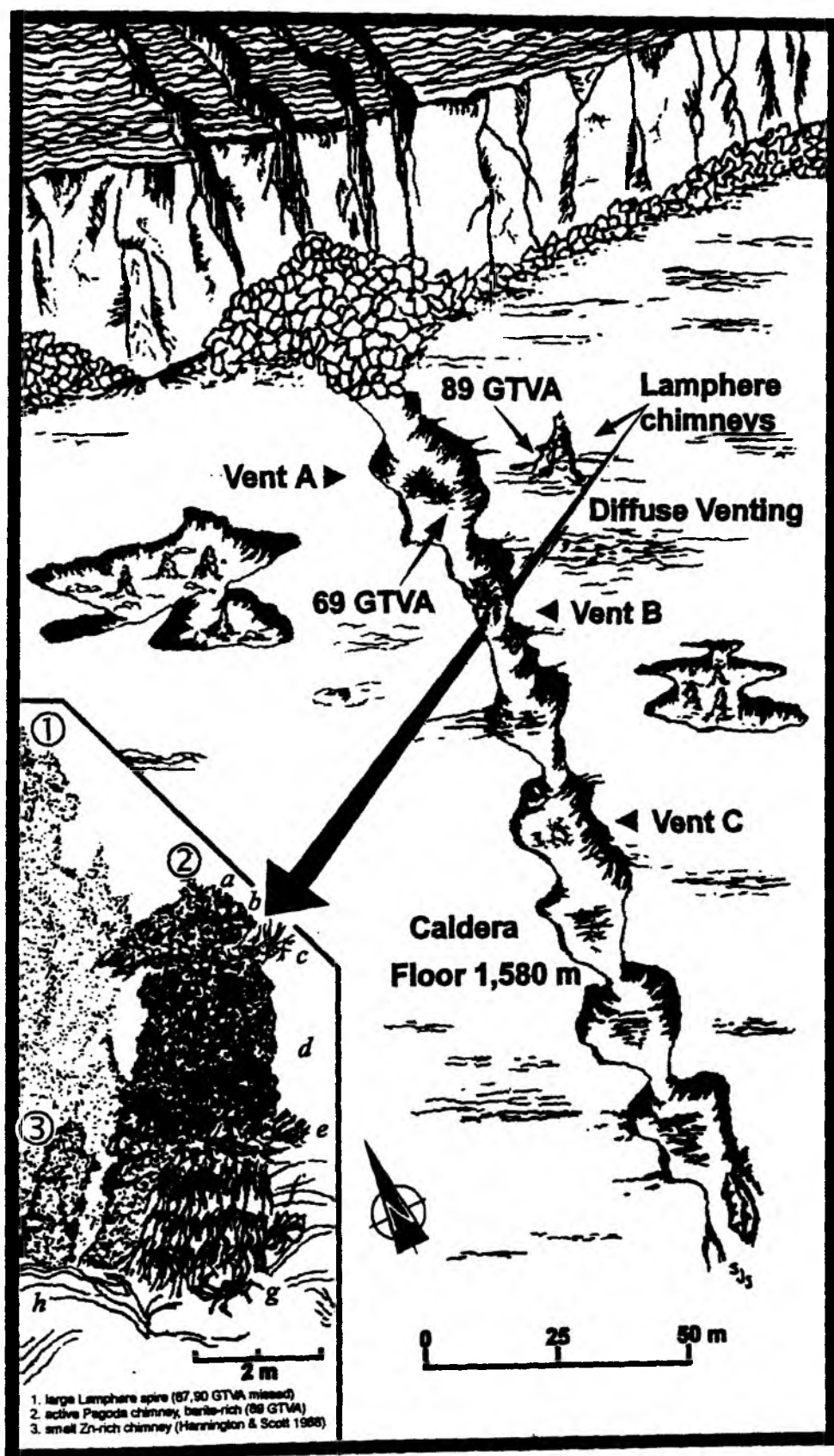


Fig. 45: Sketch of the main fissure in the CASM field showing the location and nature of the large Lamphere chimneys adjacent to the fissure. Active vents in the fissure were sampled during 69-GTVA. The large barite-rich Pagoda structure was sampled during 89-GTVA (modified from CASM II, 1985).



Fig. 46a: Plate of photographs showing samples of pyrite-sphalerite-anhydrite precipitates and sulfide-cemented breccias from beneath broken sheet flows in the main fissure of the CASM Field (69-GTVA).



Fig. 46b: Plate of photographs showing samples of pyrite-sphalerite-anhydrite precipitates and sulfide-cemented breccias from beneath broken sheet flows in the main fissure of the CASM Field (69-GTVA).

Pyrite-Sphalerite-Anhydrite Mineralization Beneath Broken Sheet Flows:

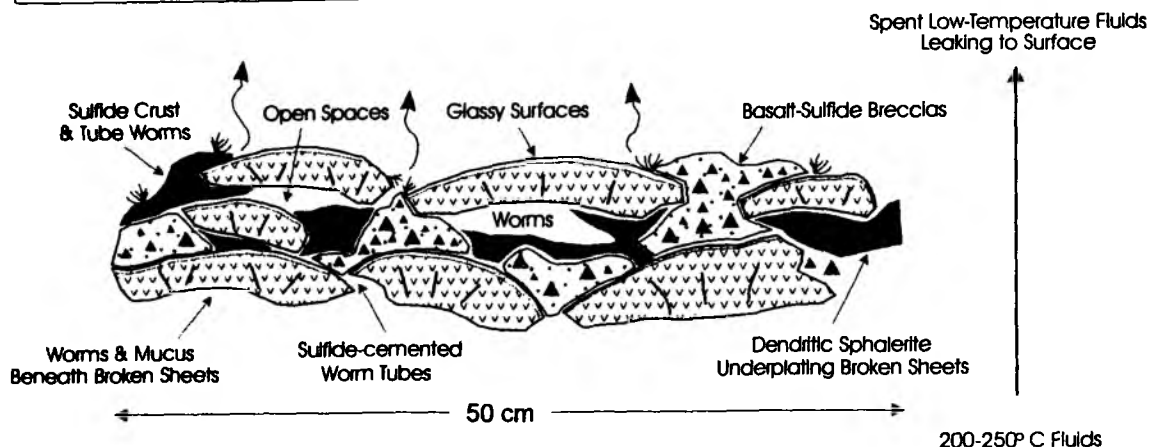


Fig. 47: Subsurface view of broken lobate and sheet flows in the main fissure of the CASM field in the vicinity of 69-GTVA. Diffuse upflow between the broken sheets is highlighted by bacterial mats and tube worms. Subsurface mineralization consists of massive sphalerite and pyrite-cemented breccias.

Basalt-Sulfide-Sulfate Breccia:

A wide range of sulfide-cemented, basalt breccias were collected. The main breccia type consists of angular blocks and chips of basalt and glass (1 to 5 cm) in a matrix of fine-grained, semi-consolidated pyrite, anhydrite (or gypsum), and rare sphalerite. The pyrite matrix is locally unconsolidated. Rare flakes or crusts of fine-grained pyrite are also present in the matrix. A second breccia type consists of fine, glassy fragments of basalt (grain supported breccia) with a fine-grained pyrite and anhydrite matrix and more dispersed, coarser fragments of basalt (up to 5 cm) floating in the finer breccia. The breccia fragments appear to have been dilated by emplacement of the pyrite-anhydrite matrix and resemble bread-crust type breccias. The basalt fragments are variably altered (usually sub-mm surficial alteration) and commonly are coated by a fine dusting of pyrite and thin films or crusts of brightly "polished" pyrite. Most of the breccias, including those attached to the undersides of the broken sheet flows, contain up to 30% anhydrite as radiating blades and felted masses infilling open spaces.

(Sample Distribution: TUBAF 4; GSC 2; NOAA 1; UF 1)

Sulfide Encrustations on Altered Basalt:

Basalt fragments and the undersides of broken sheet flows are dusted with sulfides, mainly along broken surfaces and lining fine fractures. Two types of fracture-filling and encrustations are recognized:

(A) Pyrite encrustations and thin films of ultra-fine pyrite/marcasite coat many of the glassy surfaces and exposed areas on the undersides of the sheet flows on which sulfide worms were found. The pyrite appears to be derived from the reaction between high-temperature

fluids and the sulfur-rich mucus associated with the sulfide worms. A thin film of pyrite is found beneath the white mucus, and likely forms from the S^0 in the mucus and ferrous Fe in the hydrothermal fluids. The thin films or coatings of pyrite are commonly quite smooth and can easily be rubbed off the glassy undersides of the sheets. Other pyrite crusts are thicker (up to a few mm) and more granular and resemble the marcasite crusts commonly found on the outsides of high-temperature chimneys.

(Sample Distribution: TUBAF 2; GSC 1; NOAA 1; UF 1)

(B) Granular pyrite and sphalerite commonly line fractures or occur as thin coatings (up to 1 mm) on broken surfaces throughout the basalt. The fracture-linings are dominated by fine dustings of black wurtzite crystals or sphalerite-wurtzite mixtures (check by XRD). These may represent fluid channelways through the broken sheets and lobes. Pyrite encrustations occur locally within the glassy rinds of the broken sheets or lobes, along hairline fractures. The glass is bleached and indicates that the pyrite mineralization is hydrothermal and not precipitated as a result of bacterial action (sulfur isotopes may be revealing).

(Sample Distribution: TUBAF 3; GSC 2; NOAA 1; UF 1)

Miscellaneous:

About 200 grams (wet) of bacterial mucus was collected for bacterial culture (M. Summit). GSC retained about 10gm (frozen) for chemistry. The samples came from a clot of sulfide worms in a cavity beneath the lobated sheet flows.

GSC also retained a selection of altered glass chips that display green smectite-like clays, fine disseminated pyrite, chlorite (?), and unidentified white crusts. These will be examined by XRD, SEM-EDS (quantitative), and conventional microscopy.

Two large blocks of broken sheet flow with encrustations of sulfide-cemented breccia were packaged for TUBAF (69 GTVA-7 and 69 GTVA-8).

Inferences

The sample types and mineral assemblages suggest that sulfide mineralization occurred in the shallow subsurface, by infilling of broken sheet and lobate flows and by cementation of hyaloclastite-like breccias between the broken lobes (Fig. 47). The mineralization within the basalt-sulfide-sulfate breccias appears to have caused displacement of the basalt fragments, typical of bread-crust type breccias. The mineral assemblages suggest the following conditions of formation:

- (a) Breccias contain anhydrite (\pm gypsum) and pyrite, indicating probable temperatures of 150-200°C. This can be verified by fluid inclusion measurements in coarser-grained anhydrite.
- (b) The massive sulfides contain mainly sphalerite, but with later dustings of Fe-rich sphalerite, wurtzite, and chalcopyrite. This assemblage implies temperatures in the range of

200-250°C, and possibly up to 350°C, based on similar mineralogy in active vents elsewhere in the caldera. Amorphous silica is not evident in these samples.

The higher temperatures inferred from the recently deposited sulfides within the broken sheet flows at CASM suggest that this site has experienced the same hydrothermal rejuvenation observed at ASHES in 1994-95.

CASM Lamphere chimneys

The Lamphere chimneys are part of a small sulfide deposit about 25 m to the east of the main fissure, along the contact between fractured sheets and a ridge of more rubbly, broken lavas (Figs. 40 and 45). The chimney complex was found by drifting along the main eruptive fissure to the area of most vigorous venting (69 GTVA), and then lifting the grab out of the fissure onto the broken sheet flows immediately to the east. The largest spire is up to 7 m in height and the entire complex is approximately 10-15 m in diameter. Relatively fresh, but broken lavas abut against the base of the chimneys, suggesting that the basal portion of the chimneys may be covered. The lavas immediately adjacent to the chimneys are coated in a thin film of Mn-oxides. The chimneys occur at the north end of a large area of intermittent, diffuse flow through the fractures in the broken lavas. This area is marked by local worm tube colonies and bacterial mats, and may be an older eruptive fissure covered by recent sheet flows.

The Lamphere chimneys were targeted for sampling during 89 GTVA, and the sample ultimately recovered came from the active pagoda-shaped, barite spire adjacent to the main sulfide edifice. The barite spire is up to 4 m in height. The two adjacent, twin spires of the Lamphere chimneys were 6 to 10 m in height but had no major biological colonies. The top of the largest chimney was missed, and a glancing strike on the barite spire apparently removed the cap of the chimney or a large bulge at its side (Fig. 48a+b). The barite flange was knocked off the spire and collected together with fresh basalt at the base of the chimney complex.

The grab recovered approximately 500 kg of ropy lava and 100 kg of barite (9 large pieces and a collection of smaller pieces and surface rubble). Worms, limpets, and clams were collected from the grab by V. Tunnicliffe. The outermost layers of the barite crusts were subsampled immediately for microbiology by M. Summit.



Fig. 48a: Plate of photographs showing samples of massive barite crusts from the Pagoda structure in the Lamphere chimneys, adjacent to the main fissure of the CASM Field (89-GTVA).



Fig. 48b: Plate of photographs showing samples of massive barite crusts from the Pagoda structure in the Lamphere chimneys, adjacent to the main fissure of the CASM Field (89-GTVA).

Sample Groups

89 GTVA-1	Autobrecciated, chaotic sheet flow
89 GTVA-2	Selected lava morphologies
89 GTVA-3	Selected lava morphologies
89 GTVA-4	Selected lava morphologies
89 GTVA-5	Large barite slab (35 kg)
89 GTVA-6	Large barite slab (25 kg)
89 GTVA-7	Thin barite crust (10 kg)
89 GTVA-8	Coarse-crystalline, vuggy barite crust (15 kg)
89 GTVA-9	Small barite slab (10 kg)
89 GTVA-10	Barite-cemented worm tubes (5 kg)
89 GTVA-11	Barite-cemented worm tubes (5 kg)
89 GTVA-12	Rubble from outer weathered (?) surface of barite crusts (10 kg)

General Descriptions**Composition and Morphology:**

The recovered material consists almost entirely of pure barite, with possible minor amounts of anhydrite \pm gypsum in the outer, weathered (?) portions. The interior of each large slab consists of complex cavities, vugs, and channelways lined by clusters of 1-3 mm, tabular barite, barite rosettes, and larger spheroidal masses. The coarse barite crystals are generally clear and colourless, compared to the finer-grained, massive barite which is dark grey. Zonation from the upper or outer surface of the slabs to the interior is illustrated in Figure 49 and consists of (i) soft, weathered (?) crusts of friable barite up to several centimeters in thickness (possibly secondary barite, carbonate?), (ii) a zone of barite-cemented worm tubes, 5-10 cm thick (some still occupied by alvinelid worms), (iii) a transitional zone (1-3 cm thick) of recrystallized barite in which worm tubes are completely replaced by hard, grey to black microcrystalline barite, (iv) a thick inner zone of dense, microcrystalline barite permeated by vuggy, barite-lined cavities and tortuous fluid conduits. The innermost zone probably is typical of the rest of the spire, and likely was filled with low-temperature fluids. The zone of barite-cemented worm tubes consists of dense, fine-grained white to grey barite, whereas coarser-crystalline barite occurs in the innermost zones and especially lining larger cavities and low-temperature fluid conduits. The outer, weathered (?) surface is coated in a thin film of brightly coloured, yellow-orange-brown material, especially apparent along exposed cracks in the barite crust. Previous experience with samples from this site (1986, 1988) has shown that the barite is highly enriched in radium (80000 cpm), especially around the vugs and tortuous fluid conduits (e.g., Grasty et al., 1988).

The presence of abundant fossilized worms in the barite suggests that incremental growth of the chimneys occurs within insulating colonies of tube worms, similar to those which inhabit

vents in the nearby fissure. The worm tubes on the outer surface of the Pagoda were progressively fossilized by encroaching barite as the structure grew. Within this protective framework of barite-cemented worm tubes, Zn-sulfides may form with increasing temperature. Unlike the sulfide chimneys at ASHES, the barite spires lack well-defined central orifices; barite and minor sulfides were deposited in a porous network of interconnecting channelways and cavities. Trapped fluids periodically escaped through the walls of the spire, giving rise to outgrowths and flanges of the type sampled in 89 GTVA. The growth of similar structures has been observed at temperatures as low as 150°C (e.g., Johnson & Tunnicliffe, 1985, 1986). However, there is compelling evidence for continued high-temperature mineralization, beneath the protective cap of low-temperature barite.

Sample Descriptions and Distribution

89 GTVA-1 to 4 consists of chaotic and jumbled sheet flow, autobrecciated and folded lava, and considerable agglomeratic fragmental material wrapped into sheet folds. The sheets are extensively microfractured with evidence of warm water flow penetrating each fracture (abundant Fe-staining). Thick Mn-staining (1-2 mm) is common on many of the glassy outer surfaces and also in open cavities within the lavas.

(Sample Distribution: miscellaneous pcs. to TUBAF, GSC, NOAA, M. Perfit)

89 GTVA-5 is the largest of the barite slabs from the pagoda structure. The barite crusts exhibit a layered structure and horizontal protuberances, with tube worms living on the upper surface. Weathered (?) material at the surface of the crust shows bright orange to yellow patches and thin films (with bacterial remains) and may be evidence of sulfate-reduction or sulfide-oxidation and synthesis of elemental sulfur.

(Sample Distribution: TUBAF)

89 GTVA-6 is the second largest of the barite slabs. It consists of more weathered (?) material on the upper surface, but preserves the thickest section of barite-cemented and replaced worm tubes. Large, barite-lined vugs are present in the more massive barite. The mineralogy of the weathered (?) material should be checked by XRD. A sub-sample of near surface crystalline barite was selected for microbiology (M. Summit).

(Sample Distribution: TUBAF)

89 GTVA-7 is a thin slab of the outer barite crust, with coarse crystalline barite in the interior. The surface material of this sample was scraped for microbiology (M. Summit).

(Sample Distribution: TUBAF)

89 GTVA-8 is a large slab of coarsely crystalline barite with 2-5 cm vugs and conduits lined by 2-3 mm barite blades.

(Sample Distribution: TUBAF)

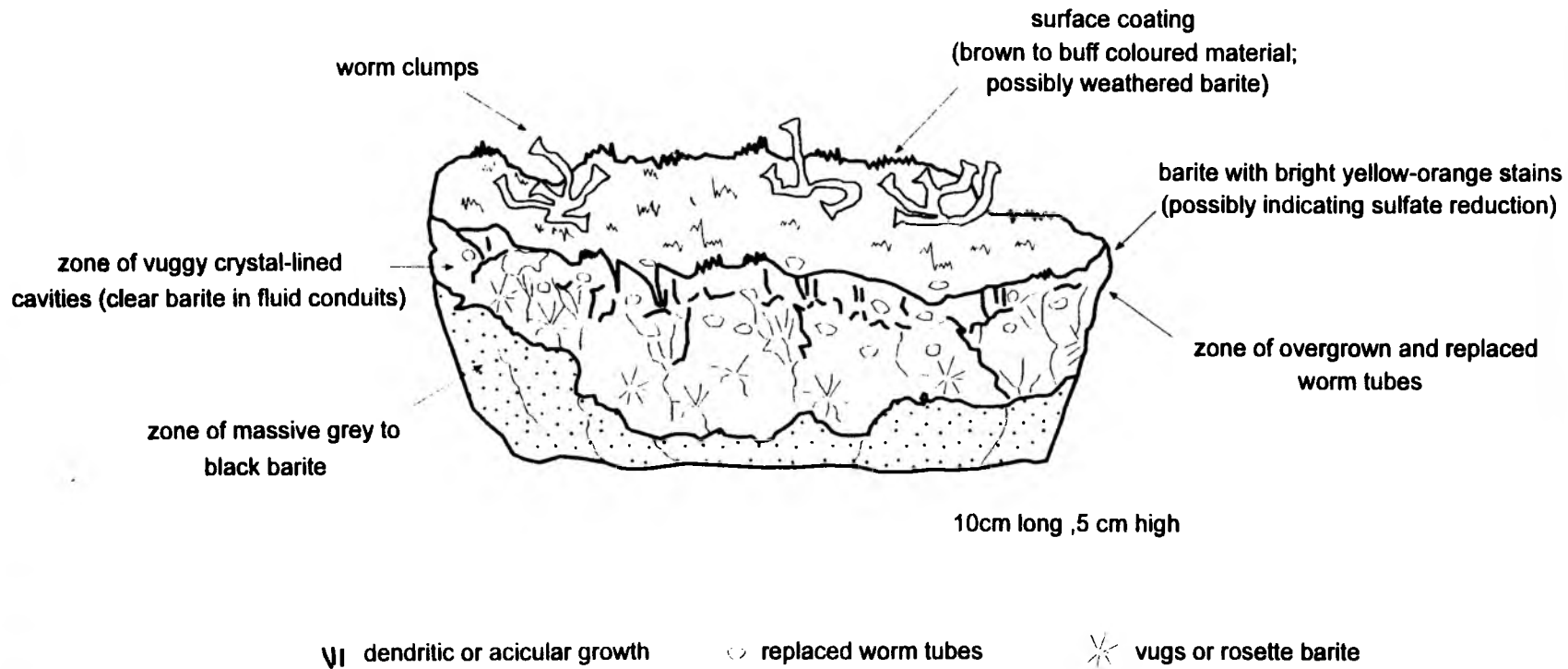


Fig. 49: Typical mineralogical zonation in barite crusts recovered from the Pagoda structure of the Lamphere chimneys (89 GTVA-9).

89 GTVA-9 consists of several smaller slabs of barite with crystalline barite on the interior of the crust.

(Sample Distribution: GSC)

89 GTVA-10 and 11 consist of barite-cemented and replaced worm tubes. The worm colonies formerly occupied the outer surface of the active chimney and were overgrown by barite as the spire developed. A new or secondary barite crust formed beneath the worm tubes, sealing off the chimney.

(Sample Distribution: TUBAF 1; GSC 1)

89 GTVA-12 is a collection of barite rubble derived from the broken weathered surface of the barite crusts.

(Sample Distribution: TUBAF)

Inferences

The sampled structure was a large, pagoda-shaped or tiered structure (up to 4 m in height), covered by dispersed worm colonies. On breaking, the massive barite smells strongly of H_2S . This, coupled with the presence of fine, snow-white, linings of barite needles on the innermost cavities suggests that the structure was still hydrothermally active at the time of sampling. The presence of worms also suggests that the fluids were sulfidic. The structure sampled was the same chimney observed at this site in 1983, 1986, and 1988. Two small samples collected at this site in 1983 (PISCES 1324-2 and 1327-2) also came from the Pagoda. A sphalerite-barite chimney was sampled nearby by PISCES in 1983 (see Hannington et al., 1988), and the tall Lamphere spire adjacent to the Pagoda was sampled by PISCES in 1986 (see Grasty et al., 1988). Venting of warm water occurred after the sampling of the sphalerite-rich spire in 1983, and an active barite-sphalerite chimney was sampled at the same site by ALVIN in 1988 (ALVIN 2084). The active chimney from 2084 may have grown in place after the 1983 PISCES dive series.

In 1983, there were no hot fluids venting from the chimneys, although the biological communities on the Pagoda at that time implied leakage of warm fluids from the structure (i.e., sulfide worms and tube worms supported by low-temperature fluids leaking through the outermost crusts). Measured temperatures in tube worm patches at the surface of the Pagoda chimney were 19°C. The existence of hydrothermal fluid in the porous interiors of the larger spires was indicated by cracks in their outer walls which leaked vent fluids and were lined by filamentous bacteria. Vents (< 50°C) at open fractures in the basalt were also found in close proximity to the chimneys. ALVIN dives to this site in 1988 reported vent fluids at temperatures of 100°C emanating from the small barite-sphalerite chimney adjacent to the main spire, confirming an increase in activity between 1983 and 1988. Barite sampled from these chimneys in 1986 was dated at less than 10 years of age (with fluid residence times of

20 years: Grasty et al., 1988), indicating that the Lamphere chimneys have likely been inflated with low-temperature hydrothermal fluid for several decades, with intermittent pulses at higher temperatures. The small sphalerite-barite chimney next to the Pagoda formed at temperatures of up to 285°C, with most of the barite forming at about 185°C (Hannington et al., 1988). The unusually Ba-rich nature of the chimneys reflects mainly the low-temperature venting history of the complex, although the abundance of barite compared to the ASHES Field might also reflect important differences in the bulk fluid composition. At Axial, the basalts are slightly enriched in Ba over normal MORB, and this enrichment may also contribute to the high barite content of the deposits.

The barite chimneys at CASM may be part of the peripheral zone of higher-temperature vents located in the main fissure. The discovery of high-temperature venting during 69 GTVA (up to 250°C inferred from mineral assemblages) may support this idea, although it remains uncertain whether this is new activity or a manifestation of higher-temperature venting that was not previously documented in surveys of the main fissure. The areas around CASM are not well-explored, and the Lamphere chimneys may be distal to higher-temperature vents that have not yet been found. At ASHES, small barite chimneys were found up to 50-100 m away from the black smokers.

Summary

The samples collected and observation made during cruise of SO109-2 indicate renewed hydrothermal activity in both the ASHES and CASM Fields, most likely associated with seismic events which are known to have taken place in the caldera between 1986 and 1988. A major ground deformation event was measured at the caldera floor in 1988 (drop of 15 cm in the caldera floor: Fox, 1990) and was associated with a water column temperature anomaly and a dramatic change in bottom current velocities. Russian researchers also described an event plume above the caldera in 1986 (Lisitsyn et al., 1988). Rejuvenation of the vent fields is indicated by increasing temperatures in the ASHES Field (from a maximum of 330°C in 1988 to 348°C in 1995), the occurrence of new black smoker chimneys (81 GTVA), an increase in venting temperatures at the CASM site (from 30°C in 1983 to 100°C in 1988), and the presence of high-temperature pyrite-sphalerite-anhydrite mineralization associated with new venting in the main fissure at CASM (69 GTVA). These are the only places in the caldera where high-temperature venting has been persistent enough to produce significant accumulations of sulfides. The low tube worm mounds now developing at the edge of ASHES may eventually become mineralized by barite, as in the CASM Field.

Although hydrothermal upflow at Axial is closely associated with fissuring adjacent to the caldera wall, most of the new venting is diffuse. The unique volcanic history and morphology of the Axial caldera promote largely diffuse flow of hydrothermal fluids to the surface above the bounding faults of the caldera rim. The extent of diffuse flow is related to the highly

permeable nature of the broken and collapsed sheet flows that fill the caldera (areally extensive sheet flows cover more than 60% of the caldera floor). Large sulfide deposits are not forming at Axial, even in areas of vigorous high-temperature upflow, most likely because of extensive seafloor mineralization with open cavities in the collapsed lavas. Large volumes of hot fluid may be present within the highly permeable, near sub-surface at both ASHES and CASM (see 69 GTVA). Because of extensive subsurface mixing, manifestation of these fluids at the seafloor is limited to mainly low-temperature vents and chimneys, dominated by sphalerite- and barite-rich compositions. This is in sharp contrast to the highly focussed upflow associated with high-temperature vents elsewhere on the Juan de Fuca (e.g., Endeavour Ridge). Periodic reactivation of the ASHES and CASM Vent Fields, as observed during SO109-2, is most likely related to faulting at the margins of the caldera or dike intrusions at depth. Temporary disturbances in the ambient thermal regime and opening of new fluid pathways caused by local extension resulted in higher vent temperatures at the surface as trapped fluids escape. Reactivation of the vents has contributed to recent near-surface metal enrichment (e.g., late-stage chalcopyrite replacing sphalerite in the cores of the ASHES chimneys) and may have caused dissolution of older sulfides deposited within open spaces in the underlying lavas.

Mapping and sampling in the caldera and in the North and South Rift Zones also has contributed to better understanding of the links between volcanic, tectonic, and hydrothermal events in the caldera and in the adjacent rifts. Whereas the recent increase in hydrothermal activity in the caldera appears to have been triggered by measurable tectonic events, more recent seismicity recorded at the North and South Rift Zones does not appear to have been associated with a similar increase in hydrothermal activity. Despite numerous events recorded during and immediately preceding the cruise, no evidence of new volcanic eruptions or new vents was observed in the rift zones. This observation suggests that, in many cases, seismic events recorded acoustically may correspond only to minor cracking or the intrusion of magma at depths too great to influence hydrothermal activity at the seafloor. The more dramatic response in hydrothermal upflow at ASHES and CASM may relate to the closer proximity of shallow magma chambers within the caldera.

The most recent volcanic eruptions in the area, on the CoAxial Segment, spawned a vibrant biological community in 1993, together with abundant ferruginous deposits. The hydrothermal sediments were mainly a product of the interaction of hot lavas with the ambient seawater, and only limited hydrothermal venting occurred. A survey of the HDV site showed that cooling of new lavas and the collapse of low-temperature hydrothermal upflow associated with diking events may occur in less than 2-3 years.

References

- CASM II, 1985, Hydrothermal vents on an axis seamount of the Juan de Fuca Ridge: *Nature*, v. 313, p. 212-214.
- Embley, R.W., Murphy, K.W., and Fox, C.G., 1990, High-resolution studies of the summit of Axial Volcano: *Jour. Geophys. Research*, v. 95, p. 12785-12812.
- Embley, R.W., Chadwick, W.W., Jonasson, I.R., Butterfield, D.A., and Baker, E.T., 1995, Initial results of the rapid response to the 1993 CoAxial event: Relationships between hydrothermal and volcanic processes: *Geophysical Research Letters*, v. 22, p. 143-146.
- Fox, C.G., 1990, Evidence of active ground deformation on the mid-ocean ridge: Axial Seamount, Juan de Fuca Ridge, April-June 1988: *Jour. Geophys. Research*, v. 95, p. 12813-12822.
- Grasty, R.L., Smith, C.W., Franklin, J.M., and Jonasson, I.R., 1988, Radioactive orphans in barite-rich chimneys, Axial caldera, Juan de Fuca Ridge: *Canadian Mineralogist*, v. 26, p. 627-636.
- Hammond, S.R., 1990, Relationships between lava type, seafloor morphology, and the occurrence of hydrothermal venting in the ASHES Vent Field of Axial Volcano: *Jour. Geophys. Research*, v. 95, p. 12875-12894.
- Hannington, M.D., and Scott, S.D., 1988, Mineralogy and geochemistry of a silica-sulfide-sulfate deposits in the caldera of Axial Seamount, N.E. Pacific Ocean: *Canadian Mineralogist*, v. 26, p. 603-626.
- Harvey-Kelly, F. E.L., Jonasson, I.R., Franklin, J.M., and Embley, R.W., 1988, Sulfide deposits of Axial Seamount: mineralogy and chemistry [abs]: *EOS, Trans. AGU*, v. 69, p. 1499.
- Johnson, H.P., and Embley, R.W., 1990, Axial Seamount: An active ridge axis Volcano on the Central Juan de Fuca Ridge: *Jour. Geophys. Research*, v. 95, p. 12689-12696.
- Johnson, H.P., and Tunncliffe, V., 1986, Time-lapse camera measurements of a high-temperature hydrothermal system on Axial Seamount, Juan de Fuca Ridge [abs]: *EOS, Trans. AGU*, v. 67, p. 1283.
- Johnson, H.P., and Tunncliffe, V., 1985, Time-series measurements of hydrothermal activity on the northern Juan de Fuca Ridge: *Geophys. Research Letters*, v. 12, p. 685-688.
- Lisitsyn, A.P., et al., 1988, Report of 1986 Cruise to Axial Seamount (translated from Russian, Dept. Secretary of State, Translation Bureau, Ottawa). GSC library.

4.4.3 Water Column Program

by Reinhold Bayer, Anke Bleyer, Klaus Becker, Stephan Lammers and Peter Linke

General

The water column sampling team surveyed the water column for tracers of fluid venting - hydrothermal fluids at Axial Seamount and cold seep fluids at the Oregon Margin subduction zone complex. The instrumentation used was the new GEOMAR Sea-Bird CTD/rosette system. This included a Sea-Bird 911 plus CTD, SeaTech light transmissometer, altimeter, and bottom trigger. The rosette system was a Sea-Bird Model 32 12-position rosette pylon with 10-L Niskin-type water sample bottles. Sampling depths were selected based on the downcast data and tripped on the upcast. Sample data was post-processed using the recommended set of Sea-Bird utilities. As during SO109-1, most likely due to incorrect transmissometer calibration coefficients, the transmissometer values were slightly incremented (the calculated mid-water light transmissions were over 93%) and the data should be reprocessed after the cruise.

Water samples collected by various participants in SO109-2 included helium isotopes (Bayer), methane and methane isotopes (Lammers and Whiticar), nutrients (Bleyer), and other trace elements (Becker). Methane and nutrients were measured onboard, analyses of the other tracers will be performed onshore.

Station description

The first and major part of the cruise focused on Axial Seamount an active ridge axis Volcano on the central Juan de Fuca Ridge with several vent fields including high- and low-temperature vents. As the ROPOS system could not be deployed for direct sampling of vent fluids as originally planned, we performed a set of 18 CTD/rosette stations positioned inside and outside the Axial caldera to locate and characterize the hydrothermal plumes emerging from local venting. The sampling was mainly restricted to the depth range between the bottom (about 1.500 m inside and close by the Axial caldera) and 1.300 m water depth to obtain the maximum resolution of the hydrothermal plume. Outside the Caldera we collected 12 CTD/rosette profiles, most of them in the direct vicinity of the Caldera completing the station set obtained during SO109-1 which now allows a three dimensional mapping of vent fluid related plumes close to Axial Seamount. A few stations were positioned further off the Caldera and give information on the extend and the transition of vent signals emanating from Axial Seamount as well as on the local background signatures. A detailed listing of the station positions is given in the Appendix of the cruise report.

Six deployments of the CTD instrument package were completed inside the Axial Caldera, one at the CASM Vent Field (station 59 CTD), one in the central caldera (80 CTD), two (78, 85 CTD) at the ASHES Vent Field with the only known high-temperature vents and another

two (76, 83 CTD) east of ASHES. At three of these positions (78 CTD, 83, 85 CTD) a sub-transponder attached to the CTD/rosette and the transponder net operated by the NOAA group was used for navigation of the system. At these stations the instrumentation was first lowered close to the ground and subsequently it was moved horizontally and vertically (tow-yo) to detect vent fluids locally injected, and to sample these fluids as close to their source as possible (see below).

Oregon Margin subduction zone cold seeps were sampled during the second part of the cruise. The sample site was located on the second pressure ridge of the slope complex near the "Bioherm" vent site also investigated during SO109-1. We collected 9 CTD/rosette profiles in search of the source of several remarkable methane plumes sampled by the rosette (see cruise report section by S. Lammers).

Preliminary results

The data from Axial Seamount clearly demonstrate the presence of plumes which were similar to previous observations by other investigators. The distributions suggest that the fluids emanating at different sites at Axial Seamount had been advected to the south at the time of sampling. Inside and in close vicinity of the Axial caldera at most sampling sites below about 1,450 m depth, a vent plume layer with a thickness of 20-40 m was indicated by local minima of light transmission (decline from background several permille) and gentle potential anomalies of 0.01-0.02°C (e.g. station 76 CTD, Fig. 50). The plume was also characterized by its methane content clearly elevated above the background signal (see cruise report section by S. Lammers). Elevated signals in potential temperature anomaly were recorded at station 83 CTD located close to "Axial Gardens" (0.05-0.07°C, Fig. 51) reflecting a higher vent fluid fraction in the lower water column. Highest vent fluid signals were obtained from the transponder navigated tow-yo CTD stations (e.g. station 78 CTD of the hot "Inferno Vent" of the ASHES Vent Field, Fig. 52) revealing a decrease in light transmission up to 2% and potential temperature anomalies between 0.05°C and 0.3°C several meters above ground. The maximum signals were not confined in distinct layers but rather in narrow patches sporadically detected, indicating the turbulent and most probably buoyant propagation of the vent fluids next to the vent site.

At the shallow "Bioherm" site at the continental margin a strong heterogeneity in water masses and the distribution of particulate mats was observed. As during SO109-1 we did not observe any consistent signature of fluid injection from the CTD profiles. However, we carefully collected water column samples with the rosette and shipboard methane analyses demonstrated several strong plumes in distinct depth (density) levels above the ridge. We continued to sample these depths intensively to locate the origin of the

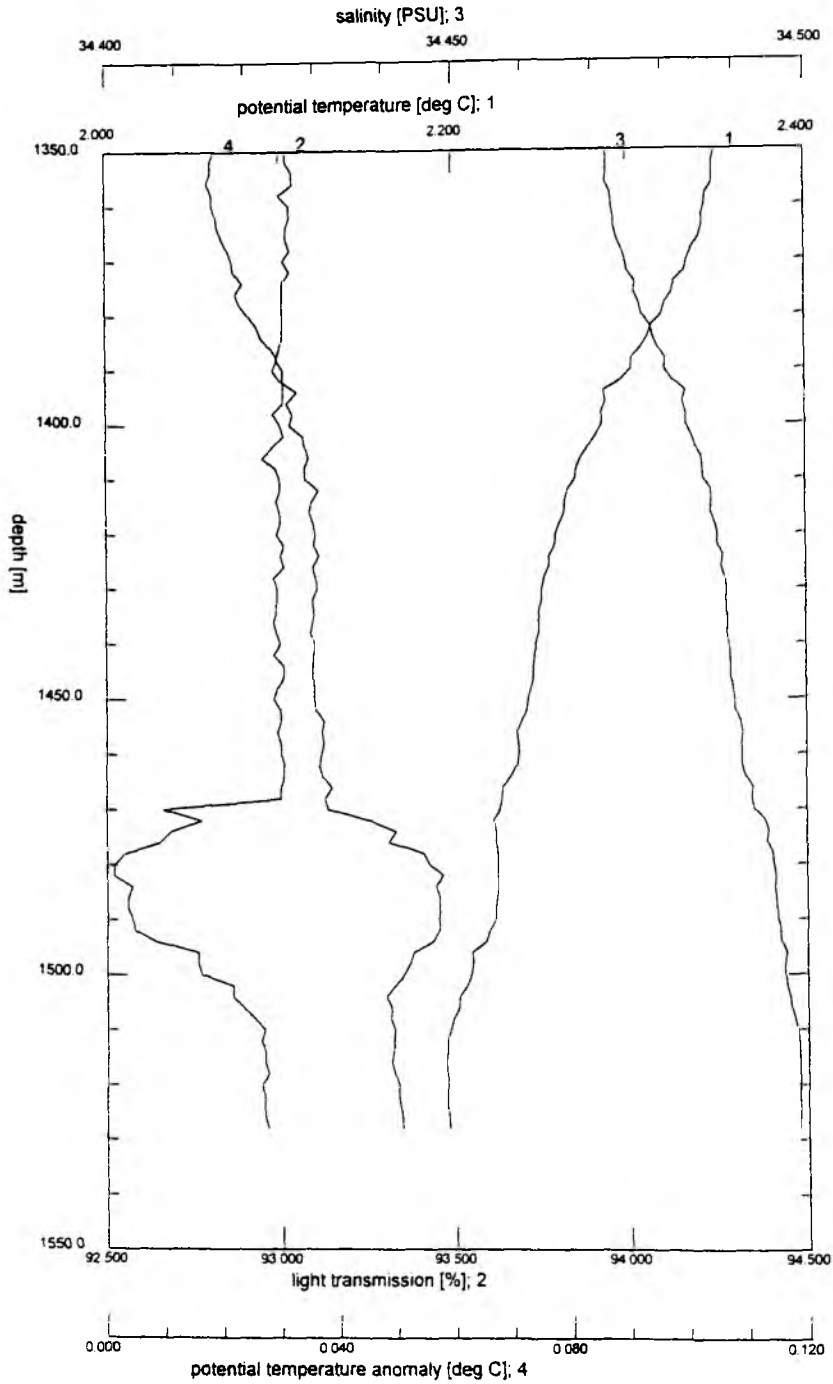


Fig. 50: CTD profiles of potential temperature (1), light transmission (2), salinity (3), and potential temperature anomaly (4) for station 76 CTD east of the ASHES Vent Field inside the Axial caldera. The calculation of the potential temperature anomaly is based on the deviation from the linear correlation of potential temperature and salinity as observed at station 4 CTD (SO109-1) next to the ASHES Vent Field. The hydrothermal plume indicated by transmission and temperature anomalies has a thickness of about 40 m and it's lower boundary is located ca. 30 m above ground.

methane anomaly, yet we were obscured by the high temporal variability of the methane distribution which we assume to be caused by tidal currents. For example a station at the "Bioherm" site showing extreme methane signals in the water column was reoccupied within 10 hours, which resulted in the detection of only two minor methane anomalies in the same

density range (see cruise report section by S. Lammers). This feature clearly depicts the requirement of a ROV for detection and sampling of vent sites.

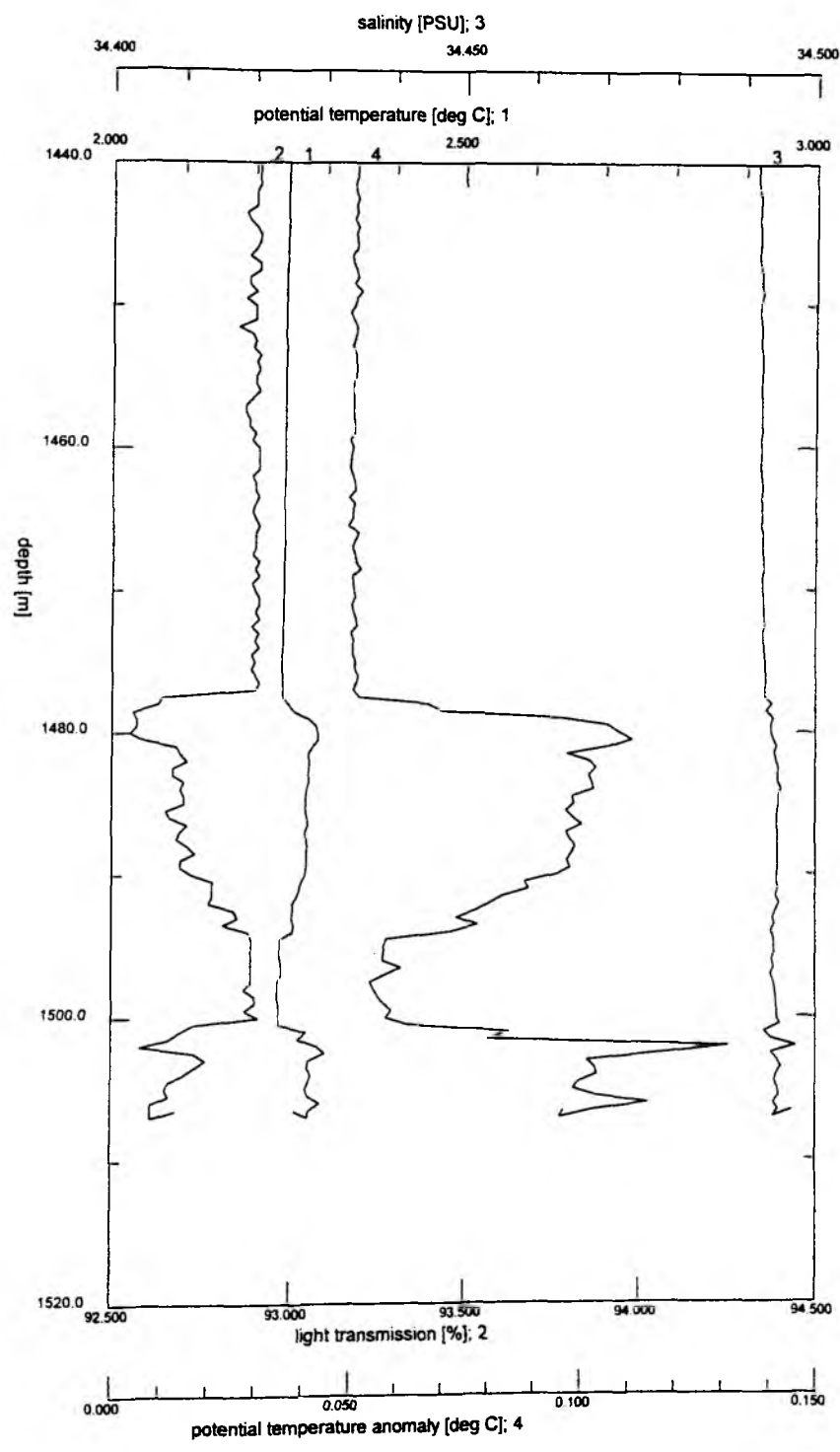


Fig. 51: CTD profiles (see Fig. 50) for station 83 CTD located at the eastern edge of the caldera north of 'Axial Gardens'. Compared to station 76 CTD the vent signatures are clearly elevated and show a more complex structure indicating nearby venting. Potential temperature (1), light transmission (2), salinity (3), and potential temperature anomaly (4).

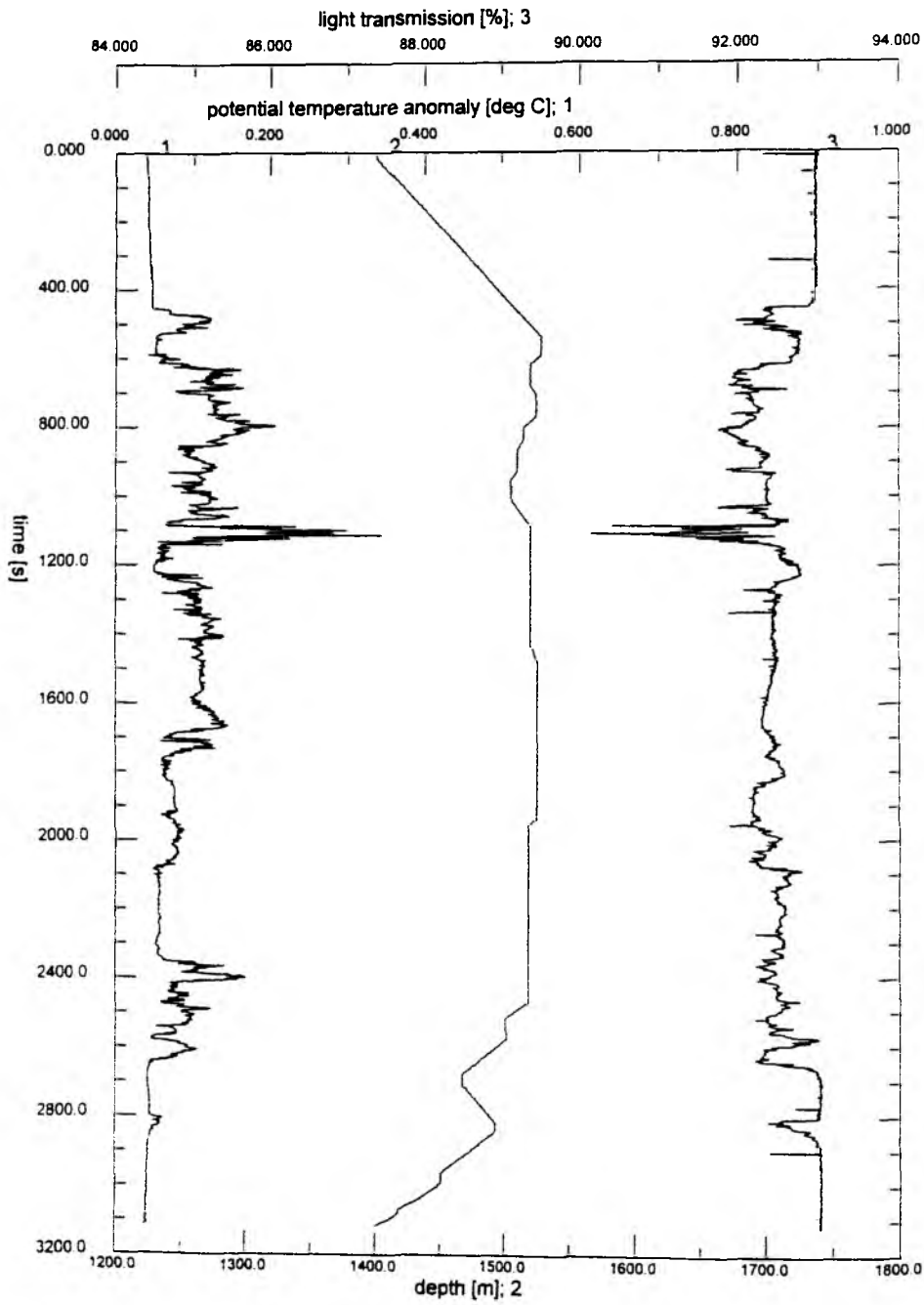


Fig. 52: Signals obtained from a tow-yo CTD next to 'Inferno Vent' of the ASHES Vent Field plotted versus relative time of the measurement. During the deployment the CTD was towed in a circle of about 50 m diameter. During this deployment we detected the maximum hydrothermal vent signatures (transmission: (2), temperature anomaly (4)) of the SO109-2 leg (see text). A more direct occupation of the hot vent fluids cannot be achieved without a ROV. Potential temperature (1), salinity (3).

4.4.4 Methane Analyses on Hydrocast Samples

by Stephan Lammers

Introduction

Measurements of dissolved methane in the water column served as an immediate indicator of either hydrothermal or cold vent activity in the main target areas of the SONNE 109 expedition, i.e. Axial Seamount and the Oregon subduction margin. Water samples, mostly from the near-bottom section, were taken from the hydrocast rosette and immediately degassed by vacuum-ultrasonication and analyzed by GC as a quick reference for vent influence. Additionally, samples were taken for high precision shore analyses of CH_4 and d^{13}CH_4 by helium stripping and GC/GC-C-IRMS determination.

Methods

Two techniques were applied for the determination of dissolved methane in water samples taken during SONNE 109-2 cruise. On board analyses were performed using a vacuum-ultrasonication degassing method (Schmitt et al., 1991, Lammers & Suess, 1994) and subsequent determination with a Shimadzu GC 14A gas-chromatograph. This technique yields 70% with 5% standard deviation of measurements (subject to modification after the intercalibration with the He-stripping). This simple and easy-to-handle method has the advantage of a higher sensitivity compared to normal head-space techniques and allows for the results from 1 hydrocast (max. 12 samples) within 3 hours after recovery.

On shore high precision analyses of CH_4 and d^{13}CH_4 are performed on selected samples at the School of Earth and Ocean Sciences at the University of Victoria using a total yield helium stripping technique and GC/GC-C-IRMS determination. This method yields 100% of the dissolved methane with standard deviations of less than 2%, mostly determined by the gas-chromatography. The results of the He-stripping will be used for an improved calibration of the vacuum-ultrasonic method.

However, the vacuum-ultrasonic method was once again appreciated as a quick tool for the detection of fluid expulsions which avoids interference with He isotope measurements.

Preliminary Results

During cruise SONNE 109-2 the data set of dissolved methane in the water column of leg 109-1 could be very successfully completed by a total of 336 samples from 28 hydrocasts. The methane data set acquired on both cruises comprises 24 hydrocasts in the Axial Seamount area and 17 around the "Bioherm" stations at the Oregon margin. To enforce the ability of vent detection through hydrocast deployments, several CTDs were towed over a distance of 1-2 miles and run in a yo-yo-technique ("tow-yo") within 10-100 m above the

bottom (see cruise report section by R. Bayer). In fact, these surveys yielded the highest methane signals in both working areas.

The compilation of the measurements from the Axial area provides a coincident view of methane distribution patterns and their relation to oceanographic parameters within and adjacent to the caldera. On the contrary, locations and extensions of methane plumes in the

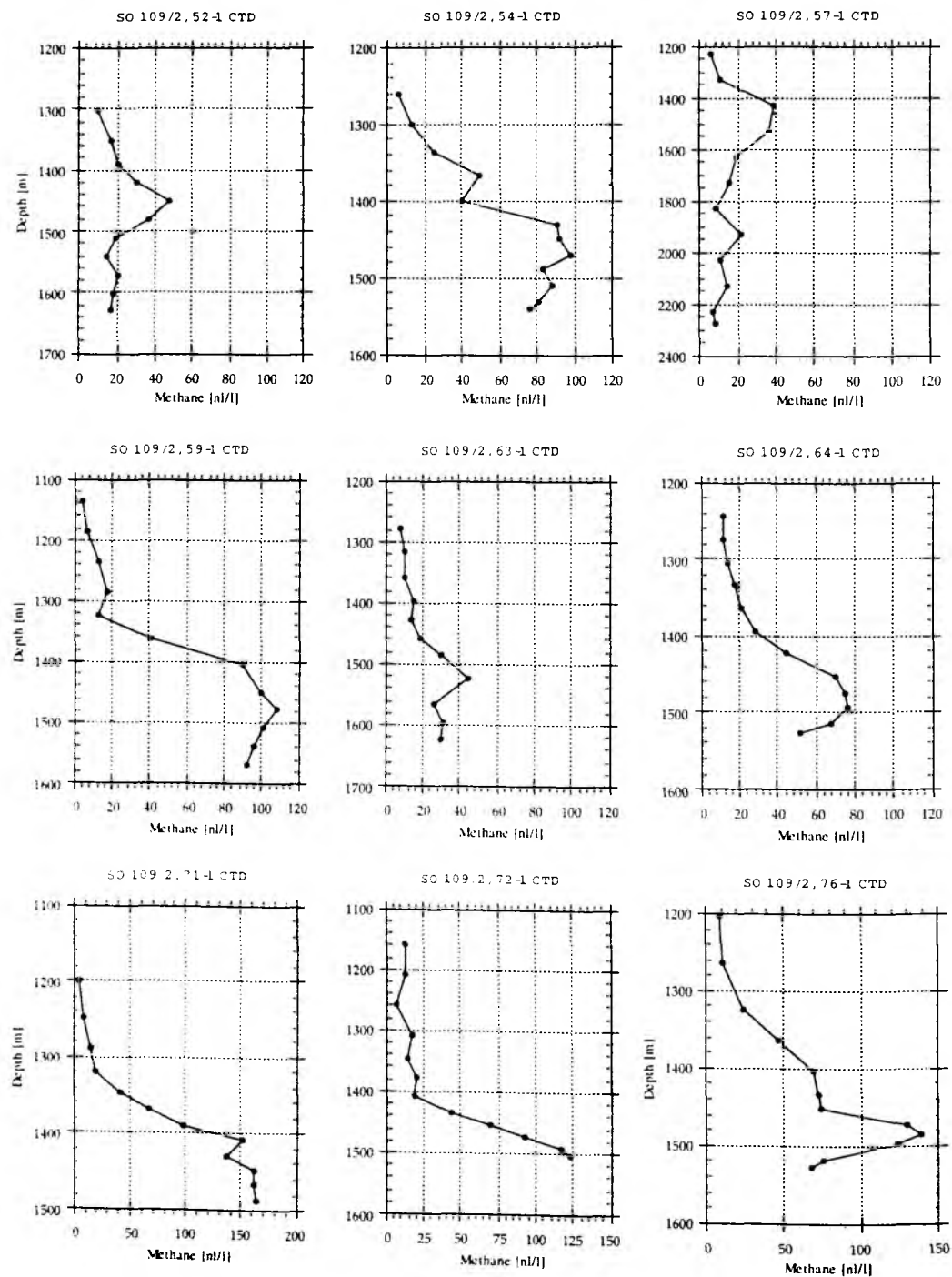


Fig. 53: Methane profiles at Axial Seamount.

"Bioherm" region have to be considered highly variable as a result of tidal influences. Repeated casts on the same location exhibit drastic contrast in methane distributions, on time scale of 2 weeks as well as 10 hours with no relation between methane maxima and water density being found.

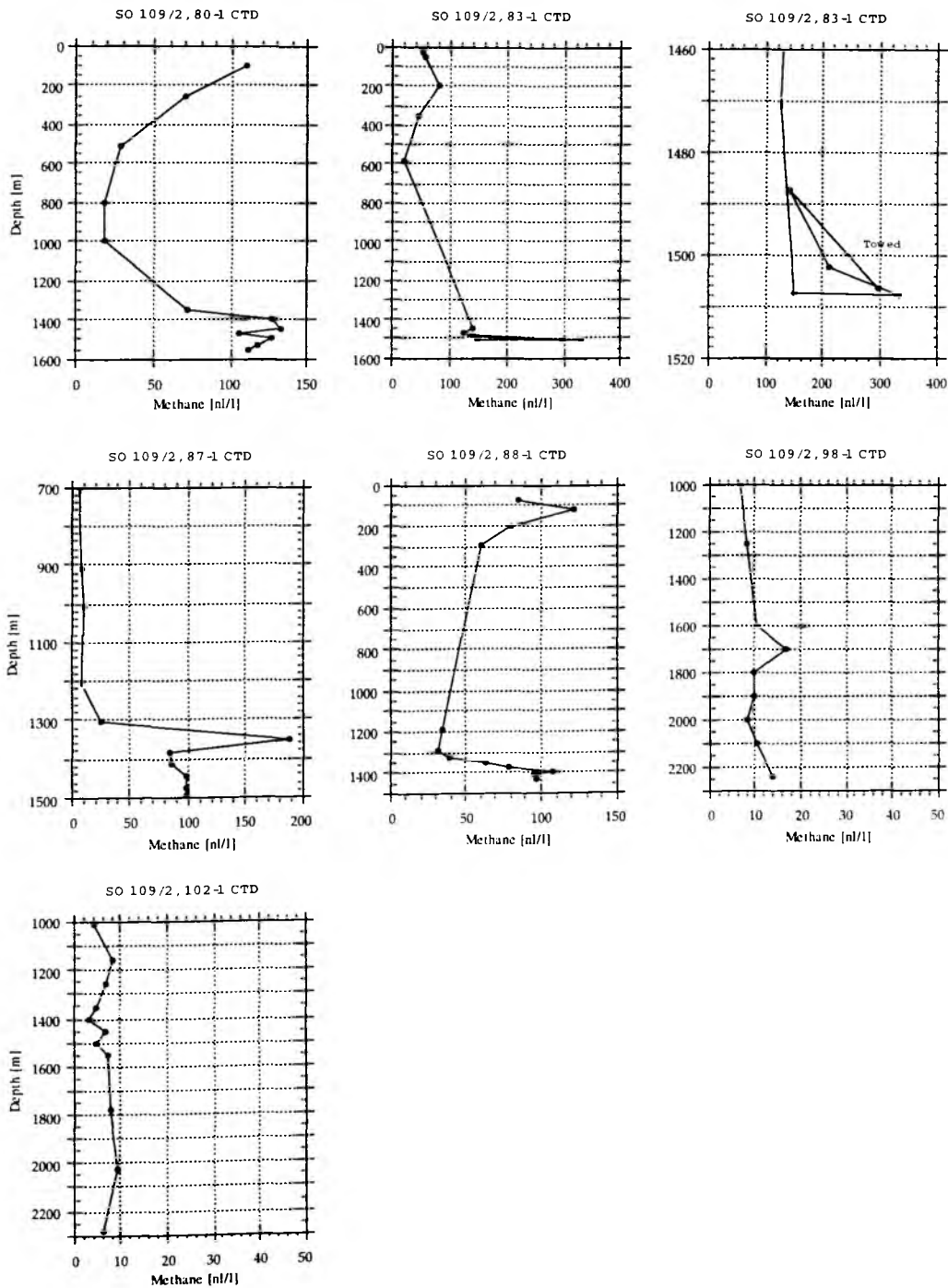


Fig. 54: Methane profiles at Axial Seamount (continued)

Although the "tow-yo" technique allowed for a better approach to the vents and thus higher methane signals compared to SO109-1, the intensities were remarkably higher in the cold

vent area of the Cascadia Margin (maximum of 4,700 n/l at Station 120 CTD) than at Axial Seamount (680 n/l at Station 78 CTD).

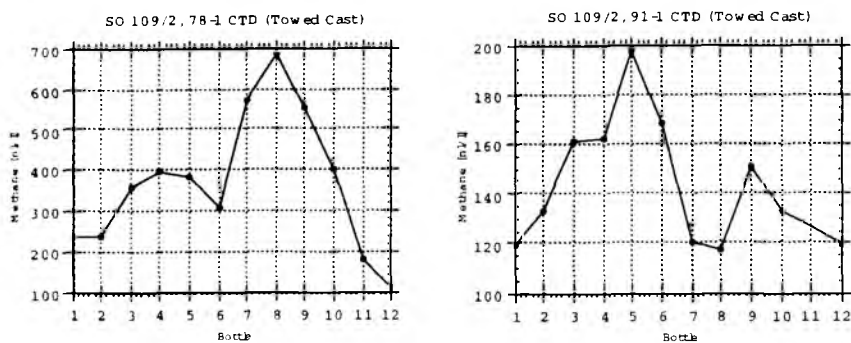


Fig. 55: Towed CTD casts at Axial Seamount.

Axial Seamount Region

Bottom near methane maxima ranged between background values of 6 n/l at station 57-1 CTD northeast of the caldera (Fig. 53) and 680 n/l at station 78-1 CTD at the hydrothermally active ASHES Vent Field (Fig. 55). For comparison, station 102-1 CTD E of Axial Seamount features a background methane profile typical for this part of the NE Pacific. The most widespread CH₄ plume is observed in the vicinity of the ASHES Vent Field at the SE of the caldera, showing maximum concentrations of 120-150 n/l at about 1500 m depth. The distribution pattern of bottom-near CH₄ at this site is reflected by a profile consisting of the CTD stations 72, 78, 76, 83 and 64 crossing the ASHES Vent Field from E to W in this order. Hydrocast 78-1 CTD was the first attempt to achieve a small-scale horizontal profile closest to the source (Fig. 55), and in fact yielded the highest CH₄ signal and also considerable variability over horizontal distances of only tens of meters. The cast was "tow-yoed" for 30 minutes at a speed of 0.5 knots over the inferno vent site in a NW-SE direction, where bottles 1-9 cover the first 9 minutes (i.e. roughly 150 m of horizontal extension) of the survey. A second equally intensive although apparently less widespread vent plume was approached at the CTD stations 54, 59, 71 and 80. For comparison with the vent activities, an image of the surface-near distribution of methane in the Axial area can be derived from a compilation of measurements from the CTD casts 80, 83, 88 and 96 showing a subsurface CH₄ maximum of 100 n/l at about 100 m depth.

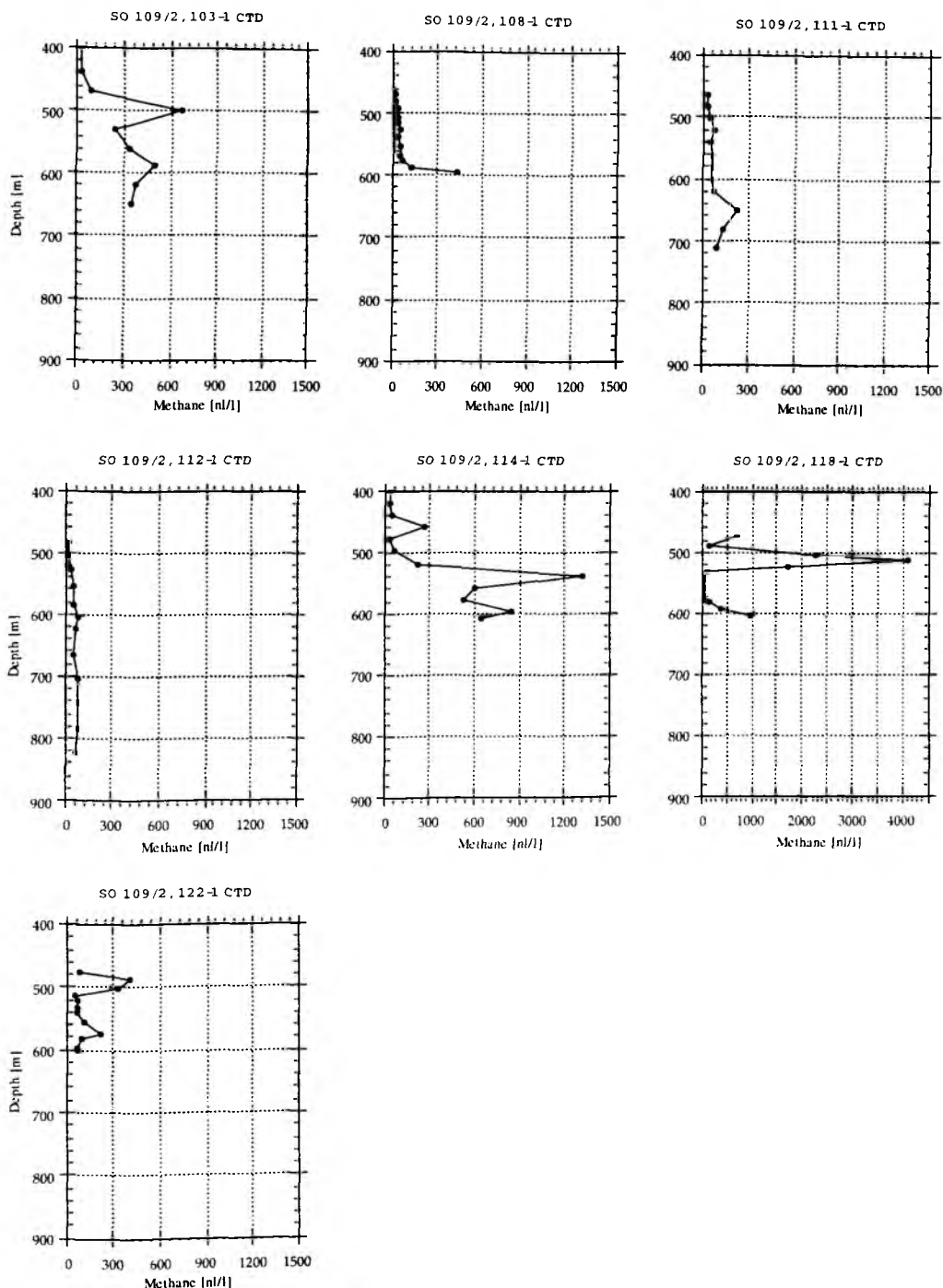


Fig. 56: Methane profiles at Cascadia Subduction Zone ('Bioherm').

Cascadia Margin

The last 3 of 15 days of the SO109-2 leg were dedicated to the continuation of the 109-1 hydrocast surveys at the "Bioherm" stations, where CH_4 signals of up to 12 nl/l had been observed at depths of 120-150 m over the top of the seamount. Although on SO109-2 considerably higher CH_4 concentrations could be measured in samples from "tow-yoed" casts, it was found impossible to re-allocate either the concentration level of the maxima or

the water depth at which they were previously observed. There was also no correlation between water density and occurrence of methane maxima. The most drastic variability with time is shown by the profiles from CTD casts 118-1 and 122-1 (Fig. 56), taken at the same location with a time span of 10 hours in between. Nevertheless, the "tow-yoed" cast 120-1 CTD yielded a record concentration of 4,700 nI/l. The small scale extension of this particular plume can be seen in the profile 118-1 CTD, where CH₄ concentrations cover a range of 100 - 4,000 nI/l within 10 m of water depth. This immense variability with time is most likely attributed to a complete change of the water current regime due to tidal influences. Taking into account the tidal exchange of water masses around the „Bioherm“,

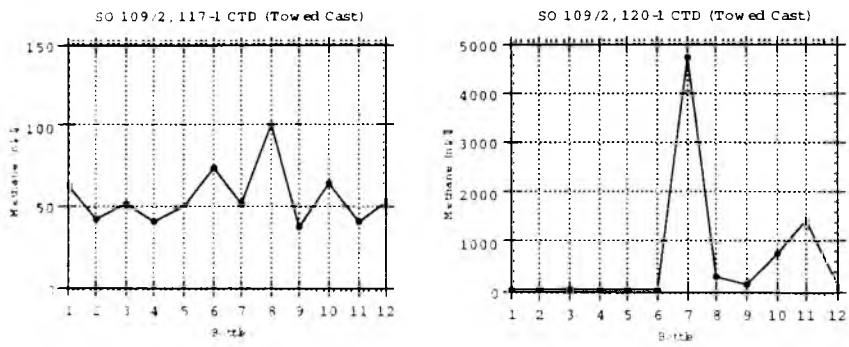


Fig. 57: Towed CTD casts at Cascadia Subduction Zone ('Bioherm').

the vent activities at this side might be considered even higher than suggested from the maximum concentrations. At first sight, the results obtained from both surveyed hot and cold vent locations suggest a comparatively stable methane distribution at moderate concentration levels at the hydrothermal sites of Axial Seamount whereas highly variable distribution patterns at high concentration levels are encountered at the „Bioherm“ sites. Further approach to the active cold vents requires recordings of the water current regime and ROPOS operation.

References

Schmitt, M., Faber, E., Botz, R. and Stoffers, P. (1991). Extraction of methane from seawater using ultrasonic vacuum degassing. *Anal. Chem.*, 63: 529-531.

Lammers, S. and Suess, E. (1994). An improved head-space analysis method for methane in seawater. *Mar. Chem.*, 47: 115-125.

4.4.5 Nutrient and Pore Water Studies

by Anke Dähmann, Klaus Wallmann and Anke Bleyer

Nutrient Analyses

Nutrient analyses were carried out as described for leg 109-1 in chapter "pore water analyses". Results are shown for selected stations at Axial Seamount (Fig. 58) and Cascadia Margin (Fig. 59). Plotted stations are chosen from the evidence for hydrothermal activity from light transmission, potential temperature and methane data. Hydrocasts throughout the whole water column result in typical nutrient profiles for the North Pacific which can be found by comparison with data from cruise SO 97 (ref. leg 109-1). Even samples from greater depth taken with a higher resolution do not show greater effects of temperature anomalies or methane plumes on nutrient concentrations. The somewhat higher values for silicate of CTD 78 (Axial Seamount, Fig. 58) with its methane concentration of above 500 nI/ (1510 m) is not very expressive compared to the data of CTD 76 with a maximum of only 140 nI/l methane.

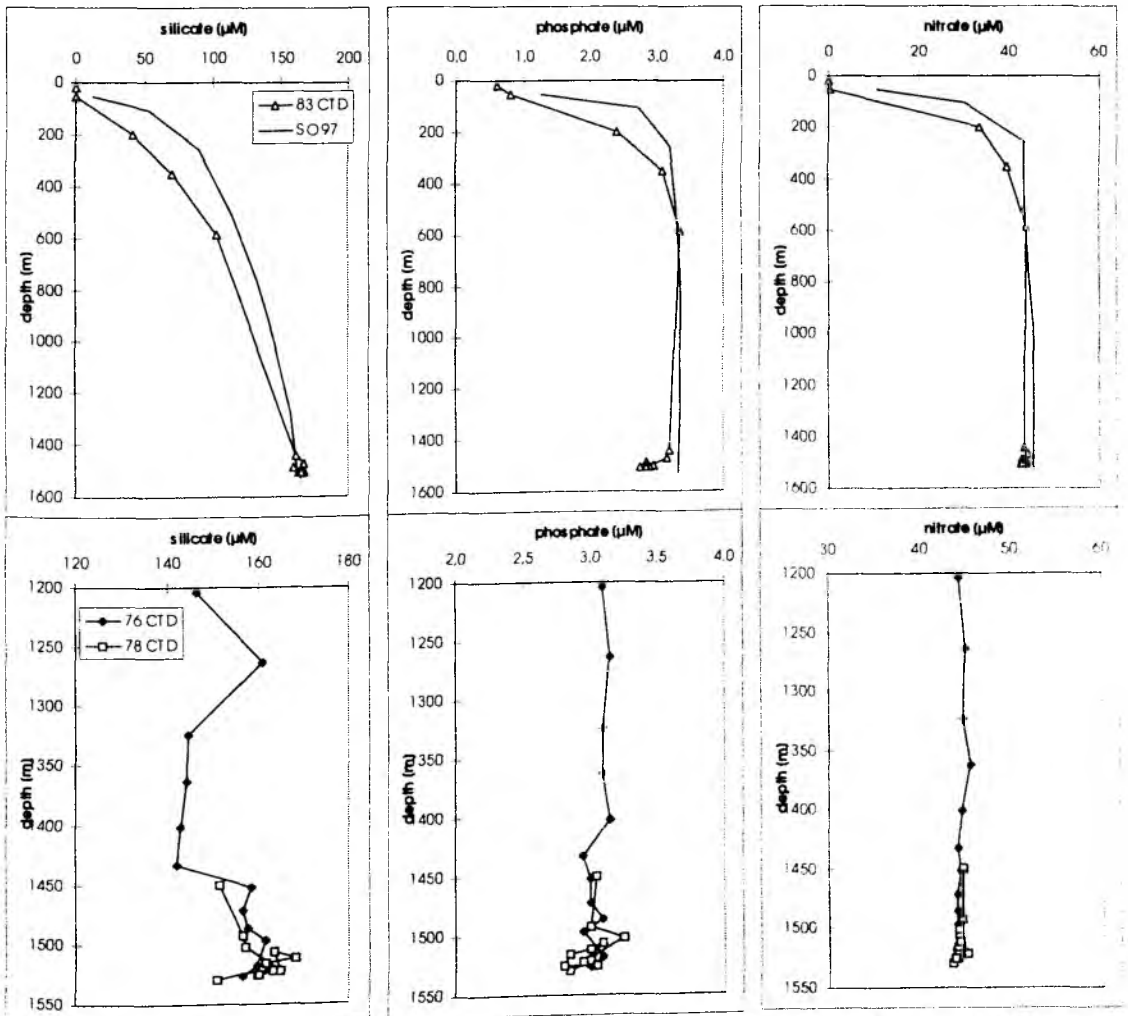


Fig. 58: Nutrient concentrations for CTD stations 76, 78, and 83 at Axial Seamount. Solid lines indicate nutrient profiles of cruise SO 97, North Pacific, for comparison.

For CTD 114 (Cascadia Margin, Fig. 59) a methane plume of more than 1300 nI/l goes along with lower phosphate concentrations, whereas the phosphate peak of CTD 120 at 522 m does not correspond directly to the detected methane plume of about 4800 nI/l (528 m).

Table 9: Synopsis of cores, samples and geochemical analyses

station	no. of subcores	core depth [cm]	no. of pore water samples	analyses
GKG 53	1	27	9	SiO ₂ , PO ₄ , NO ₃ , NH ₄
GKG 55	1	48	12	SiO ₂ , PO ₄ , NO ₃ , NH ₄
GKG 58	1	9	3	SiO ₂ , PO ₄ , NO ₃ , NH ₄
TVG115	3	10 / 14 / 20	5 / 7 / 10	SiO ₂ , PO ₄ , NH ₄
TVG119	2	24 / 19	12 / 13	SiO ₂ , PO ₄ , NH ₄ , Cl, Ca, Mg

SiO₂, PO₄, NO₃, NH₄: nutrient analysis in pore water
Cl, Ca, Mg: titration of pore water

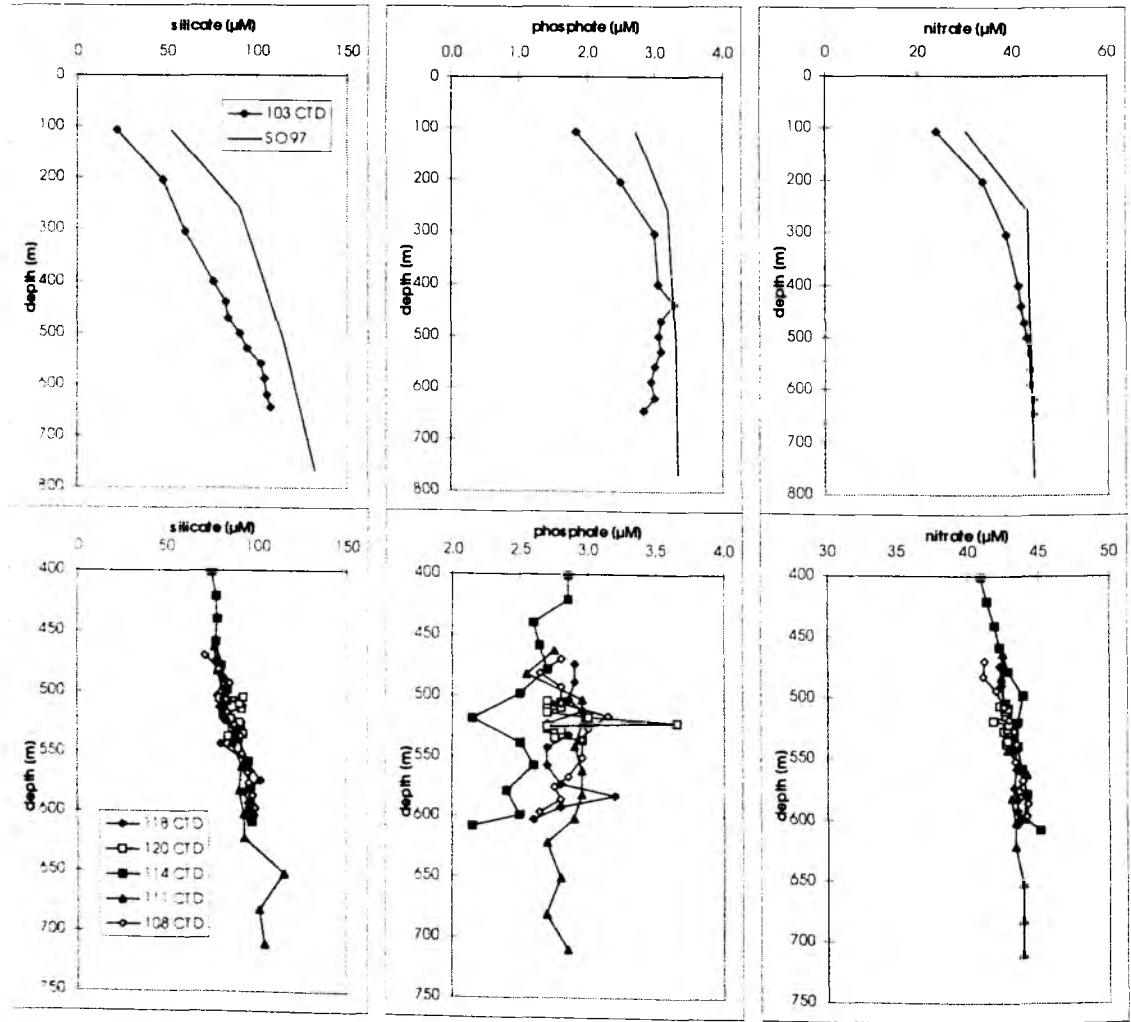


Fig. 59: Nutrient concentrations for CTD stations 103, 108, 111, 114, 118, and 120 at Oregon Margin. Solid lines indicate nutrient profiles of cruise SO 97, North Pacific, for comparison.

Pore water studies

Subcores were pushed into the sediment taken by boxcores (GKG) and TV-guided grabs (TVG), respectively. They were segmented in the cold room (4°C) and pore water was collected with a polypropylene squeezer. Methods for sampling and nutrient analyses are described in detail in chapter "pore water studies" of leg 109-1. Selected samples of TV grabs were additionally analysed for chloride, calcium and magnesium. A synopsis of cores, samples and geochemical analyses performed on board is given in Table 9.

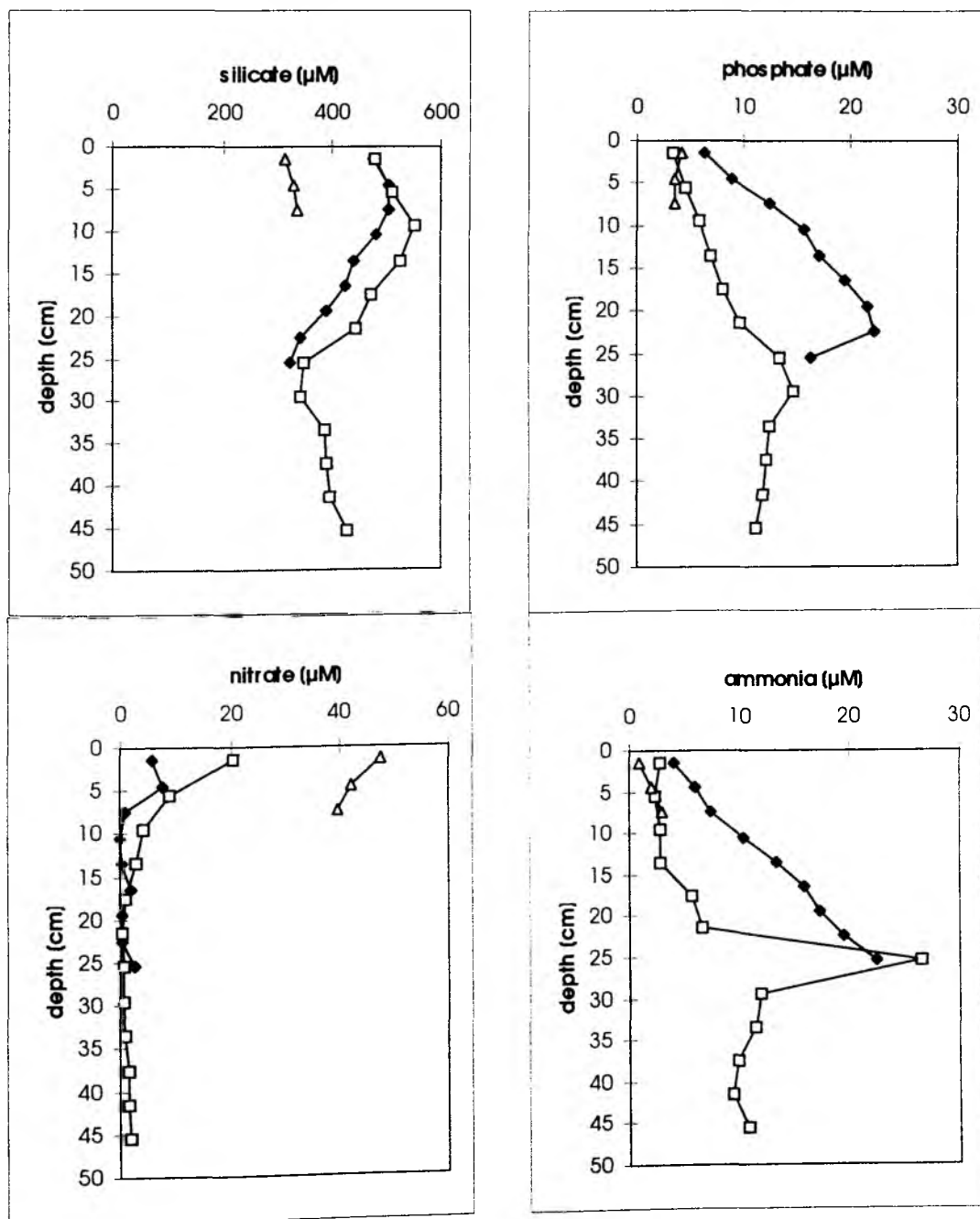


Fig. 60: Nutrient concentrations in pore water for stations GKG 53, 55, and 58 at Axial Seamount.

Juan de Fuca Ridge

The silicate profiles of pore water samples from stations 53, 55, and 58 differ from typical profiles by a decrease between 5 and 25 cm and a slight increase below 25 cm (Fig. 60). This might be due to irrigating bottom water. The suboxic layer is very shallow. Nitrate is reduced to zero at 10 to 15 cm (GKG 53, 55). The slight increases in pH and ammonia are due to oxidation of organic matter.

Oregon Margin

There is evidence for decomposing gas hydrates from the chloride data (Fig. 61). At station 115 a reduction of Cl concentration in pore water of about 2% at 11 cm depth (relative to 19 and 1 cm) is observed. At station 119 the reduction is also about 2% from 21 to 11 cm depth. Low concentrations (545 and 542 mM) could be due to dilution effects caused by dissolution of gas hydrates that are thermodynamically unstable at this site, but they are within the

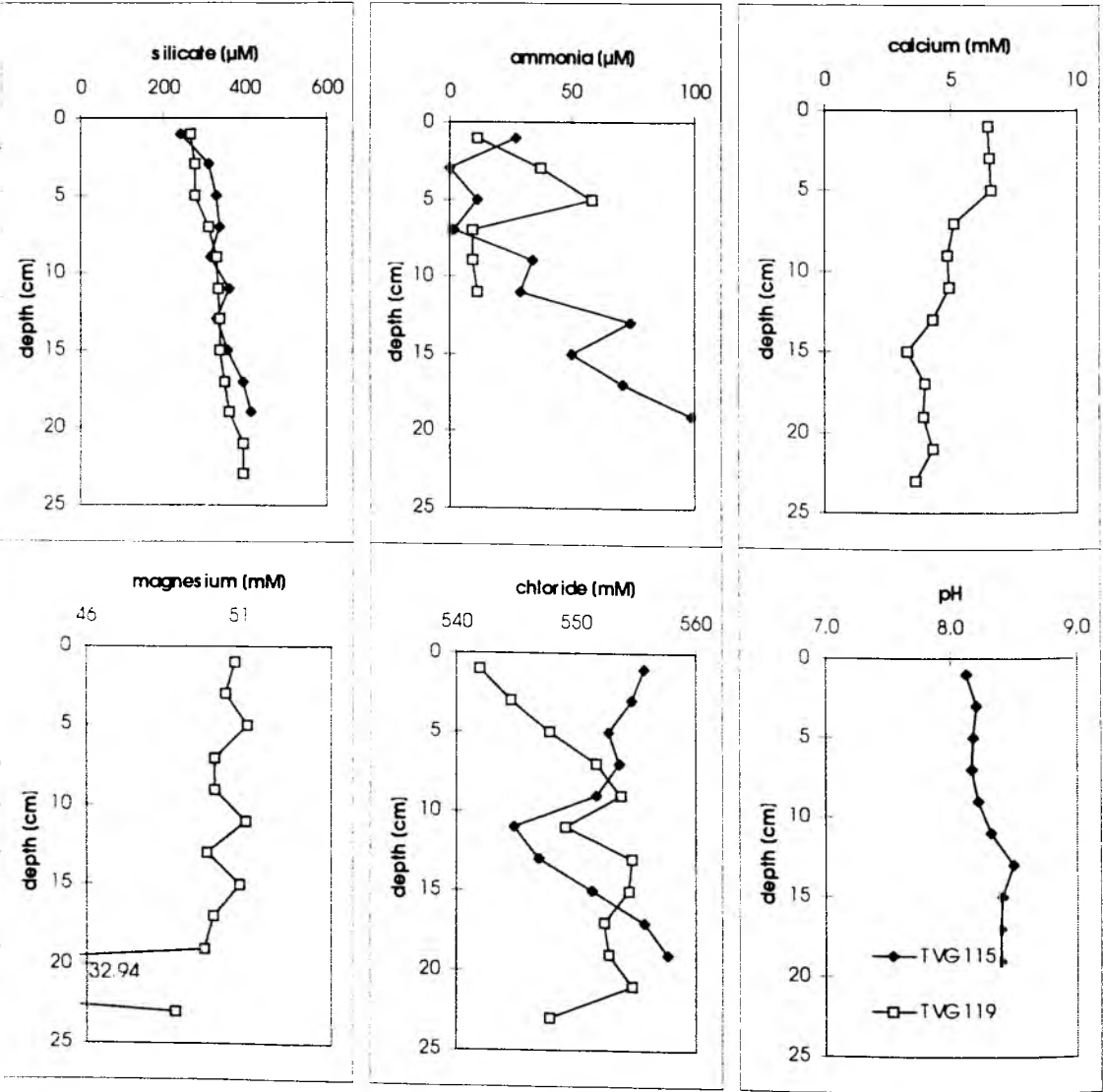


Fig 61: Nutrient concentrations in pore water for stations TVG 115 and 119 at Oregon Margin.

range of sea water chlorosity (CTD 12 and 16, SO110-1a: 533 - 555 mM). In general, chloride of TVG 115 and 119 is much higher concentrated than on leg 109-1 (TVG 43-1), whereas Ca and Mg concentrations are much lower (TVG 36-4). The silicate profile with its smooth increase with depth do not show any evidence for advective fluid flow or dilution. Sulfide was smelled but not analysed.

4.4.6 SUAVE Operations

by Gary J. Massoth

SUAVE (SUBmersible System Used to Assess Vented Emissions) is an integrated system comprised of an array of physical sensors and a chemical analyzer, all adapted for in situ deployment. SUAVE was designed expressly to detect and quantify hydrothermal fluxes to the oceans. Physical properties measured by SUAVE include: temperature, conductivity, pressure, and light attenuation and scattering. Up to four different chemical species may be determined simultaneously by SUAVE, with in situ calibration effected using an onboard valve system. Chemical species include: iron (II) and iron (III), manganese, reactive silicate, ortho-phosphate, and hydrogen sulfide. Physical sensor information is recorded internally at 1-2 Hz while each chemical channel is read every five seconds. Real-time communication is possible when SUAVE is linked to a control station via a conducting or fiber optic cable. Alternatively, autonomous operating protocols are embedded within an onboard control module. The large dynamic range of SUAVE sensors allow data collection throughout a broad spectrum of hydrothermal intensities that includes direct measurement of seafloor vent fluids at temperatures up to 120°C and highly-diluted non-buoyant hydrothermal plumes. SUAVE is a robust and dependable instrument system with over 1,300 hours of in situ deployment accumulated on a variety of platforms including manned submersibles (ALVIN and SHINKAI 6500), ROV's (ROPOS and VENTANA), CTD and camera (EXPLOS a first) tow-frames, and in unattended monitoring mode on the seafloor (up to 96 hour duration). Repetitive deployments at depths up to 5,800 m with short turn-around times are routine.

SUAVE External Unit

Frame dimensions (L x W x H): 48.3 x 40.6 x 45.7 cm (tube extension 80 cm x 5 cm dia.)

ROPOS configuration, Al frame with epoxy coating

Weight in air: 40.8 kg

Weight in water: 21.3 kg

Sensing-intake probe: 3.6 m-long, 22ga. flexible electrical cable with attached 1.59 mm

OD teflon tubing line; temperature sensor tip is 4 cm long and same diameter as electrical cable; scanner intake is a plastic filter about same diameter as

temperature probe. The flexible probe line is easily adaptable to variously configured deployment platforms.

Electronics connections:

12-channel peristaltic pump: 24-30 vdc, 0.5 amps; cable extends 1.5 m from connection at motor pressure case with RMG-4-FS marine connector at end.

CTD pump: 12-18 vdc, .15 amps; 4.2 m cable with RMG-4-FS marine connector at end (not used on EXPLOS).

RS-232 communication: cable extends 2.4 m from electronics case to end with RMG-4-FS marine connector; four wires are required: Rx, Tx, 9 vdc, and common.

SUAVE Operation with EXPLOS

SUAVE, in ROPOS configuration (see above), was fitted at sea for use on the EXPLOS camera sled. Specially-designed clamps were fabricated onboard to secure SUAVE to the top, left, middle section of the EXPLOS frame. Power (24 VDC) was provided by wiring two EXPLOS deep sea batteries (12 VDC) in series and mating with a SUAVE power cable. A Sea Tech 6000LS light scattering sensor was mounted to the upper forward sled frame. Temperature and chemistry intake probes were mounted low on the EXPLOS frame.

SUAVE Deployments

A total of 18.5 hours of in situ determinations were achieved during four deployments of SUAVE on EXPLOS:

<u>Operation</u>	<u>Date</u>	<u>Site</u>	<u>Comments</u>
79 EXPLOS	15 June	South Rift, Axial Volcano	5.0 h: ΔT, LS, Mn, H ₂ S
82 EXPLOS	16 June	along SW caldera wall	3.5 h: ΔT, LS
84 EXPLOS	17 June	HDV vent, CoAxial Segment	9.0 h: ΔT, LS, Fe, H ₂ S
100 EXPLOS	20 June	South rift, Axial Volcano	1.0 h: aborted operation

*note: ΔT indicates a temperature anomaly and LS a light scattering anomaly.

Results

(1) The utility of deploying SUAVE on a towed camera sled to chemically prospect for venting systems was clearly demonstrated. At both Axial Volcano and CoAxial segment, thermochemical venting signatures were determined within the camera tow realm. Perhaps the most convincing demonstration of SUAVE's vent finding ability is the record obtained at CoAxial segment (HDV vent) during 84 EXPLOS. At no time during this dive was there a visible indication of venting, even though site markers were imaged. Unambiguous thermal and chemical anomalies were detected, however, 6 out of 8 times between 2,000 and 2,010 m, during this tow. Unfortunately, because real-time communication with SUAVE was not available, we were not able to focus sampling in this depth range, and thus enhance our

chances of imaging the venting system that was detected chemically. Interestingly, on a subsequent TV-grab at this exact site (97 GTVA), a venting system was imaged, thus two operations were required where one might have sufficed using remote telemetry and SUAVE.

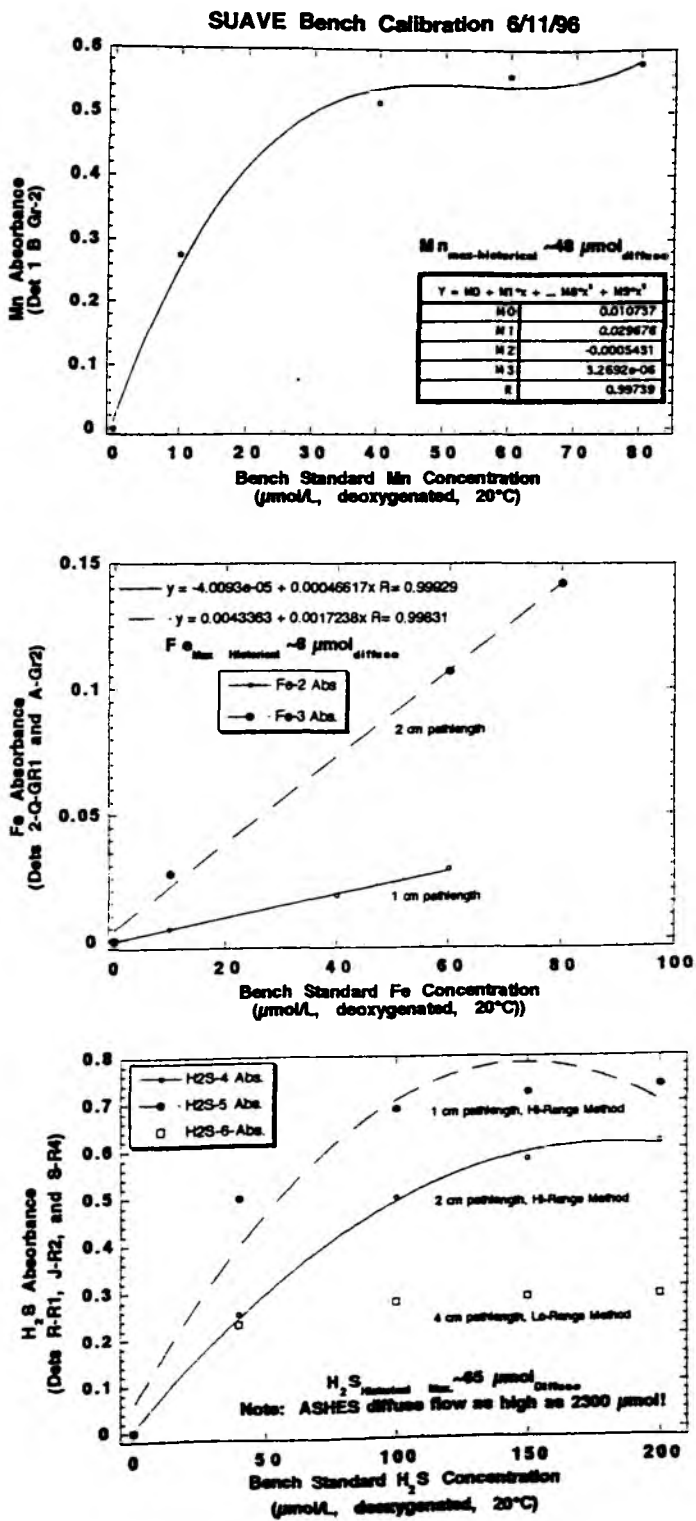


Fig. 62: SUAVE Bench Calibration.

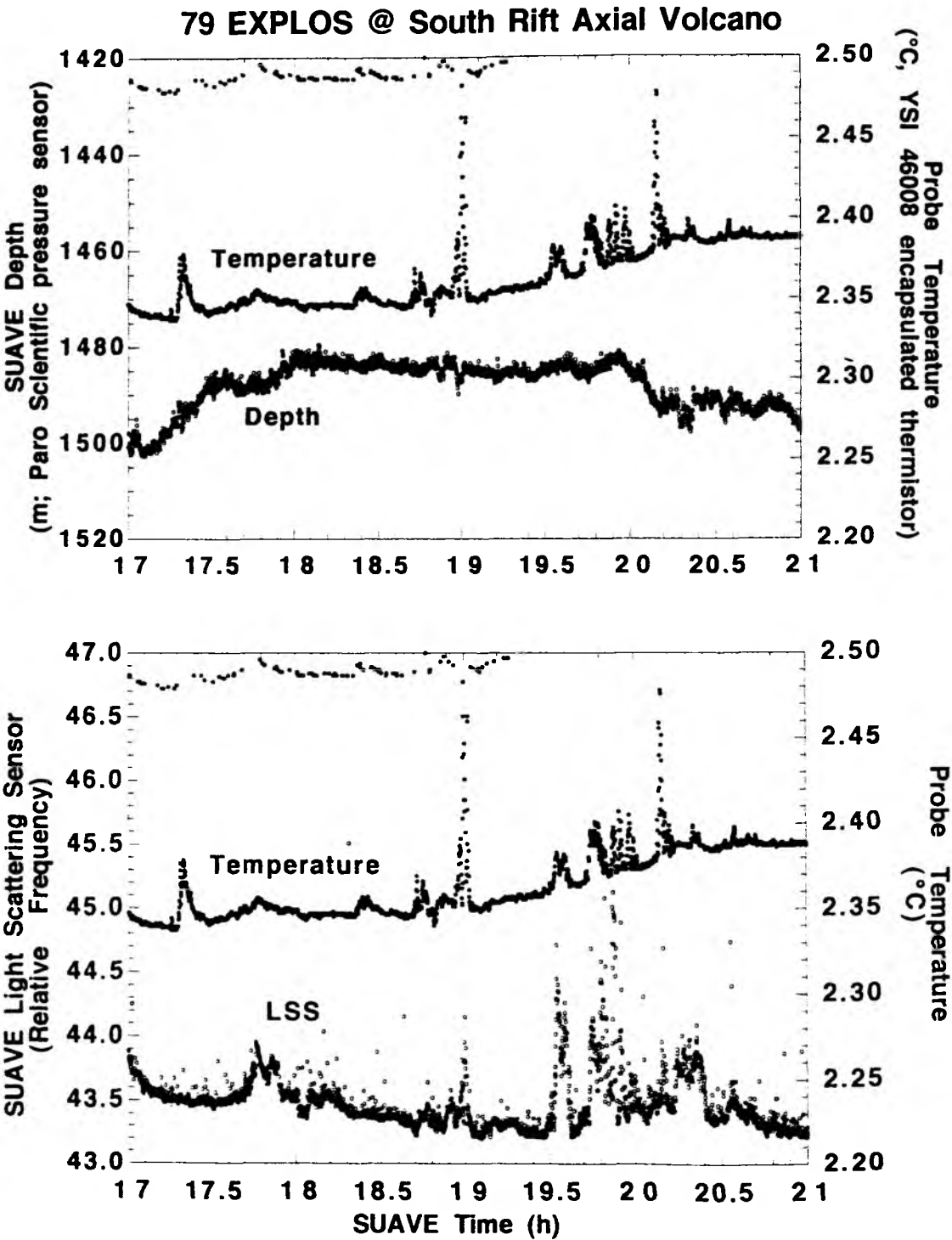


Fig. 63: SUAVE Diagramms.

(2) Bench calibrations of SUAVE for Mn, Fe (II+III), and H₂S (Figure 62) conducted onboard demonstrated that the respective ranges of determination were appropriate relative to the historical data for most diffuse vent fluids at Axial and CoAxial. Empirically determined combinations of reagents and flow analysis configurations were used to extend the ranges of determination for SUAVE to those shown in Figure 62. Surprisingly, much lower

concentrations were everywhere detected, and thus provided a challenge to the equilibrium type chemical methods utilized (PAN for Mn, FerroZine for Fe (II+III)), and methylene blue for H_2S). In retrospect, because the concentration levels for Mn and Fe were typical of non-buoyant hydrothermal plumes, the kinetic catalytic methods usually employed there (Mn catalyzed oxidation of leucomalachite green with nitrilotriacetic acid activator for Mn and Fe catalyzed oxidation of hydrogen peroxide for Fe) may be more appropriate for camera sled work, even though they are too sensitive for direct measurement of vent fluids. A direct comparison of the kinetic catalytic and equilibrium methods for Mn was configured for testing during 100 EXPLOS, which, unfortunately, was aborted only one hour after deployment.

(3) Thermochemical results are shown as SUAVEgrams in Figures 63-67.

Note that on 82 EXPLOS only the fully-autonomous pressure, temperature, and light scattering sensors were deployed along with the SUAVE electronics bottle (i.e., no deep sea batteries were required). This physically reduced configuration allowed attachment of the various parts within the EXPLOS frame, and thus provided extra protection for this potentially dangerous tow through unknown terrain.

During 79 EXPLOS, temporally coherent anomalies in temperature, light scattering, Mn, and H_2S are evident (Fig. 63). Note, also, that for each parameter measured, isolated anomalies in time occur. Thus, sole reliance on any of the venting tracers measured may lead to incomplete or false detection of venting. Simultaneous signals for multiple hydrothermal tracers is a preferred condition for positive identification of a venting site.

Examination of the baselines for the chemical analytes suggests that the operational limits of detection for Mn, Fe, and H_2S (using the low-sensitivity chemical methodologies employed during this cruise) are about 20nmol/L, 35nmol/L, and 40nmol/L, respectively. These determination limits represent ~ 200- to 2500-fold dilutions of diffuse fluids sampled directly at Axial Volcano (Fig. 62).

Thermochemical anomalies ($\text{Mn}/\text{heat}(=\text{Q})$, Fe/Q , and $\text{H}_2\text{S}/\text{Q}$) at the South Rift of Axial Volcano and HDV vent at CoAxial segment are generally representative of diffuse fluids sampled at other chronic venting sites. The high Fe/Q value (13.7 nmol/J) at CoAxial is similar to data from South Cleft segment, where the most Fe-rich fluids along the global ridge crest have been found. That multiple instances of more normal Fe/Q fluids (~ 0.65 nmol/J) were detected at CoAxial during 84 EXPLOS suggests the high anomaly may be artifact (the thermal anomaly was very small, 0.016°C) or an isolated occurrence. Interestingly, $\text{H}_2\text{S}/\text{Q}$ at CoAxial (5.3 nmol/J, Fig. 67) is similar to the value measured in 1995 (3.8 nmol/J), and much lower than the pulse of high $\text{H}_2\text{S}/\text{Q}$ (32 nmol/J) that followed by one year a dike injection at this site. Based on this sole observation, it appears that venting at Floc site, CoAxial segment has not been re-invigorated since the 1993 intrusion.

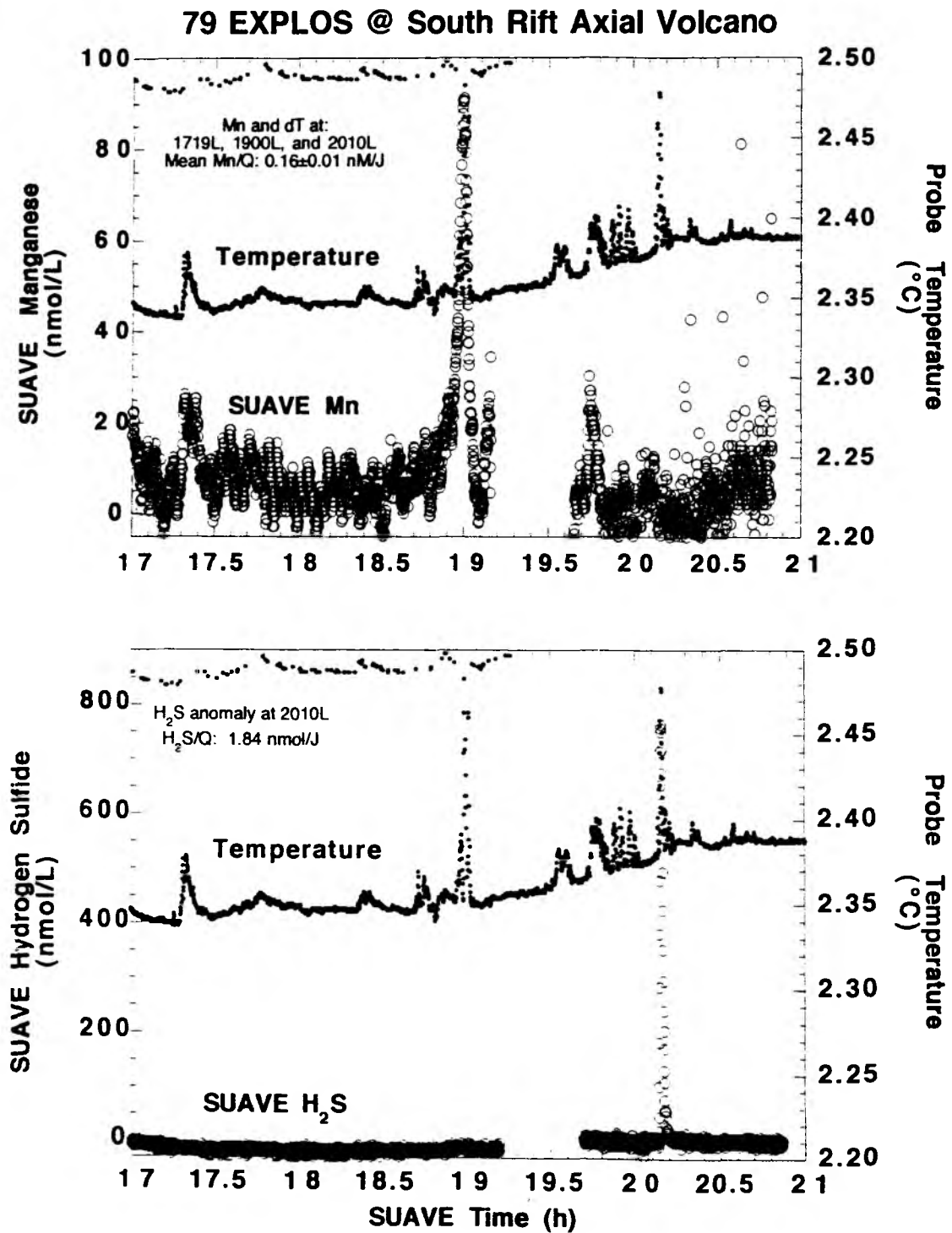


Fig. 64: SUAVE Diagramms.

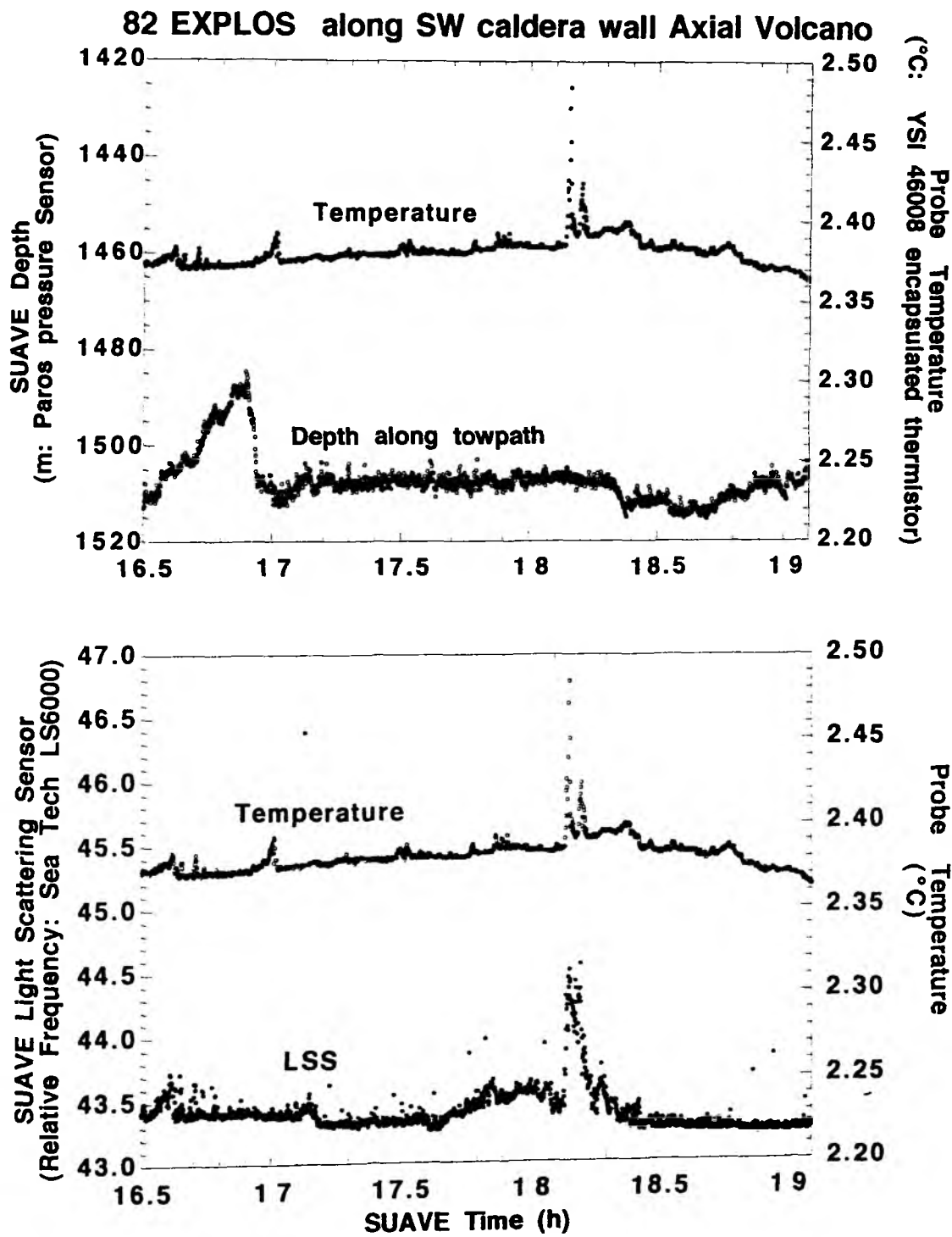


Fig. 65: SUAVE Diagramms.

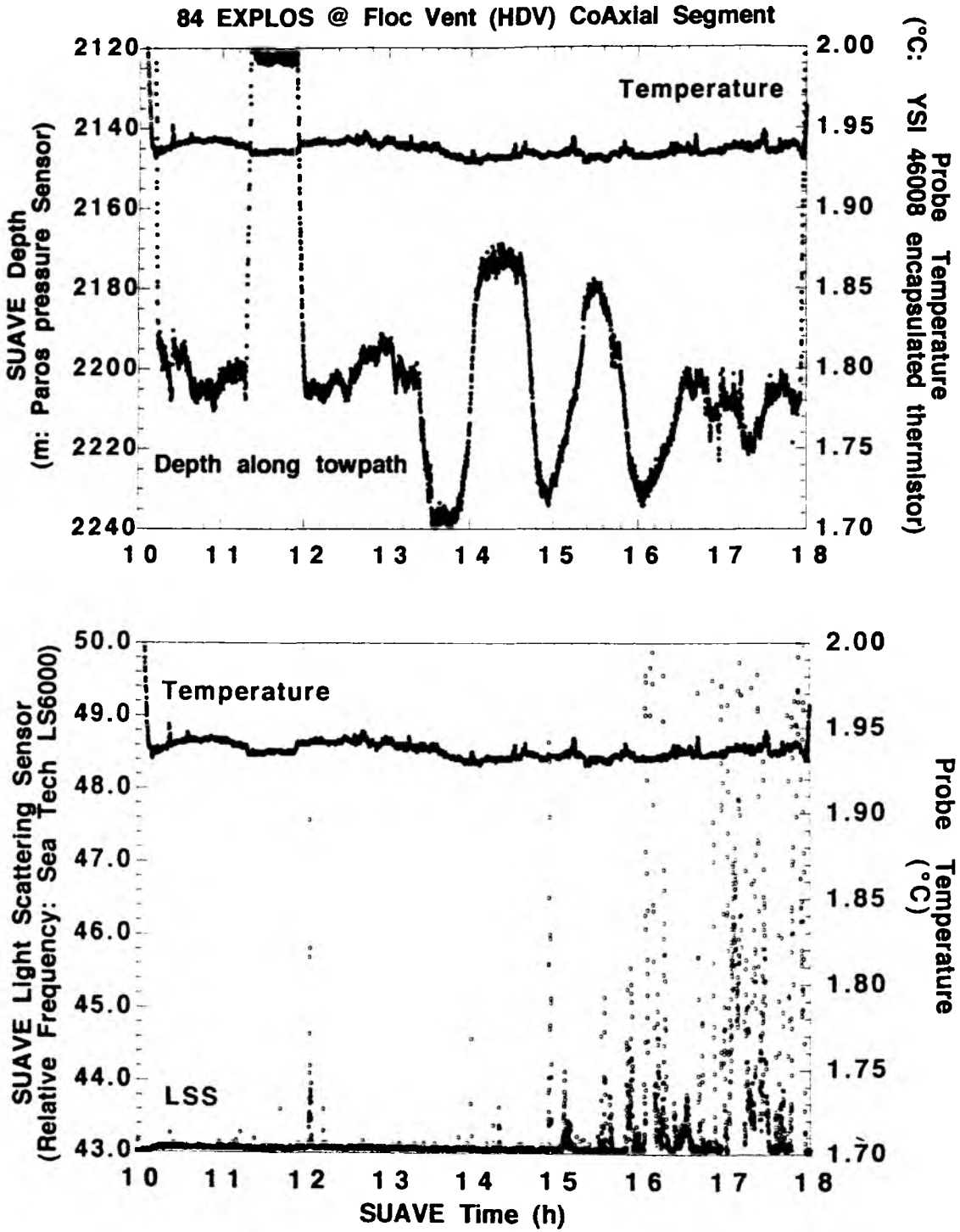


Fig. 66: SUAVE Diagramms.

84 EXPLOS @ Floc Vent (HDV) CoAxial Segment

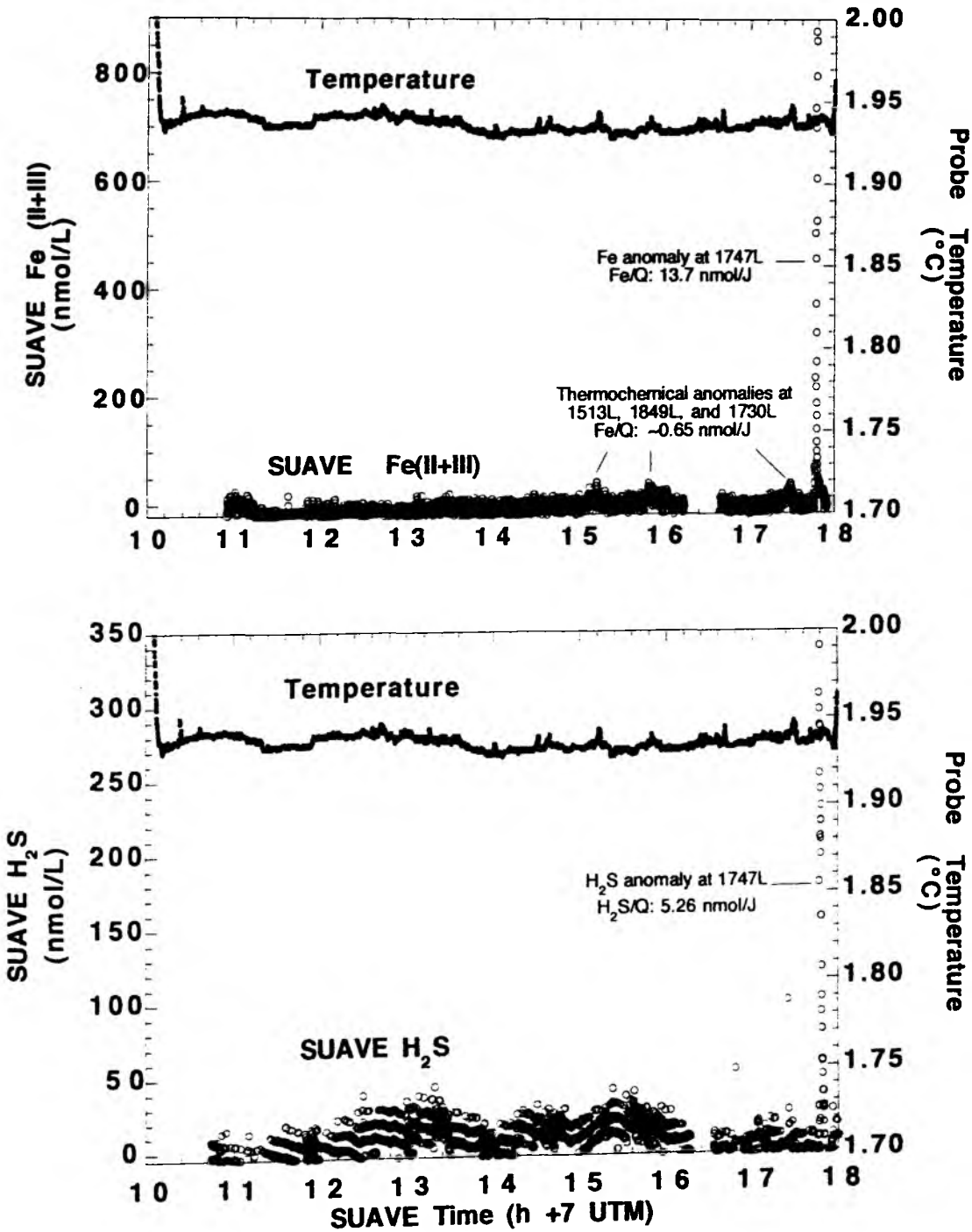


Fig. 67: SUAVE Diagrams.

4.4.7 Biology Report

by Verena Tunnicliffe and Peter Linke

The account below considers the biota associated with bottom samples and camera observations.

Box Core SE of Axial Seamount 46° 05.2' N/ 130° 10.0' W 2.807 m (53 GKG)

one burrowing anemone retrieved (Cerianthidae)

Disposition: P. Linke

The CASM Vent Field was sampled for biology in 1983 and 1986. Figure 68 is a representation of the fauna inhabiting the fissure in 1983. With the GTVA, we saw that much of this area was still active - if not expanded. A major biology objective is to determine if the site has accumulated species over the last 13 years or if it is in a steady state. The grab samples were insufficient to conclude but certainly indicate that the community has sustained itself.

CASM Vent Field (61 GTVA)

Sparse vent animals retrieved in remarkably good condition considering the collection technique. Interesting to note the high abundance of predaceous polychaetes among the bivalves: the same association (*Calyplogena* and *Nereis*, but different species) was evident in Lihir Seamount samples from the western Pacific. One limpet was recovered that previously was not recognize as a know Juan de Fuca vent inhabitant. The assemblage represents one of very low hydrothermal flow - but enough to support the symbionts in the clams.

Bivalve	<i>Calyplogena pacifica</i>	15 live, 10 shells
Polychaete	<i>Nereis piscesae</i>	10
Polychaete	<i>Hesiodeira(?) glabra</i>	1
Polychaete	<i>Nicomache venticola</i>	10
Snail	<i>Provanna variabilis</i>	2
Limpet	?n. sp.	1
Tube worm	<i>Ridgeia piscesae</i>	10
Amphipod	unknown - possible contaminant	1

Disposition: V. Tunnicliffe

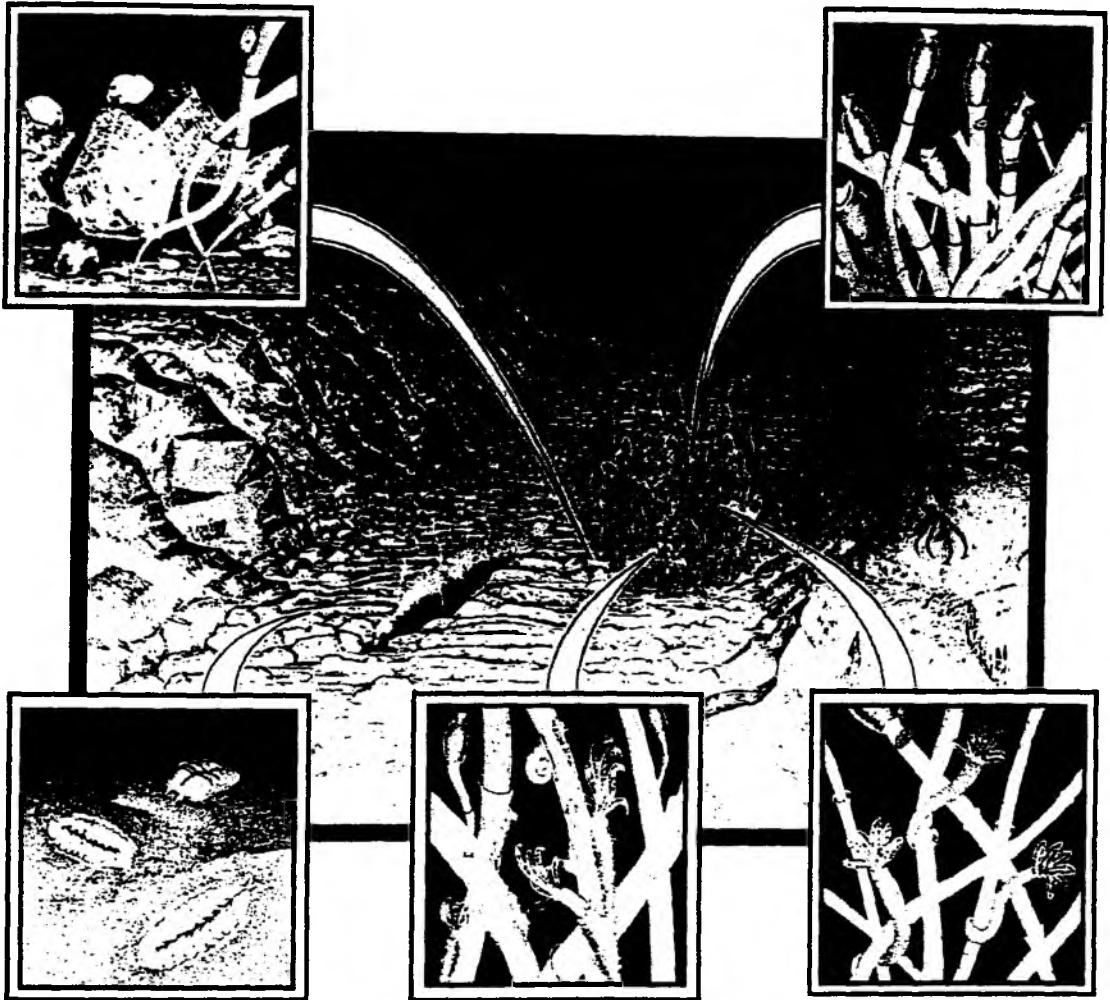


Fig. 68: Representation of the fauna inhabiting the main fissure (CASM) in 1983.

CASM Vent Field (69 GTVA)

This grab sampled basalt and newly deposited sulfides. While the high-temperature venting may be very recent, the largest animals are at least 6 to 12 months old. Several animals were located under the basalts among the depositing sulfide. Some soft sulfides were already entombing worm tubes. The assemblage is indicative of a moderate temperature biotic habitat although two higher temperature species were present in low numbers. The association with sulfide deposition is curious and an intriguing dive target. Both the assemblage and the sulfide indicate a flow temperature not present in 1983 or 1986. Most animals were retrieved in fine condition and many were still alive four hours after delivery to the surface.

Tube worms	<i>Ridgeia piscesae</i>	100's
Limpets	<i>Lepetodrilus fucensis</i>	1000's
Palm worms	<i>Paralvinella palmiformis</i>	100's
Pandora worms	<i>Paralvinella pandorae</i>	100's

Sulfide worms	<i>Paralvinella sulfincola</i>	several
Scale worms	three species	10's
Snails	<i>Depressigyra globulus</i>	100's
unsorted material		half bucket

Disposition: V. Tunnicliffe

CoAxial Segment: Floc Site (83 EXPLOS)

Attempted to tow along the fissure over known active area with camera sled fitted with the SUAVE scanner. Weather conditions and resultant use of bow thruster on SONNE resulted in poor return on the navigation in the southern (Marker 26) area. Both long and ultra-short baseline systems improved in the northern (HDV) area and several passes were made with the camera over the vent target. While several markers and ALVIN dive weights were spotted, the small target of the vent area was not seen. Visual and SUAVE observations indicate that regional venting has not increased since the 1993 eruption. The fissure that previously had patchy signs of venting (1994) was virtually bereft of hydrothermal indicators. The minuscule signature from the SUAVE even so close to HDV (within 30 m) suggests that this site likely diminished in effluent from 1995 observations.

CASM Site Axial Seamount (89 GTVA)

Grab of part of Lamphere Chimney - in vicinity of GTVA's 61 and 69. This time the biological return was fairly small. The sulfide probably came from the lower, cooler flank of the chimney. Few high temperature animals were present and the tube worms retrieved were mostly thin, with lower haemoglobin (pale pink rather than red) and the organ with symbiotic bacteria was reduced. The few good tubeworm specimens were dissected for subsequent work on the ultrastructure of reproductive systems and frontal musculature. The alvinellid polychaetes were used in an attempt to culture thermophilic bacteria from the guts.

Tubeworms	<i>Ridgeia piscesae</i>	20
Palmworms	<i>Paralvinella palmiformis</i>	4
Sulphide worms	<i>Paralvinella sulfincola</i>	8
Limpets	<i>Lepetodrilus fucensis</i>	10's
Scale worm	<i>Lepidonotopodium piscesae</i>	1
Crab	<i>Paralomis verrilli</i>	1

Disposition: V. Tunnicliffe

HDV Vent, Floc Site, CoAxial Segment (87 GTVA)

This grab was a failed attempt to sample biota at the vents formed in 1993 in conjunction with the new lava eruption. Navigation was excellent and the site was located within a half hour. However, in the pillow terrain, we did not grab the rocks. A tubeworm bush was

retrieved but lost from the top of the grab. To be successful, the basal substratum must return to the surface. We did not redeploy for fear of damaging the site too greatly before the occasion of a possible ROPOS dive.

Second Accretionary Ridge, Oregon Margin, 600 m (109 GTVA)

Noted abrupt transition from dense population of sea urchins, sea stars and flatfish close to the "bioherm" summit to hard grounds mostly uncolonized by fauna (the rare gorgonian coral). I find this unusual given that local topography in this area tends to concentrate currents and augment suspension feeder populations. My guess is that the effluent from the mound is a major deterrent to colonization by the indigenous fauna. Between the blocky chunks of apparently indurated muds, we began seeing clam shells scattered on the surface. Grabbed a relatively clear area but the amount of material retrieved was small. Consisted of heavily packed clays, some hardened chunks and clam shells. Most dead shells were still articulated and little dissolution was evident. Biologic material retrieved:

Live clams	<i>Calymene</i> sp.	about 45
Dead clams	<i>Calymene</i> sp.	about 100
Dead leather clams	<i>Solemya</i> sp	6
Neogastropods	two species (shells only)	4
Rag worm	<i>Nereis</i> sp	1

Disposition: P. Linke

Calymene specimens were collected and stored alive in the cool room. An aquarium with ambient sediment and bottom water was prepared and some of the collected *Calymene* were placed here for cultivation experiments, which were started in the subsequent leg. The sediment seemed to contain a lot of H₂S and had a greyish colour.

Summit of the Second Accretionary Ridge, Oregon Margin (110 GTVA)

Grab about 50 m from previous. Taken in terrain with large indurated sediment masses. Grab closed on cable and most sediment and clams were lost. However, three large indurated masses were retrieved. Carbonate surfaces were irregular and pitted. The undersides represented a reducing environment. These chunks housed a specialized epifauna: some animals appear to be normal deep-sea but capable of coping with the ambient H₂S while others - many on the undersides - are most likely seep indigenous.

Dead leather clams

from sediment	<i>Solemya</i>	6
Chitons	unknown & unusual	1 large, 2 sm.
Sponges	unknown	3

Limpets	seep endemic likely	~20
Brittle stars	unknown sp	3
Sea feathers	unknown hydroids	5
Worms	3 spp. polychaetes	5
Scale worms	seep endemic likely	3
Red blobs	?? Anthozoa	5

Disposition: P. Linke (some limpets to V. Tunnicliffe for DNA work).

Summit of the Second Accretionary Ridge (113 EXPLOS)

South to north profile through the centre of the elevation. The profile showed a prevailing southern bottom water current in the drifting particle. Ripple marks were visible on the more sediment-covered areas being a good indicator for strong bottom water currents.

Western Crest of “Bioherm” on Oregon Margin (115 GTVA)

Grab returned a couple hundred kilos of sediment and carbonate blocks and started degassing close to sea surface. Biological material included hundreds of live and dead clams and numerous other small species associated with vents. This material was not sorted but retained by Peter Linke for later use. Like 110 GTVA, of particular interest was the fauna associated with the carbonate blocks. Clams and snails were embedded in the lithifying matrix; a stiff mud overlayer was inhabited by live animals but the zone of accretion must slowly move outward enveloping some of these animals. Most noteworthy was a “golden slime” coating rock and sediment on the underside of the blocks. This organism is surely prokaryotic (maybe a slime mould?) and able to cope with this highly reducing habitat; gas bubbles were escaping while removing it from the clay layer. I believe this to be quite a novel beast worthy of close attention.

Disposition: P. Linke

Western Crest of “Bioherm” on Oregon Margin (116 GTVA)

Several deployments without luck, no sediment recovery. Several targets for later ROPOS dives were observed, but could not be sampled with the TV grab.

Western Crest of “Bioherm” on Oregon Margin (119 GTVA)

After 3. deployment a full grab with grey sediment was recovered, bubbles came out of it. Those spots were sampled with sediment cores. The conduits had a more coarser appearance with yellow and white crystals and grains. The sediment was very consolidated with almost no porewater in it, hence no much macrobiology. Some echinorid worms were recovered, whereas the stones were colonized by small vestimentiferans.

Western Crest of "Bioherm" on Oregon Margin (121 GTVA)

This grab recovered a dead community dominated by Calyptogena and numerous buccinid gastropods and small vestimentiferans. Obviously these organisms experienced a shut-down in the supply of seep fluids - there was no odor of H₂S.

4.4.8 Microbiology

by Melanie Summit

The focus of the microbiological studies at Axial Seamount was on organisms that grow at thermophilic (55°C) and hyperthermophilic (90°C) temperatures. Anaerobic culture tubes containing elemental sulfur and 0.6% (w/v) organic carbon were inoculated with samples of hydrothermal minerals, whole or dissected animals, and water from hydrocasts. Turbidity after incubation is an indication of potential growth, which will be confirmed by phase-contrast microscopy. Samples from selected hydrocasts and grabs were preserved in 4% formalin for direct bacterial counts via epifluorescent microscopy, in 2% grade I glutaraldehyde for electron microscopy, and frozen at -20°C for CHN analysis. Filtered water samples and samples of organic slime (69 and 114 GTVA) were buffered for DNA extraction. A list of samples tested for the presence of high-temperature microbes and preserved for shorebased analyses is included.

Preliminary results indicate that hyperthermophilic micro-organisms are present in sphalerite (81 GTVA), barite (89 GTVA), paralvinellid guts (81 GTVA), and the ASHES Vent Field plume (78 and 91 CTD). Hyperthermophiles have not previously been cultured from chronic vent field plumes. Thermophilic floc-producing organisms were cultured from a navigated hydrocast over a site of diffuse venting in the South Rift Zone (83 CTD). Thick mucus associated with a mass of *P. palmiformis* tucked underneath a slab of basalt produced hyperthermophilic cultures (69 GTVA). Confirmation of growth, purification, and identification will take place in the laboratory of John Baross at the University of Washington.

Sample list and descriptions

epi-	sample preserved for epifluorescent microscopy
EM-	sample preserved for electron microscopy
CHN-	sample frozen for CHN analysis
cult-	sample added to culture media and incubated at 55°C and/or 90°C
DNA-	sample preserved for DNA extraction
58 GKG	epi, EM from crushed basalt, 20 cm from sediment surface
59 CTD	epi from odd-numbered bottles
	cult from bottle # 1
64 CTD	epi from all bottles
	cult from bottle # 1
69 GTVA	cult from <i>Paralvinella palmiformis</i>
	cult from limpets
	cult, EM, DNA, CHN from thick white slime

	cult from sulfide layer above slime
76 CTD	epi from all bottles
78 CTD	epi from all bottles
	cult from all bottles
	EM, DNA from bottle # 4
80 CTD	epi from all bottles
81 GTVA	cult from <i>Paralvinella palmiformis</i> & <i>sulfincola</i> guts
	cult, CHN from sphalerite
83 CTD	epi from all bottles
	cult from # 1-6
89 GTVA	cult, CHN from surficial and interior barite
	cult from limpet gills
	cult from <i>Paralvinella palmiformis</i> & <i>sulfincola</i> surface and guts
	cult from nereid worm surface and gut
92 CTD	epi, cult from all bottles
	EM, DNA from bottles # 8-11
96 CTD	epi from bottles # 3-8
102 CTD	epi from even-numbered bottles
	cult from bottles # 6 and 8
	DNA, EM from bottle # 8
114 GTVA	epi, EM, DNA from mud
	epi, EM, DNA from orange organic slime
	putatively positive cultures (subject to microscopic confirmation)
<u>55°C</u>	
83 CTD	bottle # 3 (produced flocculent material)
89 GTVA	surficial barite
<u>90°C</u>	
69 GTVA	thick white slime (confirmed at sea by reinoculation)
	limpets
	worms
	sulfide
78 CTD	bottles # 2, 5, and 6
81 GTVA	worm guts
	sphalerite
89 GTVA	surficial barite
	interior barite
91 CTD	bottle # 6 and bottle # 10 (1 out of 3 replicates)

4.4.9 Petrology and Volcanology

by Mike Perfit

Introduction

Axial Seamount represents the present locus of volcanic activity related to the Cobb Hotspot. Its location, anomalous size and structural features are a consequence of excess volcanism on the axis of an accretionary plate boundary. Fresh lavas, sulfide mineralization and active hydrothermal vents in the summit caldera attest to the concentrated and recent magmatic history of the Volcano. Karsten and Delaney (1989) suggest that the seamount began to form when the Juan de Fuca Ridge jumped westward over the hotspot about 0.5 ma. However, more recent dating of the Cobb-Eickelberg seamount chain suggests the ridge slowly overrode the hotspot during the last 0.4 ma.

The geochemistry of lavas from Axial and adjoining rift zones has been discussed by Rhodes et al. (1990) and Perfit et al. (1988). Axial Seamount basalts have rather homogeneous, evolved compositions that probably reflect the presence of a long-lived, well-mixed magma chamber. Unlike most hotspot volcanoes, lavas from Axial Seamount do not show a clear geochemical signature associated with enriched mantle sources or plume. Lavas include typical normal mid-ocean ridge basalts (N-MORB) and transitional varieties but not enriched types (E-MORB) or alkalic basalts that characterize many hotspot volcanoes. Compared to lavas from the Cleft segment however, Axial lavas are slightly enriched in incompatible elements but have similar Sr and Nd isotopic compositions (Smith et al., 1993, Perfit et al., unpublished data). In comparison to the ridge, lavas from the Cobb-Eickelberg Seamount chain (Desonie and Duncan, 1990), which extends northwestward from Axial, have slightly enriched compositions. Axial Seamount appears, therefore to be mainly a consequence of a thermal anomaly in the mantle rather than one associated with an enriched source or mantle plume - a rather unique situation. How much of an influence the hotspot has on magma and fluid/gas chemistry has yet to be addressed in detail.

Because the samples discussed by Rhodes et al., (1990) were recovered by dredge and over a large area, it is difficult to relate subtle changes in chemistry to relative ages, structural and Volcanological features, and lava type. More recent sampling of Axial with submersibles indicates lavas in the caldera are quite homogenous (although some contain unusually abundant phenocrysts) and lavas recovered along the rift zones have more diverse compositions. TV-grabs should help elucidate the spatial and temporal relationships of magmatism. Of particular interest is the apparent difference in composition between young lavas at the Flow site on the CoAxial segment and those in Axial's caldera and North Rift Zone which preclude them from being derived from the same mantle source. Recovery of young samples along the North Rift Zone will provide critical information regarding

subsurface plumbing systems and the relationships between recent seismic events and eruptions.

The distribution of different lava morphologies in Axial caldera based on side-scan and photographic images has been discussed by Embley et al., (1990) and Hammond (1990). Lava types are divided into three basic varieties that are commonly transitional from one to the other: (1) Pillow lavas; (2) Lobate flows; and (3) Sheet flows (including lineated, ropy and jumbled). Pillow lavas are uncommon in the caldera although they are abundant in the faulted walls and a constructional cone (fissure cone) in the northern section of the caldera. Lobate flows comprise 50% of the lavas observed in bottom photos, and sheet flows comprise 42% (29% of the total are jumbled sheet flows). Relative ages of flows have also been estimated based on apparent glassiness and sediment cover. Relatively unsedimented flows in the CASM area appear to be some of the youngest in the caldera. Sheet flows in both the North and South Rift Zones also appear to be young. An area of young-looking pillow mounds has also recently been discovered approximately 19km north of CASM along the North Rift Zone. One of the objectives of this cruise was to sample flows from specific sites by TV-grab in order to examine their flow morphologies in detail so that correlations could be made with sidescan images and bottom photographs. In addition, it will also enable us to place constraints on eruptive mechanisms.

The composition of relatively small near-axis seamounts adjacent to the Juan de Fuca Ridge and close to Axial Seamount is not well known. Samples from some of these seamounts south of Axial (e.g. Vance Seamounts, Jinja) are N-MORB with depleted geochemical characteristics similar to near-ridge seamounts on the East Pacific Rise (e.g. Lamont Seamounts; Fornari et al. 1988). Samples from Rogue Seamount, northeast of Axial, will provide additional information regarding the composition and genesis of these common submarine volcanoes.

Methods

Sample handling, classification and distribution

Rock specimens that were recovered by TV-grab or dredging were emptied onto the aft deck. Members of the scientific party, including M. Perfit, sorted through the material on deck, selecting samples of reasonable size that were representative of the suite recovered or somewhat unusual in appearance. The selected rocks were transported to the lab in plastic containers for detailed examination while the remaining material was disposed of. Rock samples were divided into groups on the basis of their surficial morphologic characteristics, relative ages, mineralogy and degree of alteration/ weathering. In many cases the rocks were of similar age and had identical mineralogic characteristics, so samples were selected based on morphologic differences (eg. ropy sheet flow vs. jumbled sheet or vesicular samples vs. non-vesicular). Although it is possible that most or all of the

samples could have identical compositions, it was deemed important to test this by subsequent chemical analysis and to document the variability in flow morphology in individual eruptive units. Samples were macroscopically examined for crystal content, vesicularity, glass and sheet thicknesses, and alteration/mineralization. Mineralogical and textural identifications were determined with the aid of a hand-lens and binocular microscope.

Individual rocks were given unique alpha-numeric identifications which consist of the station number (47-100), operation type (DR=dredge, GTVA=TV-grab, specimen number (1-10) and alphabetic designation for splits of each specific sample. The following designations were adhered to during the distribution of samples; UF-sample split "A", TUBAF-"B", NOAA-"C" and GSC-"D". A separate of glass was also taken from each sample and bagged to be hand-carried for analysis at the University of Florida (UF). If samples were large enough, splits were given to all interested parties (generally TUBAF and NOAA). Particularly large samples were also kept by TUBAF to put in their permanent archive.

Stations and Recovery

58 GKG

Setting

Helium Basin. Samples of fragmental glass recovered in the box core were taken to look for evidence for explosive volcanism or hydromagmatic eruptions. The site is at the base of a steep (~ 30°) north-facing wall of Axial Volcano. Perfit and Jonasson had an ALVIN dive along this wall down to the basin in 1988 and documented constructional volcanism (mostly pillow basalts) associated with normal faults and scarps. Much of the sediment from the wall appears to accumulate in the basin at the base. Thick deposits of basaltic debris were not obvious during the dive.

Sample Groups

- | | |
|-----------|--|
| 58 GKG-5 | Glass and sediment from uppermost, thin fragmental layer at 5 cm. |
| 58-GKG-10 | Glass from top of thick glass layer that extends to bottom of core. Sample taken from 10 cm below top of box core. |
| 58-GKG-20 | Glass from central region of core at 20 cm. |
| 58 GKG-30 | Glass from coarse layer at 30 cm at bottom of core. |

General Descriptions

Extremely fresh, fragments of basaltic glass are layered with brown to red colored mud. The uppermost layers of glass are relatively thin but distinct and interbedded with a white-to-green pelagic clay/ooze. The thick lower layer is almost entirely glass fragments/shards that range in size from a few mm to 1 cm in diameter. There are some fragments of crystalline rock dispersed throughout the glass. All of the glass is very angular and there are crudely, graded beds that fine upwards. *The is no indication of an explosive eruption.*

Only the coarse layer at 30 cm was examined with a microscope

58 GKG-30

This layer of the core is primarily comprised of fresh, angular fragments of basaltic glass. There are minor quantities (< 5%) of angular crystalline rock (commonly attached to glass fragments) and foramaniferal ooze. Sizes of rock/glass fragments vary by at least an order of magnitude. None of the glass shards show evidence of hydromagmatic eruption.

(Sample Distribution: UF 4 small bags of glass ; TUBAF)

Miscellaneous

Samples were taken for microprobe and XRF analyses to see how much chemical variation exists in the chemistry of the parental rocks and if there has been a change in composition through time. The compositions will be compared with lavas recovered in 1988. Evidence that the shards are a consequence of an explosive eruption rather than simply deposition of epiclastic debris will be examined.

Inferences/Interpretations:

The physical appearance and observed bedding of the glass suggests that it represents deposition of fragmental debris plus pelagic sediments probably from turbidity currents that originate along the steep slope of the north side of Axial Volcano. Seismic activity and local tectonic events may trigger such episodes of deposition.

60 GTVA

Setting

Southwest rift zone of Axial Seamount just outside the caldera.

Recovered about 300 kg of basalts which are similar in appearances.

Sample Groups

60 GTVA-1	Basalt; small folded sheet flow with smooth glassy interior, aphyric to glassy interior
60 GTVA-2	Basalt; large jumbled sheet flow with many irregular cavities and brecciated glassy crust; very fresh
60 GTVA-3	Basalt; small folded sheet flow with irregularly shaped cavities on bottom; glass may be a bit altered
60 GTVA-4	Basalt; jumbled sheet flow with many cavities (both glassy and crystalline)
60 GTVA-5	Basalt, ropy sheet flow
60 GTVA-6	Basalt agglomerate or autobreccia; with glassy fragments
60 GTVA-7	Basalt; contorted, jumbled sheet flow
60 GTVA-8	Altered basalt; piece of larger sample; contains sulfides in irregular vesicles and cavities

General Descriptions

Most of the samples are jumbled sheet flows, but morphologies range from ropy to chaotic. Individual flow thicknesses range from a few cm to 15 cm. No significant sediment on rock surfaces; but a few samples have cavities containing brown foram ooze. Samples have minor amounts of iron staining and some have thin Mn coatings. Interiors of flows are mostly aphyric with rare plagioclase crystal clots or xenocrysts. A large number and great variety of vesicles and irregular cavities characterize these samples. Rounded vesicles and pipe vesicles comprise < 2% of rocks. Larger irregularly shaped cavities range from cm-size to 10 cm in diameter. Some of the samples (e.g. 6) have highly folded surfaces upon which the glass appears to have been broken and subsequently annealed to the underlying molten lava; hence their agglomeratic appearance. A few samples have interior portions that have a "bleached" (light gray) appearance and are associated with pyrite.

(Sample Distribution: UF 1,2,3,4; TUBAF 2,4,5,6; GSC 7,8)

Miscellaneous

TUBAF has 3 or 4 large samples for curation.

Inferences/Interpretations:

The abundant cavities and irregular distribution of pipe vesicles within the jumbled sheets appear to be the consequence of seawater being trapped by the advancing and folding flow. The heat from the flow would cause the water to vaporize (probably phase separate) and expand in volume. This vapor and possibly some magmatic vapor would try to escape from the lava and could form irregular cavities within the lava when the vapor pressure was no longer great enough to break through the quenched lava surface. If the lava surrounding the vapor-saturated cavities was able to dissolve some of the volatiles, it is possible that the liquidus of the melt could have been lowered enough to inhibit crystallization along the walls thereby creating some of the glassy textures observed on the cavity walls and undersides of sheet flows. On the other hand, some of the cavities are rather coarsely granular and have crystallites (plagioclase?) protruding into them. It is unclear what process would result in this unusual texture.

The angular brecciated surface on some of the samples may be the result of autobrecciation of the initial glass rinds that form on sheet flows. As sheets begin to fold and contort, the smooth glass rind shatters and the glass shards are engulfed in magma breaking out from the interior of the flow; then partially remelted/annealed by the liquid. In some places, it appears that angular vugs were formed as the lava folded over brecciated zones and partially melted the glass.

61 GTVA

Setting

CASM site at the NW end of Axial Seamount near the caldera wall. East of fissure near Lamphere chimneys. Approximately 300 kg of basalt was recovered in an attempt to sample sulfides.

Sample Groups

- | | |
|-----------|---|
| 61 GTVA-1 | Basalt; Ropy sheet flow; plagioclase phyric |
| 61 GTVA-2 | Basalt; Ropy sheet flow; very glassy |
| 61 GTVA-3 | Basalt; Flat sheet flow, may be older, slightly vesicular (< 5%), aphyric with no glassy rind |
| 61 GTVA-4 | Basalt; Ropy sheet flow; very fresh and glassy |
| 61 GTVA-5 | Basalt; Folded, jumbled sheet flow, rare plagioclase crystals, very glassy |

General Descriptions

Most of the grab consisted of thin (< 5 cm thick) ropy and jumbled sheet flows. They are very glassy with negligible sediment and very slight Mn-coatings on glass surfaces. Folding is intense in some sheet flows creating open cavities lined by glass in interiors of samples (similar to some jumbled sheet flows in 60 GTVA). Cavities with smooth, glassy interiors are up to 4 cm diameter and 5 cm long. Some samples have very finely textured glass surfaces with delicate stretch marks. Others are very fractured and an angular fragmental appearance (similar to 60 GTVA). Rocks are mesocrystalline, mostly aphyric with rare plagioclase and very rare olivine microphenocrysts. Very rare plagioclase clots.

(Sample Distribution: UF 1,2,3,4,5; TUBAF 2,3,5; NOAA 6)

Miscellaneous

A number of larger pieces were taken by TUBAF for curation.

Inferences/Interpretations:

The samples appear to be very young based on the abundance and freshness of the glass and the lack of sediment or Mn-coatings on the surfaces. The lack of any alteration or mineralization is of interest considering the proximity to active hydrothermal vents.

62 DR

Setting

Rogue Seamount, on the Juan de Fuca plate southeast of Flow site on CoAxial segment. It is a small, near-axis seamount that has never been sampled. Dredging was done from the northwest to the southeast up the steepest side of the cone. The cone rises steeply from 2,400 m to 2,100 m and has a flatter top that rises to 1,900 m. Most of the samples were probably recovered from the upper parts of the cone. Side-scan images suggest that there may be some relatively recent volcanic activity associated with the seamount. Sample recovery was very successful (750 kg recovered); the dredge bag was completely full.

Sample Groups

The lava types can be divided into 6 groups based on morphology and age.

(1) Young pillow lavas; (2) Plagioclase phyric pillow buds or tubes; (3) Jumbled (autobrecciated) sheet flows; (4) Older pillow to lobate flows; (5) Older pillow lavas; and (6) altered sheet flows. Of these groups, young pillow lava fragments comprise approximately 70% of the total.

- | | |
|---------|--|
| 62 DR-1 | Basalt; Pillow lavas, relatively young with glassy crusts and moderate Mn-coatings. Contain < 2% plagioclase phenocrysts with rare olivine phenocrysts. Interior of flows have Fe-staining on fractures and thin (1-2 mm) weathering rinds. Very fine-grained, microvesicular in some zones. |
| 62 DR-2 | Basalt; pillow bud, plagioclase phyric (~ 40%) with rare olivine microphenocrysts |
| 62 DR-3 | Basalt; Older appearance. Large piece, very irregular shape with coarse, brecciated top surface. Slightly plagioclase phyric (< 3%). May be lightly altered glass. Mn-coating is prominent. Cavities filled with tan-brown pelagic sediment. |
| 62 DR-4 | Basalt, very large piece of lava that is transitional from pillow to lobate flow. Well preserved surface glass with moderate Mn-coating. Rare plagioclase phenocrysts in a fine-grained matrix. |
| 62 DR-5 | Basalt; fractured pillow basalt with rare plag; fresh microcrystalline interior. |
| 62 DR-6 | Altered Basalt; vuggy, vesicular green-colored fragments without glass, could be pieces of altered sheet flow. |
| 62 DR-7 | Basalt; thin, flat, small pieces of sheet flow, young looking. |

General Descriptions

A wide variety of basalt morphologies were recovered during this dredge, in part a consequence of the rather long distance it was towed. At least two ages of flows were recovered and the youngest pillows were likely sampled from the upper part of the cone. The oldest samples appear to be the jumbled sheet flows with brecciated surfaces and palagonitized glass. Cream to white colored pelagic ooze was attached to some of the pieces of weathered basalt. Pillow basalts are the most abundant rock type and jumbled/ropy sheet flows and lobate flows comprise < 15% of the samples. Small (< 8 cm diameter), rounded pillow buds or fragments of ropy sheets are plagioclase-rich, containing zones in the glass rinds with as much as 40% plagioclase crystals (0.2-0.7 cm long). Vesicles are common; up to 0.5 cm diameter.

(Sample Distribution: UF 1,2,2E,2G,3,4,5,6,7,X; TUBAF 1,2,2F,3,4,5,6;
NOAA 1,2,3,4,5,6; GSC 2.)

Miscellaneous

Sample type 3, with brecciated surfaces, looks like the submarine equivalents to AA flows.

Inferences/Interpretations:

The abundance of pillow lavas and the presence of plagioclase-rich basalts is typical of near-axis seamounts on the Juan de Fuca Ridge. The freshness of the basalts and lack of thick sedimentary or Mn-coatings suggest the seamount was volcanically active in the recent past.

69 GTVA

Setting

CASM site at the NW end of Axial Seamount near the caldera wall. In fissure to west of Lamphere chimneys. Possibly recovered from beneath the surface within the basaltic foundations. Area may have recently been hydrothermally reactivated. Approximately 150 kg of basalt was recovered and included sulfide and biologic material.

Sample Groups

- | | |
|------------|--|
| 69 GTVA-1 | Basalt; fresh glassy ropy to folded sheet flows with some lobate forms. |
| 69 GTVA-2 | |
| and GTVA-6 | Basalt; sheet flow or lobate top, slightly altered with sulfide mineralization and thin coating of chlorite and sulfides on surfaces. |
| 69 GTVA-3 | Altered basalt; more highly altered with thick coatings of sphalerite, rare wurtzite, and thin coatings of pyrite. Veins of anhydrite common. Broken interiors and some glass remains fresh. |
| 69 GTVA-4 | Basalt-sulfide breccia; basalt fragments and cemented by anhydrite/sphalerite, some fresh glass remains. |
| 69 GTVA-5 | Sulfides (see sulfide chapter for complete listing and descriptions). |

General Descriptions

Fresh to moderately altered and mineralized basalts were recovered in this TV-grab. The lavas appear to be sheet flows and lobates. Basaltic-sulfide breccias are common. Most of the samples are covered with bacterial mats and biogenic mucus. The freshest sheet flows (1) are 8 cm thick with fine glass on both top (1 cm-thick) and bottom (0.5 cm) surfaces. Pipe vesicles common 1 cm from glass interface on top and 1.5 cm from bottom. Sheets are aphyric with rare ~ 0.5 cm plagioclase phenocrysts (xenocrysts?). Lobates show more alteration; least altered have some sulfide mineralization in vesicles and bleached appearance of crystalline rock but more typically they are moderately altered and have surfaces completely covered with sphalerite.

(Sample Distribution: UF 1A,1B,2,3,4,5,6; TUBAF 1A,6 , NOAA 1A,4,6; GSC 3,4,5;
see sulfide chapter for distribution of sulfides)

Inferences/Interpretations:

The range of alteration/mineralization of the basalts is of interest. It suggests that hydrothermal venting is not pervasive over a wide area but rather concentrated along narrow zones (fissures) in the basalt carapace. It is also surprising that some of these samples are so altered and mineralized compared to those nearer the chimneys (e.g. 61 GTVA) since these are in the fissure away from concentrated venting. It is consistent with the hypothesis that rejuvenation of the hydrothermal system in the CASM site has caused a shift in the locus of venting and the basalts are reflecting this change.

70 GTVA

Setting

CASM site at the NW end of Axial Seamount near the caldera wall. Near Lamphere chimneys. Approximately 300 kg of basalt with a small amount of biologic material was recovered.

Sample Groups

- 70 GTVA-1 Basalt; lobate to pillow forms with light Mn-coating. Slightly plagioclase or plagioclase and olivine phyric, rare plagioclase crystal clots up to cm diameter.
- 70 GTVA-2 Basalt; ropy to jumbled sheet flows with bleached surfaces and glass; common large cavities in interiors and glassy flanges on bottom. Mostly aphyric with rare plagioclase clots and olivine microphenocrysts. Some vesicles have pyrite.
- 70 GTVA-3 Basalt; youngest-looking folded, ropy sheet flow similar to those in 69 GTV
- 70 GTVA-4 Various pieces of sheets similar with large crystal clots.

General Descriptions

Basalts appear to be somewhat older (thicker Mn-coating) than previously recovered lavas from CASM and have a more lobate to pillow-like morphology (85% fall into this category). Some of these had tubeworms on them. Bubble walls and flanges on bottom of samples suggest interaction with water/vapor. Concentrations of pipe vesicles in bottom 0.5 cm and 0.5 to 1 cm of top glass. Slightly plagioclase-phyric with common plagioclase clots that might also contain clinopyroxene. Vesicles are often attached to crystal clots. Approximately 10% of samples are small pieces of glassy sheets with pahoehoe-like folds on their surface. Some of these have a bleached appearance and contain vugs/cavities with sulfides. Less than 5% of samples are young-looking, glassy ropy sheet flows containing cavities with rough texture in centers of folds/ropes. These also contain rare plagioclase clots and olivine microphenocrysts.

(Sample Distribution: UF 1,2,3,4; TUBAF 1,2,3,4; NOAA 1,2,3; GSC 2)

Inferences/Interpretations:

The greater proportion of lobate/pillow forms here suggest slower effusion rates and or more viscous lavas compared to other sites in the CASM area. Evidence for lava-seawater/vapor interaction is present (see discussion of samples from 85 GTVA). The presence of pyrite on a few of the slightly altered samples suggests these lavas have recently experienced hydrothermal flow; the presence of tubeworms is consistent with this.

81 GTVA

Setting

ASHES Vent Field along southwestern wall of caldera in Axial Seamount. Recovered about 100 kg of massive sulfides containing only small glass fragments. See more detailed description of sulfide samples in sulfide chapter.

Sample Groups

81 GTVA-1 Basalt glass; very fresh; (possibly from previous sites)

81 GTVA-2 Sulfides (see descriptions in sulfide chapter)

General Descriptions

Small glass chips were taken from the chimneys. They may have been incorporated from the surrounding flows but there is a possibility that they were picked up from the ships deck when the chimneys were dropped from the TV-grab.

(Sample Distribution: UF 1; see sulfide chapter for distribution of sulfides)

85 GTVA

Setting

CASM site at the NW end of Axial Seamount near the caldera wall; near Lamphere chimneys. Approximately 300 kg of fresh and glassy basalt was recovered.

Sample Groups

85 GTVA-1 Basalt; small ropy sheet samples with well-developed surficial textures.

85 GTVA-2 Basalt; Large jumbled sheet flow, very glassy with multiple folds, each rope is 3-5 cm thick, cavities in cores of folds up to 1 cm wide and 6 cm long, rare plagioclase crystal clots more rarely with olivine.

85 GTVA-3 Basalt, thin sheet flow with fine glass entirely covering sample, contains a few oblong cavities, pipe vesicle zone 1-1.5 cm from glass, rare plagioclase clots.

85 GTVA-4

and GTVA-5 Basalt, large folded sheet flow with fine surficial glass with thin Mn-coating, few oblong cavities with rough textures, rare plagioclase clots.

85 GTVA-6 Glass from bottom of buckets, to test for average composition.

General Descriptions

Very glassy and fresh-looking ropy to jumbled sheet flows. Most have finely textured, thick glass rinds (up to 1.5 cm thick) with light Mn-coating. Many of the thin sheets (3-5 cm thick) are folded over on themselves to form ropes or tubes with cavities (as large as 1 cm wide and 6 cm long) in their cores. Typically, the cores are open cavities with rough textures (a result of vesicles and crystallites protruding into the cavities) and Fe-staining. A few cavities have small lava protrusions that have been intruded into the cavities (squeeze-outs). Surface glass is commonly brecciated (as seen in other CASM jumbled sheets) and forms a rough agglomerated surface. Lavas contain rare plagioclase crystal clots and phenocrysts (xenocrysts?) and very rare olivine phenocrysts set in a glassy to microcrystalline matrix. Concentrations of small (1 x 3 mm) pipe vesicles (radially oriented) exist approximately 1.5 cm below the bottom of the glass rind. Glass has only rare rounded vesicles. Prominent Fe-staining on interior of samples extends along microfractures to the more crystalline zone near the pipe vesicles. A few sheet flows have drip-structures and thin flanges associated with smooth, mats surface on underside.

(Sample Distribution: UF 1,2,3,4,6; TUBAF 2,4; NOAA 2,4; GSC 1,5)

Inferences/Interpretations:

The lavas are petrographically and morphologically very similar to the majority of others that have been recovered at the CASM site. The high proportion of jumbled sheet flow suggests that extrusion rates were high but that topographic restrictions in the caldera floor caused the low-viscosity sheet flows to pile up into jumbled and contorted masses. During the early stages of folding, seawater may have been trapped in the open cavities between sheets and subsequently trapped as the layers annealed. Reaction of the superheated vapor and exolving magmatic gases, and cooling lava created some of the unusual features observed in the cavities. Smooth textured surfaces, drip structures and thin flanges may have formed by trapped seawater beneath rapidly flowing sheet flow s.

86 GTVA

Setting

CASM site at the NW end of Axial Seamount near the caldera wall, near Lamphere chimneys. Approximately 250 kg of basalt with very similar appearance to 85 GTVA was recovered and included small pieces of barite chimney material.

Sample Groups

86 GTVA-1 Basalt; tubular morphology with rounded upper surface and flat lower surface. Large irregular cavity (2 cm by 8 cm long) in center. Aphyric with rare plagioclase clots.

- 86 GTVA-2 Basalt; similar to 1 but has features that suggest it is an overturned piece of folded sheet flow.
- 86 GTVA-3 Basalt; flat sheet flow with thin top glass (< 0.7 cm) that has a dull luster and no bottom glass, microcrystalline to glassy interior with rare vesicles.
- 86 GTVA-4 Basalt; jumbled sheet flow that is totally contorted with a zone on bottom with autobrecciated texture (similar to 89 GTVA-3A)
- 86 GTVA-5 Basalt; thick (10 cm) jumbled sheet flow characterized by extremely brecciated and vesicular zones on the underside and interior of sample. Surface glass has large vesicles that emanate from crystalline interior.

General Descriptions

Samples are very similar to those recovered in 85 GTVA, but some of these basalts have distinctive flow morphologies that have not previously been seen (e.g. tubular). The majority of samples are jumbled sheet flows but brecciated varieties and folded/tubular sheets were also recovered.

Sediment cover and Mn-coating are light but samples have more Fe-staining on top surfaces (and less along fractures) than basalts from 85 GTVA.

(Sample Distribution: UF 1,2,3,4,5; TUBAF 1,3,4,5; NOAA 1,3,4,5)

Inferences/Interpretations:

The rounded morphologies of the tubular flows would look like small pillows from above so it is important to note that these apparently form as small tubes or folded sheet flows that flatten on the bottom surfaces.

Brecciated textures like those described in 60 GTVA are probably a result of autobrecciation during lava flow, quenching and deformation (see 60 GTVA for more details).

89 GTVA

Setting

CASM site at the NW end of Axial Seamount near the caldera wall; probably from Pagoda barite chimney site. Approximately 500 kg of basalt was recovered and included the barite chimney and biologic material.

Sample Groups

- 89 GTVA-1 Basalt; fresh-looking, ropy sheet flow, with finely textured glass rind covered with very light sediment and Mn coatings. Bottom is smooth with large (2-3 cm diameter) bubble-like structures. Zone in center of multiple sheets that is agglomerated glass shards, similar to brecciated layers on other samples. Aphyric.
- 89 GTVA-2 Basalt; sheet flow, slightly folded with large number of cavities (0.2-1cm wide and 0.5 -2 cm long) and a few large vesicles in glass surface, rare

plagioclase clots, comprised of multiple thin sheets (0.5-2 cm thick), lava drips on bottom surface.

- 89 GTVA-3 Basaltic breccia; agglomerated texture on surfaces and interior, bottom surface is mostly smooth with bubble-like forms, relatively vesicular with many round and irregularly shaped cavities (some related to space between angular annealed glass shards). Some of surface glass appears hydrated/altered but bottom remains fresh.
- 89 GTVA-4 Basalt; folded sheet flow with lava drip swirled between layers of sheets. Rare plagioclase clots.

General Descriptions

Samples are more altered and undersides have fairly thick coatings of soft, granular, black Mn-oxide. Basalts range from relatively glassy, jumbled sheet flows to somewhat altered, Mn-encrusted, chaotic flows - some of which have brecciated zones on the surface or within the matrix. Some sheet flows have very clear examples of bubbles breaking the surface glass. Others show large (few cm diameter) bubble-like structures (glassy walls and flanges) which generally have a smooth, satin-like surface texture. This group of basalts does not contain as many plagioclase crystal clots as observed in previous samples from CASM.

(Sample Distribution: UF 1,2,3, 3 (altered) 4; TUBAF 1,2,3,4; NOAA 1,3)

(See sulfide chapter for distribution of sulfides/barite)

Inferences/Interpretations:

Many of the jumbled and contorted sheet flows are a composite of multiple thin sheets (< 4 cm) that have been “welded” together during the rapid eruption. In the process, they entrain seawater which creates some of the large cavities in the interiors of the lavas.

Samples that have abundant zones of brecciated glass, or just agglomerated shards, might be considered the submarine equivalent to Aa flows. They must form when the surfaces are glassy and quenched but the interiors are still plastic and hot enough to remelt the glass. This could also happen if there are multiple sheet flows erupted rapidly in one area.

The drip-like swirl in sample 4 provides evidence for the relatively fluid nature of the underside or interior of a sheet flow even after the upper surface has quenched. The question remains if a vapor phase enhances the viscosity and or lowers the melting point of the lava it is directly in contact with.

90 GTVA

Setting

CASM site at the NW end of Axial Seamount near the caldera wall; near Lamphere chimneys. Approximately 75 kg of jumbled basalt was recovered.

Sample Groups

- 90 GTVA-1 Basalt; jumbled sheet flow with large lava protuberance (squeeze-out) in cavity in central part of flow; rare plagioclase clots, some Fe-staining on inside fractures and some cavities.
- 90 GTVA-2 Basaltic breccia, similar to that in 89 GTVA; consists almost entirely of angular basalt fragment with hyalohaline textures, some annealing of fragments is present, voids between fragments have lava squeeze-outs; rare plagioclase clots.
- 90 GTVA-3 Basalt, ropy sheet flow , typical of sheets in this grab; only glass taken for analysis

General Descriptions

Mostly fresh, glassy and friable sheet flows, jumbled to chaotic morphologies. Many have large cavities, some contain pockets of sediment. Basaltic breccias are similar to those previously recovered from this area. No indication of mineralization or alteration in samples.

(Sample Distribution: UF 1,2,3; TUBAF 1,2; NOAA 1,2)

Inferences/Interpretations:

See discussion in interpretations of TV-grabs 85, 86, and 89.

99 GTVA

Setting

North Rift Zone of Axial Seamount. High area in middle of region of young pillow basalts in the middle of the axial rift. This portion of the north rift is subparallel to the CoAxial sites and may be contemporaneous. Pillow field is relatively extensive (based on numerous camera tows through the region) and has sections of significant relief (> 20 m). The area does not appear as a recent anomaly on repeat SeaBeam maps and hence is unlikely to be less than ~ 10 years old or the pillows are extensive but have little relief (unlikely). Grab site was in the middle part of the field on a bathymetric high. Observations during the grab showed that the area was covered with large (> 2 m diameter) pillows that have very distinct striated textures, minor amounts of sediment cover and very little inter-pillow accumulations of sediment. Near the top of the pillow mound, distinct pillows were transitional to lobate forms. No collapse areas or sheet flows were observed. No older lavas could be seen through the pillows. No fissures or fractures were observed and nearly all of the pillows seemed to be in place. Large size and in situ nature of the pillows made them impossible to sample with the TV-grab. The sample that was recovered was the only one observed that was detached from the mound. The entire pillow would not fit in the grab so it was broken during impact with the seafloor. We recovered approximately half of the original pillow and this was weighed more than 300 kg.

Sample Groups

99 GTVA-1 Pillow basalt; only one very large sample that broke into several fragments was recovered. It has thick striated glass crust over a very complex interior that has many large cavities and varies from microcrystalline to holocrystalline; rare plagioclase crystal clots that rarely contain olivine, plagioclase and olivine phenocrysts are also rare. Surface glass contains minor quantities of microphenocrysts. Vesicles are abundant near the outer surface but rare in the massive interior. Cavities with rough textures contain abundant crystals (plagioclase?) and are extremely vesicular. Sample was divided into numerous sub-samples for description and distribution. 1F- sample from more massive interior of pillow, 1G- flat slab with extensive crystal growth on one side and a vesicular, quenched texture on the reverse surface.

General Description

Exterior glass rind is striated with some breadcrust texture; it is very friable and easily removed leaving fresh glass beneath it. Phenocrysts of plagioclase and lesser olivine are present in the glass. The upper 10 cm of the pillow is quite vesicular (up to 5%) - they are mostly round 0.5-2 mm diameter and extend into the glass but not into the striated outermost rind. The vesicles are evenly distributed except where they concentrate to form a rough textured cavity that is 12 cm from the glass boundary. This cavity is similar to those observed in jumbled sheets in previous sites. In this case, the cavity is lined with macroscopic white to clear, rhombohedral crystals growing out of a very jagged and vesicular surface. Most of the crystals (which may be quenched crystallites with plagioclase cores similar to what is seen in the quenched portions of glass rinds) are singular and extend outward into the void space. These same textures and crystal forms are present in many other cavities in the rock and have formed along cooling fractures after the lava started to solidify. Microscopic inspection of the crystals indicates that they are not secondary or related to alteration. They also grow in the small rounded vesicles in other portions of the rock. The interior portions of the pillow are holocrystalline and massive (fractures in a platy fashion, subparallel to the rounded surface). Abundant plagioclase microlites and clinopyroxene are present; vesicles are rare (< 1%). Pipe vesicles are abundant in zones proximal to large cavities in the interior of the pillow. Some of the cavities, and crystals in them, are coated with an oxidized Fe-coating. Not all of the cavities are rough-textured; some are smooth similar to the undersides of some sheets. Its possible that these represent periods of growth of the pillow when water/vapor

interacted with the cooling magma but was subsequently covered by the expanding pillow exterior. Rare sulfides are present along some fractures and in vesicles.

(Sample Distribution: UF 1A,1B,1D,1E,1F,1G; TUBAF largest piece of pillow ,
NOAA 1C,1F; GSC various small pieces)

Miscellaneous

X-Ray diffraction of the crystals growing in the cavities confirmed that they are plagioclase plus augite.

Because this sample is so large it is possible to see a variety of textures and features not generally observed or recovered with pillow basalts. In particular, it should be noted that pieces that broke off the outer ~ 15 cm have pyramidal forms and radial joints that suggest the pillow may have had a diameter on the order of 30-40 cm - clearly this is not the case as this pillow's diameter is greater than 1 m. The reason the pillow broke in these pieces is because below this level the rock becomes more massive, with few fractures and hence very difficult to break. Large elongate cavities also exist at about this level and facilitate fracturing of the upper parts of the pillow. The largest part of the sample was boxed to be sent to TUBAF.

The sample appears to be highly magnetic so a sub-sample (1E) was given to Paul Johnson at UW. Fe-stained portions were given to Gary Massoth.

Inferences/Interpretations:

Pillow basalts may have a more complicated history of development than previously believed. The variety of textures observed in this pillow and the large cavities lined with vesicles and crystallites suggest some sort of magma-vapor interaction that has not yet been recognized. Implications for the degassing of magmas could be significant. The grab also confirms the relative youthfulness of this field of pillows. The crystallinity of the sample is similar to that in the CoAxial Flow but the presence of olivine in this lava indicates it is more mafic.

109 GTVA

Setting

Cascadia Subduction Zone, Oregon continental margin. Grab was from a large constructional high or mound on the second accretionary ridge from the trench axis. Mound is about 100 m high and as much as 1km across. Observed area of clam beds, bacterial matss, some outcrops of slab-like rocks. Surface sediments look winnowed with a large proportion of dark, sandy material.

Sample Groups

109 GTVA Carbonate breccia

- 109 GTVA Carbonate mudstone, elongate to branching tubular shapes, quite indurated in cores, contain a few % forams and abundant sand sized grains of glauconite (?).
- 109 GTVA Carbonate mudstone; less indurated, more angular pieces, quite indurated and dense in cores, some bioturbation; no glauconite.
- (Sample distribution: all to GEOMAR)

General Description

Recovery was mostly small (< 10 cm) light-gray to cream colored, fine-grained carbonate sedimentary rocks. These were in a very viscous mud with biologic material.

Inferences/Interpretations

Elongate samples appear to be concretions of mud/ooze cemented by carbonate in fluid channels

110 GTVA

Setting

Same as above (see 109 GTVA)

Sample Groups

- 110 GTVA Mudstone, glauconite-rich
- 110 GTVA Massive silty mudstone, weakly laminated
- 110 GTVA Massive silty mudstone, with FeS precipitate in crust beneath white bacterial? matss, at edge of reduced zone. Bleached zones on underside of slab.
- 110 GTVA Sediment; silty green mud

(Sample distribution: all to GEOMAR)

General Description

Large pieces of massive carbonaceous mudstone with weak bedding and some bioturbation. Surfaces are very pitted, brown to orange surfaces. Both Fe and FeS stains and coatings are present. Interiors are finely bedding in places, gray - tan color; more indurated and less carbonate towards the cores.

Inferences/Interpretations

Samples may have formed by cementation of silty mud by calcium carbonate fluids. Fluids also rich in FeS. Oxidized rinds had CaCO_3 added during formation.

115 GTVA

Setting

Same as 109 GTVA; Cascadia Subduction Zone

Sample Groups

115 GTVA Carbonate concretions, with minor silt to pebble sized rock fragments and glauconite, wood chips and sulfurous mud
(Sample distribution: most to GEOMAR; small pieces to UF and GSC)

General Description

Grab was half full of green, sulfurous, silty mud and carbonate concretions that comprise entire rocks as large as 20 kg. Abundant biological material was associated with the rocks and mud. The carbonates have very strange morphologies (similar to individual pieces recovered in 109 GTVA) created by the cementation of tubular forms of the concretions that lie in all directions and the open irregular cavities that lie between them. Sizes and shapes of the tubes vary but most seem to be 2-3 cm diameter and 3-10 cm long. Some of the cavities appear to be channel ways for fluids and may represent dissolution channels. Silty mud is loosely incorporated between the concretions. The mud is rich in FeS.

119 GTVA

Setting

Same as 109 GTVA; Cascadia Subduction Zone

Sample Groups

119 GTVA Carbonate breccia

General Description

Large blocks of calcium carbonate breccia were recovered with viscous green-gray mud. Sand to pebble sized sedimentary clasts are supported by soft white carbonate cement. Calcium carbonate fills conduits which were probably diffuse fluid channels. Other clasts include larger, rounded mudstones that show burrowing features

Inferences/Interpretations

Larger mudstone clasts appear to be an older generation of sedimentary rocks and breccias that have been incorporated into a more recent carbonate matrix, forming a breccia.

(Sample distribution: all to GEOMAR)

121 GTVA

Setting

Same as 119 GTVA; Cascadia Subduction Zone

Sample Groups

121 GTVA Various fragments of mudstone

General Description

Small platy fragments of mudstone (look oxidized) enclosed in thick, viscous green-gray mud. Abundant clam shells and other biogenic material also recovered. Shells are partially dissolved and beginning to be cemented together. (Sample distribution: all to GEOMAR)

References

- Desonie, D.L. and Duncan, R.A., 1990, The Cobb-Eickelberg Seamount Chain: Hotspot volcanism with mid-ocean ridge basalt affinity. *J. Geophys. Research*, 95, 12,697-12,711.
- Embley, R.W., Murphy, K.M., and Fox, C.G., 1990, High-resolution studies of the summit of Axial Volcano. *J. Geophys. Research*, 95, 12,785-12,812.
- Fornari, D.J., Perfit, M.R., Allan, J.F. and Batiza, R., et al. 1988, Geochemical and structural studies of the Lamont seamounts: seamounts as windows into mantle processes, *Earth Planet Sci. Lett.*, 89, 63-83.
- Hammond, S.R., 1990, Relationships between lava types, seafloor morphology, and the occurrence of hydrothermal venting in the ASHES Vent Field of Axial Volcano. *J. Geophys. Research*, 95, 12,875-12,893.
- Karsten, J.L. and Delaney, J.R., 1989, Hot spot-ridge crest convergence in the northeast Pacific. *J. Geophys. Research*, 94, 700-712.
- Perfit, M.R., Heatherington, A.L., Hughes, S., Jonasson, I.R., and Franklin, J.M., 1988, Geochemistry of basalts from Axial Volcano: An example of a well-mixed axial magma chamber. *EOS, Trans. Amer. Geophys. Union*, 69, 1467.
- Rhodes, J.M., Morgan, C., and Liias, R.A., 1990, Geochemistry of Axial Seamount Lavas: Magmatic Relationship Between the Cobb Hotspot and the Juan de Fuca Ridge. *J. Geophys. Research*, 95, 12,713-12,733.
- Smith, M.C., Perfit, M.R. and Jonasson, I. R., (1994) Spatial and temporal variations in the geochemistry of lavas from the S. Juan de Fuca Ridge: Implications for petrogenesis *J. Geophys. Research*, 99, 4787-4812.

4.4.10 Acoustic Extensometer Deployment and Navigation

by Bill Chadwick

The acoustic extensometers are instruments designed to measure distances very precisely on the seafloor. We hope to actually measure seafloor extension associated with dike intrusions along the rift zones of Axial Volcano. The instruments are deployed in a line with 100-200 m spacing between them. The system can measure baselines of up to about 1km with a precision of about 1 mm. The current instruments can make one measurement per day for a year, but future modifications will enable deployments of up to 5 years.

We had hoped to deploy the instruments with ROPOS, but when it became obvious that this was impossible, we decided to deploy the instruments from the surface. This is not the ideal deployment method, but was preferable to not deploying the instruments at all.

On June 20, five extensometer instruments were deployed from the SONNE along a line across the north rift of Axial seamount. The line started at 46°01.08' N/-130°00.45' W and ended at 46°01.24' N/-130°01.62' W.

The drop positions and times for the instruments were as follows:

Unit 1	46°01.134' N/-130°00.846' W	00:21:40
Unit 2	46°01.152' N/-130°00.961' W	00:36:35
Unit 3	46°01.159' N/-130°01.036' W	00:44:45
Unit 4	46°01.171' N/-130°01.113' W	00:52:00
Unit 5	46°01.192' N/-130°01.267' W	01:03:40

The instruments and recorded data will be recovered in summer 1997.

We also brought on board a prototype seafloor benchmark that we hope to use in future extensometer deployments (the benchmarks will be permanent, and the instruments can be placed into them and later replaced to continue long-term time-series measurements). We still hope to deploy one benchmark on the next leg at Axial and have ROPOS pick up and move it while on the bottom. The benchmark design is preliminary and we want to make sure the ROV can move it easily on the bottom and that the benchmark will be stable, once deployed.

Acoustic Navigation

Three transponder nets were deployed and calibrated during leg 2. The first net was deployed on the north rift of Axial seamount and consisted of 5 transponders. The second net had 3 transponders and covered the ASHES Vent Field within Axial caldera and the upper South Rift Zone (note that one transponder had to be replaced in this net late in the cruise - so there is an ASHES 1 net and an ASHES 2 net. The ASHES 1 net was used during this leg and the ASHES 2 net will be used on the next leg with ROPOS). The third net was deployed on the continental margin so that some of the operations originally planned for leg 3 could be accomplished on leg 2.

The NOAA ATNAV rangemeter was connected to the ship's transducer and controlled from a PC with NOAA's SeaScape navigation software. The bottom transponders at Axial were all Benthos TR-6000 transponders (that interrogate at 9kHz) and we navigated the EXPLOS, CTD, or TV-grab by having a Datasonics relay transponder (11kHz interrogate/9kHz reply) attached to the cable above the navigated package. A remote navigation computer was placed on the bridge, so that they could see the same information displayed on the main navigation computer in the lab. The Margin Net consisted of 4 Sonartech transponders from the SONNE which interrogate at 11.0 kHz. An additional Sonartech transponder was used as a relay in this net (9 kHz interrogate/11 kHz reply). For the next leg with ROPOS, the ROPOS group's relays are also available to use in this net (9.5 kHz and 10.0 kHz interrogate and 11 kHz reply).

In general, the acoustic navigation was very good. All the EXPLOS camera tows were acoustically navigated, as were 3 CTD's (stations 78, 83, and 91), and one TV-grab (station 97) at Axial, plus additional TV-grabs in the Margin Net. Occasionally noise from the ship would interfere with the acoustic navigation, but usually only for brief periods. The one day we had rather rough seas (the June 17 camera tow at the CoAxial FLOC site) the acoustics with the ship's transducer were poor. Midway through the tow, we deployed a tow-fish transducer, which worked much better. Perhaps bubbles were getting under the ship and interfering with the acoustics around the ship's transducer.

The calibrated positions (frequency/latitude/longitude/depth) for the transponders were as follows (absolute calibration positions):

North Rift Net

8.5/A	46°00.4030' N	130°00.4401' W	1296.73
9.5/C	46°01.1159' N	130°01.9318' W	1397.88
10.0/D	46°02.1267' N	129°59.7439' W	1447.87
10.5/E	46°03.1542' N	130°01.1311' W	1456.36
11.5/G	46°03.8870' N	129°58.3242' W	1492.94

ASHES 1 Net

8.5/A	45°56.0125' N	129°58.7529' W	1301.58
10.0/G	45°56.4923' N	130°00.0253' W	1332.88
11.5/G	45°55.4952' N	130°00.0546' W	1330.16

ASHES 2 Net

9.5/C	45°55.9110' N	129°58.7415' W	1306.39
10.0/G	45°56.4918' N	130°00.0374' W	1327.36
11.5/G	45°55.4909' N	130°00.0552' W	1328.09

Margin Net

11.5	44°39.9762' N	125°05.9771' W	502.28
12.0	44°40.6565' N	125°07.3148' W	598.04
12.5	44°40.7308' N	125°05.2367' W	572.20
8.5	44°39.5021' N	125°05.0720' W	540.66

Note that the initial calibration on the Margin Net was done without differential GPS (the satellite link was down). This net will be recalibrated during leg 3 when the DGPS is back on line.

4.4.11 Appendix

compiled by Sven Petersen

A Station List

Abbreviations: CTD = hydrocast, DR = dredge, EXPL = TV/camera sled EXPLOS, EXT = extensometer, GKG = box corer, GTVA = TV-grab A, TSP = transponder.

Coordinates are given as differential GPS (DGPS) coordinates if not stated otherwise. The coordinates given for TV-grabs and camera tows are generally positions for the instrument at first and last bottom contact. Position for transponders is the actual position at the seafloor after deployment and calibration. Positions for CTD's and box corer is ship position at bottom contact. Position for dredges is ships position. Depths for TV-grabs and camera tows is the actual minimum and maximum cable length if not stated otherwise. For TV-grabs the cable length at the site of sampling is given in brackets. Depths for dredges is Hydrosweep depth. Hydrosweep depths are always marked with (HS). Depth for hydrocasts results from the depth calculated by the CTD pressure sensor added to the altitude at the sampling site. Depth for sediment stations is cable length at bottom contact. Depth for transponders is actual depth of the transponder position. Station numbers are continued from SO109-1.

Axial Seamount

station	area	location (N W)	depth (m)	objectives	brief description
47 TSP	North Rift Zone	46°00.403' 130°00.440'	1297	deploy transpon. 1	NOAA transponder 8.5 / A; responding
48 TSP	North Rift Zone	46°01.116' 130°01.932'	1398	deploy transpon. 2	NOAA transponder 9.5 / C; responding
49 TSP	North Rift Zone	46°02.127' 129°59.744'	1448	deploy transpon. 3	NOAA transponder 10.0 / D; responding
50 TSP	North Rift Zone	46°03.154' 130°01.131'	1456	deploy transpon. 4	NOAA transpon. 10.5 / E; responding
51 TSP	North Rift Zone	46°03.887' 129°58.324'	1493	deploy transpon. 5	NOAA transpon. 11.5 / G; responding
52 CTD	North Rift Zone	46°02.29' 130°00.78'	1637	sample area of diffuse venting	12 bottles fired; background CTD values; weak Methane anomaly at depth (max. 40 n/l)
53 GKG	basin of Axial Smt.	46°05.00' 130°10.00'	2807	tracer mapping in sediments	34 cm layered sediment; muddy dark brown top layer, greyish brown clay-rich layer; blue-green sandy bottom
54 CTD	crater rim north of CASM	46°00.00' 130°01.00'	1544	tracer mapping in water column	12 bottles fired; no apparent CTD anomalies; methane anomaly below 1400 (up to 100 n/l)

station	area	location (N W)	depth (m)	objectives	brief description
55 GKG	basin SE of Axial Smt.	45°46.001' 130°18.997'	2725	tracer mapping in sediments	45 cm layered sediment; muddy dark brown top layer, grey-brown clay-rich layer; blue-green sandy bottom
56 EXPL	North Rift Zone	46°04.781' 130°00.683' to 46°02.488' 130°00.851'	1780 to 1526	detailed zig-zag mapping of North Rift Zone	found several areas of diffuse hydrothermal fluid flow and associated fauna and bacterial mats
57 CTD	Helium Basin	46°00.19' 129°56.32'	2280	tracer mapping in water column	12 bottles fired; background CTD values; weak Methane anomaly at 1450 depth (40 n/l)
58 GKG	Helium Basin	46°00.210' 129°56.307'	2276	tracer mapping in sediments	30 cm; 3 cm of muddy brown sediment at the top followed by 2 discrete layers of volcanic epiclastics separated by 1 cm of mud
59 CTD	CASM	45°59.130' 130°01.350'	1573	sample area of hydrothermal venting	12 bottles fired; no apparent CTD anomalies; methane anomaly below 1350 (up to 110 n/l)
60 GTVA	South Rift Zone	45°55.196' 129°58.340' to 45°55.204' 129°58.376'	1549 to 1553 (1550)	sampling of hydrothermal spire	ca. 300 kg of basaltic material with some Fe-staining; pyrite and pyrrhotite observed in vesicles
61 GTVA	CASM	45°59.442' 130°01.614' to 45°59.365' 130°01.610'	1481 to 1586 (1583)	sample barite spire in CASM field	approx. 300 kg of very fresh basaltic material with abundant glass
62 DR	Rogue Volcano	46°23.558' 129°29.062' to 46°22.774' 129°27.711'	2472 to 1903 (HS)	sample volcanic material from the NE slope of Rogue volcano	ca. 750 kg of basaltic material including old pillows, younger glassy pillows and several pieces of phrycaterial
63 CTD	SE of Axial caldera	45°54.99' 129°55.04'	1630	tracer mapping in water column	12 bottles fired; background CTD values; background methane values (up to 45 n/l)
64 CTD	SE entrance of Axial caldera	45°56.00' 129°57.98'	1531	tracerapping in water column	12 bottles fired; background CTD values; moderate methane anomaly below 1400 (up to 80 n/l)
65 EXPL	North Rift Zone	46°01.306' 130°01.127' to 46°03.683' 130°00.150'	1598 to 1715	explore fissure at North Rift Zone	found several areas of diffuse hydrothermal fluid flow and associated fauna and bacterial mats
66 TSP	North Rift Zone	46°03.887' 129°58.324'	1493	release transpon. 5	released
67 GTVA	CASM	45°59.367' 130°01.477' to 45°59.354' 130°01.557'	1557 to 1585	sample barite spire at CASM hydrothermal field	chimney located but grab didn't close
68 TSP	North Rift Zone	46°00.40' 130°00.44'	1297	release transpon. 1	released
69 GTVA	CASM	45°59.344' 130°01.557' to 45°59.356' 130°01.582'	1559 to 1574 (1574)	sample barite spire at CASM hydrothermal field	150 kg of basaltic breccia with sulfide lining and anhydrite in cavities; abundant vent fauna
70 GTVA	CASM	45°59.364' 130°01.570' to 45°59.382'	1537 to 1570 (1568)	sample barite spire at CASM hydrothermal field	300 kg of relatively fresh basalt with glassy surface

station	area	location (N W)	depth (m)	objectives	brief description
		130°01.577'			
71 CTD	NW of Axial caldera	45°59.01' 130°02.50'	1492	tracer mapping in water column	12 bottles fired; moderate anomalies in transmission, potential temperature and methane (160 nl/l) below 1350
72 CTD	SW of Axial caldera	45°56.03' 130°02.95'	1510	tracer mapping in water column	12 bottles fired; small anomalies in transmission, potential temperature and methane (125 nl/l) below 1400
73 TSP	ASHES	45°56.492' 130°00.025'	1333	deploy transpon. 6	NOAA transpon. 10.0 / D; responding
74 TSP	ASHES	45°56.013' 129°58.753'	1302	deploy transpon. 7	NOAA transpon. 8.5 / A; responding
75 TSP	ASHES	45°55.495' 130°00.055'	1330	deploy transpon. 8	NOAA transpon. 11.5 / G; responding
76 CTD	ASHES	45°56.02' 129°59.99'	1533	tracer mapping in water column	12 bottles fired; small anomalies in transmission and potential temperature; increase in methane below 1300 with distinct peak (140 nl/l) at 1480
77 EXPL	South Rift Zone	45°54.63' 129°59.34'	1545	detailed mapping of South Rift Zone	station aborted due to electronic failure
78 CTD	ASHES	45°56.000' 130°00.832'	1535	transpon. navigated mapping of the plume over Inferno Vent	12 bottles fired at depths below 1450; strong temperature and transmission anomaly; methane values range from 100 to 700 nl/l
79 EXPL	South Rift Zone	45°54.656' 129°59.301' to 45°57.255' 129°59.247'	1541 to 1510	map diffuse flow along South Rift Zone with SUAVE scanner mounted on EXPLOS	found several areas of diffuse hydrothermal fluid flow and associated fauna and bacterial mats
80 CTD	inside Axial caldera	45°58.17' 130°00.95'	1560	sample inside Axial caldera	12 bottles fired; small anomalies in transmission, potential temperature and methane (135 nl/l) below 1350
81 GTVA	ASHES vent field	45°56.012' 130°00.820' to 45°56.036' 130°01.876'	1527 to 1533 (1531)	sample base of Virgin Mound	ca. 100 kg of massive sulfides (pyrite-marcasite-sphalerite-chalcopyrite) and abundant vent fauna at new chimney, Virgin vent not found.
82 EXPL	ASHES	45°55.177' 130°00.295' to 45°56.700' 130°01.285'	1521 to 1560	reconnaissance mapping east of ASHES vent field with SUAVE CTD mounted on EXPLOS	found several areas of diffuse hydrothermal fluid flow and associated fauna and bacterial mats
83 CTD	Axial caldera	45°55.961' 129°58.934'	1512	transpon. navigated plume mapping north of Axial Garden	12 bottles fired; moderate anomalies in transmission and potential temperature; methane anomaly below 1400 with peak at 1500-1520 (max. 330 nl/l CH ₄)

station	area	location (N W)	depth (m)	objectives	brief description
84 EXPL	CoAxial segment Floc site	46°17.141' 129°42.946' to 46°18.542' 129°42.429'	2200 to 2297	detailed mapping along the main eruptive fissure up to the HDV site with SUAVE scanner mounted on EXPLOS	found several areas of diffuse hydrothermal fluid flow and associated fauna and bacterial mats
85 GTVA	CASM	45°59.353' 130°01.559 to 45°59.360' 130°01.558'	1557 to 1560 (1560)	grab barite spire at CASM site	ca. 300 kg of very fresh glassy basalt
86 GTVA	CASM	45°59.334' 130°01.602' to 45°59.382' 130°01.570'	1560 to 1570 (1562)	sample altered rock and talus at base of spire at CASM site	ca. 250 kg of very fresh glassy basalt with few very small barite pieces
87 CTD	east of Axial caldera	45°58.01' 129°59.00'	1499	tracer mapping in water column	12 bottles fired; moderate anomalies in transmission and potential temperature; methane anomaly below 1300 with peak at 1350 and decrease to ca. 100 nl/l further below
88 CTD	west of Axial caldera	45°57.500' 130°02.517'	1437	tracer mapping in water column	12 bottles fired; moderate anomalies in transmission and potential temperature; methane anomaly below 1300 (up to 110 nl/l CH ₄)
89 GTVA	CASM	45°59.332' 130°01.543' to 45°59.388' 130°01.584'	1559 to 1568 (1566)	sample CASM barite spire	ca. 100 kg of massive barite with some vent fauna and 500 kg of basalt with indication of low-temperature hydrothermal activity
90 GTVA	CASM	45°59.376' 130°01.560' to 45°59.363' 130°01.591'	1544 to 1574 (1564)	sample CASM barite spire	ca. 75 kg of fresh sheet flow lava
91 CTD	ASHES vent field	45°56.032' 130°00.847'	1531	transpon. navigated plume mapping of ASHES hydrothermal field	12 bottles fired, anomalies in transmission and potential temperature; up to 200 nl/l methane found
92 TSP	North Rift Zone	46°01.116' 130°01.932'	1398	release transpon. 2	released
93 TSP	North Rift Zone	46°02.127' 129°59.744'	1448	release transpon. 3	released
94 TSP	North Rift Zone	46°03.154' 130°01.131'	1456	release transpon. 4	released
95 EXT	North Rift Zone	46°01.134' 130°00.846' to 46°01.192' 130°01.267' (ship's drop position)	...	deploy 5 NOAA extensometer	deployed on a straight line with a spacing of 100 to 200
96 CTD	west of Axial caldera	45°54.00' 130°05.50'	1951	tracer mapping in water column	12 bottles fired, background transmission and potential temperature; methane values at depth are generally below 20 nl/l with a small peak at 1450
97 GTVA	CoAxial	46°18.529'	2218 to	sample biology at	grabbed vent fauna, sample

station	area	location (N W)	depth (m)	objectives	brief description
	segment Floc site	129°42.450' to 46°18.562' 129°42.460'	2240 (2238)	HDV site CoAxial segment	washed out
98 CTD	CoAxial segment Floc site	46°18.512' 129°42.471'	2247	tracer mapping in water column	12 bottles fired, small anomalies in transmission and potential temperature; methane values below 25 nI/l with small peak at 1700
99 GTVA	North Rift Zone	46°09.72' 129°55.24' to 46°09.718' 129°55.220'	1823 to 1842 (1842)	sample youngest flows at this segment of the ridge	single fresh pillow, ca. 300 kg
100 EXPL	South Rift Zone	explore South Rift Zone for hydrothermal activity around main fissure using SUAVE on EXPLOS in low- sensitivity mode	aborted, transpon. (8.5 kHz) was accidentally shut off during station TSP 92-94
101 TSP	ASHES vent field	45°55.911' 129°58.742'	1306	transpon. release and deployment	transpon. Released (8.5 kHz) and deployed (9.5 kHz)
102 CTD	East of Juan de Fuca ridge	45°40.017' 129°47.005'	2538	tracer mapping in water column, background station	12 bottles fired, background values for transmission, potential temperature and methane (<10 nI/l)

Cascadia Margin

station	area	location (N W)	depth (m)	objectives	brief description
103 CTD	bioherm	44°38.97' 125°06.00'	654	tracer mapping in water column	12 bottles fired, no transmission and potential temperature anomalies; two distinct methane peaks at 500 (660 nI/l) and 580 (500 nI/l)
104 TSP	bioherm	44°39.976' 125°05.977'	502	deploy Sonartech transpon. (11.5 kHz)	deployed, no differential GPS during deployment
105 TSP	bioherm	44°40.657' 125°07.315'	598	deploy Sonartech transpon. (11.5 kHz)	deployed, no differential GPS during deployment
106 TSP	bioherm	44°40.731' 125°05.237'	572	deploy Sonartech transpon. (11.5 kHz)	deployed, no differential GPS during deployment
107 TSP	bioherm	44°39.502' 125°05.072'	541	deploy Sonartech transpon. (11.5 kHz)	deployed, no differential GPS during deployment
108 CTD	bioherm	44°40.32' 125°05.73'	601	tracer mapping in water column	12 bottles fired, strong methane peak below 580 (450 nI/l CH ₄)
109 GTVA	bioherm	- to 44°40.170' 125°05.796'	(598) (HS)	sample vent fauna at cold seeps	grey-green sediment, H ₂ S, ca. 40 living Calyptogenia

station	area	location (N W)	depth (m)	objectives	brief description
110 GTVA	bioherm	44°39.950' 125°05.791' to 44°40.225' 125°05.841'	602 to 611 (602) (HS)	sample vent fauna at cold seeps	carbonate blocks with numerous specimens (polychaetes, gastropodes)
111 CTD	bioherm	44°41.375' 125°05.755'	714	tracer mapping in water column	12 bottles fired, moderate methane anomaly of 250 n/l CH ₄ at 650 depth
112 CTD	bioherm	44°39.50' 125°0450'	827	tracer mapping in water column	12 bottles fired, background values for transmission, potential temperature; methane values show no distinct peak but are generally around 100 n/l
113 EXPL	bioherm	44°39.426' 125°05.762' to 44°39.799' 125°05.627' (ship's pos.)	582 to 646	map bioherm area	drifting particles revealed a southern bottom current, which has implications for the extend of the plume and hence the following CTD casts
114 CTD	bioherm	44°39.52' 125°05.97'	614	tracer mapping in water column	12 bottles fired, strong methane anomaly below 520 with peak of ca. 1300 n/l CH ₄ at 540 depth
115 GTVA	bioherm	44°40.378' 125°06.110' to 44°40.293' 125°06.296' (ship's pos.)	603 to 618 (616)	sample vent fauna at cold seeps	grey green sediment, sediment started degassing in the water column, H ₂ S, living Calyptogena and some carbonate precipitates
116 GTVA	bioherm	44°40.341' 125°06.117' to 44°40.063' 125°06.842' (ship's pos.)	621 to 640 (640) (HS)	sample vent fauna at cold seeps	3 deployments without sample recovery
117 CTD	bioherm	44°40.25' 125°05.40'	~600	tow-jo in SSW direction	12 bottles fired, methane values range from 35 to 100 n/l
118 CTD	bioherm	44°40.13' 125°06.54'	608	tracer mapping in water column	12 bottles fired, strong methane anomaly between 490 and 540 (up to 4200 n/l). Second smaller anomaly beneath 580 depth (1000 n/l)
119 GTVA	bioherm	44°40.423' 125°06.066' to 44°40.146' 125°06.685' (ship's pos.)	620 to 625 (625) (HS)	sample vent fauna at cold seeps	grey green consolidated sediment, H ₂ S, some echinorid worms and vestimentiferans
120 CTD	bioherm	44°40.45' 125°06.48'	609	tracer mapping in water column tow- yo	12 bottles fired, few samples with elevated methane but bottle 7 showed record 4700 n/l Methane
121 GTVA	bioherm	44°40.233' 125°06.568' to 44°40.193' 125°06.605' (ship's pos.)	622 to 627 (622) (HS)	sample vent fauna at cold seeps	recovered dead community in grey-green sediment dominated by Calyptogena with numerous buccinid gastropodes and vestimentiferans
122 CTD	bioherm	44°40.14' 125°06.55'	606	tracer mapping in water column	12 bottles fired, "small" methane anomaly between 480 and 520 (900 n/l)

B Cruise statistics

Station	Date	Time (UTC)				latitude	longitude	latitude	longitude	Type of Station and duration in minutes								
		begin	on bott.	off bott.	end	on bottom / start profile		off bottom / end profile		HS	CTD	DR	GKG	EXPL	GTV	EXT	TSP	Transit
leaving Victoria, transit to Axial Seamount																		
	06.08.	17:06			20:38	-	-	-	-									1652
47-51 TSP	06.09.	20:38	-	-	23:13	46°00.403'N	130°00.440'W	46°03.887'N	129°58.324'W	-	-	-	-	-	-	-	155	50
52 CTD	06.10.	0:03	0:42	-	1:40	46°02.29'N	130°00.78'W	-	-	-	97	-	-	-	-	-	-	14
HS 01		1:54	-	-	5:31	46°02.40'N	130°01.91'W	46°02.90'N	130°00.50'W	217	-	-	-	-	-	-	-	-
HS 02		5:31	-	-	6:16	46°02.90'N	130°00.52'W	46°05.00'N	130°10.00'W	45	-	-	-	-	-	-	-	10
53 GKG		6:26	7:27	-	8:45	46°05.00'N	130°10.00'W	-	-	-	-	-	139	-	-	-	-	8
HS 03		8:53	-	-	9:54	46°05.00'N	130°10.00'W	46°00.00'N	130°01.00'W	61	-	-	-	-	-	-	-	6
54 CTD		10:00	10:45	-	11:40	46°00.00'N	130°01.00'W	-	-	-	100	-	-	-	-	-	-	10
HS 04		11:50	-	-	14:08	46°00.00'N	130°09.90'W	45°46.00'N	130°19.00'W	138	-	-	-	-	-	-	-	9
55 GKG		14:17	15:10	-	16:15	45°46.001'N	130°18.997'W	-	-	-	-	-	118	-	-	-	-	3
HS 05		16:18	-	-	18:54	45°48.99'N	130°19.14'W	46°04.80'N	130°00.80'W	156	-	-	-	-	-	-	-	28
56 EXPLOS		19:22	20:15	7:39	8:38	46°04.781'N	130°00.683'W	46°02.488'N	130°00.851'W	-	-	-	-	796	-	-	-	6
HS 06		8:44	-	-	9:17	46°02.80'N	130°01.20'W	46°00.20'N	129°56.30'W	33	-	-	-	-	-	-	-	10
57 CTD	06.11.	9:27	10:18	-	11:35	46°00.19'N	129°56.32'W	-	-	-	128	-	-	-	-	-	-	20
58 GKG		11:55	12:51	-	13:54	46°00.210'N	129°56.307'W	-	-	-	-	-	119	-	-	-	-	-
HS 07		13:54	-	-	14:29	46°00.20'N	129°56.30'W	45°59.10'N	130°01.35'W	35	-	-	-	-	-	-	-	9
59 CTD		14:38	15:14	-	16:08	45°59.130'N	130°01.350'W	-	-	-	90	-	-	-	-	-	-	4
HS 08		16:12	-	-	16:40	45°59.08'N	130°01.33'W	45°55.18'N	129°58.40'W	28	-	-	-	-	-	-	-	5
60 GTVA		16:45	17:41	19:10	20:05	45°55.196'N	129°58.340'W	45°55.204'N	129°58.376'W	-	-	-	-	-	200	-	-	13
HS 09		20:18	-	-	20:57	45°55.18'N	129°58.40'W	45°59.45'N	130°01.65'W	39	-	-	-	-	-	-	-	13
61 GTVA		21:10	21:50	3:13	4:10	45°59.442'N	130°01.614'W	45°59.365'N	130°01.610'W	-	-	-	-	-	420	-	-	21
HS 10	06.12.	4:31	-	-	4:57	45°59.20'N	130°00.00'W	46°02.00'N	129°56.50'W	26	-	-	-	-	-	-	-	86
HS 11		6:23	-	-	8:41	46°05.00'N	129°57.50'W	46°23.50'N	129°29.00'W	138	-	-	-	-	-	-	-	14
62 DR		8:55	9:44	11:25	12:20	46°23.558'N	129°29.062'W	46°22.774'N	129°27.711'W	-	-	205	-	-	-	-	-	162
63 CTD		15:02	15:38	-	16:37	45°54.99'N	129°55.04'W	-	-	-	95	-	-	-	-	-	-	45
64 CTD		17:22	17:56	-	18:52	45°56.00'N	129°57.98'W	-	-	-	90	-	-	-	-	-	-	176

Station	Date	Time (UTC)				latitude longitude		latitude longitude		Type of Station and duration in minutes								
		begin	on bott.	off bott.	end	on bottom / start profile		off bottom / end profile		HS	CTD	DR	GKG	EXPL	GTV	EXT	TSP	Transit
65 EXPLOS		21:48	22:48	1:59	2:43	46°01.306'N	130°01.127'W	46°03.683'N	130°00.150'W	-	-	-	-	295	-	-	-	22
66 TSP	06.13.	3:05	-	-	3:54	46°03.89'N	129°58.32'W	-	-	-	-	-	-	-	-	-	49	65
HS 12		4:59	-	-	5:42	46°00.60'N	129°48.50'W	45°58.20'N	129°41.00'W	43	-	-	-	-	-	-	-	11
HS 13		5:53	-	-	6:37	45°57.30'N	129°41.30'W	45°58.80'N	129°48.80'W	44	-	-	-	-	-	-	-	17
HS 14		6:54	-	-	7:52	45°59.20'N	129°47.00'W	45°55.80'N	129°57.30'W	58	-	-	-	-	-	-	-	21
HS 15		8:13	-	-	8:25	45°54.70'N	130°00.90'W	45°53.40'N	130°02.40'W	12	-	-	-	-	-	-	-	15
HS 16		8:40	-	-	9:16	45°53.60'N	130°04.40'W	45°57.30'N	130°00.00'W	36	-	-	-	-	-	-	-	23
HS 17		9:39	-	-	10:50	45°59.40'N	130°03.60'W	46°04.50'N	130°15.00'W	71	-	-	-	-	-	-	-	12
HS 18		11:02	-	-	12:04	46°02.90'N	130°15.00'W	45°58.30'N	130°05.00'W	62	-	-	-	-	-	-	-	10
HS 19		12:14	-	-	13:07	45°57.40'N	130°06.30'W	46°01.30'N	130°15.00'W	53	-	-	-	-	-	-	-	18
HS 20		13:25	-	-	14:10	45°59.30'N	130°15.00'W	45°56.40'N	130°07.30'W	45	-	-	-	-	-	-	-	15
HS 21		14:25	-	-	15:01	45°55.50'N	130°08.80'W	45°57.90'N	130°15.00'W	36	-	-	-	-	-	-	-	14
HS 22		15:15	-	-	15:42	45°56.30'N	130°15.00'W	45°54.50'N	130°10.40'W	27	-	-	-	-	-	-	-	43
67 GTVA		16:25	18:56	19:18	20:40	45°59.367'N	130°01.477'W	45°59.354'N	130°01.557'W	-	-	-	-	-	255	-	-	13
68 TSP		20:53	-	-	21:26	46°00.40'N	130°00.44'W	-	-	-	-	-	-	-	-	-	33	54
69 GTVA		22:20	23:02	23:39	0:30	45°59.344'N	130°01.557'W	45°59.356'N	130°01.582'W	-	-	-	-	-	130	-	-	27
70 GTVA	06.14.	0:57	1:38	2:35	3:20	45°59.364'N	130°01.570'W	45°59.382'N	130°01.577'W	-	-	-	-	-	143	-	-	40
HS 23		4:00	-	-	4:05	45°54.60'N	130°01.10'W	45°55.30'N	130°01.30'W	5	-	-	-	-	-	-	-	52
HS 24		4:57	-	-	5:21	45°55.00'N	129°51.00'W	45°55.50'N	129°46.60'W	24	-	-	-	-	-	-	-	31
HS 25		5:52	-	-	6:25	45°52.00'N	129°45.90'W	45°56.50'N	129°42.40'W	33	-	-	-	-	-	-	-	17
HS 26		6:42	-	-	6:51	45°56.00'N	129°41.60'W	45°57.00'N	129°40.70'W	9	-	-	-	-	-	-	-	46
HS 27		7:37	-	-	8:22	46°02.40'N	129°41.40'W	46°05.20'N	129°50.30'W	55	-	-	-	-	-	-	-	-
HS 28		8:22	-	-	9:43	46°05.20'N	129°50.30'W	46°09.20'N	130°03.80'W	81	-	-	-	-	-	-	-	12
HS 29		9:55	-	-	10:31	46°09.50'N	130°05.90'W	46°05.00'N	130°06.90'W	36	-	-	-	-	-	-	-	22
HS 30		10:53	-	-	11:28	46°05.00'N	130°10.30'W	46°09.50'N	130°09.10'W	35	-	-	-	-	-	-	-	16
HS 31		11:44	-	-	12:21	46°09.50'N	130°11.90'W	46°05.00'N	130°13.20'W	37	-	-	-	-	-	-	-	55
71 CTD		13:16	14:27	-	15:21	45°59.01'N	130°02.50'W	-	-	-	115	-	-	-	-	-	-	44
72 CTD		16:05	16:39	-	17:34	45°56.03'N	130°02.95'W	-	-	-	89	-	-	-	-	-	-	35

Station	Date	Time (UTC)				latitude longitude		latitude longitude		Type of Station and duration in minutes								
		begin	on bott.	off bott.	end	on bottom / start profile		off bottom / end profile		HS	CTD	DR	GKG	EXPL	GTV	EXT	TSP	Transit
73-75 TSP		18:09	-	-	21:20	45°56.492'N	130°00.025'W	45°55.495'N	130°00.055'W	-	-	-	-	-	-	-	191	46
76 CTD		22:06	22:42	-	23:47	45°56.03'N	130°02.95'W	-	-	-	101	-	-	-	-	-	-	68
HS 32	06.15.	0:55	-	-	4:02	45°53.40'N	130°05.80'W	45°51.70'N	129°43.80'W	187	-	-	-	-	-	-	-	29
HS 33		4:31	-	-	7:00	45°49.90'N	129°39.60'W	45°52.20'N	130°07.70'W	149	-	-	-	-	-	-	-	18
HS 34		7:18	-	-	9:54	45°50.80'N	130°09.50'W	45°48.40'N	129°39.50'W	156	-	-	-	-	-	-	-	45
HS 35		10:39	-	-	10:50	45°53.10'N	129°47.50'W	45°54.10'N	129°46.00'W	11	-	-	-	-	-	-	-	58
HS 36		11:48	-	-	12:48	45°57.50'N	129°58.20'W	46°01.70'N	129°48.40'W	60	-	-	-	-	-	-	-	41
HS 37		13:29	-	-	14:40	46°03.80'N	129°39.50'W	46°07.80'N	129°51.90'W	71	-	-	-	-	-	-	-	17
HS 38		14:57	-	-	16:54	46°08.80'N	129°49.40'W	46°05.60'N	129°39.50'W	117	-	-	-	-	-	-	-	41
77 EXPLOS		17:35	-	-	18:30	45°54.63'N	129°59.34'W	-	-	-	-	-	-	55	-	-	-	30
78 CTD		19:00	20:02	-	21:55	45°56.000'N	130°00.832'W	-	-	-	175	-	-	-	-	-	-	38
79 EXPLOS		22:33	23:19	4:30	5:15	45°54.656'N	129°59.301'W	45°57.255'N	129°59.247'W	-	-	-	-	402	-	-	-	15
80 CTD	06.16.	5:30	6:06	-	6:57	45°58.17'N	130°00.95'W	-	-	-	87	-	-	-	-	-	-	54
HS 39		7:51	-	-	8:22	45°50.20'N	130°08.50'W	45°46.70'N	130°13.40'W	31	-	-	-	-	-	-	-	23
HS 40		8:45	-	-	11:53	45°47.70'N	130°11.00'W	45°44.80'N	129°39.50'W	188	-	-	-	-	-	-	-	118
HS 41		13:51	-	-	16:25	45°46.30'N	129°39.50'W	45°49.00'N	130°09.10'W	154	-	-	-	-	-	-	-	54
81 GTVA		17:19	18:11	21:00	21:45	45°56.012'N	130°00.820'W	45°56.036'N	130°01.876'W	-	-	-	-	-	266	-	-	56
82 EXPLOS		22:49	22:29	2:10	2:50	45°55.177'N	130°00.295'N	45°56.700'N	130°01.285'W	-	-	-	-	241	-	-	-	22
83 CTD	06.17.	3:12	3:54	-	5:04	45°55.961'N	129°58.934'W	-	-	-	112	-	-	-	-	-	-	73
HS 42		6:17	-	-	6:44	45°51.90'N	130°13.10'W	45°55.00'N	130°13.10'W	27	-	-	-	-	-	-	-	90
HS 43		8:14	-	-	9:00	46°05.00'N	130°12.80'N	46°01.50'N	130°06.70'W	46	-	-	-	-	-	-	-	91
HS 44		10:31	-	-	10:39	46°04.90'N	129°46.60'W	46°05.40'N	129°45.40'W	8	-	-	-	-	-	-	-	36
HS 45		11:15	-	-	11:48	46°07.90'N	129°39.50'W	46°09.40'N	129°45.00'W	33	-	-	-	-	-	-	-	40
HS 46		12:28	-	-	12:52	46°08.10'N	129°54.20'W	46°09.40'N	129°58.00'W	24	-	-	-	-	-	-	-	118
84 EXPLOS		14:50	17:14	1:00	1:52	46°17.141'N	129°42.946'W	46°18.542'N	129°42.429'W	-	-	-	-	662	-	-	-	132
85 GTVA	06.18.	4:04	5:10	5:16	6:11	45°59.353'N	130°01.559'W	45°59.360'N	130°01.558'W	-	-	-	-	-	127	-	-	2
86 GTVA		6:13	7:15	7:26	8:23	45°59.334'N	130°01.602'W	45°59.382'N	130°01.570'W	-	-	-	-	-	130	-	-	26
87 CTD		8:49	9:24	-	10:30	45°58.01'N	129°59.00'W	-	-	-	101	-	-	-	-	-	-	49

Station	Date	Time (UTC)				latitude	longitude	latitude	longitude	Type of Station and duration in minutes								
		begin	on bott.	off bott.	end	on bottom / start profile		off bottom / end profile		HS	CTD	DR	GKG	EXPL	GTV	EXT	TSP	Transit
88 CTD		11:19	11:54	-	13:00	45°57.500'N	130°02.517'W	-	-	-	101	-	-	-	-	-	-	76
HS 47		14:16	-	-	15:49	45°46.20'N	130°16.0'W	45°43.80'N	129°58.0'W	93	-	-	-	-	-	-	-	96
89 GTVA		17:25	18:22	19:51	20:40	45°59.332'N	130°01.543'W	45°59.388'N	130°01.584'W	-	-	-	-	-	195	-	-	16
90 GTVA	06.19.	20:56	21:37	3:58	4:50	45°59.376'N	130°01.560'W	45°59.363'N	130°01.591'W	-	-	-	-	-	474	-	-	10
HS 48		5:00	-	-	8:30	45°50.00'N	130°15.90'W	46°10.00'N	130°15.50'W	210	-	-	-	-	-	-	-	15
HS 49		8:45	-	-	11:24	46°10.00'N	130°17.80'W	45°48.50'N	130°18.20'W	159	-	-	-	-	-	-	-	37
HS 50		12:01	-	-	13:09	45°46.70'N	130°10.30'W	45°44.80'N	129°57.30'W	68	-	-	-	-	-	-	-	13
HS 51		13:22	-	-	15:01	45°44.30'N	129°58.00'W	45°42.20'N	129°39.50'W	99	-	-	-	-	-	-	-	104
91 CTD		16:45	17:33	-	19:23	45°56.032'N	130°00.847'W	-	-	-	158	-	-	-	-	-	-	51
92 TSP		20:14	-	-	20:50	46°01.116'N	130°01.932'W	-	-	-	-	-	-	-	-	-	36	20
93 TSP		21:10	-	-	21:56	46°02.127'N	129°59.744'W	-	-	-	-	-	-	-	-	-	46	19
94 TSP		22:15	-	-	22:57	46°03.154'N	130°01.131'W	-	-	-	-	-	-	-	-	-	42	24
95 EXT		23:21		-	1:04	46°01.134'N	130°00.846'W	46°01.192'N	130°01.267'W	-	-	-	-	-	-	103	-	50
96 CTD	06.20.	1:54	2:38	-	3:42	45°54.00'N	130°05.50'W	-	-	-	108	-	-	-	-	-	-	96
HS 52		5:18	-	-	8:50	46°10.00'N	130°20.00'W	46°10.00'N	129°39.00'W	212	-	-	-	-	-	-	-	17
HS 53		9:07	-	-	12:41	46°11.60'N	129°39.00'W	46°11.60'N	130°20.00'W	214	-	-	-	-	-	-	-	147
97 GTVA		15:08	16:02	16:48	17:46	46°18.529'N	129°42.450'W	46°18.562'N	129°42.460'W	-	-	-	-	-	158	-	-	16
98 CTD		18:02	18:50	-	20:22	46°18.512'N	129°42.471'W	-	-	-	140	-	-	-		-	-	80
99 GTVA		21:32	22:23	23:50	0:40	46°09.72'N	129°55.24'W	46°09.718'N	129°55.220'W	-	-	-	-	-	188	-	-	81
100 EXPLOS	06.21.	2:01	-	-	3:20	-	-	-	-	-	-	-	-	79	-	-	-	18
101 TSP		3:38	-	-	6:45	45°55.911'N	129°58.742'W	-	-	-	-	-	-	-	-	-	187	105
102 CTD		8:30	9:24	-	10:58	45°40.017'N	129°47.005'W	-	-	-	148	-	-	-	-	-	-	-
HS 54		10:58	-	-	4:22	44°40.52'N	125°07.33'W	44°43.20'N	125°01.90'W	1044	-	-	-	-	-	-	-	-

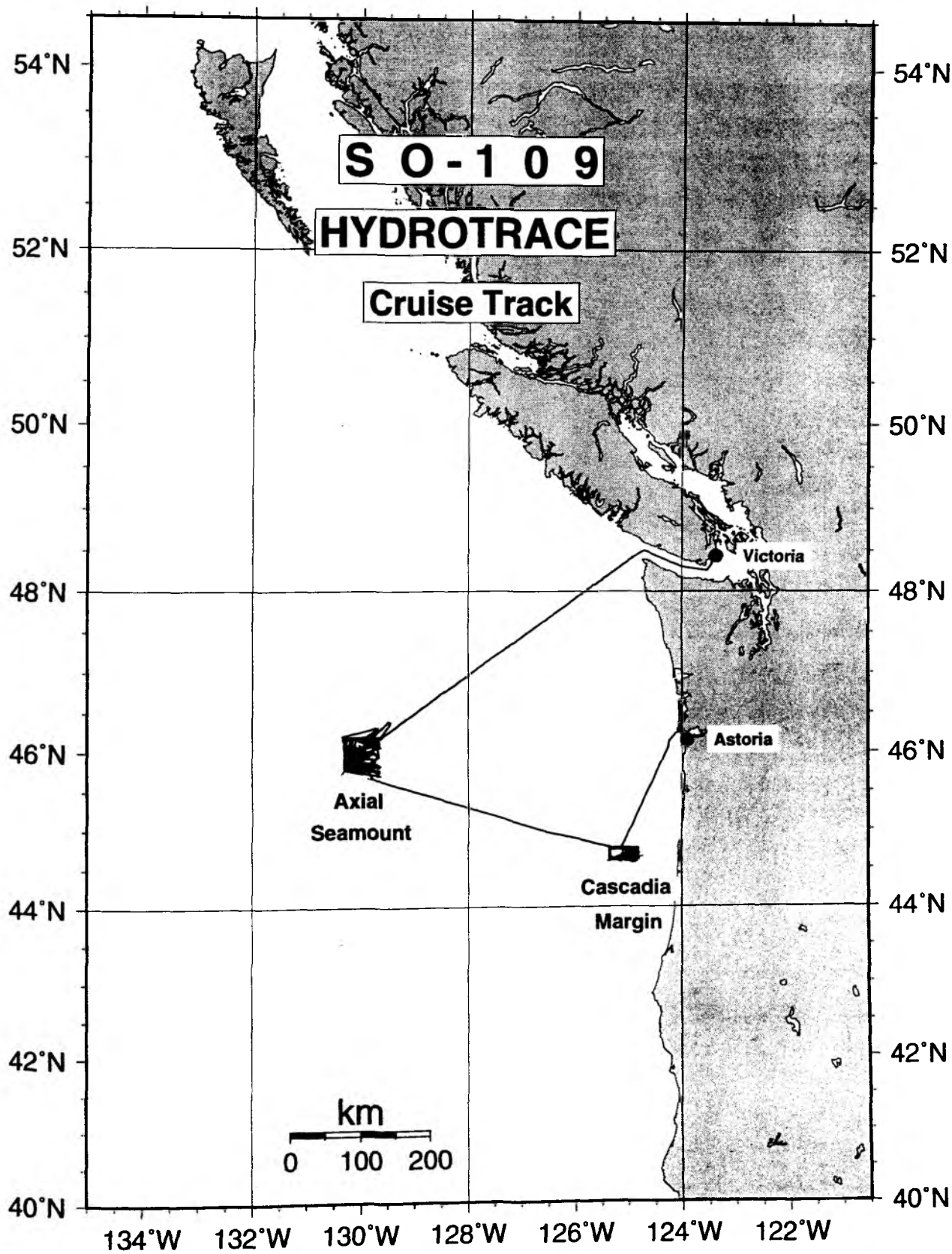
Cascadia Margin

Station	Date	Time (UTC)				latitude longitude		latitude longitude		Type of Station and duration in minutes								
		begin	on bott	off bott	end	on bottom / start profile		off bottom / end profile		HS	CTD	DR	GKG	EXPL	GTV	EXT	TSP	Transit
HS 55	06.22.	4:22	-	-	4:38	44°43.20'N	125°01.90'W	44°43.20'N	124°58.90'W	16	-	-	-	-	-	-	-	20
HS 56		4:58	-	-	5:39	44°43.50'N	124°57.50'W	44°42.90'N	124°50.10'W	41	-	-	-	-	-	-	-	9
HS 57		5:48	-	-	6:32	44°42.20'N	124°49.90'W	44°42.90'N	124°58.50'W	42	-	-	-	-	-	-	-	20
HS 58		6:52	-	-	7:50	44°42.10'N	125°00.80'W	44°41.60'N	124°49.90'W	58	-	-	-	-	-	-	-	11
HS 59		8:01	-	-	8:50	44°41.00'N	124°49.80'W	44°41.00'N	124°59.20'W	49	-	-	-	-	-	-	-	27
HS 60		9:17	-	-	9:27	44°41.30'N	125°02.40'W	44°40.10'N	125°02.20'W	10	-	-	-	-	-	-	-	25
HS 61		9:52	-	-	10:43	44°40.10'N	124°58.60'W	44°40.20'N	124°49.50'W	51	-	-	-	-	-	-	-	9
HS 62		10:52	-	-	11:48	44°39.45'N	124°49.50'W	44°38.80'N	125°01.60'W	56	-	-	-	-	-	-	-	25
HS 63		12:13	-	-	12:39	44°38.30'N	125°01.50'W	44°38.50'N	125°06.30'W	26	-	-	-	-	-	-	-	-
HS 64		12:39	-	-	13:16	44°38.50'N	125°06.30'W	44°37.70'N	125°13.10'W	37	-	-	-	-	-	-	-	15
HS 65		13:31	-	-	14:08	44°36.20'N	125°13.10'W	44°37.90'N	125°06.20'W	37	-	-	-	-	-	-	-	-
HS 66		14:08	-	-	14:33	44°37.90'N	125°06.20'W	44°37.30'N	125°01.40'W	25	-	-	-	-	-	-	-	34
103 CTD		15:07	15:25	-	16:00	44°38.97'N	125°06.00'W	-	-	-	53	-	-	-	-	-	-	34
104-107 TSP		16:34	-	-	19:44	44°39.976'N	125°05.977'W	44°39.502'N	125°05.072'W	-	-	-	-	-	-	-	190	41
108 CTD		20:25	20:42	-	21:21	44°40.32'N	125°05.73'W	-	-	-	56	-	-	-	-	-	-	15
109 GTVA		21:36	22:19	23:49	0:20	-	-	44°40.170'N	125°05.796'W	-	-	-	-	-	164	-	-	12
110 GTVA	06.23.	0:32	1:00	1:43	2:55	44°39.950'N	125°05.791'W	44°40.225'N	125°05.841'W	-	-	-	-	-	143	-	-	10
111 CTD		3:05	3:24	-	3:56	44°41.375'N	125°05.755'W	-	-	-	51	-	-	-	-	-	-	40
HS 67		4:36	-	-	5:45	44°37.60'N	125°01.60'W	44°39.00'N	124°49.50'W	69	-	-	-	-	-	-	-	13
HS 68		5:58	-	-	7:00	44°38.80'N	124°49.50'W	44°36.60'N	125°01.60'W	62	-	-	-	-	-	-	-	20
HS 69		7:20	-	-	7:52	44°36.20'N	125°01.40'W	44°37.00'N	125°06.30'W	32	-	-	-	-	-	-	-	36
HS 70		8:28	-	-	9:14	44°35.30'N	125°01.30'W	44°36.50'N	125°09.50'W	46	-	-	-	-	-	-	-	24
HS 71		9:38	-	-	9:58	44°35.10'N	125°08.00'W	44°35.80'N	125°11.30'W	20	-	-	-	-	-	-	-	11
HS 72		10:09	-	-	10:52	44°36.70'N	125°13.00'W	44°38.80'N	125°20.10'W	43	-	-	-	-	-	-	-	9
HS 73		11:01	-	-	11:47	44°38.80'N	125°20.10'W	44°44.60'N	125°20.10'W	46	-	-	-	-	-	-	-	10

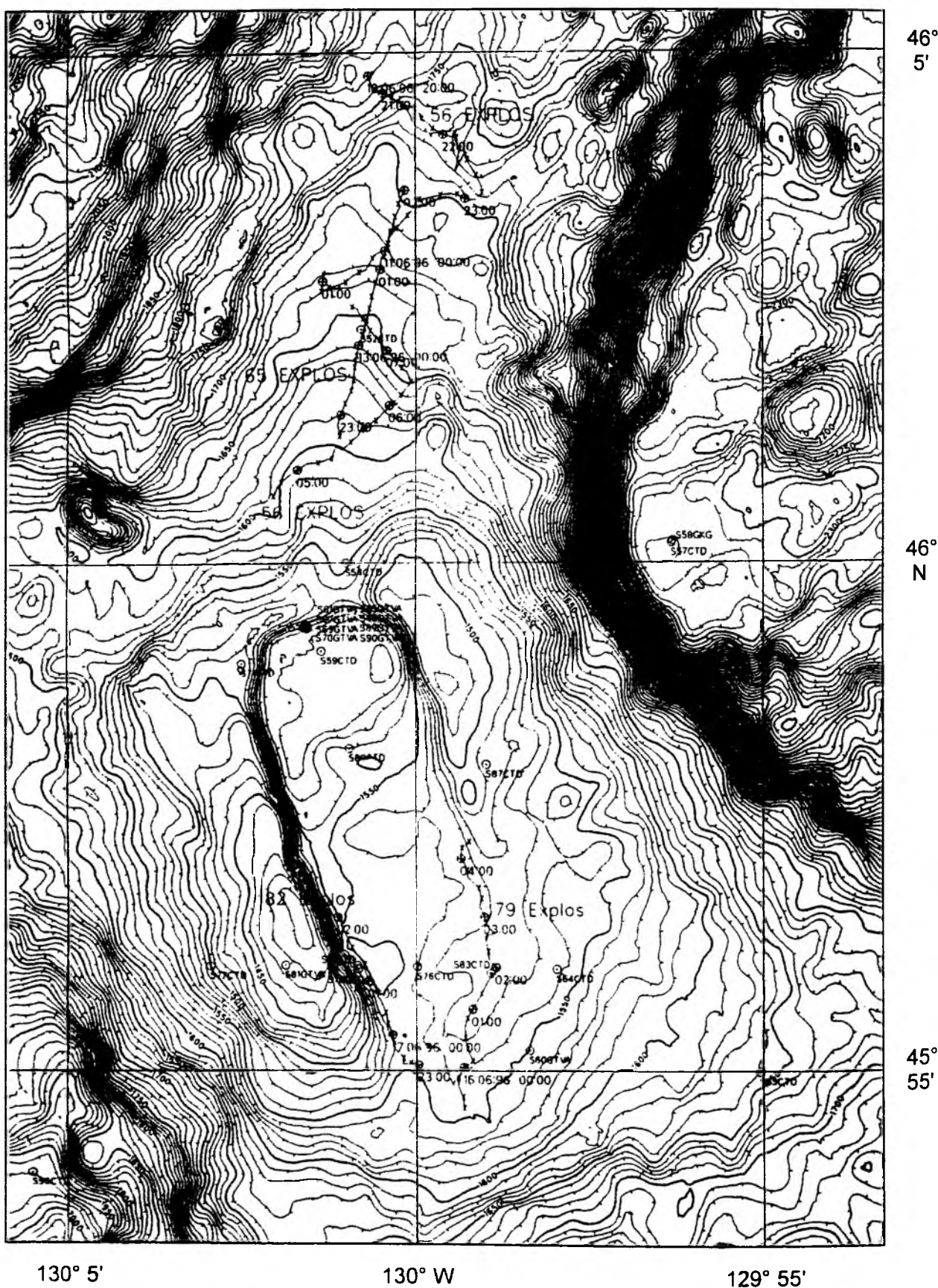
Station	Date	Time (UTC)				latitude longitude		latitude longitude		Type of Station and duration in minutes								
		begin	on bott.	off bott.	end	on bottom / start profile		off bottom / end profile		HS	CTD	DR	GKG	EXPL	GTV	EXT	TSP	Transit
HS 74		11:57	-	-	13:00	44°44.60'N	125°20.10'W	44°44.60'N	125°08.00'W	63	-	-	-	-	-	-	-	20
HS 75		13:20	-	-	14:47	44°44.60'N	125°04.70'W	44°44.60'N	124°49.00'W	87	-	-	-	-	-	-	-	8
HS 76		14:55	-	-	15:23	44°44.10'N	124°49.00'W	44°44.10'N	124°55.00'W	28	-	-	-	-	-	-	-	53
112 CTD		16:16	16:37	-	17:16	44°39.50'N	125°04.50'W	-	-	-	60	-	-	-	-	-	-	19
113 EXPLOS		17:35	18:03	19:56	20:24	44°39.426'N	125°05.762'W	44°39.799'N	125°05.627'W	-	-	-	-	169	-	-	-	28
114CTD		20:52	21:13	-	21:50	44°39.52'N	125°05.97'W	-	-	-	58	-	-	-	-	-	-	15
115 GTVA		22:05	22:39	23:09	0:03	44°40.378'N	125°06.110'W	44°40.293'N	125°06.296'W	-	-	-	-	-	118	-	-	37
116GTVA	06.24.	0:40	1:08	2:20	2:48	44°40.341'N	125°06.117'W	44°40.063'N	125°06.842'W	-	-	-	-	-	128	-	-	22
117 CTD		3:10	3:26	5:56	6:17	44°40.25'N	125°05.40'W	-	-	-	187	-	-	-	-	-	-	18
HS 77		6:35	-	-	7:50	44°38.10'N	125°02.50'W	44°39.20'N	124°49.00'W	75	-	-	-	-	-	-	-	17
HS 78		8:07	-	-	8:25	44°36.80'N	124°49.00'W	44°35.20'N	124°51.70'W	18	-	-	-	-	-	-	-	15
HS 79		8:40	-	-	9:10	44°35.20'N	124°53.50'W	44°37.30'N	124°49.00'W	30	-	-	-	-	-	-	-	11
HS 80		9:21	-	-	10:01	44°37.70'N	124°49.00'W	44°35.20'N	124°55.80'W	40	-	-	-	-	-	-	-	20
HS 81		10:21	-	-	11:14	44°35.20'N	124°58.50'W	44°38.10'N	124°49.00'W	53	-	-	-	-	-	-	-	9
HS 82		11:23	-	-	12:33	44°38.50'N	124°49.00'N	44°35.30'N	125°01.50'W	70	-	-	-	-	-	-	-	32
HS 83		13:05	-	-	13:24	44°37.50'N	125°06.90'W	44°35.20'N	125°08.70'W	19	-	-	-	-	-	-	-	16
HS 84		13:40	-	-	14:33	44°35.80'N	125°11.50'W	44°35.80'N	125°21.10'W	53	-	-	-	-	-	-	-	61
118 CTD		15:34	15:50		16:18	44°40.13'N	125°06.54'W	-	-	-	44	-	-	-	-	-	-	10
119 GTVA		16:28	16:57	20:13	20:59	44°40.423'N	125°06.066'W	44°40.146'N	125°06.685'W	-	-	-	-	-	271	-	-	8
120 CTD		21:07	21:23	22:32	22:53	44°40.45'N	125°06.48'W	-	-	-	106	-	-	-	-	-	-	57
121 GTVA		23:50	0:13	0:32	1:05	44°40.233'N	125°06.568'W	44°40.193'N	125°06.605'W	-	-	-	-	-	75	-	-	19
disable transponder		1:24	-	-	1:43	-	-	-	-	-	-	-	-	-	-	-	19	17
122 CTD	06.25.	2:00	-	-	3:03	44°40.14'N	125°06.55'W	-	-	-	63	-	-	-	-	-	-	48
HS 85		3:51	-	-	4:13	44°36.80'N	125°17.00'W	44°36.80'N	125°21.10'W	22	-	-	-	-	-	-	-	15
HS 86		4:28	-	-	4:50	44°35.80'N	125°21.10'W	44°38.80'N	125°21.10'W	22	-	-	-	-	-	-	-	43
HS 87		5:33	-	-	5:43	44°44.60'N	125°21.10'W	44°46.00'N	125°21.10'W	10	-	-	-	-	-	-	-	12

Station	Date	Time (UTC)				latitude longitude		latitude longitude		Type of Station and duration in minutes								
		begin	on bott.	off bott.	end	on bottom / start profile		off bottom / end profile		HS	CTD	DR	GKG	EXPL	GTV	EXT	TSP	Transit
HS 88		5:55	-	-	8:45	44°46.00'N	125°21.10'W	44°46.00'N	125°49.00'W	170	-	-	-	-	-	-	-	19
HS 89		9:04	-	-	9:31	44°45.45'N	124°49.00'W	44°45.45'N	125°00.00'W	27	-	-	-	-	-	-	-	21
HS 90		9:52	-	-	10:22	44°45.30'N	125°04.80'W	44°45.30'N	125°08.30'W	30	-	-	-	-	-	-	-	27
HS 91		10:49	-	-	11:46	44°44.20'N	124°54.20'W	44°43.50'N	124°49.00'W	57	-	-	-	-	-	-	-	21
HS 92		12:07	-	-	12:25	44°40.50'N	124°49.00'W	44°41.00'N	124°54.50'W	18	-	-	-	-	-	-	-	-
leaving Cascadia margin for Astoria																		
		12:25	-	-	22:00	-	-	-	-	-	-	-	-	-	-	-	-	575
						TOTAL time used for stations (hours):				112,28	45,22	3,42	6,27	44,98	59,75	1,72	15,80	86,35
						percentages:				38,79	15,62	1,18	2,17	15,54	20,64	0,59	5,46	29,83
06.08.1996 17:06 to 06.25.1996 22:00 UTC						37,12				transit to Axial Smt. and from Cascadia M. to Astoria hours of station work hours of transit between stations								
						289,43												
						86,35												
						412,90												
						of				hours of ship time								
412,90																		

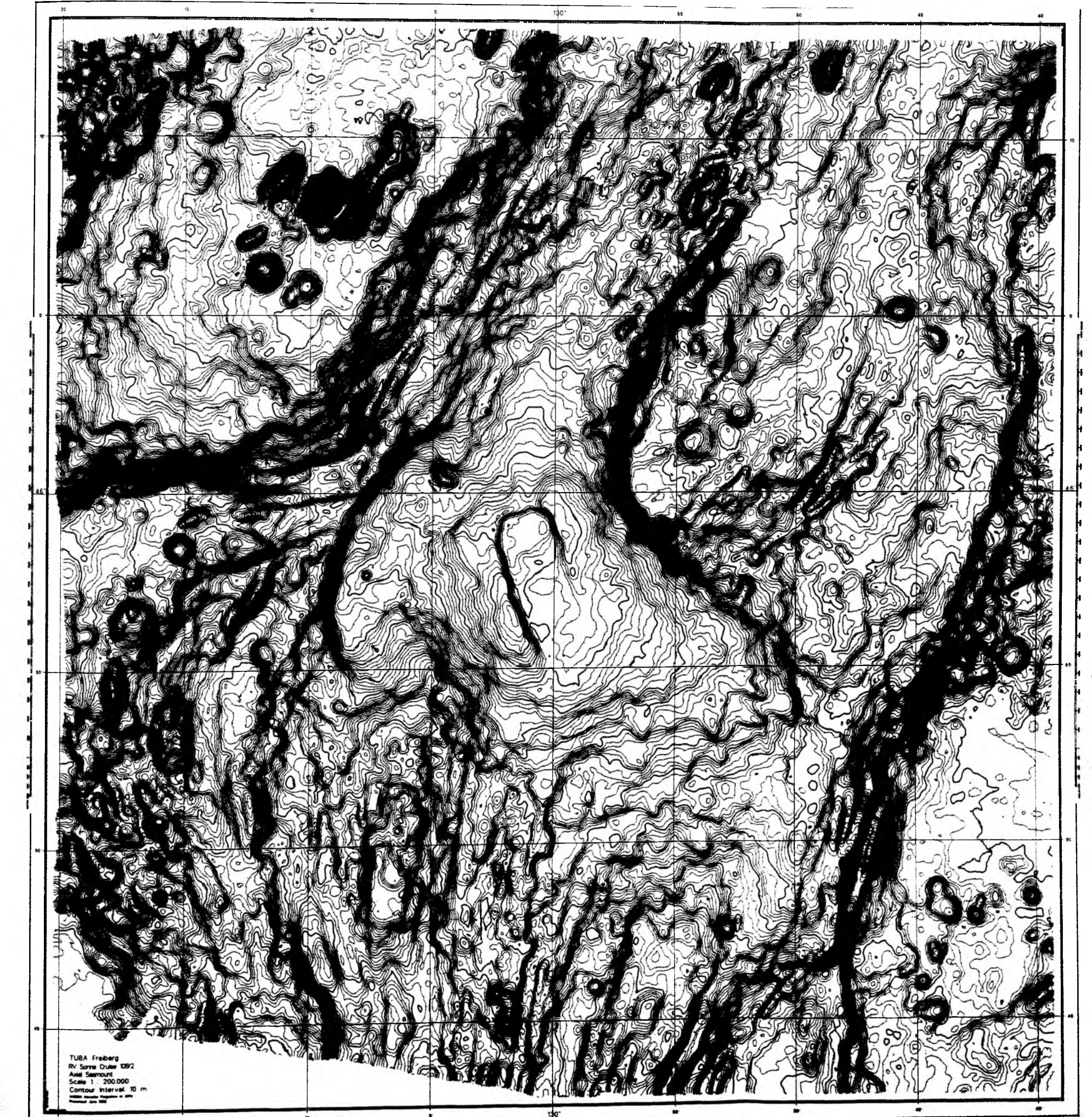
C Maps



Map 1: Track of cruise SO109-2



Map 2: Location of stations SO109-2 in and around Axial Caldera



This is a detailed topographic map of the TUBA Freberg area. The map features a grid with latitude and longitude markings. The contour lines are dense and irregular, indicating a rugged terrain with many peaks and valleys. The map is oriented with North at the top. The grid lines are spaced at 10-minute intervals. The map is titled 'TUBA Freberg' and includes information about the survey and scale.

TUBA Freberg
RV Sonne Cruise 1092
Axis Sarmouth
Scale 1: 200,000
Contour Interval 10 m
1988/89 Marine Magnetic Data
Processed June 1990

Map 3: Bathymetry of Axial Seamount collected during SO109-1 and SO109-2, 10 contour interval.

5. Leg SO109-3

5.1 Cruise Objectives

by Peter Linke

An important engineering objective of SO109-3 was to demonstrate the full range of technical abilities of ROPOS (**R**emotely **O**perated **P**latform for **O**cean **S**cience) operating from the German RV Sonne. Until now, the ROPOS has been operated from only two research vessels with a demonstrated compatibility with the system (a DFO vessel in Canada and a NOAA vessel in the U.S.). The HYDROTRACE expedition was the first deployment of ROPOS from a non-Canadian/non-U.S. vessel and the first real test of its portability. The testing of ROPOS during SO109-3 has provided the German research community with the opportunity to observe the capabilities of the vehicle and will stimulate further collaborative research between German, Canadian and U.S. partners. Germany has made a substantial investment in ROPOS operations for 1996-97, and testing of the ROV during SO109-3 was a critical step in the development of ROPOS as an international scientific facility (Canadian Scientific Submersible Facility - CSSF).

ROPOS was designed and developed in Canada as a cost-effective, fully-equipped, remotely-operated deep-submergence vehicle with complete sampling capabilities. GSC, NOAA, and U. Victoria have worked together to develop ROPOS for the ongoing study of active volcanic and hydrothermal sites on the Juan de Fuca Ridge, including Axial Volcano, since 1990. Researchers at GSC and at partner institutions in Canada and in the U.S. have employed ROPOS extensively on the Juan de Fuca.

GSC and its partners at NOAA and the University of Victoria provided the full logistical support for the operations of the ROV, including navigation, video, and water sampling. GSC's principal contribution to SO109-3 was to underwrite the ROPOS costs, including rental of equipment and extra contract pilots for the work on Axial Volcano. U. Freiberg (P. Herzig), GSC (M. Hannington and I.R. Jonasson), and NOAA (D. Butterfield and J. Lupton) were supposed to conduct shore-based research on the fluid and sulfide samples collected during SO109-3. P. Linke (GEOMAR), V. Tunnicliffe (U. Vic.), K. Juniper (CSSF) and D. Butterfield (NOAA-PMEL) coordinated ROV operations for the Freiberg-GSC-NOAA-U. Victoria group during this leg.

Major modifications to the ROPOS system were made to undertake operations during HYDROTRACE, including the preparations for installation of a new 5,000 m fiber optic cable. Engineering tests and method development also included the implementation of long-baseline navigation (SeaScape) for ROPOS, establishing links between shipboard navigation and the NOAA SeaScape bottom transponder system, installation and testing of

the NOAA-PMEL manifold sampler for high-temperature fluid sampling, and operation of the new U. Victoria high-resolution BETACAM video system.

5.2 Cruise Narrative and Summary of Results

by Peter Linke

After loading additional scientific equipment the RV SONNE left the port of Astoria on June 26th at 09:00 pm in order to load the meanwhile operational 3000 m ROPOS winch in Victoria on June 27th. The RV Sonne tied up in Victoria at the Esquimalt Graving Docks at 03:15 pm. We had a tonnage test of the A-frame before the winch was put on board. The more than 30 t weighing winch was attached on two double T-bars in order to be fitted in the deck's 20 ft raster unit and was welded firmly amidships at the container space (Fig. 69A). During the next two days the connections between the ROPOS garage and the winch as well as between the winch and the ship were established and step by step the ROPOS system was put into operation. The first port test was performed on June 30th. After this it became obvious that all the additional work could be conducted on board so that the RV SONNE left Victoria at 04:00 pm. In the evening the first shallow water dive in the Strait of Juan de Fuca demonstrated a perfectly working ROPOS system. It became clear for all participants what kind of a complex system was installed on board by the unremitting efforts of technicians and crew members.

During the next morning at the exit of the Strait of Juan de Fuca three more deployment and recovery manoeuvres were performed to ensure a close handling coordination between the ship's and ROPOS' crews. After these tests were completed successfully and the nautical manoeuvres were optimized RV SONNE headed for the Axial Seamount working area. The transit was interrupted in the morning of the 2nd for 2.5 h to test the ROPOS system for the first time in the deep sea under perfect weather conditions. During this test ROPOS left the garage in a water depth of approx. 400 m and while different manoeuvres were performed the whole crew had an insight into the system's operational abilities. Garage and ROV were recovered separately in order to simulate a failure of one unit. RV SONNE continued the transit to the working area after completing this test.

We reached the working area at the Axial Seamount in the afternoon of June 2nd. Equipped with suction sampler, sampling tray and Pac Man, a specialized claw, ROPOS left its garage 30 m above seafloor at the ASHES vent field for sampling sulfid minerals at the chimneys of the hydrothermal vent sources (#123/Dive 331). Reaching the seafloor the ROV offered all observers who were up until now only familiar with conventional deep-towed videosystems a completely new perspective of the seafloor.

Immediately after the first bottom view a new hydrothermal chimney was observed which was named PHOENIX. As it was desired by the scientists the ROPOS pilot was able to cut off the top of the chimney. The most spectacular pictures were possible at the INFERNO vent from which high-temperature fluids were expelled showing flame alike cones above the orifice which indicate a “boiling” of the fluids. This phenomenon could until now only be observed in the ASHES vent field and is considered to be an important process in the formation of mineral deposits. The sampling here and at two more vents (MUSHROOM and VIRGIN) was successful.

After this first 12 h lasting successful scientific dive ROPOS was re-equipped with the manifold sampler for the high-temperature fluid sampling (Fig. 69E). This instrument is designed for taking a series of single discrete and gas-tight water samples by the ROV, until now only separate sampling had been possible. Unfortunately the integration of this system had to be stopped after three trials because its functioning was considerably interfered by problems with the energy supply. While waiting for the re-equipping of the ROV the time was used for tests with the time-laps camera and the newly installed software for the long-baseline transponder navigation. We also realized an EXPLOS survey (#124) at the Southern Rift Zone.

During this survey we were able to discover two unknown vent fields which could be recorded precisely in cooperation with the new transponder navigation and the on board of the RV SONNE installed differential GPS. The fields were characterized by temperature and Eh-anomalies. In the morning of July 5th we succeeded for the second time in working at the ASHES vent field with ROPOS (#126/Dive 333). In addition to the sampling of the already visited location on the first the top of the HILLOCK chimney was sampled. Beside this a completely new anhydrite vent was discovered, which was populated by some sulfide worms as a kind of pioneer species. The pilot was able to take excellent close-up images with the new BETACAM videosystem. After sampling the hydrothermal rocks and the vent fauna as well as the detailed sampling of cold to warm hydrothermal influenced seawater with the suction sampler ROPOS showed up again on the surface after an 8h dive with a filled sampling tray. After recovery of the three NOAA transponders SONNE headed for the 600 m deeper CoAxial segment equipped with the biobox and two water samplers in order perform detailed sampling and mapping of the biological community.

Reaching the seafloor a high voltage ground fault at the ROPOS garage forced us to break off the dive. Alternately a profile (#129) with the EXPLOS was conducted which was towed close along the desired vent location. The repeated trial to bring ROPOS back to the vent site after repairing it once again failed because another high voltage ground fault occurred in a water depth of 1400 m. The scientific working program was terminated in the evening of July 6th and SONNE headed for Victoria in order to gain time for troubleshooting during the

transit. During three technical test dives in the next morning the cause for the ground faults was found and the manifold sampler was tested successfully. Since one of the three existing fibre optic connections broke the working program had to be terminated at 03:30 pm and SONNE continued the transit to Victoria. During transit the fibre optic cable was cut and the winch system newly organized for the preparation of the upcoming cruises. RV SONNE tied up in Victoria, Ogden Point on July 8th at 10:00 am.

5.3 Operations Background

by Peter Linke

Without any doubts is this leg of cruise SO109 one of the highlights of the HYDROTRACE project. Not only the ROPOS system was employed successfully, after adverse circumstances in the beginning but also new scientific territory was entered by the selective employment of the measuring, observing and sampling capacities. This includes the observed "boiling" of the fluids, the discovery of new active hydrothermal vents, the selective sampling of mineral precipitates, biological communities, volcanic glasses and their alteration products. The numerous problems document that ROPOS is a very complex technical system but nevertheless it seems to be outstandingly appropriate to realize new research features also due to the well developed instrumental and personnel conditions offered on the RV SONNE.

5.4 ROPOS Operation

by Keith Shepherd and Peter Linke

5.4.1 Specifications

ROPOS is a thirty horsepower electro-hydraulic ROV designed and built by International Submarine Engineering (ISE). In deep-water mode, it is a caged system with 300 m of flying tether that has been extensively modified and upgraded to reliably conduct missions to 5000 m depth (Fig. 69A, B). As of January 1996 it has worked four seasons offshore in up to 2400 m of water. In shallow water mode, the vehicle "liveboats" or operates without the cage. In this configuration it routinely operates down to 350 m depth. The vehicle is equipped with two video cameras, two manipulators, sonar, a variety of custom sampling tools and several digital data channels. The vehicle and cage are normally navigated with an acoustic long baseline tracking system that is calibrated with differential GPS.

Typically the vehicle, when it is in shallow water mode, conducts surveys and retrieves samples from coastal waters and operates from small ships (up to 150 ft.). It weighs 1600 kg and operates directly from the deck winch (3600 kg). Deep water operations require larger

ships capable of carrying the large winch and cage (Fig. 69A, B). To date the vehicle has over 1100 h of operation during 320 "dives" in shallow and deep modes.

Cameras

The vehicle is equipped with two video cameras, a wide angle SIT low light camera and a three CCD, broadcast quality colour camera with 16 x zoom (Fig. 69C). We can also fit a still camera. The cage has one colour camera. All cameras use the NTSC format.

Video Recorders

Video is recorded in NTSC format, RGB for the vehicle colour, Super VHS for the vehicle black and white. We can also record the cage or sonar on other Super VHS decks.

Manipulators

The vehicle has two manipulators, a Kodiak (Magnum) seven function that has been modified and improved, and a five function that has also been substantially improved. The manipulators can be fitted with "Pac-man", a clamshell sampler, or can carry many tools with a 3/4 inch "T" bar handle such as a rope cutter, snap hooks and core tubes (Fig. 69C).

Sonar

A Mesotech 971 scanning sonar is fitted. It has been modified with a lower frequency and narrow beam head for better long range information.

Extra services

Six spare data channels are available for other user provided equipment. These are RS-232 format at up to 9600 baud. The configuration of individual channels can be changed to accomodate different data string characteristics. We have fitted chemical scanners, high temperature probes and data links with drill hole data loggers.

Specialty tools

We have developed many tools to improve our scientific capacity. A marker dropper can deposit up to 25 discrete markers throughout the worksite. A rotating sample tray has four separate compartments that can also be subdivided. A suction sampler can sample up to eight discrete, two litre samples (Fig. 69D). The filter size of each container can be changed to allow samples of bacteria through to large animals. "Pac-man" is a clamshell shaped sampler that can be fitted on either manipulator. It is useful for sampling sediments, fragile rock or animal colonies. Laser scalers are fitted on the colour camera. They put out parallel beams for scaling of video frames. Other tools available through users include a chemical scanner for near real time analysis of vent fluids, a stainer for marking tube worms and a manifold sampler for high temperature fluid samples. We will be fitting a multiple barrelled rock drill in the fall of 1996. This will collect samples of rock up to 36 inches long. It may also be used for coring other materials such as steel.

Navigation

We use long baseline navigation for accurate deep-water surveys but have also operated with only the ship using DGPS for long initial site surveys. Our long baseline system integrates data from the acoustic seafloor net, DGPS, ship heading, wind speed and direction, and puts it on one screen with a display for the ROV operators and a remote display used for station keeping the ship. We can absolutely position objects on the seafloor within 5 m. Our acoustic nets can also span up to 8 km.

Launch and Recovery

At present we have used the A-frames present on research ships for launch and recovery, and must use ship based A-frames or cranes. The A-frame dimensions should be a minimum of 12 ft wide and 22 ft tall as the A-frame swings clear of the deck edge. The A-frame must be rated for 14 t or greater.

Ship Requirements

The system requires 460VAC at 250 Amps and 60 Hz to operate the ROV and winch. It is desirable to have 117VAC 60 Hz on a UPS system available.

System weights and size

- Deep system

The vehicle is 7 ft tall, 5 ft wide and 9 ft long. It weighs 6000 lb. (2700 kg).

The cage is 13 ft tall, 7 ft wide and 11 ft long. It weighs 11,000 lb. (5000 kg).

The winch is 7 ft tall, 9.5 ft wide and 13 ft long. It weighs 70,000 lb. (31,800 kg)

The winch power supply is 5 ft tall, 7 ft long and 6.5 ft wide.

The overboard sheave is 7 ft tall.

- Shallow system

The vehicle is 6 ft tall, 5 ft wide and 9 ft long. It weighs 3600 lb. (1600 kg).

The winch is 8 ft tall, 8 ft wide and 7 ft long. It weighs 8000 lb. (3600 kg).

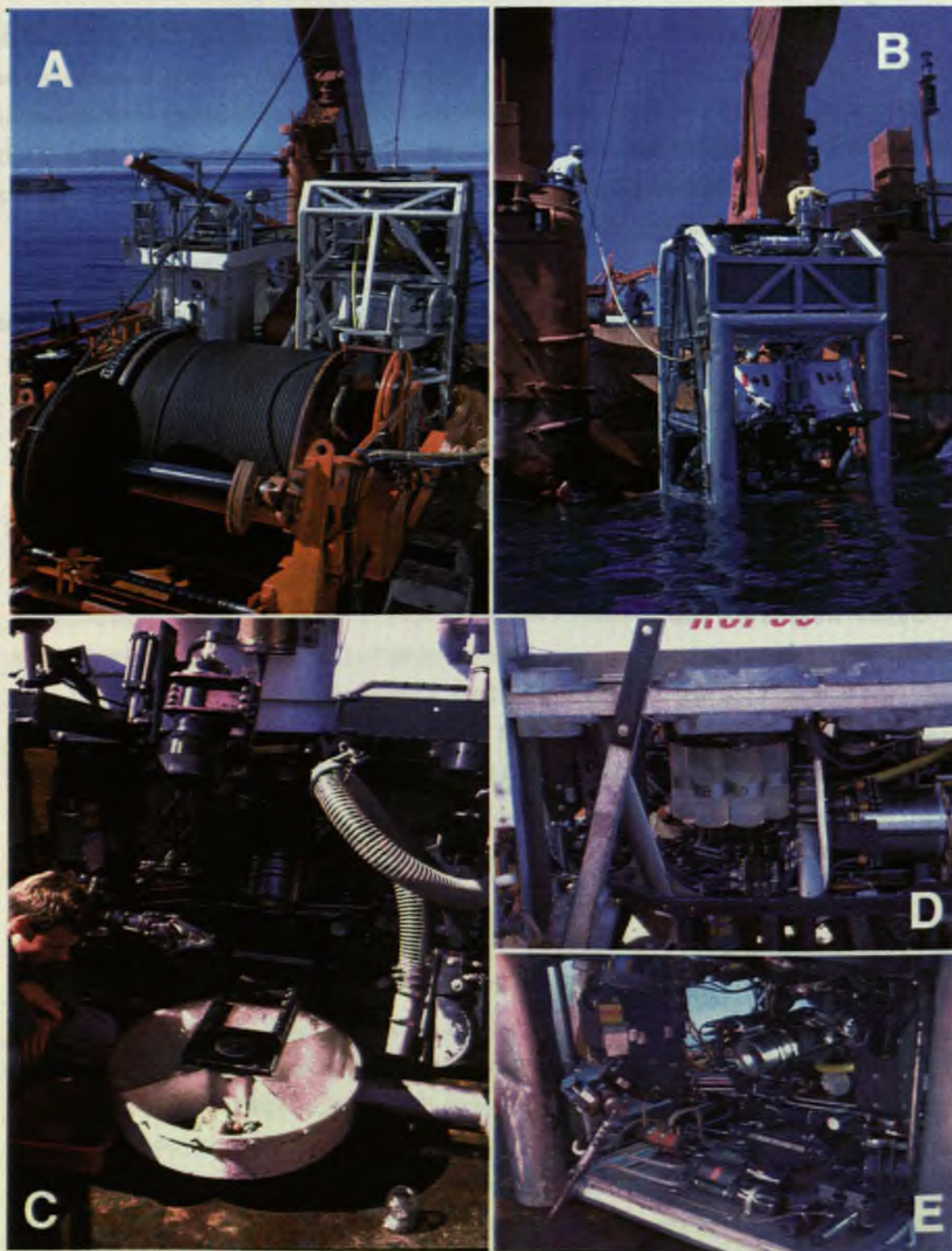


Fig. 69: A). ROPOS winch and cage with vehicle installed on the back of RV SONNE. B). Recovery of ROPOS within the cage at calm weather after successful dive to the Juan de Fuca Ridge. C). Front of ROPOS equipped with sampling tray, 2 manipulators (the right one equipped with the clamshell shaped sampler PacMan and the intake of the suction sampler), 3-ship colour camera with 16 x zoom (middle of picture) and wide angle SIT low light camera (top of picture). D). Side of ROPOS with 8 sampling jars of the suction sampler. E). Front of ROPOS equipped with manifold sampler which can accommodate 6 discrete water samples.

5.4.2 Technical Problems

ROPOS installation on board the research vessel Sonne was delayed because of delivery problems with the new winch drum. The delivery delay became so long that the decision was made to install our old drum with the old 3500 m cable onto the vessel. This was a major undertaking as the old drum, which had started to yeild, was partially disassembled. The drum needed engineering design, repair and reinforcement, and the old cable installed. The slip rings needed to be installed, lebus grooved shells refit, new drive sprocket machined and mounted, cable tensioned and wound onto the drum, cable electrics and fibres terminated at each end and mechanical termination made. This was done in less than two weeks. Due to the rush and pressure to set up on the ship and commence diving some mistakes were made. Following is a brief history of the first leg of the cruise with ROPOS, documenting the technical problems encountered.

- | | |
|---------|---|
| June 25 | Old, rebuilt drum delivered. Lebus grooved shells installed |
| June 26 | New large chain fit, cable tensioned and wound |
| June 27 | Slip rings installed, trucks loaded, ship loaded |
| June 28 | Installation of cables, welding winch to deck, power up of winch and cage. |
| June 29 | Alongside in Victoria. Delayed sailing because of problems. Power conditioner failure, - connector installed incorrectly. This connector is inaccessible and difficult to install. The pins were slightly misaligned and shorted two pins together. This caused a fault in the electronics, although the unit still does regulate power. Fibre problems, winch termination, - cable fibres found to be extremely fragile at the surface end of the cable. The fibres at the surface end of the cable were fragile with visible micro fractures throughout them. The fibres had been functional when the cable was last used, but the unspooling and respooling, after the cable had been stored under tension for years caused micro fractures in the last 500 to 1000 m. Only three fibres were successfully terminated leaving the colour camera in composite mode and no spare fibres. |
| June 30 | Dockside test dives for handling, welding winch to ship's deck PDU flood, - blanking plate not installed when new power conditioner cable installed. Inexperienced technician neglected to reinstall penetrator blanking plate. Only 3 fibres ok - difficult termination due to fragile fibres. |
| July 1 | Test dives for handling science telemetry alive and dead, - science telemetry was tested and functional. After power up checks with the sub motor on, the CPU failed. |

- July 2 Science dive at Axial Seamount. Science power problems, voltage would swing wildly with sub motor on. No navigation, communications with the PS-8000 rangemeter were not installed. No scientific telemetry, removed after CPU failure and science power problems. No arc lights
- July 3 Rigging for manifold on, off, on. Vehicle telemetry failed @ 1600 hrs.
- July 4 Manifold off, too many power problems. Rebuilt vehicle telemetry, replaced line drivers on CPU, found wire off in 7function term box that was affecting telemetry power.
- July 5 Rebuilt still camera cable, camera cable found to have faulty connector. 7f opened, closed, re-routed control signal through new relay. High voltage ground fault - cage motor connector had slow weep causing condensation in can.
- July 6 Repaired science power (wires swapped), replaced cage motor connector. another high voltage ground fault, disappears on deck, aborted dives until ground fault could be found.
- July 7 Test dives for high voltage, ground fault, large E.O. connector on power distribution unit had a ground fault at depth and it would disappear on deck. Connector was removed and reinstalled.
- Video fibre broke. The system was stationary on deck. Retermination of the winch end of the cable necessary.
- Manifold sampler installed and tested. Test was successful.

Outstanding problems: arc lights do not light, science telemetry not installed, camera control not installed, colour camera video intermittent, retermination of winch end of cable required.

5.5 Results:

5.5.1 ROV Operations

by Verena Tunnicliffe

ROPOS Dive 330, test dive, no samples (Axial Seamount)

ROPOS Dive 331

July 2, 1996

Target: ASHES Ventfield, Axial Seamount

Objectives: To test the vehicle systems, assess venting in the ASHES field and sample smoker sulphides.

Summary: Several operational problems were detected: communication with the Datasonics transponder was not possible, problems in the science can meant inoperative controls for the still camera and TV camera, fluctuating power caused loss of two main lights thereby limiting visibility.

The lack of navigation hampered entry to the ventfield. The ship was eventually repositioned to bring the cage nearer to the field whereupon the smoker plume was encountered while the vehicle was in the cage and we could drop into the field. We soon came upon a smoker previously unknown (now "Phoenix") that appears to lie about 25 m east north east of Hell. About 2 m high, it forked from a thin base and was venting from one finger. The top was collected and about 20 cm retained after the beehive disintegrated. Sonar was helpful in locating other chimneys. Hell was sampled next - it was venting in the same position as 1995 but the south side had too much diffuse hot flow from black anhydrite belts to allow ROPOS purchase; only detrital pieces could be retrieved from the fragile chimneys. At Inferno, the "flame" was still burning. The whole structure is larger than in 1986 (three adjoining structures now). While only one double orifice behaved as a smoker, large areas of the chimney sides were uncolonized, black anhydrite diffused hot water. Both the volume of water and the biomass on the chimney was greater than 1986. It was difficult to perch and difficult to sample the smoker top (Pac Man failed at this point). However, a 3/4 round orifice was retrieved intact. Mushroom Vent had scored a hit from the TV grab in the previous SONNE leg but the damage was not severe. Three smoker tips were present but all were broken and lost in sampling attempts. Virgin Vent was difficult to find. It no longer is a brilliant white and sits in a slight depression. A 0.5 m anhydrite spire was toppled and a piece retrieved. Ribbons of pyrite were evident showing through the grey-white apron. Subsequently, the suction sampler was used to pump samples of background water and diffuse flow for microbial analyses. A couple of basalt samples were retrieved. Considerably more was accomplished in this dive than anticipated especially considering technical limitations imposed.

ROPOS Dive 332, test dive, no samples (Axial Seamount)

ROPOS Dive 333

July 5, 1996 ASHES Ventfield, Axial Seamount

Launch target is in the southeast quadrant of the field

Objectives: Sulphide sampling, video, water with suction sampler, animal sample.

Summary: Field was located very rapidly. Acoustic navigation worked fine when the cage was not in the immediate vicinity (which it was for most of the dive for easy working conditions). We could verify that Phoenix Vent is indeed a new find - it is located about 25 m east-northeast of Hell. Sampled a smoking "bulb" from Hillock; passed by Hell and arrived at Inferno (still flaming). Voltage problems precluded good lighting for video, a problem compounded by a fault that lost us all color video for part of the dive. About half of dive spent trying to obtain more of the most recent sulphide from Inferno. Collected a worm clump near Hell then spent about half an hour locating Virgin. Tried to grab into the anhydrite with PacMan but it was heavily indurated and impossible to pull more than a crust off. Another small anhydrite spire (about 25 cm) was located about 8 m southwest of Virgin (Daughter of Virgin). It was vigorously venting but a few sulphide worms had colonized the structure. Relatively good video was possible here.

ROPOS Dive 334, test dive, no samples (Co-Axial Segment, Floc Area)

ROPOS Dive 335, test dive, no samples (Co-Axial Segment, Floc Area)

ROPOS Dive 336, test dive, no samples (Co-Axial Segment, Floc Area)

ROPOS Dive 337, test dive, no samples (between Co-Axial Segment and entrance of Juan de Fuca Street)

ROPOS Dive 338, test dive, no samples (between Co-Axial Segment and entrance of Juan de Fuca Street)

5.5.2 Mapping and Sulfide Sampling

by Peter Buchholz and Thomas Seifert

Sampling

Initial dives with ROPOS were used to remap and sample sulfides in the ASHES vent field. This work was designed to characterize the evolution of the vent complexes in the field since they were last visited in 1988 and 1995. Samples from venting chimneys were collected as a prelude to water sampling. This suite will be used to make detailed comparisons between the fluid chemistry and the mineralogy and bulk composition of boiling and non-boiling vents. Two dives (dives 331 and 333) were successfully carried out at about 1535 m water depth (Appendix). Several test dives focussed on solving technical problems of the system (dives

332, 334-338). Diving time was 11.5 h on the first dive on July 2/3, 1996, and 7 h on July 5, 1996. Five active black and white smoker vents have been sampled with a 7-finger arm, the Pack Man grab system, and a suction sampler: Inferno, Hell, Hillock, Virgin Mound and a new vent (Phoenix). Sulfide samples were emplaced in a sampling tray with 4 compartments. Fluid samples were pumped into plastic water bottles using the suction sampler. The ROPOS system offered a unique opportunity to video-tape the venting scenario and to observe macro and microorganisms as well as boiling of the vent fluids, certainly a unique feature of the Ashes field. The most encouraging subject is that detailed mapping and sampling was successfully carried out within a confined area of centimeter scale. Sulfide sampling was concentrated on the top areas of active chimneys to investigate the interacting processes of fluid boiling and mineral precipitation.

Sample description

ROPOS Dive 331, station R 123 (Ashes Vent Field)

During ROPOS deployment of dive 1 (dive 331), Phoenix, Hell, Inferno, and Virgin Mound vents were observed and sampled. The system was rigged with 7-function and Pack Man arms, sampling tray, suction sampler and video camera. At Mushroom vent, it was not possible to take a sample, because the Pack Man grab arm of ROPOS was blocked after the second deployment at Hell vent. At seven stations, sulfide (R 123-1 to 3, 5, 6, 9) and water (R 123-4, 7, 8, 10; see Appendix Sample list) samples have been taken.

R 123-1 PHOENIX VENT

After about two hours of orientation in the Ashes vent field (transponder system was not operating), a new black smoker chimney (Phoenix vent) was found NE of Mushroom vent. The chimney is approximately 3 m high and characterized by black smoker venting out of a single orifice. One sample (R-123-1-1) was taken from the top of the active vent (diameter about 20 cm). During grabbing, the uppermost 10-15 cm broke off.

The largest sample (2.5 kg) consists of a cavernous to cellular edifice with one major and several smaller fluid channels. Fine crystalline anhydrite has a relict framework and dissolution textures. In the centre of the vent, a tube-like anhydrite aggregate was found. Anhydritization of a tube worm was discussed. Anhydrite is strongly replaced by sphalerite, which is the dominant sulfide phase. Sphalerite crystals (up to 5 mm) have a needle-like texture and form fibrous bunches. The texture is due to replacement of anhydrite. Some of these dark-grey sphalerite needles show a white, transparent appearance at the end of the spire (relict anhydrite). Chalcopyrite is a minor phase and has a filigree texture. The paragenetic relationship between chalcopyrite and sphalerite is not yet clear.

R 123-2 HELL VENT

Several small samples and one larger sample (40 g) (R 123-2-1 and R 123-2-2) have been recovered from the top of the active black smoker chimney. The friable edifice with its cavernous structure consists mainly of sphalerite and anhydrite. Anhydrite is characterized by roundly shaped dissolution textures. Bush-like crystals are covered and replaced by fine grained sphalerite I, giving the anhydrite a grey to dark-grey color. Pseudomorphs of sphalerite I after anhydrite are very common. Sphalerite II is grown onto sphalerite I. Filigree pyrite/marcasite aggregates are relatively late in relation to sphalerite and anhydrite.

R 123-3 INFERNO VENT

Inferno Vent is the most interesting chimney in the Ashes field. It has three major branches splitting off a basal stump. Two active vents in the central part and on the north side have been observed. The central most active vent is characterized by a flame-like fluid flow (visible boiling) coming out of the orifice, well documented by video recording. The recently formed vent is about 50 cm high and has a diameter of 8-10 cm. The hard oval shaped carapace is 1-2 cm thick. The inner fluid channel is characterized by a mosaic-like texture

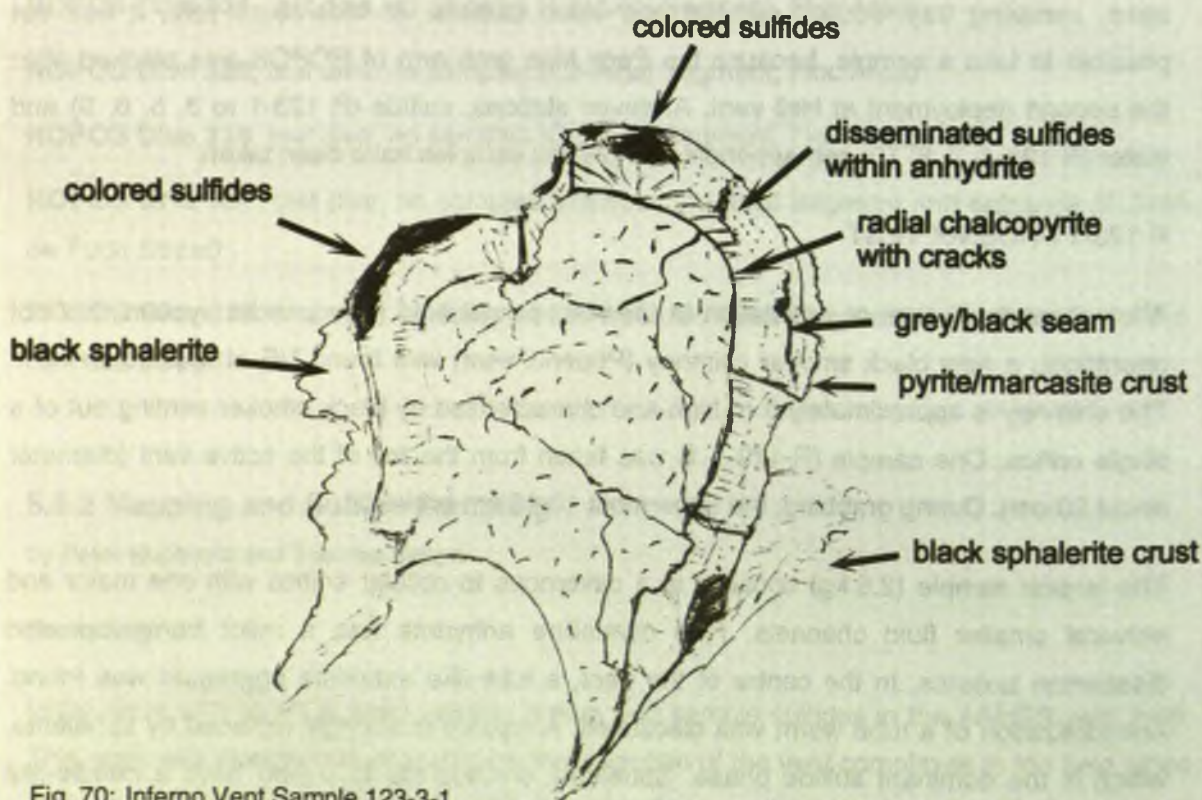


Fig. 70: Inferno Vent Sample 123-3-1

and has a shiny yellow to golden colored surface (sample R 123-3-1). It completely consists of radial shaped chalcopryite forming an almost plane surface of the conduit wall (Fig. 70 and 71). Fractures up to 0.5 mm wide irregularly cross-cut the vents' surface. Sphalerite crystals were observed inside these fractures. The chalcopryite grains are 0.1-1.5 mm in size

and highly porous. The pores' diameter range from 0.2 cm to $< 50 \mu\text{m}$. White coatings were observed to cover some parts of the structure after washing. Towards the outer surface, chalcopyrite is strongly intergrown with anhydrite. Disseminated sulfides occur within this zone. Close to the rim, oxidized and colored sulfide grains of several mm in size, probably bornite, were found. Marcasite (pyrite?) as well as later sulfides of bluish to reddish color form the outer hummocky crust of the vent.



Fig. 71: Zoned chalcopyrite-anhydrite vent from the boiling zone of Inferno Vent

R 123-4 MUSHROOM VENT

Mushroom vent was video-mapped for a detailed biological investigation. The 7-function arm of ROPOS was deployed to take a sample from the active top of the black smoker, but no sulfide sample could be recovered. In the vicinity of the black smoker chimney, a small, approximately 50 cm tall anhydrite spire, was found.

R 123-5 SHEET FLOWS

A relatively fresh basalt sample with a glass crust was taken from the top of a sheet flow for petrological investigations.

R 123-6 VIRGIN MOUND

Virgin Mound is a white smoker within the Ashes field. The chimney mainly consists of anhydrite with a major spire growing from a cone-shaped pedestal. On the basal flanks, shiny yellow sulfide crystals have been observed on several spots (Fig. 72). The shimmering fluids itself are very clear and contain only few white smoke particles. The first approach for

sampling using the 7-function arm failed and the main spire was broken off. One sample was eventually recovered (~ 80 g). It consist of strongly dissolved and cavernous anhydrite. Hexagonal brown to reddish, translucent sphalerite (wurtzite) and chalcopyrite were probably recently precipitated within the cavities, revealing a major change in the fluid composition and physico-chemical conditions of the fluids.



Fig. 72: Anhydrite with recently precipitated sulfides from Virgin Mound

R 123-9 SHEET FLOWS

A relatively fresh basalt sample with a glass crust was taken from the top of a sheet flow for petrological investigations.

ROPOS Dive 333, station R 126 (Ashes Vent Field)

During ROPOS dive 333, Hillock, Inferno, and Virgin Mound vents were observed and sampled. The system was rigged with 7-function and Pack Man arms, sampling tray, suction sampler, and BETACAM color camera. At stations R 126-3, 4, and 9, sulfide samples have been collected. At stations R 126-1, 2, 5-8, 10-13, water samples were taken with the suction sampler (Appendix: Sample list).

R 126-3-1 HILLOCK VENT

At Hillock, one major active vent with a black, smoky plume was observed. Two larger pieces of vent carapace (total ~ 30 g) and some smaller pieces have been recovered at the south side of the chimneys' top (R 126-3-1, Appendix: Sample list).

The chimney material consists of fine grained sphalerite I replacing the anhydrite edifice. Later hexagonal sphalerite II (wurtzite) occurs in cavities and is followed by chalcopyrite mineralization. Marcasite has roundly shaped crystal aggregates probably formed at the final stage.

R 126-4 INFERNO VENT

Inferno vent was approached from the same site as during station R 123-3. Samples were taken from the lower part of the chimney close to the boiling vent. One larger vent sample (R 126-4-1, ~ 800 g) is completely mineralized, relict fluid channelways can still be seen. A cross section of the vent shows zoned mineralization pattern. Sphalerite I is the dominant sulfide phase. Minor components are sphalerite II (wurtzite), pyrite/marcasite, chalcopyrite and anhydrite. On the outer crust of the sample, pseudomorphs of pyrite/marcasite after tube worm structures (*Vestimentifera* *ridgia*) as well as pseudomorphs of sphalerite after sulfide worms (*Paralvinella* *sulfincola*) are obvious. Cavities of the tube worm relicts are mineralized with anhydrite. Mineralization is comparable to that at Hell and Hillock vents. Smaller samples (R 126-4-2) comprise the same mineral assemblage as the sample described above. Anhydrite is strongly replaced by sphalerite I. Additionally, pseudomorphs of marcasite after sphalerite II (hexagonal crystals, wurtzite) were found. Fe-oxihydroxides cover the crust of the chimney fragments.

R 126-9 VIRGIN MOUND

Three larger samples (~ 70 g each) and a couple of smaller pieces from Virgin Mound were taken from the pedestal (R 126-9-1, Appendix). They consist of fine grained, cavernous anhydrite. Later sulfides (sphalerite, chalcopyrite and pyrite/marcasite) occur in cavities. Dark to light-grey spots of anhydrite with a strongly dissolved surface structure indicate replacement by sulfides (mainly sphalerite).

Strongly hydrothermally altered basalts from the same site have a light greenish to grey color and are characterized by disseminated sulfide mineralization. Sulfides and anhydrite additionally occur along micro-fissures and cover basalt surfaces.

Conclusions

The recovered samples from the Ashes hydrothermal field mainly consist of massive sulfides and sulfide-bearing anhydrite chimney fragments and contain different types of vent fauna. Three types of mineralization can be distinguished at the Ashes field:

Type 1: Massive anhydrite samples, which show dissolution textures and recent sulfide overgrowth (sphalerite, chalcopyrite, pyrite/marcasite) at Virgin Mound.

Type 2: Sulfide-rich samples from chimneys without visible boiling (Hell, Hillock, and Phoenix vents). The anhydrite framework of the chimneys is typically replaced by sulfides (mainly sphalerite I; minor phases are sphalerite II, chalcopyrite, pyrite/marcasite).

Type 3: Sulfide-rich samples (mainly chalcopyrite) from the active boiling zone of Inferno vent.

Since the last observation by ALVIN in 1995, Virgin Mound must have changed with respect to fluid chemistry and mineral precipitation. Sulfide mineralization onto the anhydrite indicates an intensifying stage of the hydrothermal activity (type 1). Samples from the Hell, Hillock and Phoenix vents probably represent an intermediate stage characterized by a more intense replacement of the anhydrite chimneys by sphalerite I (type 2). Typical textures are relicts of anhydrite. Precipitation associated with the active boiling at Inferno vent is probably the latest stage of hydrothermal evolution in the Ashes field and represents sulfide-rich high-temperature endmembers (type 3).

5.5.3 Water Sampling

by Dave Butterfield

The manifold vent fluid sampler was reconstructed for SO-109 to expand its cross-platform use, i.e., operating from various submersibles and remotely-operated vehicles. The present manifold sampler, which can accommodate 6 discrete water samples, has been used successfully on the DSRV ALVIN for eight years. Dave Butterfield was lead scientist on sampling of the vent fluids and also was responsible for sample processing and shipboard analysis of pH, alkalinity, H_2S , silica, ammonia, and anions by ion chromatography. J. Lupton (NOAA) also provided 4 evacuated, gas-tight bottles for analyses of rare gases in the vent fluids. Because of the highly gaseous nature of the vent fluids at ASHES, gas-tight samplers are required to effectively trap the volatiles (He , CO_2 , H_2S , CH_4 , H_2 , and rare gases). Lupton's bottles are compatible with both manifold and discrete sampling and are particularly suited for highly-overpressured, gas-charged fluids of the kind presently venting in the ASHES Field. GSC and U. Victoria provided 4 major samplers (two pairs of titanium water bottles) for additional sampling. Two full-time technicians were on board to assist with installation of the manifold sampler and the handling of water samples (one person requires 12 hours to process a load of samples and prepare the samplers for another deployment).

The purpose of NOAA/PMEL's participation in this leg was to demonstrate the capability of ROPOS to collect multiple vent fluid samples on a single dive using the manifold sampler. This was identified as a top priority in discussions with Peter Herzig, Mark Hannington, and

Ian Jonasson. Our primary objective was to sample hot vent fluids in the ASHES vent field to compliment and augment the study of solid sulfides and mineralization processes. This goal was not met primarily because of problems interfacing the manifold sampler to ROPOS. The manifold was installed and functioned properly on deck, and entered the water twice on ROPOS, but suffered from severe power supply problems that caused the manifold computer interface program to stop. On the last day of the cruise, the ultimate cause of the problem was identified as incorrect wiring in the science can. This is what prevented the manifold sampler from functioning properly. It was a simple matter to correct the wiring, and once that was done, the manifold sampler was successfully tested in the water at 1000 meters depth on the way back to Victoria. It was shown that the manifold sampler is technically capable of taking at least 5 samples per dive on ROPOS. Payload limits the number of samplers that can be used per dive and also limits other instruments and equipment that can be attached to the ROV during water sampling dives. Installation and removal of the sampler requires minimal mechanical and electronic connections to the ROV, and can be accomplished in two hours under most circumstances. Although the scientific results were disappointing, the manifold sampler holds promise for using ROPOS to systematically sample hydrothermal fluids in future expeditions.

Gisela Winkler (U. Heidelberg) was trained in the use of the titanium major samplers for use on the next leg of Sonne/ROPOS at cold seeps.

After temporarily giving up the effort to make the manifold sampler work, we set up a pair of titanium major samplers in the arm with a hydraulic actuator. The actuator was attached directly to the samplers, rather than to the arm, to avoid movement of the samplers during triggering. Test firing was successful. This method should be very reliable for collecting a single pair of samples on a dive.

Although no titanium samplers were deployed at vents, we used the suction sampler to collect ambient seawater and diffuse fluids at ASHES. These fluids were analyzed on board for pH, alkalinity, H_2S , and nutrients. Aliquots were stored for later analysis of major elements and trace metals on shore.

5.5.4 Microbiology

by Melanie Summit

Microbiological studies were concerned with the microbial community exiting the subseafloor from sites of diffuse flow. A site of diffuse flow (temperature unknown) NE of Mushroom was sampled on dive #331 with the suction sampler. This site and six samples of background water were checked for the presence of high-temperature organisms and subsamples were preserved for bacterial counts, electron microscopy, and DNA analysis. High-temperature

organisms were cultured at 55°C and 90°C from the diffuse fluids and from some of the background samples. Further analyses will take place in the laboratory of John Baross at the University of Washington.

5.5.5 EXPLOS operations

by Thomas Kuhn

During Leg 3 of R/V SONNE cruise 109 two EXPLOS surveys were conducted. EXPLOS is a video-controlled deep-towed device equipped with a video camera (OSPREY), a photcamera (BENTHOS), a CTD as well as a Eh electrode (with courtesy Mr. K. Nakamura) was mounted. The first deep tow (124 EXPLOS) was carried out on the South Rift area of Axial Seamount caldera, the second EXPLOS profile (129 EXPLOS) was realized along the Floc Area of CoAxial segment.

The objective of the deep tow on the South Rift was to look for hydrothermal activity and its extension according to the vents and chimneys mapped by Embley et al. (1990). Hydrothermal indicators in the water column (temperature and Eh) as well as on the sea floor (active-inactive chimneys, hydrothermal fauna, hydrothermal sediments) should give informations about the current hydrothermalism whereas sea floor structures as well as lava types point towards its tectonic and volcanic control.

5.5.5.1 Survey

Station 124 EXPLOS started just southeast of the Axial Gardens in about 1,560 m water depth heading north. Before the first appearance of hydrothermal activity northeast of the Axial Garden the sea floor is built up of alternating jumbled and lineated sheet flow lava. Small collapse structures cause a rugged topography which is further modified by single cracks. A thin sediment coverage is only observed along small fissures. Ideal formed large pillows also occur.

From 45°56.00' N and 129 °59.05' W through the end of the track at 45°56.88' N and 128°59.20'W hydrothermal indicators play a dominant role of the sea floor structures. A big chimney probably 5 m high is situated just northeast of Axial Gardens. Further north at about 45°56.00' N and 129°58.92'W bacterial mats and a great deal of tube worm bushes cover the sea floor. They most often appear to be bound to cracks and fissure through which hydrothermal fluids may be venting. Clams and mussels feed on the bacterial mats and large crabs sit on hard rocks. Sea floor coverage of hydrothermal fauna partly reaches 50 % or more. The density of the animals decreases north of 45°56.10 'N and 129°59.00 'W to a nearly constant coverage with animals occurring on hydrothermal sediments along fissures and cracks, only. Beyond 45°56.40 'N and 129°50.10 'W there is an increasing amount of hydrothermal material, especially Fe-Oxyhydroxides, altered basalts as well as copper

sulfides (blue precipitations see Foto). Active vents and sulfide chimneys could not be observed. Deep collapse structures that might have caused by outflow of lava of low viscosity along subsurface channels create a very rugged topography. The rim of the collapse structures are often covered by brown Fe-oxyhydroxides. Jumbled sheet flow and lineated sheet lava are still the main lava types. The bottom water over hydrothermal areas is characterized by a high amount of hydrothermal flocs which reasons low visibility. Temperature anomalies increases from 0.03°C northeast of Axial Garden to 0.2°C at the Worm Garden (Fornari & Embley 1995), Eh anomalies are highest northeast of Axial Garden (Δ 220 °C) and reach 120 mV further north.

Station 129 EXPLOS was objective to search for venting areas on the Floc Area in the rift valley of the CoAxial Segment. The venting should be caused by the dike injection event which took part along CoAxial Segment in June-July 1993. The event started at the southern end of CoAxial and traveled about 40 km to the north passing Floc Area and eventually causing lava outflow at the Flow Site at the northern end of CoAxial Segment.

The deep tow started at 46°18.87' N and 129°42.27' W at 2275 m water depth heading WSW along the rift valley. The sea floor was mainly built up of pillows and lobate lava with pure sediment coverage. A rugged topography was cause by different size of the pillows and by cracks striking oblique to the rift axis. Large deep cracks characterize the southern part of the track. It was at such a big crack (46°18.44' N, 129°42.49' W) that an Eh anomaly of about 10 mV appeared. However temperature anomalies could not be measured. Coverage of the sea floor by benthic fauna was also poor but a great amount of mineralized flocs caused a poor visibility in the benthic layer. The mineralized flocs are probably the anorganic result of bacterial metabolism which had been forced out of the subsurface sea floor due to the dike injection (V. Tunnicliffe, pers. commun.).

References

- D.J. Fornari & Robert W. Embley: Tectonic and Volcanic Controls on Hydrothermal Processes at the Mid-Ocean Ridge: An Overview Based on Near-Bottom and Submersible Studies. In S.E.Humphris, R.A. Zierenberg, L.S. Mullineaux & R.E. Thomson(eds.): Seafloor Hydrothermal Systems. Geophys. Monograph 91, American Geophysical Union, 1-46, 1995.

5.5.5.2 Eh-measurements

by Ko-ichi Nakamura

Introduction

Off-line based in-situ Eh measurement system was equipped to the EXPLOS sledge frame near its CTD unit during the EXPLOS station works of the SO109-3 cruise at the Co-axial Seamount in the Juan de Fuca Ridge to detect hydrothermal emissions along the survey lines.

The in-situ Eh measurement has been used in the surveys of seafloor hydrothermal systems since 1993 by the author. The system recorded significant electric potential drops up to several hundreds of mV when it encountered the hydrothermal fluid (plume) during the tow-yo CTD survey, deep-towed side-scan sonar survey and near bottom TV sledge survey in different places (South-East Pacific Rise (Nakamura et al., 1994, cf. Urabe et al., 1995), TAG hydrothermal field in the North Atlantic (Nakamura, 1994, in unpublished cruise report of R/V Knorr TAG cruise, cf. Kleinrocket al., 1995), Okinawa Trough hydrothermal sites (Nakamura et al., 1996) and a hydrothermal site near the Rodriguez Triple Junction in the Indian Ocean (K. Tamaki, 1996, in unpublished cruise report of R/V Meteor, M 33/2 (Hydrock I cruise)).

Equipment and operation

The Eh measurement system was composed of two electrodes and a datalogger. The electrodes were a Pt electrode and a reference electrode, which has a Ag-AgCl electrode contained in a pressure balanced zircaroi tube filled with saturated KCl solution. The data logger recorded the electric potential of seawater between the two electrodes at the interval of two seconds. At the EXPLOS stations 124 and 129, it was fixed to the EXPLOS frame near the CTD sensor and 80 cm above from the bottom of the sledge. Both the electrodes of Eh and CTD were located within 10 cm distance.

Results and discussion

Figure 73 and 74 shows the results of Eh measurements during the EXPLOS 124 and 129 survey, respectively. The Eh records do not indicate any absolute redox potential values at each time (point). Because the EXPLOS sledge passed through different seawater masses (i.e. ambient seawater, various kinds of hydrothermally emitted vent fluids and their mixtures) along the survey tracks before the electrodes equilibrated to the surrounding seawater. However, the drops of the Eh value were the quick response of the electrodes against the entrance into reduced water mass (mostly hydrothermally emitted) from the more oxygenated ambient seawater. The electrodes tended to be equilibrated to the ambient seawater along the logarithmic curve when the sledge went out from the reduced water mass. The drop intervals of Eh values are indicated by dots on the time axes. During the EXPLOS 124 survey many Eh drops were observed. These drops were mostly coincident

with the temperature anomalies and the observations of chimneys, vent organisms and bacterial mats. For example, although the Eh drop (1.8 mV) and the temperature anomaly (0.02°C) were very small at 23:08, crabs were observed along a collapsed structure. A 1 mV small Eh drop near the end of the EXPLOS 129 survey line corresponds to 0.025°C

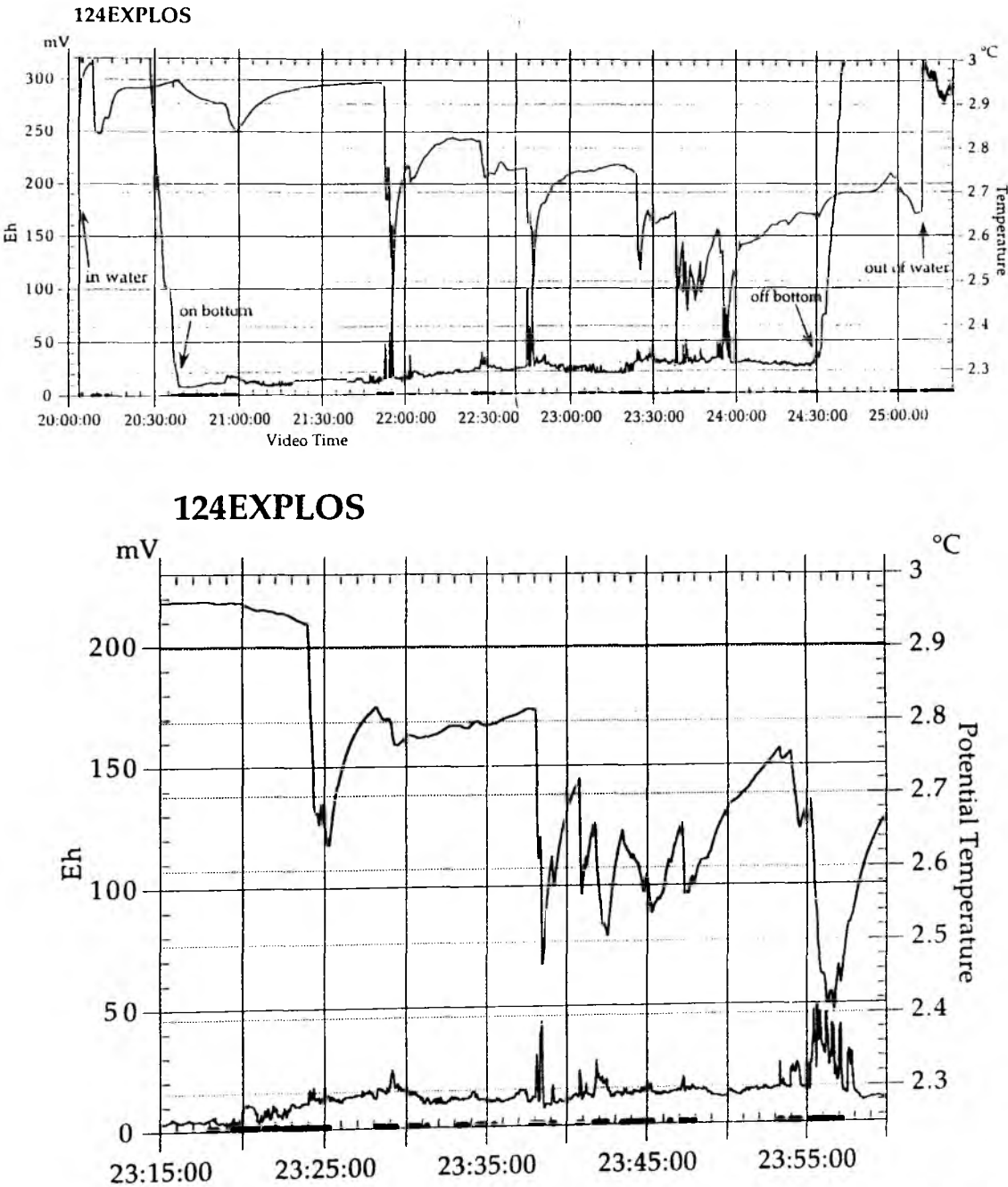
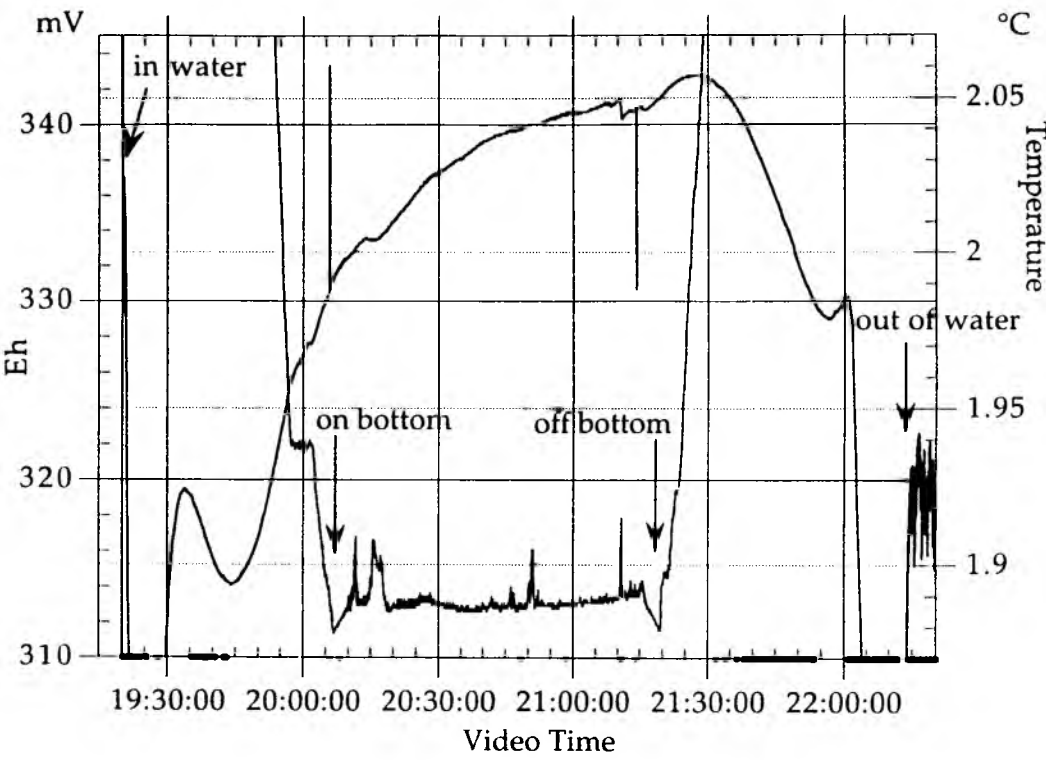


Fig. 73: Eh (black line above) and temperature (grey line below) records of EXPLOS 124 survey along the time record of video and observation sheets. The reference time of these records ('video time') was different from either GPS time or CTD record time. The intervals of the drops of Eh values are indicated by dots on the time axis. a) Whole records. b) Detailed records during the seafloor survey between 23:15 and 00:00.

129EXPLOS



129EXPLOS

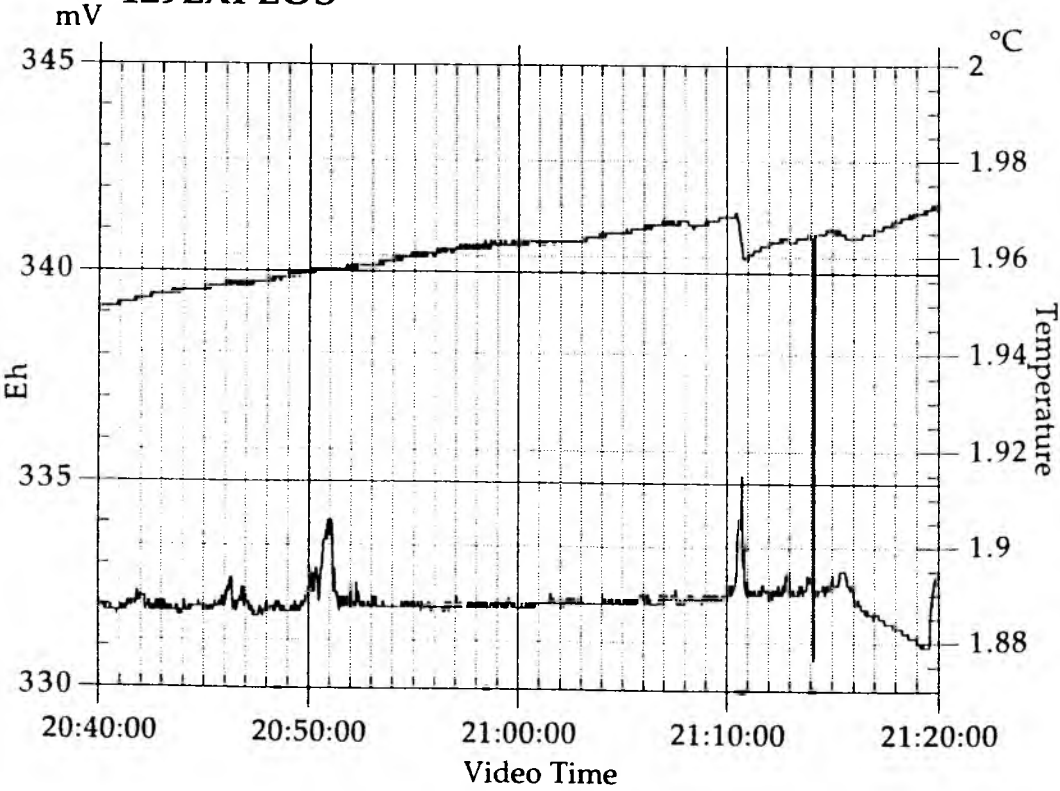


Fig. 74: Eh and temperature record of EXPLOS 129 survey. Lines, the reference time record and dots on the time axis are as those in the figure 73. a) Whole records. b) Detailed records during the seafloor survey between 20:40 and 21:20.

temperature anomaly. A large and deep fissure was observed at the same time through the EXPLOS TV camera. Based on the information of Dr. Tunnicliffe, this fissure might be a continuation of one of the fissures of the neighboring known hydrothermal field. The drop might be an indication of diffusive(?) hydrothermal emission.

References

- Kleinrock, M. C., Humphris, S. E., Shaw, P., Bowen, A., Crook, T., Davis, C., Elder, R., Gleason, D., Goff, J., Goldstein, L., Handley, W., Howland, J., Hussenoeder, S., Koga, K., Lerner, S., Nakamura, K., Rashid, M., Reiser Wetzels, L., Sellers, W., Sulanowska, M., Van Dover, C. and Whitcomb, L. (1995). Detailed structure and morphology of the TAG active hydrothermal mound and its geotectonic environment. In: Humphris, S. E., Herzig, P. M., Miller, D. J., et al., Proc. ODP, Init. Repts., 158: 5-21, College Station, TX (Ocean Drilling Program).
- Nakamura, K., Baker, E. T. and Ridge Flux / R/V Melville Westward Expedition Leg 1 onboard scientific party (1994). Characterization of hydrothermal plumes in the East Pacific Rise by in-situ Eh measurements during Tow yo surveys. Abstracts of 1994 Joint Meeting of Japan Earth and Planetary Science, 167.
- Nakamura, K., Maeda, K., Murayama, N., Saito, N. and Ito, M. (1996). Mapping active hydrothermal sites in the Izena Hole in the Okinawa Trough by Eh and CTD in-situ measurements and its implication for future hydrothermal prospecting. Abstracts, 8th annual meeting of the Japan Society for Marine Surveys and Technology, 22.
- Urabe, T., Baker, E. T., Ishibashi, J., Feely, R. A., Marumo, K., Massoth, G. J., Maruyama, A., Shitashima, K., Okamura, K., Lupton, J. E., Sonoda, A., Yamazaki, T., Aoki, M., Gendron, J., Greene, R., Kaiho, Y., Kisimoto, K., Lebon, G., Matsumoto, T., Nakamura, K., Nishizawa, A., Okano, O., Paradis, G., Roe, K., Shibata, T., Tennant, D., Vance, T., Walker, S. L., Yabuki, T. and Ytow N., 1995, The effect of magmatic activity on hydrothermal venting along the superfast-spreading East Pacific Rise. *Science*, 269: 1092-1095.

5.5.6 Appendix

SO109- Leg 3 Station list

Station	area	location N W	depth m	objectives	brief description
123 ROPOS DIVE #331 date: 02.07.96	ASHES vent field	45°56.0812' 130°00.846'	1485 to 1537	first deep dive of ROPOS from R/V SONNE with massiv sulfide sampling	ROPOS was nearly 10 h working; succesful sampling of 4 different vent sides with Pac Man; boiling at Inferno Vent documented and sampled (chimney tip); one new vent discovered and named Phoenix Vent; anhydrite sampled at Virgin Mound; altered basalt sampled at Virgin Mound and inbetween vent sites; water samples taken with suction sampler at Virgin Mound, near and at Mushroom Vent
124 EXPLOS date: 04.07.96	South Rift area Axial SMT.	45°55.994' 129°58.610' to 45°56.883' 129°59.199'	1565 to 1562	Mapping South Rift Zone to map hydrothermal activity found during Leg 2	Two hydrothermal fields observed, one field inactive but large chimney structures up to 5 m (EXPLOS-coord.: 45°55.60'N, 129°58.78'W), temperature ($\Delta 0.03$ °C) and Eh anomalies ($\Delta 220$ mV); second hydrothermal field (EXPLOS coord.: 45°56.43'N, 129°59.053'W to 45°56.883'N to 129°59.199'W) was probably touched peripherrily with a lot of tube worm „bushes“, clams and bacterial mats being located along fissures within sheet flow lava, suggusting it is an active field, temperature ($\Delta 0.2$ °C) and Eh anomalies ($\Delta 120$ mV); seafloor mainly characterized by sheet flow lava, very rough topography due to collapse structures (range: some m up to far more than 10 m)
125 ROPOS DIVE #332 date: 04.07.96	ASHES vent field	45°55.900' 130°00.800'	20	Test of ROPOS equipped with Manifold Sampler	Problems with telemetry partly caused by wrong interferences of Manifold software with ROPOS telemetry. It made it impossible to control the single units of ROPOS properly or if at all. Test failed and was stopped after a few attempts.
126 ROPOS DIVE #333 date: 05.07.96	ASHES vent field	45° 55.96' 130° 00.76'	1507 to 1537	sample massive sulfides, water samples as well as to map the sea floor with 3- chip color camera	Dive took 8 hours 20 min. Basically all the features of station # 124 could be detected again. Sampling of massive sulfides at Inferno Vent (boiling zone) and Hilloch Vent, of biological samples near Hell Vent (tube worm bush) and Mushroom Vent (basalts covered with bacteria mats) as well as water samples at the begin and end of the dive.
127 ROPOS DIVE #334 06.07.96	CoAxial segment	46°18.450' 129°42.420'	1000	look for hydrothermal vents at Floc Site and take biological and water samples ROPOS equipped with bottles of Manifold Sampler	Operation failed due to cage problems, probably a ground fault
128 ROPOS DIVE #335 06.07.96	CoAxial segment	46°18.582 129°42.511'	2215	look for hydrothermal vents at Floc Site and take biological and water samples ROPOS equipped with bottles of Manifold Sampler	Operation failed due to high voltage ground fault, cage back to ship

Station	area	location N W	depth m	objectives	brief description
129 EXPLOS	Floc Area on CoAxial Segment	46°18.622' 129°42.345' to 46°18.132 129°41.959'	2232 to 2282	to look for venting sites on the Floc Area in rift valley of CoAxial Segment	No hydrothermal venting could be detected; rugged sea floor made up of pillows and lobate lava; high amount of mineralized flocs in benthic water layer caused low visibility; large cracks striking oblique to axial valley; one big crack shows small Eh anomaly of 10 mV
130 ROPOS DIVE #336 date: 06.07.96	Floc Area on CoAxial Segment	46°18.132 ' 129°41.959'	1475	look for hydrothermal vents at Floc Site and take biological and water samples ROPOS equipped with bottles of Manifold Sampler	Operation failed due to high voltage ground fault, cage back to ship
131 ROPOS test	Midway between Floc Area and Victoria, B.C.	47°44.20' 126°36.90' DGPS	1300	ROPOS test in water column	Operation failed due to cage problems, probably a ground fault
132 ROPOS test	Midway between Floc Area and Victoria, B.C.	47°45.15' 126°37.57' DGPS	1750	ROPOS test with Suction Sampler in water column	Suction Sampler worked well, but no images on screens of board units

ROPOS coordinates are the transponder navigation coordinates of the launch target at the beginning of the dive if not stated otherwise. Depth is the actual depth of the transponder position. Station numbers are continued from SO109-2, ROPOS Dive # derives from consecutive numbering of ROPOS deployments.

Appendix ROPOS logs

Dive No. 331 Station No. 123 Date: 2.7.96 Launch Target N 45.56.0812; W 130.00.846 Dive Axial Seamount-Ashes vent field, 1st deep dive of ROPOS to sample Objectives sulfides; Rigging: PAC-MAN, Sampling Tray, Suction Sampler, Still Camera					
Item	Time	Observations/Activities	Z	X	Y
1	2.7.96 17:15	Launch	0	0	0
2	2.7.96 17:31	Back on deck. Air in cage hydraulic system.			
3	2.7.96 18:12	Launch ROPOS, lowering rate ca. 35m/min	0	0	0
4	2.7.96 19:04	stopped at position	1511		
5	2.7.96 19:06	leaving cage, compass heading (H) 190, 214, approaching ashes field from NE	1511		
6	2.7.96 19:08	see bottom, sheeted lava, Fe-oxides, H-214	1533		
7	2.7.96 19:11	undifferentiated sheet flows, water full of micro organisms ?	1534		
8	2.7.96 19:16	lava flows, rough surface	1536		
9	2.7.96 19:19	sheet flows, H-226	1531		
10	2.7.96 19:21	sheet flows, covered partly with sediments, fissures	1533		
11	2.7.96 19:23	flows, rough surface	1534		
12	2.7.96 19:24	broken lavas, Fe-oxides abundant, spider crab	1532		
13	2.7.96 19:26	100m away from cage, 90m from wall, H-216	1518		
14	2.7.96 19:28	sheet flows with cooling fractures	1535		
15	2.7.96 19:31	new spot after direction change, H-43,	1533		
16	2.7.96 19:32	new heading, H-239, many micro organisms (marine snow) in water column	1533		
17	2.7.96 19:33	H-241, jumbled lava ?	1535		
18	2.7.96 19:37	H-232, sheet flows, sediments, some broken lava	1535		
19	2.7.96 19:41	sheet flows with fissures, sediment filled	1532		
20	2.7.96 19:42	H-121, sheet flows, plain surface, fissures filled with sediments	1532		

Item	Time	Observations/Activities	Z	X	Y
21	2.7.96 19:43	clam deposit, ropy sheet flows, lobated at end, H-126, 60m off the wall	1535		
22	2.7.96 19:45	jumbled lava flows ? H-127	1533		
23	2.7.96 19:47	system check, H-121, spider crab, jumbled lava, fractured?	1534		
24	2.7.96 19:49	sheet flows, sedimented fissures	1535		
25	2.7.96 19:49	driving in the SW, lot of marine snow, yellow particles	1535		
26	2.7.96 19:51	changing course, H-355, rough surface, jumbled sheet flows, oxides cover in places 50% of surface	1533		
27	2.7.96 19:54	H-348, contact sheet flows and jumbled flows	1535		
28	2.7.96 19:55	H-301	1533		
29	2.7.96 19:55	H-308, jumble flows	1535		
30	2.7.96 19:56	new chimney, sulfides?, black smoke out of orifice, close to ships (cage) position is N45.55.9920, W130.00.8414 (position of pointer at screen !!)	1531		
31	2.7.96 19:59	shimmering water, same chimney, tube warms on pedestal, possibly bacteria, H-351	1533		
32	2.7.96 20:02	approaching chimney to get sample, one orifice on top of the chimney, one branch on top seems to be extinct, black on top is anhydrite, first framework?, anhydrite possibly replaced by sulfides (see comments V. Tunnicliffe).	1532		
33	2.7.96 20:06	pack man is now beeing deployed, chimney about 1m high,	1533		
34		grabbing, soft particles falling down, no sample, grabbing, top 3-5cm were falling down, wide top and narrow bottom hold in pack man, sample tray box No. 5 (station/sample 123-1-1), successfully sampled, organisms on top and aside of sample	1533		
35	2.7.96 20:13	returning to chimney, H 95	1532		
36	2.7.96 20:17	cracked lava flows	1533		
37	2.7.96 20:18	tube worms in lava fissures	1534		
38	2.7.96 20:19	just passed small Fe-oxide chimneys	1534		
39	2.7.96 20:21	H-24,	1531		
40	2.7.96 20:22	H-344, passing oxide chimneys again, yellowish colour, H-321, jumbled lava flows, rough surface, Fe-oxides in fissures, some oxide chimneys, little fish	1534		
41	2.7.96 20:25	clams, tubeworm bushes, bacterial mats , lobated (pillowed lavas), H-268, more bushes	1534		
42	2.7.96 20:26	undifferentiated lava flows with Fe-oxides, lot of broun to yellow marine snow,	1535		
43	2.7.96 20:28	sea star, H-266, problems with orientation,	1536		
44	2.7.96 20:30	H-321, new compass heading , approaching crater wall, rough flow surface, next heading to the SE	1532		
45	2.7.96 20:34	new heading H-128, sheet flows	1530		
46	2.7.96 20:35	just passed sea star	1533		
47	2.7.96 20:36	lobated lavas contacting jumble lavas? H-139	1531		
48		change of topography, small escarpment (depression) to the right	1531		
49	2.7.96 20:38	jumbled sheet flows H-165, changing into flat sheet flows, fissures with sediments,	1533		
50	2.7.96 20:41	H-198, jumbled sheet flows	1531		
51	2.7.96 20:42	H-138	1531		
52	2.7.96 20:44	ropy sheet flows, H-109, yellow Fe-oxides in fissures,	1533		
53	2.7.96 20:50	ROPOS returning to cage by winging, H-339, still problems with orientation	1519		
54	2.7.96 20:55	back to cage for new orientation, cage visible in front of ROPOS,	1513		
55	2.7.96 20:57	manovering ropos into cage	1510		
56	2.7.96 20:58	ROPOS parked in cage,	1512		
57	2.7.96 21:05	finish video			
58	2.7.96 21:53	Restarting video recording.			
59	21:57	sheeted lava flows, magmatic fissures filled with sediments	1535		
60	21:59	the same chimney as sample 123-1-1, N: 45.55.9965; W: 130.00.7365; the greater chimney vent is not smoking; the smaller one is smoking (dark smoke)	1534		

Item	Time	Observations/Activities	Z	X	Y
61	22:03	25 m from the last chimney point in H289 new chimney with four vents; two smoking (dark smoke); below the chimney lobated lava to pillow lava; hydrothermal sediments in fissures; tube worm bushes; in the lower part of the chimney are light color areas;	1536		
62	22:11	the same point as 22:03; active vents are in the centre of the chimney top; the name is HELL VENT; sampling of one active vent; sample 123-2-1 (box number 6/7); N: 45.56.0021; W: 130.00.7493;	1532		
63	22:21	see 22:11; H: 342; looking for the lost sample at sample point 123-2-1; vent fish (?);	1536		
64	22:35	see 22:11; H: 60; taking a new sample from the same chimney; difficult to take the sample; H: 5-10; 22:40 next step to take a sample;	1533		
65	22:42	see 22:11; H: 30; sample 123-2-2 (sample is in the grab arm and we go to the next sampling point); sample is not in the sample box!!	1532		
66	22:48	we go to H:16-20 direction;	1534		
67	22:49	Inverno Vent; active; black smoke; one vent in the top of the chimney; very active with boiling (see video); partly covered by vent fauna;	1534		
68	22:58	see 22:49; a lot of tube worms covered the chimney;	1534		
69	23:05	see 22:49; grab arm take a chimney sample from the top (see video); sample 123-3-1 (sample box 8/1), the sample is from the point, where we see on the video boiling	1535		
70	23:10	see 22:49; we take an other sample from Inverno Vent H: 200, it is difficult; the chimney is covered by many tube worms; we see a second vent in the background; mapping of the Inverno vent; we did not take this sample (it is not possible)	1534		
71	23:39	H: 283 to 321; Mushroom Vent; mapping around the chimney; one active vent in the top of the chimney; we want to take a sample from the active top (sample 123-4-1), but it is difficult	1532		
72	23:45	around the chimney; anhydrite spire (about 20 cm high); a lot of tube worms covered the chimney; one other little vent in the middle part of the chimney;	1537		
73	23:57	mapping and looking for a sampling point around the chimney	1537		
74	3.7.96 0:10	see 23:39, sampling at the top, H: 350; sampling sample 123-4-1 is difficult	1536		
75	0:35	see 23:39, sampling 123-4-1 finished without sample (very difficult)	1536		
76	0:40	go to an other sample point (first H: 95), (leave Mushroom Vent); second H: 175; third H: 115;	1536		
77	0:44	unknown vent, H: 89; sheeted lava, tube worm bush; Fe hydroxides; sampling of basalt with a FeOOH crust 0:44 (sample 123-5; sample box 3)	1537		
78	1:01	active smoker with several vents on the top (dark smoke); H: 294, Mushroom Vent	1537		
79	1:09	go to Virgin Mound (H: 88)	1537		
80	1:11	basalt with FeOOH crusts	1537		
81	1:13	Virgin Mount (new little vent ?) ca. 50cm high with approximately 1.5m pedestal, white colour, probably anhydrite, sulfides precipitated at the flanks, shiny yellow colour, chimney broken off, black smoke and chimmering water	1537		
82	1:28	white coatings in the perimeter of the vent, trying to get a sample,	1537		
83	1:33	sample grabbed, lost, trying again, ca. 2cm thick sulfide crust covers pedestal close to chimney,	1538		
84	1:45	sample 123-6-1, Virgin Mount vent in box 2/3, small sample with white coatings,	1537		
85	1:57	no chance to get more sulfide samples at Virgin Mount, looking around for some other chimneys in the area, jumbled lava flows,	1537		
86	2:01	tube of suction sampler broken off	1537		
87	2:03	H-327, sulfide sampling finished,	1524		
88	2:07	Melanie Summit takes over, fluid sampling with suction sampler is planned, back to the bottom, bottle check	1524		
89	2:09	start sucking into bottle No. 3, 13 m off the bottom approximately above Virgin Mount, sample No. 123-7-1 (bottle 3), ca. 5 min sucking, H-318	1524		
90	2:14	stop sucking into bottle No. 3, down to the bottom	1524		

Item	Time	Observations/Activities	Z	X	Y
91	2:15	at bottom, looking for a diffuse field, jumbled lava flows, Fe-oxides in fissures	1537		
92	2:17	small Fe-oxide chimneys	1536		
93	2:20	looking for more intensive fluid flow, Verenas XYZ markers found, bushes of tubeworms,	1536		
94	2:22	site with diffusive fluid flow found, shimmering water, jumbled lava flows around	1535		
95	2:24	another site of shimmering water, lot of marine snow, fish, tabular lava blocks,	1537		
96	2:28	getting close to Virgin mount, going WSW of Virgin mount, H-238, bushes of tubeworms,	1537		
97	2:29	Mushroom vent ahead, yellow XYZ-marker on bottom, grabbing marker	1537		
98	2:34	moving east from Mushroom vent, crossing field with small lava pillars	1535		
99	2:35	site of shimmering water found, XYZ-marker No. 21, positioning tube of suction sampler just above diffusive flow	1537		
100	2:39	start pumping into bottle No. 4 of suction sampler, sample No. 123-8-1, 5 min suction time	1537		
101	2:44	stop suction into bottle No. 4, bottle No. 5 in position	1536		
102	2:49	Mushroom vent is 20-25m at bearing 250 degrees where we left marker No. 21	1535		
103	2:50	shimmering water, diffuse fluid flow, positioning tube for suction sampler,	1537		
104	2:52	lost tube connection to the suction sampler, grabbing tube and positioning over diffuse fluid exits, plenty of tubeworms	1537		
105	2:55	start sucking into suction sampler, bottle No. 5, sample No. 123-8-2, close to XYZ-marker No. 21, compass Heading-2 degrees	1537		
106	3:00	stop suction into bottle No. 5	1537		
107	3:01	V. Tunnicliffe takes over, new direction H-210 for ca. 40 m, intention is to locate the first chimney sampled at beginning of dive	1537		
108	3:04	crossing field of jumbled to lobated lava, H-218, passing large tubeworm bushes,	1537		
109	3:06	pillow lavas, Hell Vent ahead, new direction ESE, H-148,	1538		
110	3:10	ROPOS returning to cage for check, screen wobbles	1537		
111	3:12	H-265	1507		
112	3:15	suddenly all screens off, checking systems			
113	3:23	screens OK, time reset, 00:02	1485		
114	3:26	back on bottom, H-345, lavas with Fe-oxide coatings, heading to the NW, H-317, jumbled lava flows, sulfide mount chimneys, some ropy lavas ahead,	1536		
115	3:31	crossing a field of broken sheet flows, H-320,	1537		
116	3:33	lots of Fe-oxides covering fissures in lava flows, H-061	1529		
117	3:35	heavily broken lava flows, Fe-oxides in fissures, H-31,	1535		
118	3:40	jumbled flows, small lava pillars	1537		
119	3:43	sampling a little basalt pice	1537		
120	3:52	basalt sample grabbed, sample No. 123-9-1, sample still fixed in ROPOS arm	1532		
121	3:53	pumping water in bottle 6, sample No. 123-10-1, background value of sea water, no obvious hydrothermal influences	1532		
122	3:59	stop pumping into bottle 6, returning to cage	1532		
123	4:03	ROPOS close to cage, start manoeuvrating into cage	1510		
124	4:05	ROPOS parked in cage, start heaving, 20m/min	1511		
125	5:18	ROPOS at water surface	0		
126	5:20	ROPOS back on deck			

ROPOS Dive Log Dive No. 332 Station 125 Number Date: 4.7.96 Launch Target N 45° 55.9' W 130° 00.8' Dive Axial Seamount-Ashes Vent Field; ROPOS dive to sample vent fluids; Objectives rigging: MANIFOLD SAMPLER					
Item	Time	Observations/Activities	Z	X	Y
1	4.7.96 19:35	Start of station; launching ROPOS	0		
2	4.7.96 19:51	ROPOS stopped and back to ship due to ground problems	20		
3	4.7.96 23:38	launching ROPOS again after some repair			
4	4.7.96 23:41	problems with ROPOS partly caused by interactions with MANIFOLD SAMPLER			
5	4.7.96 23:45	tests failed ROPOS back to ship			
6	4.7.96 23:50	ROPOS reaches ship			
7	4.7.96 23:53	ROPOS deployment failed due to problems with MANIFOLDER SAMPLER, its software , power supply and so on could not used with ROPOS at the current state of art. It is not a problem of ROPOS' standard system use to take hard rock samples.			
8	4.7.96 23:58	ROPOS on deck; end of station			

ROPOS Dive Log Dive No. 333 Station No. 126 Protokol Th. Kuhn; P. Buchholz; Th. Seifert Date: 5.7.96 Launch N 45°55.96' W 130°00.76' Target Dive ASHES-AXIAL SMt. to sample massive sulfides, fluids and water Objectives samples as well as to map the sea floor; rigging: PAC-MAN, Suction Sampler and Color Camera (3-chip for BETACAM), PS 8000 at cage for navigation					
Item	Local time	Observations/Activities	Z	X	Y
1	5.7.96 6:27	Begin of station	0		
2	5.7.96 6:40	ROPOS in water, short look around everything o.k. then start launching with 25 m/min	50		
3	5.7.96 7:06	transponder navigation for ROPOS and cage works very well, cage is just below the ship	800		
4	5.7.96 7:29	stop at 1512 m			
5	5.7.96 7:34	ROPOS leaves the cage, heading (H) 24			
6	5.7.96 7:36	bottom view H 321, broken sheet flow	1520		
7	5.7.96 7:37	H 294,			
8	5.7.96 7:39	a lot of animals on sea floor, probably not hydrothermal			
9	5.7.96 7:40	fish			
10	5.7.96 7:40	three range fix now, exact position of ROPOS underneath the cage possible			
11	5.7.96 7:41	preparing for sampling bottle #1, pumping 5 min 5 m above ground			
12	5.7.96 7:43	start pumping, pumping stopped due to reverse pumping	1529		
13	5.7.96 7:45	try to pump the other way round			
14	5.7.96 7:48	pumping still into wrong direction, actually pumping not sucking	1529		
15	5.7.96 7:51	stop pumping, go on into field, H 286			
16	5.7.96 7:52	target on sonar about 20 m away	1534		
17	5.7.96 7:53	bottom covered with Fe-Oxides	1535		

Item	Local time	Observations/Activities	Z	X	Y
18	5.7.96 7:53	change direction to 321, target turned to be nothing, variable changing from lineated to jumbled sheet flow, Fe-Oxides	1533		
19	5.7.96 7:55	lineated sheets, alvin mark, clams nesseling down in cracks	1534		
20	5.7.96 7:56	no fixes	1535		
21	5.7.96 7:56	sheet flows lineated			
22	5.7.96 7:56	entering area of worm bushes, but only a few	1535		
23	5.7.96 7:57	H320	1536		
24	5.7.96 7:57	still alternating sheets and jumbled flows			
25	5.7.96 7:58	rising 5 m above ground taking another suction sample	1526		
26	5.7.96 7:58	start sucking into bottle #2 for 1:30 min	1527		
27	5.7.96 8:01	stopped sucking			
28	5.7.96 8:02	back to sea floor	1533		
29	5.7.96 8:02	some worm bushes in cracks, lots of marine snow	1534		
30	5.7.96 8:03	number of bushes increases, H 273 now	1535		
31	5.7.96 8:04	stop at large bush, surrounding it	1536		
32	5.7.96 8:05	having a close look at the worm tubes	1536		
33	5.7.96 8:08	color test with 3-chip camera	1536		
34	5.7.96 8:09	trying to get a fix, but ropos directly under the cage, causes difficulties	1536		
35	5.7.96 8:09	still some tests with 3-chip camera, focussing, zooming etc.	1536		
36	5.7.96 8:11	shimmering water causes problems with focussing, but eventually o.k. we are still right above the worm bushes			
37	5.7.96 8:13	still no fix cause too close to the cage	1536		
38	5.7.96 8:14	go back to the cage, cause of tether problems, teather is rapped around the cage	1507 cage depth		
39	5.7.96 8:20	trying to unrap the tether			
40	5.7.96 8:23	back down to bottom view	1533		
41	5.7.96 8:24	H 257, back on broken jumbled floww, 50 m east of Hell	1535		
42	5.7.96 8:25	heading for Hell,	1535		
43	5.7.96 8:27	lineated sheet flow	1535		
44	5.7.96 8:27	marker ahead#2, chimney ahead , approaching it its Phoenix	1533		
45	5.7.96 8:29	at Phoenix still the one arm smoking	1533		
46	5.7.96 8:30	still no fix, though cage is more off			
47	5.7.96 8:32	facing now to 308	1535		
48	5.7.96 8:32	try to find out where this vent is try to clear if it is a already known vent, H 271	1536		
49	5.7.96 8:34	found Hillock and Hell in background, so former vent is new (Phoenix) its just to the east of Hillock	1536		
50	5.7.96 8:35	look for venting to get a sample there	1535		
51	5.7.96 8:35	fishes			
52	5.7.96 8:36	guessing there is a small gab with smoke coming out			
53	5.7.96 8:37	animal (vent fish) eating a worm, zooming at it	1535		
54	5.7.96 8:39	BETACAM was just on to film the eating fish, now its off again	1535		
55	5.7.96 8:40	shimmering water about 200 °C			
56	5.7.96 8:41	still surrounding Hillock for a site to sample	1536		
57	5.7.96 8:41	zonation of animals, Hydr. worms...			
58	5.7.96 8:42	zooming at tube worms	1537		
59	5.7.96 8:44	reset color taping and try to get a focussed close image again			
60	5.7.96 8:52	still problems with color recording			
61	5.7.96 8:54				
62	5.7.96 8:55	try to get a sample at Hillock's top where there is fluid venting off and there is a small stump with Pac-Man (on the south side), still problems with color recording	1536		
63	5.7.96 8:58	grabed a smoking knob putting into box #4/5 (1 big piece)	1536		
64	5.7.96 9:01	still no color image on the color screen, try to solve the problem	1536		
65	5.7.96 9:04	look for a good basalt piece about 10 m away from Hillock	1536		
66	5.7.96 9:09	H 276 stopped trying a basalt piece going to Hell	1536		
67	5.7.96 9:10	move the ship to get a fix of ROPOS	1536		

Item	Local time	Observations/Activities	Z	X	Y
68	5.7.96 9:14	Hell is a large chimney prob. about 3 metres high, three small chimneys on top, one of them slightly smoking	1536		
69	5.7.96 9:16	power switch off and on in order to reset color recording	1513		
70	5.7.96 9:17	still no color image			
71	5.7.96 9:18	back on sea floor	1536		
72	5.7.96 9:19	power switch off and on in order to reset color recording			
73	5.7.96 9:20	still no color image			
74	5.7.96 9:22	color image back, anemonies around Phoenix Vent	1536		
75	5.7.96 9:23	second vent a bit away (Mushroom?)			
76	5.7.96 9:23	Phoenix still smoking on the one arm			
77	5.7.96 9:24	heading for Inferno H 355	1534		
78	5.7.96 9:25	jumbled sheets on the way to Inferno	1535		
79	5.7.96 9:26	clams and worm bushes on the way, H 348	1536		
80	5.7.96 9:27	heading 320	1535		
81	5.7.96 9:27	Phoenix is ENE of Mushroom	1536		
82	5.7.96 9:28	arriving at Inferno from south side (marker)	1536		
83	5.7.96 9:29	look for the boiling zone	1535		
84	5.7.96 9:31	four small chimneys of top of Inferno, two of them (on the central and north side) are smoking	1529		
85	5.7.96 9:34	looking now ESE	1534		
86	5.7.96 9:35	height about 4m	1533		
87	5.7.96 9:38	taking a sample from top of Inferno from smoking chimney	1532		
88	5.7.96 9:39	Pac Man empty, gonna try it again	1532		
89	5.7.96 9:41	try sampling again	1532		
90	5.7.96 9:42	try to push the tray with sampling arm (it does not move automatically anymore) which is a really tricky manoeuvre taking some time	1535		
91	5.7.96 9:49	into box #6/7 a lot of hydroth. material succesful sampled at Inferno (126-4-1)	1535		
92	5.7.96 9:52	go back to top of Inemo to get another sample	1536		
93	5.7.96 9:53	surrounding inferno to face SW			
94	5.7.96 9:54	NW chimney heavily smokes, wanna take a sample from there facing SE	1533		
95	5.7.96 9:55	boiling flame just where the smoke leaves the chimney	1532		
96	5.7.96 9:58	taking the sample directly from the boiling zone at In ferno	1532		
97	5.7.96 9:59	sample tray works again automatically			
98	5.7.96 9:59	sampling failed	1535		
99	5.7.96 10:08	switch power off and on to reset color recording go a bit up	1526		
100	5.7.96 10:09	bottom view again, Inferno Vent, surrounding it and try to get a nother sample	1533		
101	5.7.96 10:11	lots of tube worms with brownish organic mass inside and white tubes	1532		
102	5.7.96 10:12	shimmering water around the tube worms	1532		
103	5.7.96 10:13	H 134, turning further, boiling zone very distinct visible	1532		
104	5.7.96 10:17	sampling boiling zone of Inferno Vent top side	1536		
105	5.7.96 10:19	into box#1/8 sampling failed again	1529		
106	5.7.96 10:21	back to top of Inferno and try to sample again	1532		
107	5.7.96 10:23	H 85 lowering for sampling	1532		
108	5.7.96 10:25	first attempt failed, breaking off some parts of the chimney's top			
109	5.7.96 10:26	camera and Pac Man directly in hot fluid, can withstand it without problems	1535		
110	5.7.96 10:29	sampling attempt,	1535		
111	5.7.96 10:30	crab on the foot of Inferno Vent	1535		
112	5.7.96 10:30	into box #1/8 some hydrothermal material of succesful sampling of the boiling zone at Inferno			
113	5.7.96 10:35	lots of small fragments and some bigger parts of hydrothermal material sampled	1533		
114	5.7.96 10:36	further sampling of same boiling zone of Inferno's top	1532		
115	5.7.96 10:38	lots of tube worms sticking out of their's tubes	1532		
116	5.7.96 10:39	boiling flame visible very well on the color screen			

Item	Local time	Observations/Activities	Z	X	Y
18	5.7.96 7:53	change direction to 321, target turned to be nothing, variable changing from lineated to jumbled sheet flow, Fe-Oxides	1533		
19	5.7.96 7:55	lineated sheets, alvin mark, clams nesseling down in cracks	1534		
20	5.7.96 7:56	no fixes	1535		
21	5.7.96 7:56	sheet flows lineated			
22	5.7.96 7:56	entering area of worm bushes, but only a few	1535		
23	5.7.96 7:57	H320	1536		
24	5.7.96 7:57	still alternating sheets and jumbled flows			
25	5.7.96 7:58	rising 5 m above ground taking another suction sample	1526		
26	5.7.96 7:58	start sucking into bottle #2 for 1:30 min	1527		
27	5.7.96 8:01	stopped sucking			
28	5.7.96 8:02	back to sea floor	1533		
29	5.7.96 8:02	some worm bushes in cracks, lots of marine snow	1534		
30	5.7.96 8:03	number of bushes increases, H 273 now	1535		
31	5.7.96 8:04	stop at large bush, surrounding it	1536		
32	5.7.96 8:05	having a close look at the worm tubes	1536		
33	5.7.96 8:08	color test with 3-chip camera	1536		
34	5.7.96 8:09	trying to get a fix, but ropos directly under the cage, causes difficulties	1536		
35	5.7.96 8:09	still some tests with 3-chip camera, focussing, zooming etc.	1536		
36	5.7.96 8:11	shimmering water causes problems with focussing, but eventually o.k. we are still right above the worm bushes			
37	5.7.96 8:13	still no fix cause too close to the cage	1536		
38	5.7.96 8:14	go back to the cage, cause of tether problems, teather is rapped around the cage	1507 cage depth		
39	5.7.96 8:20	trying to unrap the tether			
40	5.7.96 8:23	back down to bottom view	1533		
41	5.7.96 8:24	H 257, back on broken jumbled floww, 50 m east of Hell	1535		
42	5.7.96 8:25	heading for Hell,	1535		
43	5.7.96 8:27	lineated sheet flow	1535		
44	5.7.96 8:27	marker ahead#2, chimney ahead , approaching it its Phoenix	1533		
45	5.7.96 8:29	at Phoenix still the one arm smoking	1533		
46	5.7.96 8:30	still no fix, though cage is more off			
47	5.7.96 8:32	facing now to 308	1535		
48	5.7.96 8:32	try to find out where this vent is try to clear if it is a already known vent, H 271	1536		
49	5.7.96 8:34	found Hillock and Hell in background, so former vent is new (Phoenix) its just to the east of Hillock	1536		
50	5.7.96 8:35	look for venting to get a sample there	1535		
51	5.7.96 8:35	fishes			
52	5.7.96 8:36	guessing there is a small gab with smoke coming out			
53	5.7.96 8:37	animal (vent fish) eating a worm, zooming at it	1535		
54	5.7.96 8:39	BETACAM was just on to film the eating fish, now its off again	1535		
55	5.7.96 8:40	shimmering water about 200 °C			
56	5.7.96 8:41	still surrounding Hillock for a site to sample	1536		
57	5.7.96 8:41	zonation of animals, Hydr. worms...			
58	5.7.96 8:42	zooming at tube worms	1537		
59	5.7.96 8:44	reset color taping and try to get a focussed close image again			
60	5.7.96 8:52	still problems with color recording			
61	5.7.96 8:54				
62	5.7.96 8:55	try to get a sample at Hillock's top where there is fluid venting off and there is a small stump with Pac-Man (on the south side), still problems with color recording	1536		
63	5.7.96 8:58	grabed a smoking knob putting into box #4/5 (1 big piece)	1536		
64	5.7.96 9:01	still no color image on the color screen, try to solve the problem	1536		
65	5.7.96 9:04	look for a good basalt piece about 10 m away from Hillock	1536		
66	5.7.96 9:09	H 276 stopped trying a basalt piece going to Hell	1536		
67	5.7.96 9:10	move the ship to get a fix of ROPOS	1536		

Item	Local time	Observations/Activities	Z	X	Y
68	5.7.96 9:14	Hell is a large chimney prob. about 3 metres high, three small chimneys on top, one of them slightly smoking	1536		
69	5.7.96 9:16	power switch off and on in order to reset color recording	1513		
70	5.7.96 9:17	still no color image			
71	5.7.96 9:18	back on sea floor	1536		
72	5.7.96 9:19	power switch off and on in order to reset color recording			
73	5.7.96 9:20	still no color image			
74	5.7.96 9:22	color image back, anemonies around Phoenix Vent	1536		
75	5.7.96 9:23	second vent a bit away (Mushroom?)			
76	5.7.96 9:23	Phoenix still smoking on the one arm			
77	5.7.96 9:24	heading for Inferno H 355	1534		
78	5.7.96 9:25	jumbled sheets on the way to Inferno	1535		
79	5.7.96 9:26	clams and worm bushes on the way, H 348	1536		
80	5.7.96 9:27	heading 320	1535		
81	5.7.96 9:27	Phoenix is ENE of Mushroom	1536		
82	5.7.96 9:28	arriving at Inferno from south side (marker)	1536		
83	5.7.96 9:29	look for the boiling zone	1535		
84	5.7.96 9:31	four small chimneys of top of Inferno, two of them (on the central and north side) are smoking	1529		
85	5.7.96 9:34	looking now ESE	1534		
86	5.7.96 9:35	height about 4m	1533		
87	5.7.96 9:38	taking a sample from top of Inferno from smoking chimney	1532		
88	5.7.96 9:39	Pac Man empty, gonna try it again	1532		
89	5.7.96 9:41	try sampling again	1532		
90	5.7.96 9:42	try to push the tray with sampling arm (it does not move automatically anymore) which is a really tricky manoeuvre taking some time	1535		
91	5.7.96 9:49	into box #6/7 a lot of hydroth. material succesful sampled at Inferno (126-4-1)	1535		
92	5.7.96 9:52	go back to top of Inerno to get another sample	1536		
93	5.7.96 9:53	surrounding Inferno to face SW			
94	5.7.96 9:54	NW chimney heavily smokes, wanna take a sample from there facing SE	1533		
95	5.7.96 9:55	boiling flame just where the smoke leaves the chimney	1532		
96	5.7.96 9:58	taking the sample directly from the boiling zone at In ferno	1532		
97	5.7.96 9:59	sample tray works again automatically			
98	5.7.96 9:59	sampling failed	1535		
99	5.7.96 10:08	switch power off and on to reset color recording go a bit up	1526		
100	5.7.96 10:09	bottom view again, Inferno Vent, surrounding it and try to get a nother sample	1533		
101	5.7.96 10:11	lots of tube worms with brownish organic mass inside and white tubes	1532		
102	5.7.96 10:12	shimmering water around the tube worms	1532		
103	5.7.96 10:13	H 134, turning further, boiling zone very distinct visible	1532		
104	5.7.96 10:17	sampling boiling zone of Inferno Vent top side	1532		
105	5.7.96 10:19	into box#1/8 sampling failed again	1536		
106	5.7.96 10:21	back to top of Inferno and try to sample again	1529		
107	5.7.96 10:23	H 85 lowering for sampling	1532		
108	5.7.96 10:25	first attempt failed, breaking off some parts of the chimney's top	1532		
109	5.7.96 10:26	camera and Pac Man directly in hot fluid, can withstand it without problems			
110	5.7.96 10:29	sampling attempt,	1535		
111	5.7.96 10:30	crab on the foot of Inferno Vent	1535		
112	5.7.96 10:30	into box #1/8 some hydrothermal material of succesful sampling of the boiling zone at Inferno	1535		
113	5.7.96 10:35	lots of small fragments and some bigger parts of hydrothermal material sampled			
114	5.7.96 10:36	further sampling of same boiling zone of Inferno's top	1533		
115	5.7.96 10:38	lots of tube worms sticking out of their's tubes	1532		
116	5.7.96 10:39	boiling flame visible very well on the color screen	1532		

Item	Local time	Observations/Activities	Z	X	Y
117	5.7.96 10:46	surrounding Inferno in order to get into good position for sampling, two attempts failed yet			
118	5.7.96 10:47	H 138 approaching for another sampling attempt on the NW side	1532		
119	5.7.96 10:50	discussion about where to take another sample: from last year's boiling zone? it could not exactly be located that's why another sample will be taken at the present boiling zone	1531		
120	5.7.96 10:53	H 131, we are still at the NW side of Inferno	1531		
121	5.7.96 10:54	retreating a bit to let the suspended material settle down	1531		
122	5.7.96 10:55	approaching again heading 75-120	1531		
123	5.7.96 10:59	sampling at boiling zone of Inferno's NW side	1530		
124	5.7.96 11:02	into box#1/8 some pieces of hydr. Mat. from boiling zone of Inferno (126-4-2)	1536		
125	5.7.96 11:04	H320 approaching Inferno again	1533		
126	5.7.96 11:05	surrounding Inferno	1534		
127	5.7.96 11:05	three finger-like chimneys on a basic stump			
128	5.7.96 11:06	two active chimneys H110, one N one S	1533		
129	5.7.96 11:08	small basis which gets a bit thicker upwards	1534		
130	5.7.96 11:09	H 252, Vent elongated E-W	1535		
131	5.7.96 11:09	one smoking chimney situated on east side	1534		
132	5.7.96 11:10	lots of worm tubes on the chimneys on all sides	1534		
133	5.7.96 11:11	s from Vent side about 10 m to sample basalt	1535		
134	5.7.96 11:13	blocky basalts looking for tube worms on basalts to sample	1534		
135	5.7.96 11:14	tube worms localized try to take samples	1535		
136	5.7.96 11:15	try to sample tube worms	1535		
137	5.7.96 11:18	try to sample with 7 function arm	1535		
138	5.7.96 11:20	two big worm bushes	1535		
139	5.7.96 11:21	location 8 m N to NW of Hell	1535		
140	5.7.96 11:22	sampling perfectly one bush and put it into box # 2/3 (126-5-1)	1536		
141	5.7.96 11:27	go up just 5 m to take water samples with sucking sampler	1530		
142	5.7.96 11:29				
143	5.7.96 11:30	start sucking 1:30 min box#3	1530		
144	5.7.96 11:31	stop sucking			
145	5.7.96 11:32	start sucking box#4, 2:30 min	1530		
146	5.7.96 11:34	stop sucking			
147	5.7.96 11:40	hoping to reach a crack vent area to take biological samples	1535		
148	5.7.96 11:40	just passed transition of sheet flows and broken sheets H-110	1534		
149	5.7.96 11:42	back in sheet flows again, broken sheets, crab, highly fractured, Fe-hydr. oxides in fissures, rough topography, tabular lava fragments	1533		
150	5.7.96 11:44	go little bit off north from now, vector up around virgin mount, position west of Phoenix vent	1535		
151	5.7.96 11:46	new heading to north H-351, probably passing Inferno vent	1535		
152	5.7.96 11:47	sheet flows, over 50 % sediment cover in some locations	1534		
153	5.7.96 11:48	jumbled sheet flows, H-355	1533		
154	5.7.96 11:50	still jumbled and broken lavas	1532		
155	5.7.96 11:50	turning west, detecting chimneys on sonar	1534		
156	5.7.96 11:51	fish, H-275	1531		
157	5.7.96 11:52	tectonically broken lava sheets, tabular fragments, jumbled, sediments in fissures, H-273	1534		
158	5.7.96 11:53	jumbled lava sheets, turning to the south H-232	1532		
159	5.7.96 11:54	big fish H-245	1532		
160	5.7.96 11:54	lava pillars and hydrothermal sediments (Fe-hydr. oxides), problems with orientation, cage is about 90 m SE of our position, we need to take a SW heading, approximately H-220, we have to find mushroom vent again for new orientation	1534		
161	5.7.96 11:57	H-235, hydrothermal yellowish to brown sediments	1533		
162	5.7.96 11:58	H-218, found XYZ-markers, stopped, turning to H-270	1536		
163	5.7.96 12:01	hydroth. sediments, lobated to pillowed lavas ahead	1532		
164	5.7.96 12:01	H-278, inferno vent ahead, H-359	1535		

Item	Local time	Observations/Activities	Z	X	Y
165	5.7.96 12:03	Mushroom vent ahead, little anhydrite spire in front of the vent, lobated lava in perimeter of the vent	1535		
166	5.7.96 12:05	H-90, orientating	1535		
167	5.7.96 12:06	jumbled lava sheets, brown coatings on lavas	1534		
168	5.7.96 12:08	basalts with white bacteria mats, intend to take a sample	1535		
169	5.7.96 12:12	yellow micro organisms, spider, wurm, white bacteria mats, on the edges of the vent there are pretty rare species living, trying to get a sample, shimmering water	1535		
170	5.7.96 12:15	still trying to grab	1535		
171	5.7.96 12:21	looking for another sample	1535		
172	5.7.96 12:24	using pack man for grabbing	1535		
173	5.7.96 12:27	just tried to get a sample with 7-function arm, not successful	1535		
174	5.7.96 12:31	content of pack man emptied in box 4/5, two bio-samples, basalt covered with white bacteria mats	1535		
175	5.7.96 12:33	H-86, going to Vergin Mount vent next, crossing a field of jumbled sheet lavas, hydr. sediments, Fe-hydr. oxides	1534		
176	5.7.96 12:34	little fish ahead, hydr. sediments, crab, bacteria mats?	1533		
177	5.7.96 12:35	sheeted lavas, yellowish to brown hydr. sediments in cavities and fissures of lava, H-83	1535		
178	5.7.96 12:36	H-83, Fe-hydr. oxides covering lavas, orientation problems, cage under back of the ship N 45.55.9784; W 130.00.7385	1535		
179	5.7.96 12:41	jumbled lava sheets, rough surface, still searching for Virgin Mount vent	1534		
180	5.7.96 12:43	arrived at Virgin Mount vent, looking around the vent	1534		
181	5.7.96 12:48	prepared for grabbing with pack man	1535		
182	5.7.96 12:54	still trying to grab a sample	1535		
183	5.7.96 12:59	grabbed sample from Virgin Mount vent, taken at pedestal, loose broken pieces broken up on first ROPOS dive, not colonized by organisms, sulphides precipitates along the flanks of the chimney, it looks like little sulphide streams			
184	5.7.96 13:03	little anhydrite spire, smoking, ca. 5 m east of Virgn Mount vent	1535		
185	5.7.96 13:06	bacterias, shimmering water, sulfide worms, highly turbulent water, zooming and recording the whole scenery, almost pure fluids without any white or black particles (particle-poor smoke)	1535		
186	5.7.96 13:13	trying to zoom and focus on sulphide worms through shimmering water, BETACAM video is now working at the end of the dive	1535		
187	5.7.96 13:17	leaving the Virgin mount area, H-191, looking for a good spot for taking a water sample using the suction sampler	1532		
188	5.7.96 13:20	checking orientation	1525		
189	5.7.96 13:23	water sampling bottle Nr. 5 for Melanie	1526		
190	5.7.96 13:27	water sampling bottle Nr. 6 for Melanie, start by 1515 m, finish by about 1500 m	1515		
191	5.7.96 13:35	finish of video recording	1510		
192	5.7.96 13:37	back in the cage	1510		
193	5.7.96 13:38	finished water sampling bottle Nr. 7 for Melanie (Water sampling in the cage)	1512		
194	5.7.96 13:41	water sampling bottle Nr. 8 (water sampling in the cage) finished	1510		
195	5.7.96 13:47	start the winch up	1511		
196	5.7.96 14:43	ROPOS on surface	0		
197	5.7.96 14:49	ROPOS back on deck; end of protokol total number of video tapes: 3			

<div><div>ROPOS Dive Log</div><div><div>Dive Number: 334</div><div>Station Number 127</div></div><div><div>Date: 05/07/96</div><div>Launch Target: CoAxial Segment, Floc area</div><div>Dive Objectives</div></div></div>				
Date/Time	Observations/Activities	Z	X	Y
	2053 sub in water I need to figure out how to use the time macro 2145ish coming back up			
5.7.96 22:03	start and stop, problems with the the cage, on deck again at about 23:00			

ROPOS

Dive Log

Dive No. 335

Station Number 128

Date: 6.7.96

Launch Target: Coaxial on northern fraction zone

Dive Objectives: fluid-sampling, sampling of biota

Equipment: 2 fluid-bottles right arm, pac man left arm, suction sampler, biota box

Item	Time	Observations/Activities	Z	X	Y
1	6.7.96 6:47	ROPOS in the water, decent descent			
2	6.7.96 7:27	ship-position: 46:18,582 N, 129:42,511 W, Waterdepth 2260 m			
3	6.7.96 8:08	cage stopped at 46o 18.58 129o 42.47 2180m			
4	6.7.96 8:13	leaving cage heading SE			
5	6.7.96 8:16	bottom sighted depth 2215m (!)			
6	6.7.96 8:19	cage lowered to 2190m			
7	6.7.96 8:21	high voltage ground fault			
8	6.7.96 8:23	bringing cage back up			
9	6.7.96 8:25	winch stopped			
10	6.7.96 8:34	coming back up, two-part recovery			

ROPOS Dive Log Dive No. 336 Station Number 130 Date: 6.7.96 Launch Target: Coaxial on northern fraction zone Dive Objectives: fluid-sampling, sampling of biota Equipment: 2 fluid-bottles right arm, pac man left arm, suction sampler, bio box					
Item	Date/Time	Observations/Activities	Z	X	Y
1		sub in water			
2	6.7.96 15:38	100m down			
3	6.7.96 15:40	all stop; unidentified ground? Or breaker trip			
4	6.7.96 15:46	going down again			
5	6.7.96 16:31	1475m ground fault; all stop			
6	6.7.96 16:33				

Appendix: Sample list

Ashes vent field

Sample No.	ROPOS Dive No.	Location/ Description	No. of pieces	Size, weight	Mineralogy
R 123-1-1	331	new vent (Phoenix Vent), pedestal of chimney	1	20x20x15 cm	anhyd, sl
			4	~ 2500 g	
			1	3-5 cm Ø	anhyd, sl
			23	4x2 cm Ø	sl, anhyd
			1	1-2 cm Ø	anhyd, sl
R 123-2-1	331	Hell Vent, fragments of chimney	1	<0.5 cm	soft powdered sulfides
			2	2x4 cm Ø	sl, very friable
			3	1-2 cm Ø	sl
R 123-2-2	331	Hell Vent, top of dark brown to black vent	1	< 0.5 cm	soft powdered sl
			4	7x4.5x1 cm	sl
			12	~ 40 g	sl
R 123-3-1	331	Inferno Vent, complete vent tube sample with mineral precipitation directly from flame-like boiling zone	4	6-6 cm Ø	sl
			1	1-3 cm Ø	sl
			1	9x5x6 cm	cpy, sl, anhyd, bn?, py/ma
			5	~ 250 g	cpy, sl, anhyd, bn?, py/ma
R 123-5-1	331	Ashes field	1	5.5x3 cm	cpy, sl, anhyd, bn?, py/ma
			1	5x4 cm	cpy, sl, anhyd, bn?, py/ma
R 123-6-1	331	Ashes field	1	1-3 cm Ø	cpy, sl, anhyd, py/ma
			1	6.5x3x3.5 cm	fresh, glass-rich basalt
R 123-9-1	331	Virgin Mound, sample from pedestal flank of the chimney	1	4x2.5x2.5 cm	fresh, glass-rich basalt
			1	7x5x4 cm	anhyd, sl
R 126-3-1	333	Hillock Vent, south side of the chimney, sample taken close to vent orifice	1	~ 80 g	
			1	10x6x5 cm	fresh, glass-rich basalt
			1	6x4 cm	sl, py/ma
			1	5x2 cm	sl, py/ma
			17	1-3 cm	sl, py/ma
			1	<0.5 cm	soft powdered sulfides

Sample No.	ROPOS Dive No.	Location/ Description	No. of pieces	Size, weight	Mineralogy
R 126-4-1	333	Inferno Vent, sample taken from the lower part of the chimney	1	8x10x9 cm ~ 800 g	sl, py/ma, anhyd
			1	6.5x4.5x4 cm	sl, cpy
			1	5x2x2 cm	ma-pseudom.
			1	3x3x1 cm	sl, cpy!
			3	1-3 cm Ø	sl, cpy
			7	1x3x1 cm	ma-pseudom. after worms
			4	1-2 cm Ø	fibrous anhyd
			17	0.5-2.5 cm Ø	sl, py/ma
R 126-4-2	333	Inferno Vent, NW side of the top, sample taken below boiling zone	1	7x8x0.5cm ~ 60 g	sl (pseudom. after anhyd; needles and small leafs, opaque); sl (wurzite, brownish trans-parent, hexa-gonal xx)
			1	6x6x0.3 cm	sl
			1	4x3.5x0.3 cm	sl (hexagonal xx typical), py/ma
			11	1-5 cm Ø	sl, partly py/ma
			1	<0.5 cm	soft powdered sulfides
R 126-9-1	333	Virgin Mound, sample from pedestal of the chimney	1	10x7x3.5 cm ~ 70 g	anhyd, sl, cpy, py/m
			1	7x5.5x3.5 cm ~ 70 g	anhyd, sl, cpy, py/ma
R 126-9-1	333	ff. Virgin Mound altered basalt samples from the bottom of the Virgin Mound Vent	1	8x5x3 cm ~ 70 g	anhyd, sl, cpy, py/ma
			1	3x3x0.5 cm	anhyd, sl, cpy, py/ma
			12	0.5x2 cm	anhyd, sl, cpy, py/ma
			1	4.5x4x4 cm	strongly hydroth. Altered basalt with greenish-grey color, sulfides and anhyd on micro-fissures and surface
			~ 30	small pieces (0.5-3 cm)	see above
			1	<0.5 cm	soft powdered sulfides

Abbreviations: sl = sphalerite ma = marcasite py = pyrite cpy = chalcopyrite anhyd = anhydrite